

**UNIVERSITÀ DEGLI STUDI DI TRIESTE
UNIVERSITÀ DEGLI STUDI DI UDINE**

XXIX CICLO DEL DOTTORATO DI RICERCA IN

Ambiente e Vita

**Mercury mobilization potential from highly
contaminated alluvial soils**

Settore scientifico-disciplinare: AGR/13 CHIMICA AGRARIA

**DOTTORANDA
GIADA ZANUTTINI**

**COORDINATORE
PROF. GIORGIO ALBERTI**

**SUPERVISORE DI TESI
PROF. MARCO CONTIN**

ANNO ACCADEMICO 2015/2016



**UNIVERSITÀ DEGLI STUDI DI TRIESTE
UNIVERSITÀ DEGLI STUDI DI UDINE**

XXIX CICLO DEL DOTTORATO DI RICERCA IN

Ambiente e Vita

**Mercury mobilization potential from highly
contaminated alluvial soils**

Settore scientifico-disciplinare: AGR/13 CHIMICA AGRARIA

DOTTORANDA
GIADA ZANUTTINI

Giada Zanuttini

COORDINATORE
PROF. GIORGIO ALBERTI

G. Alberti

SUPERVISORE DI TESI
PROF. MARCO CONTIN

M. Contin

ANNO ACCADEMICO 2015/2016

Table of Contents

SUMMARY	1
1. INTRODUCTION	5
1.1. RELEVANCE OF MERCURY PROBLEM	5
1.2. MERCURY IN THE ENVIRONMENT	5
1.2.1. Sources and transformations of mercury in the environment	7
1.3. MERCURY FRACTIONATION AND SPECIATION	10
1.3.1. Methods for mercury fractionation and speciation	12
<i>1.3.1.1. Sequential Extraction Procedures</i>	12
<i>1.3.1.1.1. SEP limitations</i>	18
<i>1.3.1.2. Thermal desorption</i>	18
<i>1.3.1.3. Comparison between SEP and TD</i>	22
<i>1.3.1.4. X-ray absorption spectroscopy</i>	23
<i>1.3.1.5. Importance of sample handling</i>	25
1.4. THE ROLE OF SOIL ON MERCURY FRACTIONATION AND BEHAVIOUR	26
1.4.1. Factors affecting mercury fractionation in soil	29
<i>1.4.1.1. Influence of dissolved anions in soil solution</i>	30
<i>1.4.1.2. Mineral and organic surfaces</i>	33
<i>1.4.1.2.1. Sorption of elemental Hg</i>	36
<i>1.4.1.3. Mercury and organic matter interactions</i>	36
<i>1.4.1.3.1. Cinnabar dissolution by NOM</i>	41
<i>1.4.1.4. Mineral Fertilizers</i>	43
<i>1.4.1.5. Organic amendments</i>	44
<i>1.4.1.6. Effect of root exudates on mercury mobility</i>	45
1.4.2. Mercury reduction and volatilization	46
2. OBJECTIVES AND HYPOTHESES	51
2.1. OVERALL AIMS AND GOALS	51
2.2. HYPOTHESES	51
3. MATERIALS AND METHODS	53
3.1. DESCRIPTION OF THE STUDY AREA	53

Table of Contents

3.2. SOIL SAMPLING AND PROCESSING	57
3.3. SEDIMENT SAMPLING AND PROCESSING	59
3.4. CLEANING PROCEDURE	61
3.5. CHEMICAL ANALYSES FOR SOIL CHARACTERIZATION	61
3.5.1. Soil pH	61
3.5.2. Soil salinity analyses	62
3.5.3. Cation Exchange Capacity analyses	62
3.5.4. Redox potential	62
3.5.5. Lime content analyses	63
3.5.6. Organic carbon and total nitrogen analyses	63
3.5.7. Determination of total metal content	63
3.5.8. Multielement analyses by neutron activation	64
3.6. TOTAL MERCURY ANALYSIS	64
3.7. PARTICLE SIZE FRACTIONATION	64
3.8. MERCURY FRACTIONATION WITH SEQUENTIAL EXTRACTION PROCEDURES (SEP)	66
3.8.1. Sequential extraction procedure by Lechler et al.	67
3.8.2. Tree steps Sequential extraction procedure	68
3.8.3. Sequential extraction procedure by Han et al.	68
3.9. MERCURY QUANTIFICATION IN SOIL EXTRACTS	70
3.9.1. CV-AAS	70
3.9.2. CV-AFS	70
3.9.3. ICP-MS	71
3.10. Hg FRACTIONATION BY THERMO-DESORPTION	71
3.11. INTERPRETATION OF MERCURY FRACTIONATION BY COUPLING TD WITH SEP	75
3.12. SOIL SPIKING WITH MERCURY-HUMIC SUBSTANCES	76
3.13. EFFECT OF FERTILIZERS ADDITION ON MERCURY STABILITY	76
3.14. VOLATILIZATION AND SOLUBILISATION EXPERIMENT	78
3.14.1. Experimental set up	80
3.15. WATER LEACHING TEST	82
3.16. QUALITY CONTROL AND QUALITY ASSURANCE	82

4. RESULTS AND DISCUSSION	83
4.1. SOIL SURVEY AND CHARACTERIZATION	83
4.1.1. Pedological characterization of soil profile	86
4.2. MERCURY SPECIATION/FRACTIONATION	94
4.2.1. Mercury distribution according to particle size	95
4.2.2. Hg speciation through three steps Sequential Extraction Procedure	99
4.2.3. Hg speciation according to Han et al.	101
4.3. COMBINATION OF SOIL MERCURY THERMAL DESORPTION CURVES AND SEQUENTIAL EXTRACTIONS	105
4.3.1. Soil spiking	126
4.4. EFFECT OF MINERAL FERTILIZERS ON MERCURY MOBILITY	128
4.4.1. Effect of mineral fertilizers on Hg thermal stability	128
4.4.2. Effect of mineral fertilizers on water extractable Hg	130
4.4.3. Effect of mineral fertilizers on Hg solubility under aerobic and anaerobic conditions	130
4.4.4. Effect of mineral fertilizer on mercury volatility under aerobic and anaerobic conditions	131
4.5. EFFECT OF ORGANIC FERTILIZERS ON MERCURY MOBILITY	132
4.5.1. Effect of organic fertilizers on Hg thermal stability	132
4.5.2. Effect of organic fertilizers on water extractable Hg	133
4.5.3. Effect of organic fertilizers on Hg solubility under aerobic and anaerobic conditions	134
4.5.4. Effect of organic fertilizers on mercury volatility under aerobic and anaerobic conditions	135
4.6. EFFECT OF ROOT EXUDATES ON MERCURY MOBILITY	137
4.6.1. Effect of root exudates on mercury solubility under aerobic and anaerobic conditions	137
4.6.2. Effect of roots exudates addition on mercury volatility under aerobic and anaerobic conditions	140
5. CONCLUSIONS	145
REFERENCES	147
APPENDIX A	173

Table of Contents

A.1. RELEVANCE OF MERCURY POLLUTION IN THE AREA STUDIED	173
A.2. IDRIJA MERCURY MINE.....	175
APPENDIX B-PICTURES OF THE STUDY AREA AND THE SOIL PROFILE	179
APPENDIX C-THERMO-DESORPTION CURVES OF FOSSALON SOIL TREATED WITH FERTILIZERS	183
APPENDIX D-PROPOSALS FOR FURTHER RESEARCH.....	197
D.1. IMPORTANCE OF NANOPARTICLES IN CINNABAR'S MOBILIZATION	197
ACKNOWLEDGMENTS	201

List of Tables

<i>Table 1.1. Properties of some Hg species: water solubility ($\mu\text{g l}^{-1}$) (WS), vapor pressure (VP) at 25 °C (Modified from Dyrssen and Wedborg, 1991; Navarro, 2008).</i>	7
<i>Table 1.2. Accessible literature data about the temperature characteristics of Hg compounds (Sedlar, 2014).</i>	19
<i>Table 1.3. Review of existing methods for temperature fractionation of Hg (Sedlar, 2014).</i>	21
<i>Table 1.4. Evolution of total Hg and Hg⁰ concentrations (mean \pm standard deviation; n = 4) with pretreatment and 10-day storage period (Reis et al., 2016).</i>	26
<i>Table 3.1. Geographical coordinates of sampling points.</i>	59
<i>Table 3.2. Size limits of texture fractions (ISSS).</i>	65
<i>Table 3.3. Type of Hg Compound, Suppliers and Purity.</i>	75
<i>Table 3.4. Application doses for some fertilizers commonly used for arable crops (corn). Application rate of N (300 kg ha⁻¹), P (100 kg ha⁻¹ P₂O₅), K (100 kg ha⁻¹ K₂O) in a depth of 5 cm.</i>	78
<i>Table 3.5. Application of organic amendments commonly used for arable crops (corn).</i>	78
<i>Table 3.6. Conditions of incubation experiments.</i>	81
<i>Table 4.1 Concentration (mg kg⁻¹) and standard deviation (n=3) of potentially toxic elements in the top 0-40 horizon of six sampling points. Threshold concentration of contamination in the soil and subsoil referred to the specific intended use of the sites to be reclaimed (D.Lgs 152/2006).</i>	84
<i>Table 4.2. Total mercury concentration along soil profiles in the six sampling points.</i>	85
<i>Table 4.3. Soil profile description. GENERAL FEATURES: Holocene Floods with water table at 200 cm. Headland at the side of a drainage ditch. COORDINATES:X: 2404985.54; Y: 5065087.10. LOCATION: Fossalon di Grado.</i>	88
<i>Table 4.4. General characterization of soil profile C23: texture, particle size, pH, soil salinity, redox potential, total lime content, cation exchange capacity, nitrogen and organic carbon.</i>	89
<i>Table 4.5. Pearson correlation coefficients between Total Hg concentration and soil parameters.</i>	91
<i>Table 4.6. Concentration of total mercury along soil profile.</i>	92
<i>Table 4.7. Texture Partition of C 31 soil sample.</i>	95
<i>Table 4.8. Organic C, total N and C/N ratio of particle-size fractions before and after heating at 180 °C.</i>	95
<i>Table 4.9. Sequential extraction procedure (Lerchler, 1999) from soil C31 and its particle-size fractions.</i>	98
<i>Table 4.10. Hg⁰ concentration desorbed from Fossalon soil at 80 °C, soluble plus exchangable Hg, OM-bound Hg, residual Hg, total Hg.</i>	99
<i>Table 4.11. Hg concentration in SEP extracts.</i>	104

Table 4.12. Peak parameters of Fossalon Soil (peak height, released temperature, height of peak 2 vs height of peak 1 ratio). 124

Table 4.13. Peak parameters of Banduzzi Sediment (peak height, released temperature, height of peak 2 vs height of peak 1 ratio). 124

Table 4.14. Concentration of Hg ($\mu\text{g kg}^{-1}$) extracted with water..... 130

Table 4.15. Concentration of Hg ($\mu\text{g kg}^{-1}$) extracted with water..... 134

List of Figures

<i>Figure 1.1. Current estimates of the fluxes and pools of Hg at the Earth's surface. Hg(II) includes both gaseous and particulate forms, plus a negligible contribution (1 Mg) from inert particulate Hg. The percentages in brackets are estimated increases in pools and fluxes due to anthropogenic activities over the past 150 years. Fluxes are in Mg yr^{-1} and reservoirs are given in Gg (Driscoll et al., 2013).</i>	8
<i>Figure 1.2. Operationally-defined phases targeted in most SEP, common extractants and respective mobility (Reis et al., 2016).</i>	16
<i>Figure 1.3. Sequential extraction methods proposed by some scientists to determine the mercury species in soils and/or sediments (Issaro et al., 2009).</i>	17
<i>Figure 1.4. Hg-thermo-desorption curves of standard materials (Gosar et al., 2006).</i>	19
<i>Figure 1.5. Comparison between SEP and TD. Procedures are compared for their target species, advantages and disadvantages. General results obtained are also presented (Reis et al., 2016).</i>	22
<i>Figure 1.6. EXAFS spectra of mercury minerals and mercury sorption complexes in the model compound database used for linear least-squares fitting of the heterogeneous mercury bearing calcines. The horizontal axis represents the conversion of energy to momentum space following the normalization of the EXAFS data to a fixed point in energy space; the vertical axis is a k-cubed weighted expression of the EXAFS function, which is modeled as the sum of scattering contributions from each neighboring shell of atoms (Kim et al., 2000).</i>	25
<i>Figure 1.7. Schematic representation of Hg mobilization in soil.</i>	27
<i>Figure 1.8. pH-Eh diagram of mercury (Navarro et al., 2008).</i>	31
<i>Figure 1.9. Proposed reaction scheme controlling Hg speciation of Hg(II) sorption to goethite. (Modified from Jiskra et al., 2012).</i>	34
<i>Figure 1.10. Oxidation states of hydroquinone: A) Fully reduced compound; B) Semiquinone state; C) Fully oxidized compound.</i>	40
<i>Figure 1.11. Scheme of mercury sulphide and dissolved organic matter under different redox status (Stallings, 2013).</i>	41
<i>Figure 1.12. The role of organic amendments in regulating various processes that include immobilization, reduction, volatilization and rhizosphere modification (Park et al., 2011).</i>	45
<i>Figure 3.1. Idrijca-Soča-Isonzo rivers system, Aussa river and location of sampling sites for soils (Fossalon) and sediment (Banduzzi channel), red spots.</i>	54
<i>Figure 3.2. Idrijca- Soča-Isonzo river system and location of sampling site (red circle) of contaminated soil (Gosar and Tersic, 2012).</i>	55
<i>Figure 3.3. Aerial view of Isonzo river mouth and location of sampling site (red circle) of contaminated soil (Google maps).</i>	56

List of Figures

<i>Figure 3.4. Aussa-Corno river system, Torviscosa chlor-alkali plant outflow from Banduzzi channel and location of sampling site of chlor-alkali contaminated sediment (redrawn from Covelli et al., 2009).....</i>	<i>57</i>
<i>Figure 3.5. Cartography of studied area in Fossalon di Grado. Red spots indicate locations of sampling points for soil survey.....</i>	<i>58</i>
<i>Figure 3.6. Aerial view of the industrial area in Torviscosa (Google maps).</i>	<i>60</i>
<i>Figure 3.7. Banduzzi channel close to the chlor-alkali plant.</i>	<i>60</i>
<i>Figure 3.8. Stainless steel Van Veen grab used for sediment sampling.....</i>	<i>61</i>
<i>Figure 3.9. Sedimentation cylinder (Appiani).....</i>	<i>66</i>
<i>Figure 3.10. Scheme of the Thermo-desorption measuring apparatus (redrawn Sedlar, 2014).....</i>	<i>73</i>
<i>Figure 3.11. Picture of Thermo-desorption measuring apparatus.</i>	<i>73</i>
<i>Figure 3.12. Scheme of the experimental setting with fertilizers.</i>	<i>77</i>
<i>Figure 3.13. Scheme of the incubation experiments.</i>	<i>79</i>
<i>Figure 3.14. Picture of the incubation experiments.....</i>	<i>80</i>
<i>Figure 4.1. Concentration of total Hg in each horizon of C23 soil profile.</i>	<i>93</i>
<i>Figure 4.2. Total Hg concentration along the soil profile.</i>	<i>94</i>
<i>Figure 4.3. Hg concentration in the leachates of three steps SEP.....</i>	<i>100</i>
<i>Figure 4.4. Hg concentration in the leachates of soluble plus exchangeable fraction and organic matter bound Hg.</i>	<i>100</i>
<i>Figure 4.5. Percentage of Hg extracted in each SEP fraction.....</i>	<i>104</i>
<i>Figure 4.6. Thermo-desorption curve of Standard of HgS pure. Released temperature is plotted versus intensity/weight ratio.</i>	<i>106</i>
<i>Figure 4.7. Thermo-desorption curve of Standard of HgCl₂ pure. Released temperature is plotted versus intensity/weight ratio.....</i>	<i>106</i>
<i>Figure 4.8. Thermo-desorption curve of Standard of HgSO₄ pure. Released temperature is plotted versus intensity/weight ratio.</i>	<i>107</i>
<i>Figure 4.9. Thermo-desorption curve of Standard of HgS plus SiO₂. Released temperature is plotted versus intensity/weight ratio.....</i>	<i>107</i>
<i>Figure 4.10. Thermo-desorption curve of Standard of HgCl₂ plus SiO₂. Released temperature is plotted versus intensity/weight ratio.</i>	<i>108</i>
<i>Figure 4.11. Thermo-desorption curve of Standard of HgSO₄ plus SiO₂. Released temperature is plotted versus intensity/weight ratio.</i>	<i>108</i>
<i>Figure 4.12. Thermo-desorption curve of Standard of HgS plus Gypsum. Released temperature is plotted versus intensity/weight ratio.</i>	<i>109</i>
<i>Figure 4.13. Thermo-desorption curve of Standard of HgCl₂ plus Gypsum. Released temperature is plotted versus intensity/weight ratio.</i>	<i>109</i>
<i>Figure 4.14. Thermo-desorption curve of Standard of HgSO₄ plus Gypsum. Released temperature is plotted versus intensity/weight ratio.</i>	<i>110</i>
<i>Figure 4.15. Thermo-desorption curve of Fossalon Soil. Desorption temperature is plotted versus intensity/weight ratio.</i>	<i>111</i>
<i>Figure 4.16. Thermo-desorption curve of Banduzzi Sediment. Desorption temperature is plotted versus intensity/weight ratio.</i>	<i>112</i>

<i>Figure 4.17. Thermo-desorption curve of Fossalon Soil after EXC-Hg extracting step. Desorption temperature is plotted versus intensity/weight ratio.....</i>	<i>114</i>
<i>Figure 4.18. Thermo-desorption curve of Fossalon Soil after ERO-Hg extracting step. Desorption temperature is plotted versus intensity/weight ratio.....</i>	<i>114</i>
<i>Figure 4.19. Thermo-desorption curve of Fossalon Soil after OM-Hg extracting step. Desorption temperature is plotted versus intensity/weight ratio.....</i>	<i>115</i>
<i>Figure 4.20. Thermo-desorption curve of Fossalon Soil after AmoFe-Hg extracting step. Desorption temperature is plotted versus intensity/weight ratio.....</i>	<i>115</i>
<i>Figure 4.21. Thermo-desorption curve of Fossalon Soil after CryFe-Hg extracting step. Desorption temperature is plotted versus intensity/weight ratio.....</i>	<i>116</i>
<i>Figure 4.22. Thermo-desorption curve of Fossalon Soil after RES-Hg extracting step. Desorption temperature is plotted versus intensity/weight ratio.....</i>	<i>116</i>
<i>Figure 4.23. Thermo-desorption curve of Fossalon Soil after HgS extracting step. Desorption temperature is plotted versus intensity/weight ratio.....</i>	<i>117</i>
<i>Figure 4.24. Thermo-desorption curve of Banduzzi Sediment after EXC-Hg extracting step. Desorption temperature is plotted versus intensity/weight ratio.</i>	<i>118</i>
<i>Figure 4.25. Thermo-desorption curve of Banduzzi Sediment after ERO-Hg extracting step. Desorption temperature is plotted versus intensity/weight ratio.</i>	<i>119</i>
<i>Figure 4.26. Thermo-desorption curve of Banduzzi Sediment after OM-Hg extracting step. Desorption temperature is plotted versus intensity/weight ratio.</i>	<i>119</i>
<i>Figure 4.27. Thermo-desorption curve of Banduzzi Sediment after AmoFe-Hg extracting step. Desorption temperature is plotted versus intensity/weight ratio.</i>	<i>120</i>
<i>Figure 4.28. Thermo-desorption curve of Banduzzi Sediment after CryFe-Hg extracting step. Desorption temperature is plotted versus intensity/weight ratio.</i>	<i>120</i>
<i>Figure 4.29. Thermo-desorption curve of Banduzzi Sediment after RES-Hg extracting step. Desorption temperature is plotted versus intensity/weight ratio.</i>	<i>121</i>
<i>Figure 4.30. Thermo-desorption curve of Banduzzi Sediment after HgS extracting step. Desorption temperature is plotted versus intensity/weight ratio.....</i>	<i>121</i>
<i>Figure 4.31. Thermo-desorption curves of Fossalon soil residues left from each extracting step: soluble plus exchangeable (EXC-Hg, black line); easily reducible oxides or Mn oxides (ERO-Hg, pink line); organic matter (OM-Hg, red line); amorphous Fe oxides (AmoFe-Hg, green line); crystalline Fe oxides (CryFe-Hg, blue line); residual, non-cinnabar Hg fraction (RES-Hg, yellow line) and cinnabar Hg (HgS, brown line).</i>	<i>122</i>
<i>Figure 4.32. Thermo-desorption curves of Banduzzi sediment residues left from each extracting step: soluble plus exchangeable (EXC-Hg, black line); easily reducible oxides or Mn oxides (ERO-Hg, pink line); organic matter (OM-Hg, red line); amorphous Fe oxides (AmoFe-Hg, green line); crystalline Fe oxides (CryFe-Hg, blue line); residual, non-cinnabar Hg fraction (RES-Hg, yellow line) and cinnabar Hg (HgS, brown line).</i>	<i>123</i>
<i>Figure 4.33. Peak ratio of Fossalon Soil (hight of peak 2 vs hight of peak 1 calculate based on the curves of .desorption temperature plotted versus intensity/weight ratio).</i>	<i>125</i>

List of Figures

Figure 4.34. Peak ratio of Banduzzi Sediment (height of peak 2 vs height of peak 1 calculate based on the curves of desorption temperature plotted versus intensity/weight ratio). 125	125
Figure 4.35. Thermo-desorption curves of Fossalon soil: soil spiked with Fulvic Acids-Hg and soil spiked with Humic Acids-Hg. 127	127
Figure 4.36. Thermo-desorption curves of native soil (sampling point C13, 0-40 cm dept) and soil amended with urea added in solution and incubated in aerobic conditions for seven days. 129	129
Figure 4.37. Mercury concentrations in added liquid solution of the “Reactor” container water in control soil, soil added with KCl and Urea. Different letters corresponds to significant differences ($P < 0.05$). 131	131
Figure 4.38. Mercury concentrations in oxidizing solution of the “Trap” container in oxidizing solution in control soil, soil added with KCl and Urea. Different letters corresponds to significant differences ($P < 0.05$). 132	132
Figure 4.39. Thermo-desorption curves of Fossalon soil and soil amended with peat and incubated in aerobic conditions. 133	133
Figure 4.40. Thermo-desorption curves of Fossalon soil and soil amended with digestate and incubated in aerobic conditions. 133	133
Figure 4.41. Mercury concentrations in added liquid solution of the “Reactor” container water in control soil, soil added with Poultry manure, Compost and Humic Acids. Different letters corresponds to significant differences ($P < 0.05$). 135	135
Figure 4.42. Mercury concentrations in oxidizing solution of the “Trap” container in oxidizing solution in control soil, soil added with Poultry manure, Compost and Humic Acids. Different letters corresponds to significant differences ($P < 0.05$). 136	136
Figure 4.43. Mercury concentrations in added liquid solution of the “Reactor” container water in control soil, soil added with L-Glutathione, L-Aspartic acid, Gallic acid, Malic acid. Different letters corresponds to significant differences ($P < 0.05$). 137	137
Figure 4.44. Redox Ladder, values of Eh for the oxidation of substances used in this work. 139	139
Figure 4.45. Mercury concentrations in oxidizing solution of the “Trap” container in oxidizing solution in control soil, soil added with L-Glutathione, L-Aspartic acid, Gallic acid, Malic acid. Different letters corresponds to significant differences ($P < 0.05$). ... 141	141
Figure A.1. Regional map presenting location of Idrija mercury mine, Idrijca and Soča Rivers flow, and Gulf of Trieste (Gosar and Teršič, 2012). 176	176
Figure A.2. Mercury contamination from the Idrija mine region to the Gulf of Trieste. 177	177
Figure D.1. SEM image of a grain containing Hg. 199	199
Figure D.2. EDX spectrum for an Hg-rich particle. 199	199
Figure D.3. SEM image of a grain containing Hg. 200	200
Figure D.4. EDX spectrum for an Hg-rich particle. 200	200

SUMMARY

Mercury (Hg) is a global pollutant that affects human and ecosystem health. Alluvial soils of the Isonzo river basin are strongly contaminated by Hg transported from the Idrjia mine (SLO), the second largest Hg mine in the world. Albeit the mine ceased operation in 1995, the Isonzo river still delivers large quantities of Hg downstream into the northern Adriatic Sea. Hg pollution continues due to the erosion and solubilization of mine waste previously deposited along the Idrjca-Soča-Isonzo rivers system. Much research has been carried on water and sediments of the river itself, of the Trieste gulf, and in the Grado and Marano lagoon, but very few studies involved contaminated soils. Most of the area in the river basin is intensively cultivated with both arable and horticultural crops, albeit Hg concentration is several times larger than the critical levels.

The mobility, bioavailability and potential biomagnification of Hg from these soils depends on its chemical and physical form. Fractionation and speciation procedures are designed to evaluate Hg mobility, but they still have many limitations and drawbacks.

The overall aim of this research was to investigate the risks connected to agricultural activities on these soils which may cause Hg mobilization toward the hydrosphere and the atmosphere.

The first aim of this study was to deeply investigate the physico-chemical characteristics of these contaminated soils, especially along the soil profile, to assess the chemical species mainly represented, and the distribution of Hg chemical forms in different size-texture fractions. The second objective was to improve Hg fractionation/speciation by combining sequential extraction procedures (SEP) with thermo-desorption measurements (TD). The third aim was to investigate the potential effect of mineral fertilizers, organic amendments and root exudates on Hg mobility (solubilization and volatilization). This was combined with redox changes, since these soils are generally under the sea level, so they are subject to frequent changes in the oxic/anoxic boundary.

Total Hg concentration is variable according to distance from the river, ranges in top soil from 7.32 to 50.6 mg Hg kg⁻¹ soil. The concentration of Hg along the soil profile did not follow a regular trend: generally it decreased with depth, but sometimes very high Hg concentration were found in deeper layers. Texture fractionation showed an accumulation of Hg in the Fine Sand and particularly in the Silt size fractions, in agreement with previous studies on sediments of the Trieste gulf. A six steps SEP on size-texture fractions

Summary

showed that the Clay fraction had the highest percentage of volatile Hg, whereas the Fine Sand and Silt fractions had the highest percentage of Hg in the sulfide and residual fractions.

Hg contamination in the studied area is coherent with a long-term gradual deposition of contaminated particulate material from the Isonzo river. Indeed, a soil survey demonstrated that the soils are alluvial soils and horizons originated from sediments of the Soča-Isonzo river.

Application of different SEP procedures showed that most Hg is strongly retained in the sulfide and/or residual fractions. Elemental and organic Hg represents in these soils only a tiny part of the total.

Thermo desorption analysis is a fractionation procedure based on the different volatility of Hg compounds, but its interpretation has several problems due either to a strong matrix effect, the overlap in the behavior of different compounds and the lack of reliable reference materials. In order to improve the thermogram interpretation, TD was coupled to a seven steps SEP, performing TD on the residue of each solubilization step. A sediment contaminated by a different source of Hg, from a chlor-alkaly plant (Banduzzi channel), was also analyzed to validate the results obtained in the soil under study (Fossalon soil).

Coupling TD measurements with SEP allowed the identification of two main Hg fractions in the Fossalon soil, the first peak at 220°C defined as “matrix-bound Hg” was attributed mainly to organic-Hg, and the second larger peak at 310 °C was attributed to HgS. In the Banduzzi sediment the “matrix-bound” Hg was the highest peak, whereas the HgS peak was very small. The “matrix-bound Hg” was separated and quantified by SEP: organic Hg represented almost 70%, Hg bound to easily reducible oxides about 13.4%, Hg bound to amorphous Fe oxides about 8%, and minor percentages for other SEP fractions.

The assignment of the peak at 310 °C was confirmed by comparison with pure HgS standard, whereas the assignment of the peak at 220 °C to organic Hg, was confirmed by TD analyses of the Fossalon soil spiked with humic acids-Hg and with fulvic acids-Hg complexes.

It can be concluded that both in the Fossalon soil and in the Banduzzi sediment the “matrix-bound” Hg peak can be principally ascribed to organic matter bound Hg and to a lesser extent to Hg bound to minerals. This work also evidenced that TD cannot be a stand-alone tool for Hg speciation mainly due to the impossibility to resolve overlapped

peaks without an appropriate SEP protocol. On the contrary, SEP may allow a more specific identification of Hg compounds.

The effect of several mineral fertilizers, organic amendments and root exudates were investigated on:

- Hg thermal stability by TD,
- Hg solubility by water extraction,
- Hg solubility and volatility under aerobic and anaerobic conditions.

All tested inorganic and organic fertilizers did not affect Hg thermal stability: thermograms of control and treated soils were practically identical.

Water Hg extractability was also little affected by fertilizer addition. Only urea increased significantly the soluble fraction of Hg, from 0.60 to 1.32 $\mu\text{g Hg kg}^{-1}$. This increase is not important in practical terms also because of the limited persistence of urea in field conditions, being subject to rapid hydrolysis.

Aerobic and anaerobic soil incubations showed different results:

- Both Hg solubilization and volatilization increased in the native soil incubated under anoxic conditions with respect to oxic conditions.
- Mineral fertilizers had no significant effect on Hg solubility and volatility neither in oxic nor in anoxic conditions.
- Organic amendments enhanced Hg mobilization in aerobic conditions but not in anaerobiosis, indeed poultry manure, compost and humic acids showed an increase in both Hg solubility and volatility in aerobic conditions, whereas only poultry manure increased Hg solubilization under anaerobic conditions.
- Root exudates compounds decreased Hg solubility both in oxic and in anoxic soil incubation, with the exception of glutathione and malic acid which increased Hg solubilization. All tested root exudates increased Hg reduction/volatilization in anoxic soil incubation.

Hypothesis on the mechanisms involved in the solubilization / volatilization have been formulated but the complexity of the system made it difficult to assign their relative importance.

The overall conclusion of this work is that although the alluvial soils under investigation are highly contaminated by Hg even in the deep horizons, this Hg is practically immobile being represented mainly by HgS, and application of mineral fertilizers do not increase

Summary

the risk of Hg mobilization by solubilization or volatilization. Notwithstanding organic amendments and root exudates could increase Hg solubilization and volatilization.

1. INTRODUCTION

1.1.RELEVANCE OF MERCURY PROBLEM

Mercury (Hg) is widely considered to be among the highest priority environmental pollutants of continuing concern on the global scale.

The biogeochemistry of Hg has become one of the most important topics in environmental sciences in the last 4 decades. This is due, in part, to some characteristics of Hg:

- Its volatility and dispersion on a global scale,
- its extreme toxicity at low levels,
- its tendency to bioaccumulate within food chains,
- the possibility of aqueous mobilization.

Indeed, Hg is recognized as a global pollutant due to its ability to transverse the globe through the atmosphere and its severe neurotoxic effects, especially on fetuses and young children (Clarkson, 2002). Methyl-Hg is the Hg-compound which represents the greatest threat to humans and wildlife due to its toxic effects and the fact that it can be highly biomagnified in the food chain, most importantly in fish (Mason et al., 1994).

Hg is a persistent pollutant, despite anthropogenic inputs have been decreased in the last 30 years. It has been used for the past 2500 years due to its unique chemical and physical properties.

Therefore, there has been a growing interest worldwide about Hg and the mechanisms that govern its concentrations and transformations in air, water and soil (Grassi and Netti, 2000).

As it will be bediscussed later, the temporal and spatial scales of Hg transport in the atmosphere and its transfer to aquatic and terrestrial ecosystems depend primarily on its chemical and physical forms.

1.2.MERCURY IN THE ENVIRONMENT

As previously mentioned, Hg is a widespread surface and groundwater contaminant throughout the world. Although it is naturally occurring, anthropogenic activities such as mining, fossil fuel burning, waste disposal, agriculture and chlor-alkali industries have led to the mobilization of increased amounts of Hg into the environment. Indeed, Hg

Introduction

pollution has been reported in many places, including Quebec in Canada (Wheatley, 1979) and the Amazon in Brazil (Malm, 1998).

A remarkable characteristic of Hg is its presence as a silvery liquid at room temperature. Elemental Hg is the predominant species emitted by anthropic activities as well as released from soils and rocks to the atmosphere. The most human exposure to inorganic Hg species is due to Hg⁰ vapor, derived from industries such as Au–Ag mining and chlor-alkali plants (Navarro et al., 2008).

In addition, Hg may have other two oxidation states, Hg⁺ (mercurous) and Hg²⁺ (mercuric), but Hg⁺ is instable in nature as it transforms to Hg²⁺ and Hg⁰ (Navarro et al., 2008).

Mercuric ion is the most abundant species in nature; it is a soft Lewis acid and has a high affinity for large, highly polarized ligands, such as soft Lewis acids, (i.e. sulfides) and a rather weak affinity to Lewis bases (i.e. R-COOH). Hg has a strong tendency to build complexes with Cl⁻, OH⁻, S²⁻, S⁻-containing functional groups of organic ligands, and NH₃ because of their high abundance and stability with Hg. Hg²⁺ forms complexes of moderate stability with Br⁻, I⁻ ions, rather weak complexes with F⁻, SO₄²⁻, and NO₃⁻ (Schuster, 1991; Gabriel and Williamson, 2004).

However, the dominant form of Hg in nature is cinnabar (HgS), a sulfide that is extremely insoluble and chemically and physically stable, this explains the low mobility of this heavy metal where it appears only in association with sulfide (Han et al., 2008, Navarro et al., 2008). Indeed, the accumulation of HgS will result in highly insoluble cinnabar (red in color, trigonal structure) or meta-cinnabar (black and more insoluble, cubic structure), which further precipitates (Gabriel and Williamson, 2004). Therefore, in reducing environments, formation of HgS can be an efficient detoxification process.

However, small amounts of Methyl-Hg are also formed from HgS in aerobic sediments (Benoit et al., 1999a). Likewise, cinnabar could dissolve in the presence of organic matter by means of surface complexation (Ravichandran et al., 1998; 2004).

Moreover, Hg exhibits a great affinity for organic matter in soils, peats and sediments. The "class B" character of the chalcophil element becomes evident in the very strong affinity to S-containing functional groups which are frequently found in organic molecules. It explains the accumulation of Hg in organic-rich, upper soil horizons and the predominance of organic Hg-binding even in mineral soil horizons. Furthermore, processes as chelation, ionic exchange, inner and outer sphere complex formation,

adsorption, and coprecipitation are likely to occur. Which type of interaction predominates will mainly depend on the properties of the humic substance and the pH of the system. About one third of the total binding capacity of the soil humus is used for cation exchange processes, about two thirds of available binding sites serve for metal complexation (Schuster, 1991).

Table 1.1 shows the solubility and vapor pressure of several Hg species.

Table 1.1. Properties of some Hg species: water solubility ($\mu\text{g l}^{-1}$) (WS), vapor pressure (VP) at 25 °C (Modified from Dyrssen and Wedborg, 1991; Navarro, 2008).

SPECIES	WS	VP
Hg⁰	56	$2 \cdot 10^{-3}$
HgCl₂	$74 \cdot 10^3$	0.1
HgS	10^{-10}	ND
HgO	$51.3 \cdot 10^3$	ND
Hg₂Cl₂	$2.0 \cdot 10^3$	ND
Hg₂(SO₄)	600 103	ND

1.2.1. Sources and transformations of mercury in the environment

Hg research has a long history and much is known about its biogeochemical cycle. However, there is still need of research, due to the low concentrations and the complexity that characterize Hg cycling and its toxicity (Selin, 2009).

Hg is a natural element, present in every major compartment of our planet at low concentrations. Primary natural Hg emissions to the atmosphere, estimated at 500 Mg/year, result from aerial and sub-aerial volcanism and gradual degassing of soil systems (Selin, 2009).

Others natural sources are sea-floor hot springs and global mercuriferous belts, where, Hg is present as cinnabar ore. Indeed, Hg has been known to human societies for millennia, and early mining activities occurred in these naturally enriched regions. For example, the Hg mine at Almaden, Spain, has produced Hg since at least Roman times

Introduction

(Tarr, 1898). Hg can be released to the atmosphere in these areas through geothermal activity or by natural releases from Hg-enriched rock and soil (Gustin et al., 2008). However, the natural flux of Hg into the atmosphere from primary geological sources is small compared to direct present-day anthropogenic emissions of Hg. On the basis of measurements of the ratio from remote lake sediment cores, it is estimated that present-day Hg deposition is three to five times larger than preindustrial deposition (U.S. Environmental Protection Agency (USEPA), 1997) (Figure 1.1). This causes an increase in Hg reservoirs and subsequent secondary Hg emissions that facilitate its global distribution (Selin, 2009).

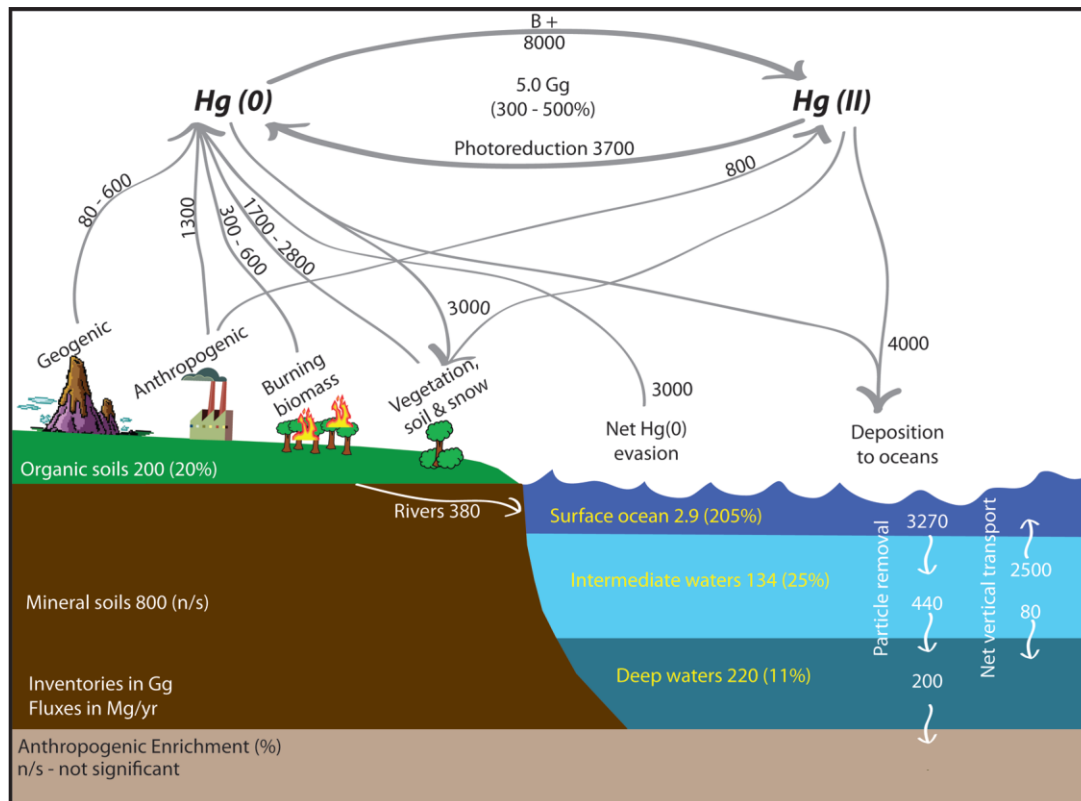


Figure 1.1. Current estimates of the fluxes and pools of Hg at the Earth's surface. Hg(II) includes both gaseous and particulate forms, plus a negligible contribution (1 Mg) from inert particulate Hg. The percentages in brackets are estimated increases in pools and fluxes due to anthropogenic activities over the past 150 years. Fluxes are in Mg yr⁻¹ and reservoirs are given in Gg (Driscoll et al., 2013).

Indeed, man-made activities have modified the natural cycling of Hg. An EPA (1997) estimate of annual Hg emission due to human activities suggested that anthropogenic sources accounted for about 50% to 75% of Hg emissions from all sources.

Prior to the 1970s, chlor-alkali plants were the dominant sources in many industrialized countries (Shroeder and Munthe, 1998). Nowadays, most Hg is released through mining and smelting, fossil fuel burning, industrial processes, and burning of municipal and medical wastes (Schierow, 2006; Selin et al., 2008; Pirrone et al., 2010; UNEP, 2013).

Hg from these sources is emitted mainly in the elemental form. In the gaseous elemental form (Hg^0), Hg is capable of moving across regional and global distances (Pirrone and Mahaffey, 2005; Pirrone and Mason, 2009; Selin, 2009). In the atmosphere, divalent forms of Hg (Hg^{2+}) partition more easily to water and particles (compared to Hg^0), resulting in much shorter distances over which Hg^{2+} travels in the lower troposphere. Thus, oxidative processes in the atmosphere strongly influence overall residence times (Lindberg et al., 2007), which can vary between several months to a year (Selin, 2009; Pirrone et al., 2010).

The ultimate fate of emitted Hg is primarily recalcitrant soil pools and deep ocean waters and sediments. Transfers of Hg emissions to largely unavailable reservoirs occur over the time scale of centuries, and are primarily mediated through atmospheric exchanges of wet/dry depositions and evasion from vegetation, soil organic matter and ocean surfaces (Driscoll et al., 2013).

There are also reemissions into atmosphere of Hg deposited onto plants, soils and other surfaces (EPA, 1997; Schroeder and Munthe, 1998). Past anthropogenic Hg emissions, deposited to soils and surface oceans have a tendency to be re-emitted back to the atmosphere. Amos et al. (2013), in a recent study, suggested that the contribution of these historical or secondary Hg emissions to modern Hg exposure is much larger than thus far appreciated.

Impacts of Hg have been assessed for three potential future anthropogenic greenhouse gasses (GHG) emission scenarios under the Intergovernmental Panel on Climate Change Special Report on Emission Scenarios (IPCC SRES). Under most GHG scenarios, primary Hg emissions will increase unless emission controls are widely implemented. The main driver for increased Hg emissions is the expansion of coal-fired electricity generation in the developing world, particularly in Asia. However, as it is discussed below, an important distinction between Hg and most other atmospheric pollutants is that environmental and health impacts are only indirectly related to total concentration (Pacyna et al., 2009; Streets et al., 2009).

1.3.MERCURY FRACTIONATION AND SPECIATION

It is known that different metal species exhibit different behavior, mobility and bioavailability in the environment, therefore measurements of total Hg in soils do not provide enough information on the potential toxicity of Hg for living organisms (Beckvar et al., 1996; Biester et al., 2002). A detailed knowledge of the chemical forms of Hg in soil is critical to evaluate the risks for humans and the environment (Navarro et al., 2008). Knowledge of the speciation of Hg is also paramount in assessing the extent and kinetics of the biologically driven conversion of Hg into Methyl-Hg. (Gerbig et al., 2011). Thus, Hg speciation is the key for risk assessment of Hg contaminated areas (Bollen et al., 2008).

Speciation is the distribution and the quantity of all different chemical forms of a substance (e.g. HgS, HgCl₂, Hg₂Cl₂, Hg⁰, Hg(OH), CH₃HgX, (CH₃)₂Hg...) in a sample, whereas fractionation means the separation of the total content in groups of substances according to different properties.

Speciation should be used only to indicate the distribution of species in a particular sample or matrix. Chemical compounds that differ in isotopic composition, conformation, oxidation or electronic state, or in the nature of their complexed or covalently bound substituents, can be regarded as distinct chemical species (Templeton et al., 2000). By this definition, terms in relation to speciation have also been determined by Templeton et al. (2000):

- *Speciation analysis is the analytical activity of identifying and/or measuring the quantities of one or more individual chemical species in a sample.*
- *The **chemical species** are specific forms of an element defined as to isotopic composition, electronic or oxidation state, and/or complex or molecular structure.*
- *The **speciation** of an element is the distribution of an element amongst defined chemical species in a system.*

In the case of Hg, it is possible to understand by speciation analysis how Hg is transported from its sources to the local environment of man and wildlife, how Hg is bound in the environment and is therefore more or less available to cause adverse effects, and how Hg is transformed and accumulated in fish and other aquatic and terrestrial foods as Methyl-Hg (Horvat, 2005).

It is sometimes impossible with speciation to determine the concentrations of the various chemical species that make up to the total concentration of an element in a given matrix, due to the possible instability of that chemical species in the sample. Species can even change

form during speciation analysis; determination of the total concentration of a particular element may therefore be impossible by such a method. A fractionation method can be used for this purpose, by which various classes of species of an element can be determined, also with the sum of their concentrations in each class (Templeton et al., 2000; Horvat, 2005).

- **Fractionation** is the process of classification of an analyte or a group of analytes from a certain sample according to physical (e.g. size, solubility) or chemical (e.g. bonding, reactivity) properties. In a case in which it is not possible to determine the concentration of the different individual chemical species that sum up the total concentration of an element in a given matrix, which means it is impossible to determine the speciation, it is a useful practice to perform **fractionation** instead.

Speciation/fractionation influences:

- Solubility: lipophilicity, hydrophilicity;
- Mobility: e.g. through leaching, volatilization, etc.;
- Bioaccessibility and bioavailability: absolute bioavailability describes the percentage of an external exposing mass that reaches the systemic circulation (the internal dose); it is the fraction actually absorbed. Bioaccessibility describes the fraction of the chemical that desorbs from its matrix (e.g. soil, dust, wood) in the gastrointestinal tract and it is available for absorption, while absorption describes the transfer of a chemical across a biological membrane into the blood circulation. By definition, Hg bioaccessibility should exceed Hg bioavailability.

In other words a chemical form is bioaccessible when it can get in contact with an organism, while it is bioavailable when it is really adsorbed by the organism (e.g. pass the cellular membrane or go through the intestinal villus to reach blood) (Davis et al., 1997; Paustenbach et al., 1997);

- Toxicity.

Han et al. (2003b) highlighted the high mobility and toxicity of alkyl species, such as Methyl-Hg and Ethyl-Hg, and the high solubility and mobility of soluble inorganic species, such as mercuric chloride (HgCl_2), in comparison with other inorganic Hg species. As observed by the same authors, alkyl and inorganic soluble Hg species contribute to the major portion of potential Hg toxicity in soil. On the other hand, chemically stable species, such as mercuric sulfide (HgS) are considerably less mobile and, therefore, less toxic (Han et al., 2003b).

1.3.1. Methods for mercury fractionation and speciation

Analytical procedures to assess Hg speciation in soils still lack consensus.

Although some steps have already been taken towards the establishment of robust and reproducible methodology, the complex chemistry of Hg, in conjunction with the intricacy of soil chemistry and the interaction of the contaminant with the soil matrix, have not yet allowed this objective to be fulfilled (Kim et al., 2000; Hesterberg et al., 2001; Gustin et al., 2002; Sladek et al., 2002).

There are three main approaches to Hg speciation in soil and sediment:

- 1) sequential chemical extractions (Issaro et al., 2009);
- 2) thermodesorption (Biester and Scholz, 1997; Reis et al., 2012);
- 3) X-ray absorption spectroscopy (mainly XAFS and EXAFS) (Kim et al., 2000; 2004; Terzano et al., 2010).

1.3.1.1. Sequential Extraction Procedures

Extraction procedures may be divided into:

1. selective extractions or single extractions,
2. sequential extractions (SEP).

The first are used to target only one fraction of interest and are currently used for estimating the most potentially mobile, bioavailable and toxic fractions, mainly organometallic fractions e.g. Methyl-Hg. Indeed many researches have focused on Methyl-Hg determination including its limitations (Bloom et al., 1997; Tseng et al., 1997; Hintelmann, 1999; Hammerschmidt and Fitzgerald, 2001; Leermakers et al., 2003). However, in contrast to sediments, this harmful Hg-species (Methyl-Hg) often represents in soils less than 1% of total Hg (Bloom et al., 1997; Bowles and Apte, 2000; Canário et al., 2004; Mailman and Bodaly, 2005; Neculita et al., 2005; Sánchez et al., 2005; Shi et al., 2005; Donkor et al., 2006).

Thus, it is in fact interesting to subdivide the other forms of Hg, especially Hg(II), into different species.

Sequential extractions are based on the chemical leaching of complex samples and have been proposed to allow the determination of the mobility of elements according to their chemical form and the various soil/sediment constituents to which they are bound. Hg mobility is defined in terms of the amount of Hg leached in the various acid and salty solutions (Issaro, 2009).

The literature vehemently stresses the need to develop speciation methods specific for Hg, as well as adequate quality control procedures and associated reference materials (Horvat, 1999; 2005). Because, the traditional sequential extractions used for the others trace metals are not fully suitable to Hg due to its complex chemistry (Wallschläger et al., 1998; Bloom et al., 2003).

Moreover, establishing easy-to-use protocols is the key to a successful risk assessment and to assess contaminant-soil interactions in contaminated areas (Bloom and Preus, 2003; Han et al., 2003b; Reis et al., 2010; Fernández-Martínez and Rucandio, 2013).

Despite several attempts to develop such methods, there is still not a consensual protocol regarding Hg fractionation and/or speciation in soil samples (Issaro et al., 2009). In fact, there are different protocols available for Hg speciation and fractionation in literature (see review of Issaro et al. (2009) and references therein).

Several different SEP have been proposed for Hg, which are very specific and depend on:

- the type of matrix (e.g. physicochemical characteristics of soil and land use);
- the Hg source (e.g. mining activity/chlor-alkali plant);
- type of Hg compounds in the samples.

Since soil is a complex and variable matrix, it is very important to choose an appropriate SEP according to its characteristics, as well as to the type of Hg compounds that are expected to be found in the samples. For example, if the objective is just to investigate the mobility of Hg in soil, a three step procedure can be applied, which subdivides Hg into mobile, semi-mobile and immobile fractions. But, if the objective is to investigate the distribution of Hg among different inorganic and organic compounds a more selective, multiple steps SEP has to be selected.

Since SEP results are influenced by substrate matrix, the application and interpretation of such extractions should be carried out with caution, and the substrate components with the environmental conditions associated have to be characterized (Reis et al., 2016).

In Figure 1.2, a summary of the most common target phases in sequential extraction schemes and respective mobility in the environment is given. While Figure 1.3 shows some examples of the most commonly used SEP procedures.

In general, sequential extraction schemes starts with the extraction of the more labile fractions: water-soluble and/or exchangeable using, respectively, distilled water and salt solutions that remove Hg by ion-exchange (e.g. NH_4Ac , MgCl_2 , CaCl_2).

Introduction

Some fractions are indicative of the Hg forms which are likely to transfer from soil to other environmental compartments (water and organisms), i.e. the more bioaccessible fractions; these fractions are usually determined by the application of mild extractants that mostly work by cation exchange, complexation and through weak acid dissolution.

Determination of the water-soluble fraction (Leermakers et al., 2003; Sladek and Sexauer, 2003) has been used to estimate the potential risk of groundwater contamination, biological uptake and toxicity for aquatic organisms when leaching, runoff, or erosion occur (Wahle and Kördel, 1997). Hg concentrations are usually low (Biester and Scholz, 1997; Renneberg and Dudas, 2001; Bloom et al., 2003; Neculita et al., 2005; Reis et al., 2014), implying that the estimation of this fraction is only worthwhile when soils are highly contaminated or the in-situ environmental conditions are favorable to leaching.

In the last steps, the less reactive species, which are strongly bound to the matrix, are extracted with strong acids, including HNO₃, HF and aqua regia. The residual fraction means the part of Hg bound to the matrix that cannot be extracted by the previous reagents.

Saturated solution of sodium sulphide (Na₂S) is used for HgS extraction to form the soluble Hg polysulphides, while most Hg-species are soluble in HNO₃ (Jing et al., 2008). The use of increasing HNO₃ concentrations as a sequential extraction to mobilize different Hg fractions prior to HgS determination in the last step was applied to sediment samples (Wallschläger et al., 1998; Palmieri et al., 2006). To optimize the dissolution of all non-HgS species, the effect of HNO₃ concentration, sample to volume ratio and the duration of extraction have been studied. For this purpose, a 2-hour extraction of 1 g of sample in 20 ml of 40% HNO₃ is recommended to separate HgS from the other Hg-forms (Hall et al., 2005). In fact, HNO₃ must be used very carefully because some oxidizing gases produced by the traces of chloride in concentrated HNO₃ may result in the dissolution of HgS (Mikac et al., 2003). According to the protocol by Fernández-Martínez et al. (2006), soil samples are firstly extracted by HNO₃ to dissolve all Hg-species other than HgS. Then, Na₂S or aqua regia was added to the remaining residue prior to HgS determination. Both reagents gave similar recoveries (85%) (Issaro et al., 2009; Reis et al., 2016).

Several works have proposed a simplified sequential extraction to separate Hg in environmental samples into “mobile”, “semi-mobile” and “non-mobile” fractions (e.g.

Biester et al., 1999; Sladek et al., 2002; Fernández-Martínez et al., 2006; Reis et al., 2010).

Fractions		Extractants	Mobility
Water-soluble	Constitutes the most mobile and potentially the most available metal and metalloid species; This fraction is usually negligible.	Sample pore solution using in situ filtration, dialysis tubes or bags; Laboratory procedure such as centrifugation, filtration or displacement	High.
Exchangeable	Includes weakly adsorbed metals retained on the solid surface by relatively weak electrostatic interaction, metals that can be released by ion-exchange processes and metals that can be coprecipitated with carbonates; Generally accounts for less than 2% of the total metals present in a sample.	Salts solutions of replaceable cations such as $MgCl_2$, NH_4OAc , $CaCl_2$, $NaNO_3$, $Mg(NO_3)_2$, $BaCl_2$, KNO_3 , $Ca(NO_3)_2$, usually at 1 M concentration.	High. Changes in major cationic composition or lowering of pH may cause a release due to ion exchange
Acid-soluble	Contains the species which are precipitated or coprecipitated with carbonate. Carbonate can be an important adsorbent when organic matter and Fe-Mn oxides are less abundant in the system. The carbonate form is a loosely bound phase and liable to change with environmental conditions. This fraction in general contains a relatively small percentage of the total concentration and is significantly modified by drying but less than the first fraction.	Generally targeted by use of a mild acid; most common is sodium acetate-acetic acid buffer at a 1 M concentration and pH 5	Medium. Changes in redox conditions may cause a release but some metals precipitate if sulfide mineral present is insoluble .
Reducible	Associated with hydrous oxides of Fe and Mn, present as coatings on mineral surfaces or as fine discrete particles. Binding can occur by any or a combination of the following mechanisms: coprecipitation; adsorption; surface complex formation; ion exchange; and penetration of the lattice. These oxides are in large proportion in soil and sediments.	1M Hydroxylamine hydrochloride in nitric, acetic or HCl acid medium	Medium.
Oxidisable	Complexation or bioaccumulation process with various forms of organic material such as living organisms, detritus or coatings on mineral particles.	The most used oxidant is H_2O_2 in acid, heated (85°C) medium. The addition of NH_4OAc prevents readsorption of the already extracted species. $NaOCl$, $Na_4P_2O_7$ both at pH 9.5, and $K_4P_2O_7$ are also used as oxidants	Low. However, with time, decomposition/oxidation of organic matter occurs.
Residue	All species that weren't extracted in previous fractions.	<i>Aqua regia</i>	Low. Only available after weathering or decomposition

free ion

soluble inorganic complexes

soluble organic complexes

Figure 1.2. Operationally-defined phases targeted in most SEP, common extractants and respective mobility (Reis et al., 2016).

Author	Reagents	Compound extracted	Percentage of total mercury extracted
Sahuquillo et al. (modified BCR-SEP)	0.11 mol L ⁻¹ CH ₃ COOH 0.5 mol L ⁻¹ NH ₂ OH/HCl (pH 1.5) 8.8 mol L ⁻¹ H ₂ O ₂ (pH 1.5)/1 mol L ⁻¹ CH ₃ COONH ₄ (pH 2) Aqua regia/HF	Exchangeable, Water soluble, and carbonates fractions bound Hg Reducible Hg Oxidizable Hg Residual	Not mentioned
Panyametheekul	Heated at 180 °C Deionized water 0.5 M MgCl ₂ 0.5 N HCl 0.02 N HNO ₃ /30%H ₂ O ₂ /Al(CH ₃ COO) ₃ Na ₂ S HgT - extracted-Hg in all fractions above	Hg ⁰ Water soluble Hg Exchangeable Hg Strongly bound Hg Organic-Hg HgS Residual	31–84 0 0.1–1.3 0.1–0.3 0.2–1.7 12–62 1.4–10
Han et al.	1 M NH ₄ OAc 0.1 M NH ₂ OH.HCl 0.01 M HNO ₃ /H ₂ O ₂ 30% 0.2 M (NH ₄) ₂ C ₂ O ₄ /0.2 M H ₂ C ₂ O ₄ 0.04 M NH ₂ OH.HCl in 25% HNO ₃ 4 M HNO ₃ Na ₂ S (saturated)	Soluble and exchangeable Hg Easily reducible oxides bound Hg Hg bound to organic matter Hg bound to amorphous iron oxides Hg bound to crystalline iron oxides Residual non-HgS HgS	0–20 20–35 10–25 <2 20–40 5–10 0–98
Lechler et al.	MgCl ₂ HCl NaOH/CH ₃ COOH Aqua regia	Exchangeable compounds Strongly bound Hg Organic Residual	<5 Ambiguous 6.5 8.1–69
Barrocas and Wasserman	NH ₄ Ac Ammonium hydroxide HNO ₃ Saturated Na ₂ S Aqua regia	Exchangeable compounds Hg bound to Humic substances Organic matter Hg bound to sulfide Residual	1 <5 >95 2 Undetectable
Burt et al.	Deionized water NaNO ₃ CH ₃ COONa/CH ₃ COOH Na ₂ OH-HCl/CH ₃ COOH HNO ₃ /H ₂ O ₂ /NH ₄ Ac HNO ₃ /HCl	Water soluble Exchangeable compounds Adsorbed/bound to carbonates Bound to Fe and Mn oxide Organic matter and sulfur Residual	Not mentioned
Wang et al.	0.1 M CaCl ₂ (pH 7) 1 M HCl + 1% CuSO ₄ 1% KOH 2 M HNO ₃ Aqua regia	Active Hg (include soluble Hg and exchangeable Hg) HCl-dissoluble Hg Organic bound Hg Hg ⁰ form Residual Hg	0.10–0.12 14.56–18.75 0.86–5.84 24.58–26.86 52.64–55.29
Boszke et al.	Chloroform/Na ₂ S ₂ O ₃ Deionized water 0.5 M HCl 0.2 M NaOH Heated at 150 °C/Aqua regia Aqua regia	Organic bound Hg Water soluble Hg Acid soluble Hg Hg associated with humic matter Hg ⁰ Residual Hg	2.3 1.0 1.5 22 17 56

Figure 1.3. Sequential extraction methods proposed by some scientists to determine the mercury species in soils and/or sediments (Issaro et al., 2009).

SEP procedures varies according to:

- time of extraction, which varies between 30 minutes and 1 hour, extraction periods should be carefully chosen in order to assess the real risk (Biester and Scholz, 1997; Renneberg and Dudas, 2001);
- shaking/stirring rate, which must be adjusted according to the particle size of the sample;
- temperature and time of heating.

In addition, by using the same sequential extraction for the same samples, divergences of more than 50% for different Hg-species and Total Hg can be found by different laboratories (Issaro, 2009).

1.3.1.1.1. SEP limitations

Sequential extraction procedures have several known limitations (Bacon and Davidson, 2008), such as:

- lack of selectivity, as they distribute Hg content into operationally defined fractions, instead of isolating specific chemical species;
- cross-contamination of samples;
- Hg losses;
- problems of re-adsorption and incomplete extraction;
- high percentage of Hg in the residual fraction.

Other problems regarding quality control and method performance evaluation are:

- lack of standardized procedures and uniformity among procedures;
- lack of certified reference materials for checking the performance both of method and the laboratory;
- lack of quality control procedures.

1.3.1.1.2. Thermal desorption

Another method of Hg fractionation is Thermo-Desorption (TD), which is widely applied in soils and sediments (Biester and Scholz, 1997; Biester et al., 2000; Higuera et al., 2003; Piani et al., 2005a; Gosar et al., 2006; Bollen et al., 2008; Rallo et al., 2010; Teršič et al., 2011a; Teršič et al., 2011b; Rumayor et al., 2013).

The basic principle of the method is the controlled heating of the sample at a known heating rate. This technique is based on the thermal decomposition, or desorption, of Hg compounds from solids at different temperatures, and the continuous determination of the released volatile Hg. Since Hg compounds have different properties, with different vapor pressures at different temperatures (Milobowski et al., 2001), the temperatures at which Hg compounds are decomposed and evaporated are therefore different (Figure 1.4). Through comparison with standards, Hg species can be identified.

Available literature suggests decomposition and sublimation temperatures for several Hg compounds (Table 1.2), which are mostly theoretically determined and do not include all the experimental conditions (Sedlar, 2014).

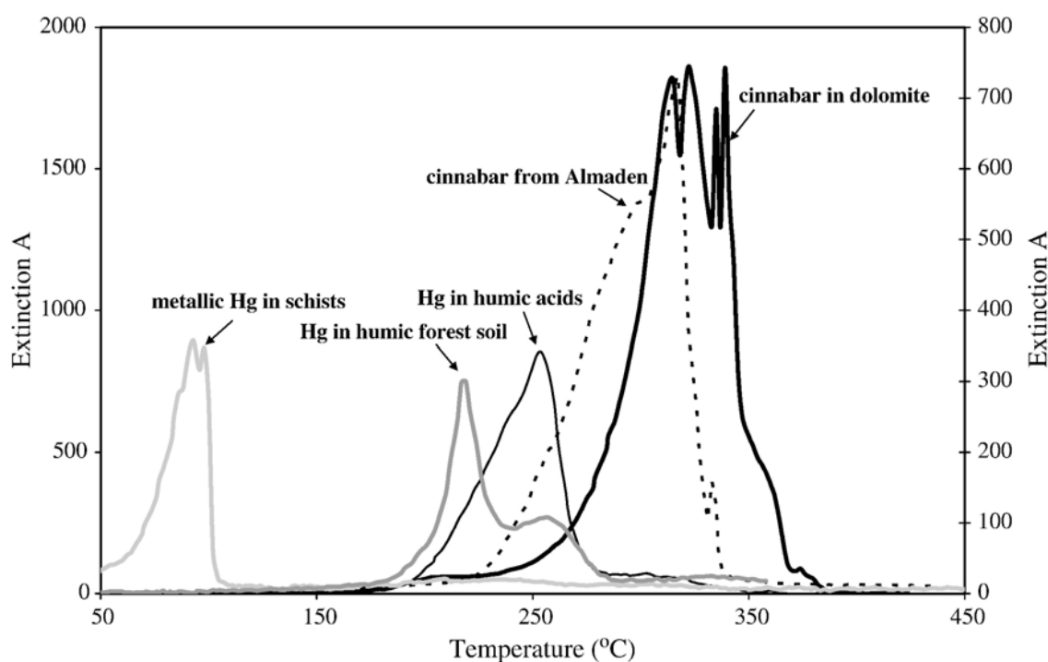


Figure 1.4. Hg-thermo-desorption curves of standard materials (Gosar et al., 2006).

Table 1.2. Accessible literature data about the temperature characteristics of Hg compounds (Sedlar, 2014).

Mercury Compound	Temperature of Decomposition or Sublimation
Mercury(I) chloride (Hg_2Cl_2)	383 °C – sublimation (Lide, 2010)
Mercury(II) chloride (HgCl_2)	277 °C – melting point, 304 °C – boiling point (Schroeder and Munthe, 1998)
Mercury(I) oxide (Hg_2O)	100 °C – decomposition (Lide, 2010)
Mercury(II) oxide (HgO)	500 °C – decomposition (Schroeder and Munthe, 1998)
Mercury(II) sulphide-Red (HgS)	344 °C – transforms to black HgS (Lide, 2010), 584 °C – sublimation (Schroeder and Munthe, 1998)
Mercury(II) selenide (HgSe)	Sublimation (Lide, 2010)
Mercury(I) sulphate (Hg_2SO_4)	335 – 500 °C – decomposition (Tariq and Hill, 1981)
Mercury(II) sulphate (HgSO_4)	450 °C decomposition (Lide, 2010), 500 °C decomposition (Tariq and Hill, 1981)
Mercury(I) fluoride (Hg_2F_2)	570 °C - decomposition/ sublimation (Lide, 2010)
Mercury(II) fluoride (HgF_2)	645 °C – decomposition (Lide, 2010)

With increasing temperature, Hg species are released in the following order: elemental Hg (Hg^0), HgCl_2 , Hg associated with Fe_2O_3 , organically bound Hg, HgS , HgO , with an overlap of organic Hg and Hg associated with oxy(hydr)oxides, called “matrix-bound”

Introduction

Hg (Figure 1.4). In fact, according to present knowledge, matrix components are known to exist as organo-mineral complexes (Biester et al., 1999; 2000). This means that Hg can either be chemically bound to functional groups of organic matter or physically adsorbed to mineral surfaces, but it is difficult to distinguish the species. In fact, both processes can happen, as Hg^{2+} -organic complexes may be specifically adsorbed onto the mineral surfaces of the matrix, forming organo-mineral Hg complexes (Schuster, 1991).

Previous studies have shown that Hg pyrolysis combined with atomic absorption spectroscopy allowed to distinguish cinnabar from “matrix-bound” Hg (Biester and Scholz, 1997).

Indeed, in the work of Reis et al. (2012), Hg bound to humic acids extracted from soil has a release peak between 100 and 240 °C that overlapped HgCl_2 .

Hg associated with iron oxides is mainly released between 100 and 285 °C, while a second, much smaller peak can be observed at 500–610 °C. This overlaps with HgCl_2 . Therefore, characterization of the sample and consideration of its origin may help to infer the species that are most likely present.

The interpretation of results may be done taking into account:

- soil characteristics,
- the percentage of iron oxides,
- the percentage of organic matter,
- the source of contamination.

Recently, Reis et al. (2015b) improved Hg TD curves interpretation by accurate soil characterization, however peaks overlapping remains an unresolved question.

Two methodologies have been proposed to perform TD speciation. The extensive work by Biester et al. (Biester and Nehrke, 1997; Biester and Scholz, 1997; Biester et al., 1999; Biester et al., 2000; Biester and Schöler, 2002) was carried out with an atomic absorption spectrometer, by means of an in-house built apparatus consisting of an electronically controlled heating unit and a Hg detection unit (Biester et al., 2000). An alternative method for Hg speciation by thermodesorption consists in the use of direct Hg analysers, such as the LECO[®] AMA-254 (Reis et al., 2012; 2015b) or Lumex[®] RA-915 + PYRO-915 (Rumayor et al., 2013; 2015) by simply adjusting combustion temperature and the heating programme.

Several models have already been made for temperature fractionation and speciation of Hg compounds. Different approaches were taken into account to get the temperatures at

which Hg compounds decompose. The results may vary due to differences in methods (Table 1.3).

Table 1.3. Review of existing methods for temperature fractionation of Hg (Sedlar, 2014).

Sample	Temperature programme	Carrier gas	Detection	Calibration	Reference
Soil samples	Linear heating: Room T-800 °C; Heating rate of 0.5 °C s ⁻¹	Nitrogen; 300 mL min ⁻¹	Perkin Elmer AAS, 3030 (AAS)	Hg standards: HgS and HgCl ₂ in SiO ₂ and Hg-bearing humic acids	Biester and Scholz, 1997
Coal samples	Linear heating: Room T-300 °C, Room T-400 °C, 200-600 °C; Heating rate of 1 °C min ⁻¹	Nitrogen; 100 mL min ⁻¹	Nippon Jarrell Ash AA855 (AAS), with a Hg reduction system AMD-D2	Comparison with results of Lide (Lide, 2010)	Iwashita et al., 2003
Soil samples	Linear heating: Room T-800 °C; Heating rate of 0.5 °C s ⁻¹	Nitrogen; 300 mL min ⁻¹	Perkin Elmer AAS, 3030 (AAS)	Comparison with results of others (Biester, 1994; Biester and Nehrke, 1997)	Bollen et al., 2008
Plankton and lake sediments	Linear heating: Room T-700 °C; Heating rate of 0.5-4 °C s ⁻¹	Air; 1-3 L min ⁻¹	Lumex RA-915+ with pyrolytic cell (AAS), and Perkin Elmer (AAS), 3030B with Hg-hydride attachment MHS-20	Hg standards: CH ₃ HgCl, HgO, HgSO ₄ and HgCl ₂ in Al ₂ O ₃ or SiO ₂ substrate. Reference materials: Soil, river sediments and dogfish liver and muscle.	Shuvaeva et al., 2008
Calibration only	Linear heating: Room T-650 °C; Heating rate of 10 °C min ⁻¹	Argon; 250 mL min ⁻¹	PS Analytical Thermogram model 50.042, (AFS) coupled to Sir Galahad Hg Analyser model 10.525	Hg standards: HgCl ₂ , HgS, HgSO ₄ , HgO, Hg ₂ Cl ₂ , Hg ₂ SO ₄ and HgBr ₂ in SiO ₂ substrate	Lopez-Anton et al., 2010
Gypsum samples from FGD	Linear heating: 40-650 °C; Heating rate of 10 °C min ⁻¹ and 20 °C min ⁻¹ with 3 isothermal intervals of 7-10 min	Argon; 250 mL min ⁻¹	PS Analytical Sir Galahad Hg Analyser model 10.525, (AFS)	Comparison with results of Lopez-Anton et al. (Lopez-Anton et al., 2010)	Rallo et al., 2010

Introduction

Thermo-desorption methods present some advantages over conventional chemical extraction methods and x-ray absorption methods, such as:

- applicable to a vast range of Hg concentrations;
- little to no sample treatment preventing the loss of volatile Hg-compounds;
- free of cross-contamination;
- a small quantity (<1 g) of sample is required;
- operational conditions are standardized and results obtained by different laboratories can be compared;
- good repeatability;
- the equipment is automated and commercially available;
- easy to use by the non-expert analyst;
- negligible losses of Hg;
- lack of residues (Reis et al., 2012).

1.3.1.3. Comparison between SEP and TD

In Figure 1.5 SEP and TD method are compared according to groups of Hg compounds targeted, including advantages and disadvantages.

	Sequential extraction	Water-soluble fraction	Exchangeable fraction	Acid-soluble fraction	Thermo-desorption
Target	•Provides information on Hg mobility (bioavailability).	•Extracts free Hg ²⁺ and Hg ²⁺ complexed with dissolved OM. •Most mobile and bioaccessible fraction.	•Extracts weakly adsorbed Hg retained on the solid surface by weak electrostatic interaction, by ion-exchange processes. •Extremely mobile and bioaccessible fraction.	•Extracts acid-soluble species, such as water-soluble, exchangeable, and carbonate associated.	•Hg species and not fractions. •Hg species: Hg ⁰ , HgCl ₂ , Hg associated with Fe, Hg bound to humic acids, HgS.
Advantages and disadvantages of the method.	✓ Fewer steps than other SEP. ✗ Hg easily lost. ✗ Time-consuming.	✓ Water is a cheap extractant. ✗ Concentration is very low and only quantifiable with extremely sensitive analytical techniques.	✓ Only one extraction step and one reagent required. ✓ Cost-effective ✓ Requires less technical skill. ✗ Hg extracted varies with extractant used.	✓ Only one extraction step and one reagent required. ✓ Cost-effective ✓ Requires less technical skill. ✗ Doesn't provide geochemical information.	✓ No extraction involved. ✓ Cost-effective. ✓ Requires low technical skill. ✗ Requires a mercury analyser. ✗ Peak overlap
General results in tested samples.	Hg mostly in semi-mobile fraction. Higher Hg mobility in anthropogenically-contaminated soils. Hg mobility enabled by Al and Mn and inhibited by organic matter and sulfur.	Equilibrium was reached at 24h. Hg removal in two stages (faster t<6h; slower t>6h). Two first-order reaction model fit data. Low % of water-soluble Hg (<2%)	Hg removal in two stages (faster t<10h; slower t>10h). Two first-order reaction and diffusion models fit data. Percentage removed <10 %.	Hg removal in two stages (faster t<10h; slower t>10h). Two first-order reaction and diffusion models fit data. Percentage removed up to 30%	Hg ⁰ and HgS are easily identifiable. Hg species associated with matrix components can sometimes be harder to clearly identify.
Chemical extractions are influenced by: Sample texture (% sand and % clay); Method of separation of the extracted solution from the residue. Results vary with the quantification method chosen.					

Figure 1.5. Comparison between SEP and TD. Procedures are compared for their target species, advantages and disadvantages. General results obtained are also presented (Reis et al., 2016).

Despite the recognized problems associated with chemical extraction procedures, they provide valuable information for Hg geochemistry interpretation in soils, allowing information to be inferred on reactivity and bioaccessibility, or response to changes in environmental conditions such as rainfall events or pH changes.

When TD analysis are performed, it is still quite impossible to completely separate all Hg species. This indicates that thermo-desorption cannot be considered a stand-alone tool in Hg speciation analysis. However, this method is a useful tool for a preliminary screening of the samples, with its results being helpful to decide on further sample analysis, including the application of extraction methods. It is also the best technique to identify and quantify Hg^0 , since it prevents Hg losses and does not require any sample preparation (Reis et al., 2016).

In light of this, the identification of Hg compounds and substances to which Hg is bound, may require the use of multiple methodologies (Issaro et al., 2009).

1.3.1.4. X-ray absorption spectroscopy

X-ray absorption spectroscopic techniques comprise a great variety of spectroscopies for solid phase speciation, allowing to investigate the structure of matter at the atomic scale. Direct measurement of Hg species by synchrotron X-ray is possible but, in most of the cases, requires total Hg concentration above 100 mg kg^{-1} , restricting its applicability to heavily contaminated sites. However, this technique has the benefit of being non-destructive, element-specific, relatively sensitive at low concentrations, and requiring minimal sample preparation. The microanalytical techniques allowed more precisely speciation even at relatively low Hg concentration (Santoro, 2009), but only small Hg-rich spots can be targeted and identified. μXRF , μXANES , μXRD are very useful when the contamination is homogeneous, otherwise the results could not be representative of the bulk of the contamination.

Thus, the use of this technique, in conjunction with standard analytical techniques such as X-ray diffraction and electron probe microanalysis, is beneficial in the prioritization and remediation of Hg-contaminated sites. Currently, there is no other known technique available to determine directly the types and relative proportions of Hg phases in such samples. Other methods, such as sequential chemical extractions and thermal desorption indirectly determine the speciation of Hg. Whereas X-ray absorption spectroscopy (XAS) may allow the identification of the atoms which Hg is bound to, as well as coordination number, bond distances and oxidation state; allowing more precise identification of

Introduction

chemical and mineralogical properties of the contaminant. It is possible to define the chemical speciation of the element at the molecular level and can be used to distinguish one chemical species from another, assuming there are sufficient differences in the spectra. XAS can help to define the crystalline structure of minerals, as well as chemical composition, chemical speciation and surface and interface characteristics.

X-ray Absorption Spectroscopy involves bombarding a sample with high energy X-rays, generating photoelectrons from a specific element in the sample when the incident beam possesses sufficient energy to excite or eject core electrons from that element. The generation of photoelectrons induces specific electronic scattering interactions between the central absorbing atom and neighboring atoms. The incident X-ray energy at that point corresponds to the absorption edge of the element for a given electron shell (K, LIII, etc.), while the electron scattering interactions give rise to the X-ray absorption near-edge structure (XANES) and the extended X-ray absorption fine structure (EXAFS) regions.

A composite EXAFS spectrum can be deconvoluted, using a linear least-squares fitting routine, into the sum of its separate components by comparison with the spectra in the model compound database. In Figure 1.6 it is shown an example of a model compounds database. Determining the relative proportion of each model spectrum's contribution to the spectrum of a sample may allow the quantification of the various phases present within the sample (Kim et al., 2000).

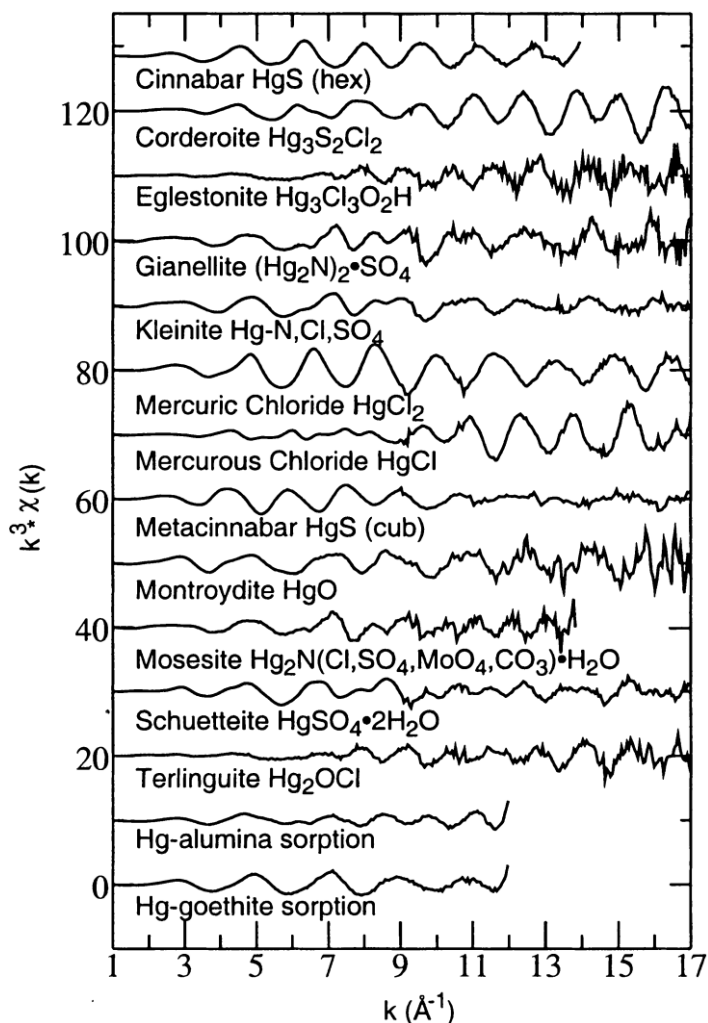


Figure 1.6. EXAFS spectra of mercury minerals and mercury sorption complexes in the model compound database used for linear least-squares fitting of the heterogeneous mercury bearing calcines. The horizontal axis represents the conversion of energy to momentum space following the normalization of the EXAFS data to a fixed point in energy space; the vertical axis is a k -cubed weighted expression of the EXAFS function, which is modeled as the sum of scattering contributions from each neighboring shell of atoms (Kim et al., 2000).

1.3.1.5. Importance of sample handling

In analytical procedures is always important to take care about sample handling storage and processing. It is important to consider soil heterogeneity, sample pretreatment and storage (Claff et al., 2010). Samples collected should be as representative as possible of the contaminated site and every precaution should be taken to ensure samples to remain unaltered. In Hg speciation assessments, particular attention must be given to potential losses of Hg. It is common practice that, for comparison among samples, or with other studies and with certified reference materials, dried (hence stable) samples are used. However, it has been observed that, while drying and sieving soils prior to analysis to

Introduction

increase sample homogeneity, Hg^0 loss can happen, with this species no longer present in samples after a short 10-day storage period (Reis et al., 2015b).

Indeed, Reis et al. (2015b) proved that, during a 10-day period, almost 32% of total Hg was lost, which mainly corresponds to the loss of Hg^0 (Table 1.4). Longer storage periods can result in a complete loss of volatile Hg^0 .

This problem may affect not only Hg speciation, but also total Hg determination in soils. Very often, it is not possible to analyze the samples immediately after sampling and these results show that Hg concentration can be underestimated due to Hg losses during sample storage.

Table 1.4. Evolution of total Hg and Hg^0 concentrations (mean \pm standard deviation; $n = 4$) with pretreatment and 10-day storage period (Reis et al., 2016).

	Total Hg (mg kg^{-1})	Hg^0 (mg kg^{-1})
Day 1	34.2 ± 2.8	9.5 ± 4.9
Day 2	32.6 ± 1.5	6.8 ± 1.3
Day 5	33.1 ± 1.5	8.9 ± 2.0
Day 10	23.4 ± 0.6	0.05 ± 0.01

1.4.THE ROLE OF SOIL ON MERCURY FRACTIONATION AND BEHAVIOUR

Soils play an important role in the biochemical cycle of Hg acting both as a sink and a source of this metal to biosphere, atmosphere and hydrosphere (Reis et al., 2010) (Figure 1.7).

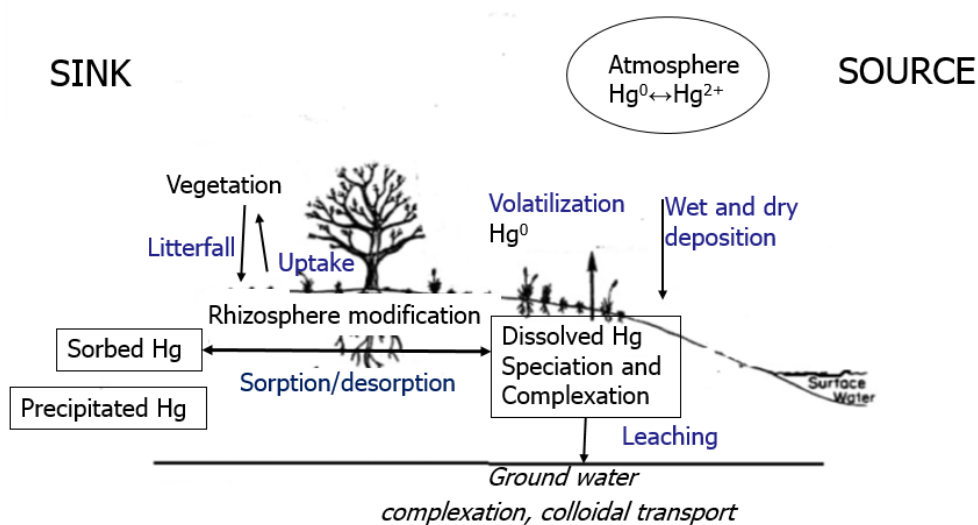


Figure 1.7. Schematic representation of Hg mobilization in soil.

Soils worldwide contain a total pool of 1.15×10^6 tons of Hg and represent the most important terrestrial sink for atmospherically deposited Hg from natural and anthropogenic sources (Selin, 2009). Indeed soil has a large capacity to sequester Hg (Welp and Brümmner, 1997).

Hg close association with soil is because of its complexation to organic and inorganic particles (Gabriel and Williamson, 2003). In fact, the largest Hg pool in soils is bound to organic and mineral soil phases, where it is immobilized (Selin, 2009). In organic topsoils, Hg is mainly bound to reduced organic sulfur groups whereas in soils and sediments with low organic matter contents, mineral phases such as iron and other metal (oxyhydr)oxides and clay minerals play an important role as sorbents (Gabriel and Williamson, 2003; Skyllberg, 2010; Jiskra et al., 2012).

Therefore, studying the behavior of Hg with these particles within soil and runoff water is crucial to understand the fate of Hg in terrestrial watersheds (Gabriel and Williamson, 2003).

Hg may occur in the soil in various forms. These are:

- dissolved (free ion or soluble complex),
- nonspecifically adsorbed (binding mainly due to electrostatic forces),
- specifically adsorbed (strong binding due to covalent or coordinative forces),
- chelated (bound to organic substances),
- precipitated (as sulfide, carbonate, hydroxide, phosphate, etc.).

Introduction

Since it is strongly bound to soil constituents, normally only trace concentrations of Hg are found in the soil solution (Schuster, 1991).

Meanwhile soil may serve as a long-term source of Hg. Hg from soils can be:

- exported to aquatic environments,
- re-emitted as Hg⁰ to the atmosphere,
- methylated under anoxic conditions (Skylberg et al., 2009; Jiskra et al., 2012).

As with other heavy metals, the mobilization of Hg in an aqueous phase can be influenced by many processes related to the aqueous phase (pore water, groundwater, etc.) and processes related to interaction with associated solid media (soil, saturated porous media of aquifers, sediments, etc.).

The main processes related to the aqueous phase are:

1. precipitation and dissolution of solids,
2. complex formation,
3. redox reactions.

The main processes related to porous media are:

1. sorption reactions,
2. phenomena associated with mobile colloidal particles (Navarro et al., 2008).

Terrestrial soils are possibly the most significant contributor of Hg to surface water (Johansson et al., 1991). It has been hypothesized that up to 60% of the atmospherically deposited Hg that reaches lakes originates from the associated terrestrial watershed (Welp and Brümmer, 1997).

In addition, due to the relatively shallow depth at which Hg concentrates in the soil column (Andersson, 1979) surface water contamination can possibly be enhanced during and after intense rainfall events due to soil erosion (Welp and Brümmer, 1997).

Moreover, organic matter and metal (oxyhydr)oxides form colloidal particles and can thus act as carriers of sorbed Hg by colloidal transport (Jiskra et al., 2012).

Thus, Hg-enriched soils are a potential source of soluble and particulate Hg species, which may be transported from contaminated areas as Hg⁰ vapor (Navarro et al., 2000; Gustin et al., 2002), as ionic soluble phases or as colloid particles (Shaw et al., 2001; Lowry et al., 2004; Navarro et al., 2008).

It is well known that the biohazard of Hg in soil is attributed not only to the total concentration of the metal but also to its different chemical species. In fact, the toxicity and phyto-accumulation of Hg for plants mainly rely on the specific species of Hg in soil

and their bioactivity. Especially from experiments with higher plants it is known that the soluble part of chemicals is responsible for its uptake and toxic power (Stalder and Wilfried, 1980; Hardiman et al., 1984). It is, therefore, important to determine the distribution and the mobility of Hg species for the assessment of their bioavailability and toxicity for plants in soil.

Not only speciation is important in soil, furthermore, it is of paramount importance to understand the relationships between Hg species and soil properties in order to assess the dynamics of Hg within the soil system. This is because the hazard potential of chemicals is highly influenced by the factor “soil” (Welp and Brummer, 1997).

In fact, the solubility and sorption of chemicals, depend on soil characteristics such as pH, redox conditions, and content of humus, Fe oxides, and clay (Brümmer and Herms, 1983; Buchter et al., 1989). Also, correlations between the microbial toxicity of heavy metals and the cation exchange capacity of soils (Bååth, 1989) and the clay content of soils can be attributed to these causes (Welp and Brummer, 1997).

So far, the interactions between the sorption of Hg in soils and his solubility, availability, and effects on microorganisms have not been investigated systematically (Welp and Brummer, 1997).

1.4.1. Factors affecting mercury fractionation in soil

There are many factors which affect Hg’s speciation in soil.

The Hg fractionation in soils can be affected by organic matter, clay minerals and metal oxides content, as well as by pH (Sánchez et al., 2005). The complexes formed by divalent Hg with soluble organic matter, chlorides and hydroxides may contribute to its mobility (Sánchez et al., 2005; Millán et al., 2006). Organic matter presence in soils can also lead to the formation of Hg complexes and inhibit Hg biomethylation processes (Bloom and Preus, 2003). The pH affects the speciation of Hg in the soil solution and influences the mobility and availability of Hg in soil (Miretzky et al., 2005; Jing et al., 2007), desorption of inorganic divalent Hg species from soil components increases with decreasing pH since, in general, trace element cations become more soluble and therefore more mobile as pH decreases (Chopin and Alloway, 2007). The presence of sulfur is very important in the chemistry of Hg, as in the presence of sulfides Hg quickly reacts with them, forming the insoluble HgS (Boszke et al., 2003). Because HgS is not very reactive or mobile; it is therefore less available for methylation and potentially less harmful to the environment.

The implications for natural soils will be that under acidic conditions prevailing for example in podzolic soils, organic matter can be expected to dominate the sorption of Hg. In neutral soil types iron oxides and clay minerals may be dominating. In soil horizons low in organic matter, the mobility of Hg will increase with decreasing pH, thus making translocations within the profile or out it increasingly probable (Reis et al., 2010).

1.4.1.1. Influence of dissolved anions in soil solution

Hg concentrations are generally low in Italian groundwaters (Brondi et al., 1986), well below the admissible limit for drinkable waters (1 mg l^{-1} ; EEC Regulation no. 80/788, converted to Italian law DPR 236) (Giammanco et al., 1998; Grassi and Netti, 2000).

Although Hg concentration in drinkable water rarely exceed admissible limits, the presence and reactivity of this element in aquatic environment, soil solution and aquifers is important to understand Hg mobilization.

As with other heavy metals, the mobilization of Hg in an aqueous phase can be influenced by different processes in:

1. the aqueous phase (surface water, pore water, groundwater, etc.),
2. the solid media (soil, saturated porous media of aquifers, sediments, etc.).

Among the processes related to the aqueous phase there is complex formation. This association may alter their adsorptive behavior, since complexation can modify the characteristics of the metal ion such as solubility, charge, size and stereochemical configuration (Elliott and Huang, 1979).

Generally, ligands with a strong affinity to Hg (OH_2 , Cl_2 and organic anions) that form highly soluble complexes are able to increase the solubility of Hg-compounds and effectively leach Hg from soils (Schuster, 1991).

The formation of Hg(II)-complexes which are of importance in natural systems was discussed by Gilmour (1971). His calculations reveal that the values of the stability constants are highest for Cl^- , OH^- , NH_3 , and several orders of magnitude lower for F^- , SO_4^{2-} and NO_3^- . The latter ligands may be excluded from further considerations because they would only be significant under unnaturally high concentrations.

However, Cl^- and OH^- are of sufficiently high concentrations and large stability constants to dominate most natural systems. Hahne and Kroontje (1972) calculated the relative abundance of Hg species dependent on the concentration of chloride and hydroxyl ions (pH). Hg(II) was calculated to hydrolyze in the pH range of 2 to 6, with the final species being the soluble $\text{Hg}(\text{OH})_2$ at about pH 6. Precipitation of $\text{Hg}(\text{OH})_2$ occurs only if the

concentration of Hg(II) exceeds $107 \mu\text{g g}^{-1}$ the intrinsic solubility of $\text{Hg}(\text{OH})_2$ being $5.37 \cdot 10^{-4} \text{ M}$. Thus, at normal pH conditions in soils, the distribution of Hg(II) will be dependent on the solubility of $\text{Hg}(\text{OH})_2$ (Schuster, 1991) (Figure 1.8). Under normal groundwater conditions, the most stable state is the one that corresponds to Hg^0 (Navarro et al., 2008). Indeed, elemental Hg released by mining operations may be stable in near-surface environments such as surface soils or groundwater and may persist largely in the elemental form (Lechler, 1999).

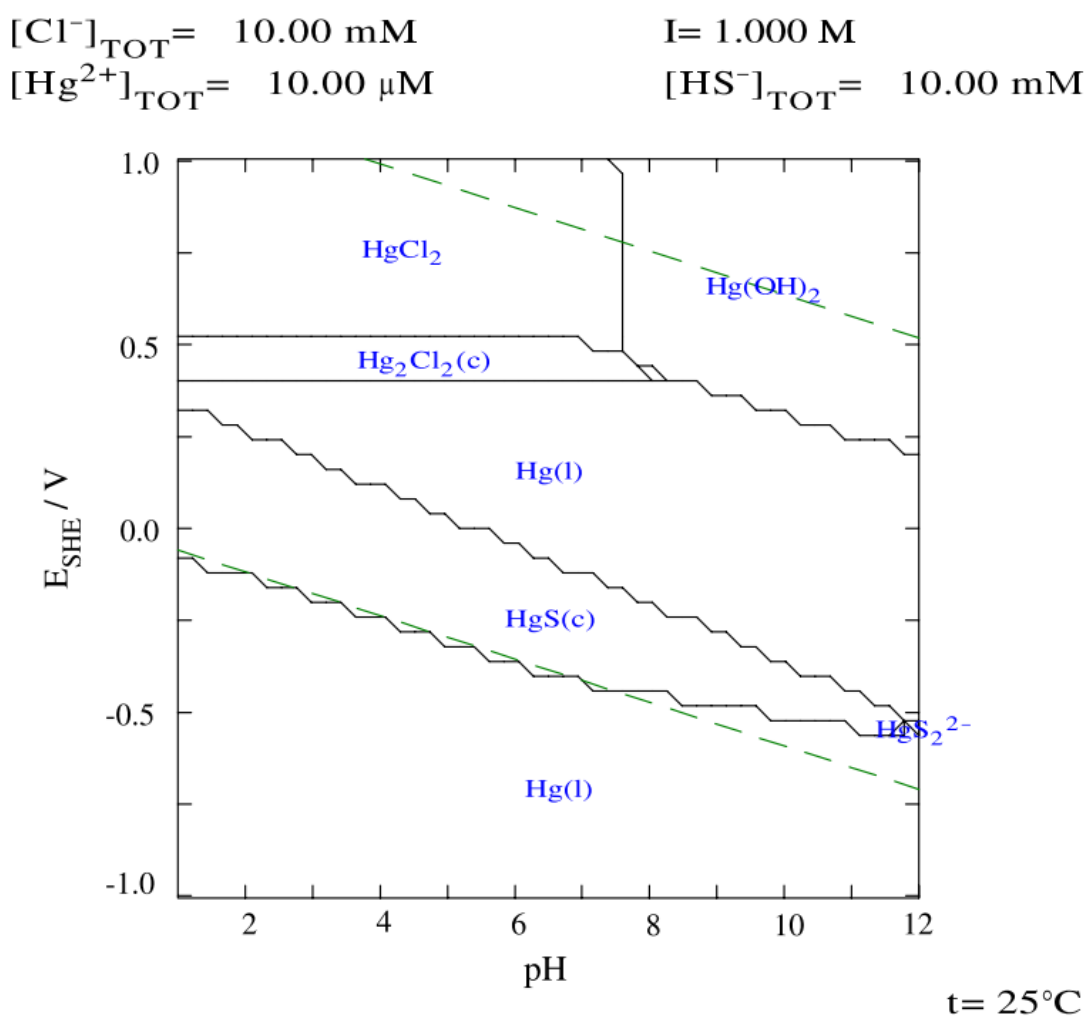


Figure 1.8. pH-Eh diagram of mercury (Navarro et al., 2008).

Under aerobic conditions, the dominant inorganic Hg species (Figure 1.8) are HgCl_2 at low pH, HgClOH at neutral pH, and $\text{Hg}(\text{OH})_2$ at high pH. Some Hg^{2+} might be bound to

Introduction

sulfides (S^{2-} and HS^-), with HgS^0 as the dominant complex at neutral pH (Davis et al., 1997; Benoit et al., 1999a).

Next to chloride and hydroxide ligands, sulfide and dissolved organic carbon are the two next major ligands that commonly complex with Hg in terrestrial and aquatic environments. Compounds such as HgS_2^{-2} , $Hg(SH)_2$, $HgSH^+$, $HgOHSH$, and $HgClSH$ are mainly found in wetland, subsurface, or lake sediment environments (Gabriel and Williamson, 2004).

The competition between Cl^- , dissolved organic carbon, and S^{2-} is mainly dictated by the concentration of each and the surrounding pH (Gabriel and Williamson, 2004).

In batch and column experiments, McLeod (1996) demonstrated that some fertilizers and NaCl solutions can remove most part of the Hg sorbed to the sediments.

Regardless of the species present in solution, crucial for the prediction of metal speciation in aquatic environments is that properly determined stability constants exist and are correctly used (Skylberg, 2008).

The use of equilibrium speciation to predict Hg bioavailability relies on these assumptions:

1. Input parameters for the model (i.e. the stability constants) are accurate; solubility products K_{s0} for minerals such as metacinnabar and cinnabar vary by orders of magnitude in the NIST database for critically selected stability constants (Smith and Martell, 1993).
2. Clear distinction can be made between fully dissolved and particulate Hg(II) concentrations in the model system (e.g. species that pass through a filter of 0.2 or 0.45 μm) (Hsu-Kim et al., 2013).
3. The partitioning of Hg between various chemical species can be represented by equilibrium chemistry.

The problem today is that there are several controversial stability constants in literature, and sometimes an inconsequent use of these. This may result in misconceptions and misinterpretations about the behavior of Hg and Methyl-Hg in soils, sediments and waters.

As an example, stability constants used for Hg-natural organic matter complexes are often unrealistically small, which lead to incorrect conclusions about the competitiveness of thiols for Hg as compared to inorganic bisulfides (Deonaraine and Hsu-Kim, 2009; Hsu-Kim et al., 2013).

Moreover, the current understanding of Hg complexation in the presence of sulfide in natural waters relies on laboratory studies and thermodynamic models that have not been validated under natural conditions (Paquette and Helz, 1997; Benoit et al., 1999a; Merritt and Amirbahman, 2007; Miller et al., 2007; Skyllberg, 2008; Drott et al., 2013).

These problems hinder the possibility of predict Hg speciation and bioavailability using equilibrium speciation models (Hsu-Kim et al., 2013).

1.4.1.2. Mineral and organic surfaces

The nature of sorption/desorption reactions taking place strongly influences Hg toxicity in surface waters (Gabriel and Williamson, 2004). Meanwhile, Hg absorbed on the soil surfaces by weak electrostatic interactive forces, is also considered to be readily available for plants because Hg in this fraction can be released through ion-exchange processes (Han et al., 2008).

It can be distinguished two types of interaction (Figure 1.9), the first is the “outer sphere” complex, it is less stable and have a faster kinetic, because it is an electrostatic bound, which occur between the charged surfaces and a charged specie of Hg, in between there is also a molecule of water. In other words, Hg exchanges another ion which is in the strato.

A more effective way to immobilize Hg regards the “inner sphere” complex in this case Hg forms a covalent or ionic bound directly with a functional group own, e.g. to clay mineral such as -COOH, where it can exchange the atom of hydrogen. This reactive capacity is pH dependent.

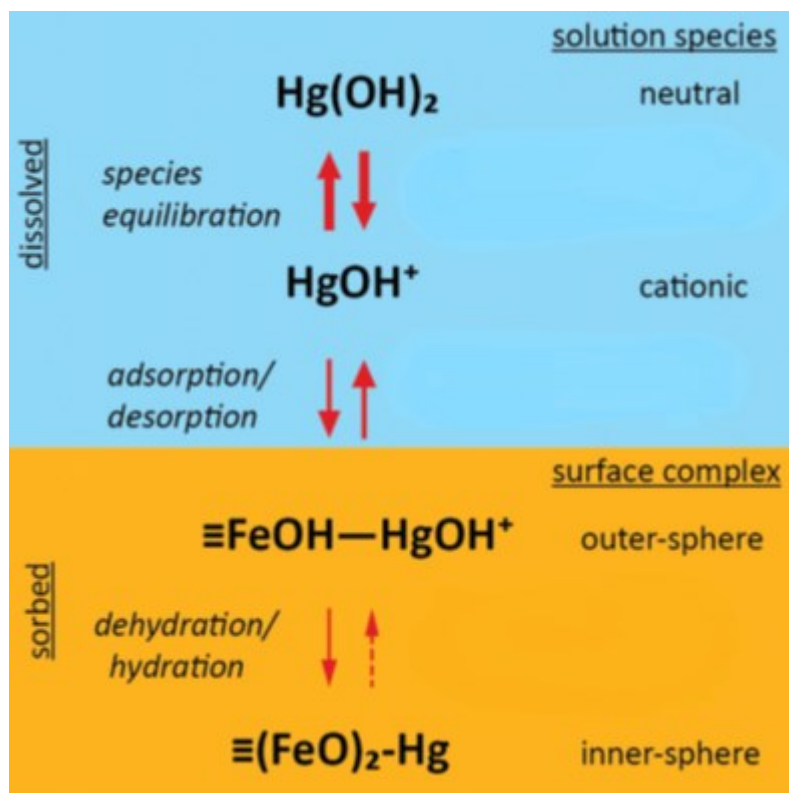


Figure 1.9. Proposed reaction scheme controlling Hg speciation of Hg(II) sorption to goethite. (Modified from Jiskra et al., 2012).

The type of complex (i.e. inner or outer sphere complex) that takes place between Hg and the adsorbent will depend upon three factors: ionic size, valence, and electronegativity. Therefore, depending upon what Hg is adsorbing to, this can ultimately determine Hg's potential availability in solution (Gabriel and Williamson, 2004). Considering that the dominant Hg species in soils are uncharged species, the mechanism of sorption on the solid phase is not ion exchange but rather long-range electrostatic forces (Schuster, 1991). In terrestrial environments there are two major types of Hg sorbents: mineral and organic surfaces. The vast majority of Hg in soil and watershed runoff are associated with each of these two materials.

Overall, it was found that the most efficient sorbent over all pH ranges was the organic matter. The retention of HgCl_2 by organic soil began to decrease starting at pH of 4 and continued to drop as pH dropped. The second most efficient sorbents over all pH ranges were illite clay and $\text{Fe}_2\text{O}_3\text{-nH}_2\text{O}$ based soil. These two soil types started to lose their adsorption capacity between a pH of 5.8 and 6.8 and went down further as pH dropped. The least effective sorbents over all pH ranges were bentonite and kaolinite clay soils.

Kaolinite adsorbed relatively very little Hg, and bentonite began to lose adsorption capacity as pH dropped below 7.

As it has already been mentioned, in acidic soils organic material is the most efficient Hg sorbent, and in neutral to alkaline soil, mineral components are the more effective sorbents (Lockwood and Chen, 1973; Reimers and Krenkel, 1974; Schuster, 1991; Jackson, 1998; Gabriel and Williamson, 2004). The two major sorbents could then be further divided into particulate ($>0.4 \mu\text{m}$) and colloidal ($<0.4 \mu\text{m}$ and >10 kilodalton (kDa)). But the distribution between these two phases in stormwater runoff is of some question (Babiarz et al., 2001). Colloids have proven to be an important downstream transport vector of Hg due to their large surface area (Babiarz et al., 2001; Gabriel and Williamson, 2004).

Ramamoorthy and Rust (1978) also showed that overall Hg adsorption to mineral and organic particles was correlated to surface area, organic content, cation exchange capacity, and grain size, in that order (Gabriel and Williamson, 2004). Due to their large surface area, the finest particles, e.g. colloidal clay particles, have the highest adsorption capacities. As a result of the high concentration of colloidal sized particles in soil pore water and the colloids' high affinity for Hg, Hg^{2+} is rapidly and efficiently removed from solution (Jackson, 1998; Gabriel and Williamson, 2004).

Some studies have also concluded that inorganic colloids contribute more to adsorption of organomercurials, whereas soil organic matter contributes more to adsorption of inorganic Hg (Jackson, 1989; Gabriel and Williamson, 2004). Moreover, if Hg is nonpolar and non-ionic, organic humus tends to be the adsorbent, and if Hg is ionic, then clay tends to be the adsorbent (Gabriel and Williamson, 2004).

The adsorption process is pH-dependent, indeed the order of adsorption of hydrolyzable metal ions with increasing pH corresponds to the order of increasing p^*K for the first hydrolysis product of the metal ion (Schuster, 1991). Correspondingly, Lockwood and Chen (1973) found a sharp increase of Hg-adsorption on hydrous MnO_2 between pH 2.5 and 3, the explanation being the formation of the hydroxide complex in this pH range.

If the dissolved species of minerals coat the surface of other minerals, Hg's sorption characteristics will vary tremendously (Jackson, 1989). For example, Hg in solution has a relatively weak bond to kaolinite. But when MnOOH ions are introduced to solution and coat the surface of kaolinite, Hg adsorption increases due to the strong bond between MnOOH and free Hg^{2+} (Jackson, 1989; Gabriel and Williamson, 2004).

1.4.1.2.1. Sorption of elemental Hg

Mineral and organic surfaces not only have a high affinity for inorganic and organic forms of Hg but also its elemental form (Hg^0). Even though elemental Hg is highly volatile, it is also readily adsorbed to soil material (Schluter, 2000). Adsorption of elemental Hg to soil is a subject of great interest because it can potentially determine whether Hg is oxidized to more soluble forms (Schluter, 2000). Experimental data indicates that kaolinite, montmorillonite and goethite adsorb air Hg^0 at higher rates, and that the mineralogical nature of soil particles may play an important role in the sorption of atmospheric Hg^0 (Xin and Gustin, 2007; Navarro et al., 2008)

Hg^0 bound to humic acids is an environmental concern due to possible transformation processes such as methylation or Hg^{2+} reduction (Navarro et al., 2008).

As it will be discussed later, humic acids have a dual role in Hg chemistry, because Hg^{2+} may be reduced, as well as complexed by humic acids. This dual role of dissolved organic matter on Hg reduction/complexation is still a matter of question and peculiar interest. Indeed complexed Hg may be retained in soil, or mobilized through leaching in colloidal particles. While Hg^0 will more easily be evaded from soil in the atmosphere (Schluter, 2000).

1.4.1.3. Mercury and organic matter interactions

There is a considerable amount of speculation on the role of Natural Organic Matter (NOM) and its association with metals. Most studies indicate that association with NOM can both increase and decrease the solubility of trace metals (Schuster, 1991).

According to Vuceta (1976) the addition of dissolved organic ligands may generally result in:

1. an inhibition of metal adsorption because of strong complex formation with the metal ion or by competing with the surface for available adsorption sites (e.g. humic acids, glycine, leucine, acetate, etc.);
2. no perceptible change in the extent of adsorption if the ligand has weak complex forming ability and exhibits a lack of affinity for the solid surface;
3. enhanced adsorption of the ligand that is capable of strong complex formation and also possesses a substantial affinity for the solid surface (Schuster, 1991).

Previous research suggests, also, that NOM can both reduce or enhance the Hg's bioavailability (Barkay et al., 1997). If Hg is bound to low molecular weight organic compounds (LMW) (e.g. cysteine), or organic matter that is itself part of a larger organic

mass that harbors bacteria capable of methylating Hg (i.e. sulfate reducing/methanogenic bacteria) it could inherently promote methylation. But if Hg binds to long chain NOM molecules this could decrease Hg's availability due the larger sizes of these organic molecules (Gabriel and Williamson, 2004).

Nevertheless, the high affinity of Hg to soil organic matter has been described in numerous papers (e.g. Nriagu, 1979; Förstner, 1991).

NOM plays a major role in determining Hg speciation through:

1. complexation,
2. redox reactions,
3. interference in mineral solubilization, aggregation and reprecipitation.

In this paragraph it will be discussed Hg complexation and reduction, while next paragraph will describe mineral and organic matter interactions.

Organic matter forms chelates throughout the bound with different functional groups, in descending strength they are: thiol SH^- , amminic NH_2^- , phenolic, OH^- and carboxylic COO^- . Weaker binding to oxygen functional groups such as carboxyls (Reddy and Aiken, 2001) occurs only at relatively high Hg concentrations, atypical of most natural settings (Waples et al., 2005). The highest strength regards the bind with thiol which can also compete with sulfide (HgS) (Skylberg, 2008a). Indeed, it is widely known that the complexing capacity of organic matter is far greater for Hg than for other metals such as Cd, Zn, Cu, and Pb, because of covalent bonds that commonly form between Hg and organic molecules (Gabriel and Williamson, 2004)

Recently, X-ray Absorption Spectroscopy (XAS) was used to obtain information on the bonding environment between Hg and soil-extracted humic matter (Xia et al., 1999; Hesterberg et al., 2001; Qian, 2001). The chemical identities of binding atoms (sulfur and oxygen in the first coordination shell and sulfur and carbon in the second coordination shell) and binding lengths were interpreted from extended X-ray absorption fine structure (EXAFS). The ratio of reduced to oxidized sulfur was obtained from X-ray absorption near edge structure (XANES). Thiol (RSH), disulfide (RSSR) and disulfane (RSSH) were proposed as the binding sites for Hg in humic acid (Xia et al., 1999). Similar results were obtained by Hesterberg et al. (2001) who showed that the fraction of increased Hg–S with increasing S/Hg ratio, which supports the possibility of a double sulfur bond at a very low Hg/S ratio.

Introduction

Spectroscopic studies of penicillamine reveal that Hg associates with two thiols at low pH (pH = 4), and with two, three or even four thiols at alkaline (pH = 11) conditions (Leung et al., 2007). Some of these thiols may be free, low molecular weight (LMW) molecules like cysteine or glutathione. The majority of the thiols, however, is associated as functional groups to high molecular weight (HMW) dissolved or particulate natural organic matter (NOM).

In mercaptoacetic acid, which does not have any amino group, the thiol group has a pKa value of 10.0. If the thiol groups in cysteine and penicillamine are assigned a pKa of 10.0, an “average” stability constant for the formation of Hg(SR)₂ complexes in LMW thiols with a pKa of 10.0 may be calculated (Skylberg, 2008).

Ravichandran et al. (1998) have demonstrated that cysteine and mercaptoacetic acid solubilized a significant amount of Hg ($\approx 0.002 \mu\text{mol/mg C}$; $\approx 0.02 \mu\text{mol/mg C}$, respectively) from cinnabar. This might be a result of the extremely high binding strength between Hg and these compounds.

The strong affinity of Hg to functional groups of soil organic matter refers to bulk particulate organic matter as well as dissolved organic ligands. As a consequence the mechanisms regulating the partition of organic matter between aqueous and solid phases should play a dominant role in the control of the concentrations and thus on the transport of those metals which are strongly complexed (both as solution complexation and adsorption) by organic matter (Schuster, 1991). Common dissolved organic ligands are salicylic and acetic acid, EDTA, and cysteine (Reddy and Aiken, 2001).

In most cases, the stronger adsorption and immobilization also mean a nonavailability and detoxification of Hg. This reflects the possible ability of soils to withdraw Hg via sorption from the liquid phase. Thus, soils can be very effective as immobilizing and detoxifying agents, depending on Hg speciation, Hg concentration, and soil characteristics (Welp and Brümmer, 1997).

It is not only the amount but also the quality of organic matter that decides about the sorption capacity for Hg. This becomes evident by comparing Hg-adsorption of soils with identical mineralogy and humus content but varying vegetation cover (= humus quality) (Semu et al., 1987). Ramamoorthy and Rust (1976) showed that sorption maximum was correlated to surface area > organic content > cation exchange capacity (CEC) > grain size whereas the bonding constant correlated in the order organic content > grain size > CEC > surface area.

Humic and fulvic acids, which make up a large percentage of organic matter, are the most important complexing agents in soils (Landa, 1978; Andersson, 1979; Beister and Scholtz, 1997; Gabriel and Williamson, 2004).

The humus rich materials revealed a by far higher adsorption capacity than pure clays. These results were verified by Landa (1978). Fulvic acid exerted a stronger affinity for Hg than did a strong cation-exchange resin (Lindberg et al., 1975).

Most organic Hg complexes also have a high degree of stability that is only weakly affected by pH even at extremely acidic or alkaline conditions (Jackson, 1998).

Besides complexes formation, NOM is also involved in redox reactions with Hg. NOM can mediate electron transfer and it is one of the most important electron shuttles in natural environments. Among the various functional groups in NOM, quinone/hydroquinone pairs (aromatic compounds) are the dominant redox active moieties, acting both as electron acceptors and donors in oxidation-reduction cycles. It is demonstrated the oxidation of Hg^0 by LMW thiol compounds, i.e. glutathione and mercaptoacetic acid, under reducing conditions. Of particular interest is the recent finding that reduced NOM can mediate both the reduction and oxidation of Hg in anoxic environments, although the exact mechanisms by which these reactions occur are not fully understood (Zheng et al., 2012).

These observations are important because previous research using microbially reduced NOM raised the possibility that microbial exudates may interfere with the redox reactions of Hg (Zheng et al., 2012).

Some research has involved quinones because of their predominance in natural organic matter and their ready participation in redox reactions.

Zheng et al. (2012) also noted that the oxidation rates of Hg^0 appeared to vary with different thiol compounds. Indeed, depending on their origins, NOM samples vary not only in thiol content, but also in reactivity of the thiols. NOM reactive sites vary in:

- sulfur oxidation state (thiols or disulfide, etc);
- variety of neighboring functional groups;
- substituent chain lengths and steric arrangements.

For aromatic compounds that contain hydroxyl groups, removal of the acidic hydrogen and stabilization of the produced intermediate increases overall reactivity, so pH could influence NOM and Hg interactions. Furthermore, depending on the conditions of the

Introduction

environment in which the reaction is occurring, NOM moieties can exist in reduced (A), semiradical (B), and oxidized (C) forms (Figure 1.10).

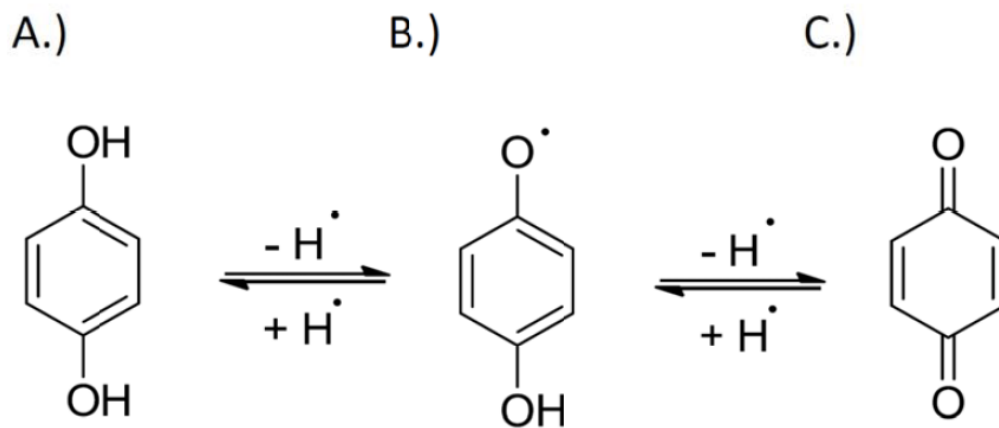


Figure 1.10. Oxidation states of hydroquinone: A) Fully reduced compound; B) Semiquinone state; C) Fully oxidized compound.

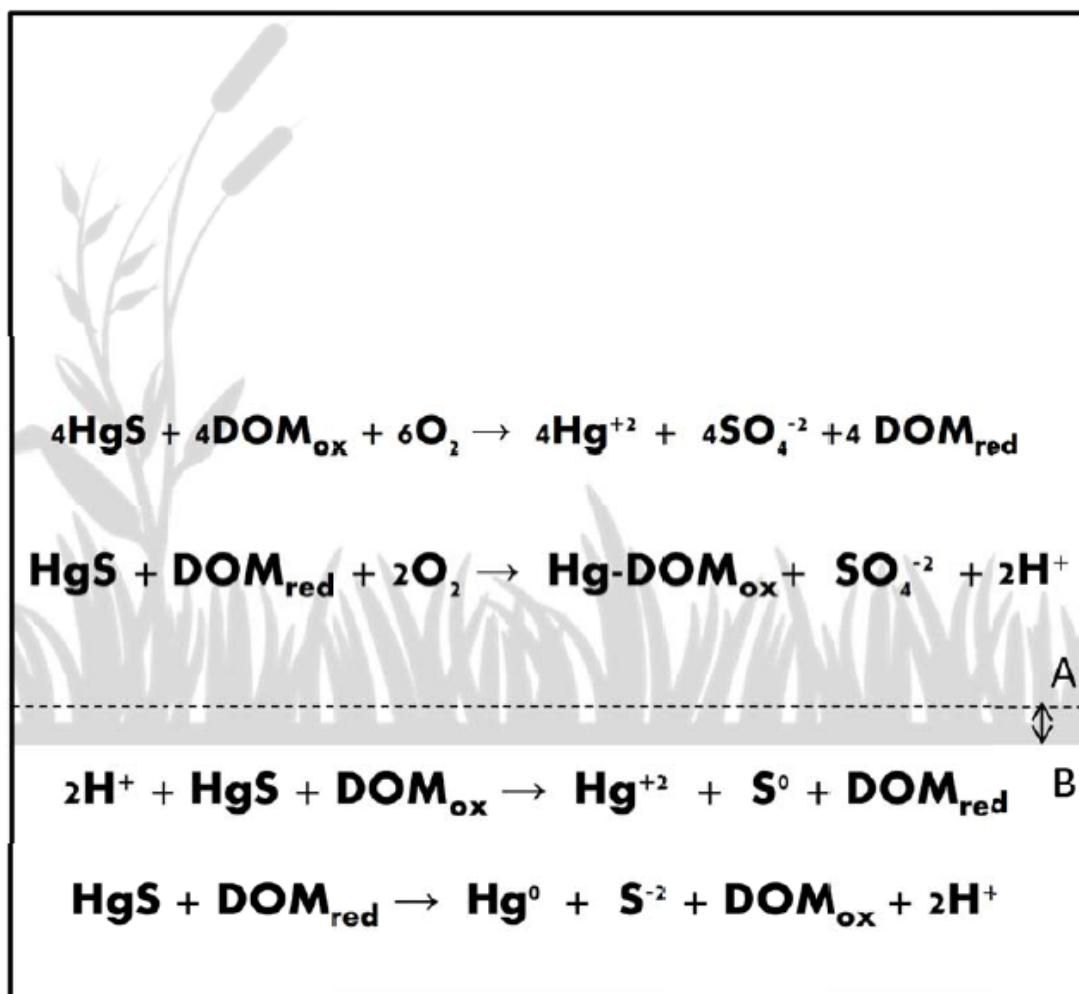


Figure 1.11. Scheme of mercury sulphide and dissolved organic matter under different redox status (Stallings, 2013).

In the soil, many redox reactions between Hg and NOM may occur, during water table fluctuations. Further, shifts in the anoxic/oxic boundary can result in a relatively sudden introduction of NOM into waters of different Eh where the redox state of NOM moieties may change (Figure 1.11).

1.4.1.3.1. Cinnabar dissolution by NOM

Formation of relatively insoluble solid Hg sulfides (HgS), cinnabar or metacinnabar, can inhibit Hg^{2+} methylation and bioaccumulation, and immobilize Hg^{2+} in reducing environments.

However, the presence of NOM produces different effects:

1. enhances the solubility and dissolution of cinnabar (Ravichandran et al., 1998), which lessens the role of cinnabar in immobilizing Hg;

Introduction

2. inhibits the precipitation of metacinnabar (Ravichandran et al., 1999).

Soil dissolved organic carbon may increase dissolution of Hg from HgS (Ravichandran et al., 1998; 2004), thus increasing Hg bioavailability in soils. Likewise, cinnabar can dissolve in the presence of organic matter by means of surface complexation (Ravichandran et al., 1998; 2004). The possible mechanisms of dissolution of HgS were suggested to include surface complexation of Hg and oxidation of surface sulfur species by the organic matter (Ravichandran, 2004; Han et al., 2008).

Hydrophobic acid (a mixture of both humic and fulvic acids) dissolved more Hg than hydrophilic acids and other nonacid fractions of dissolved organic matter (Ravichandran, 2004; Han et al., 2008). Other inorganic (chloride and sulfate) and organic ligands (salicylic acid, acetic acid, cysteine) were not found to enhance the dissolution of Hg from the mineral cinnabar (Ravichandran, 2004; Han et al., 2008).

More in detail, Waples et al. (2005) showed that the amount and rate of Hg released from cinnabar in the presence of NOM samples from a wide range of natural environments were correlated with the aromaticity of the NOM.

According to Waples et al. (2005), cinnabar dissolution rates correlates positively with three NOM characteristics:

1. specific ultraviolet absorbance,
2. aromaticity,
3. molecular weight.

It is known that certain fractions of NOM promote while others hinder cinnabar dissolution (Waples et al., 2005). Moreover S(-II) may chemically alter NOM (Heitmann and Blodau, 2006) and therefore should affect its reactivity with HgS(s).

Experimental observations, further, demonstrate that dissolution was controlled by the interaction of NOM with the cinnabar surface. The chemical mechanism that is responsible for surface cinnabar and NOM interaction is not fairly clear yet. Evidence for a surface interaction that increases the dissolution rate exists in the dialysis experiment results that showed that surface contact is necessary to enhance the amount of solubilized Hg. In a hypothetical dissolution reaction, NOM components sorb to the cinnabar surface and facilitate some change in the coordinative environment of Hg causing the Hg-S bond to break. Hg is then removed to solution, possibly as a Hg-NOM complex.

Cations such as Ca^{2+} , Mg^{2+} , and Al^{3+} can inhibit NOM-promoted HgS(s) dissolution (Waples et al., 2005).

Moreover, the presence of a NOM component that reduced the surface area of cinnabar that can be dissolved is indicated by the negative correlation between dissolution rates and concentrations of sorbed NOM (Waples et al., 2005). The sites, or functional groups that bind Hg to aqueous NOM are distinct from those sites in the NOM that participate in the rate-limiting step in the dissolution mechanism. Simultaneously, other NOM components sorb irreversibly to the cinnabar surface, alter the surface in a way that reduces subsequent dissolution, and cause the remaining NOM to have different bulk characteristics.

Other evidence that a surface sorption step drives cinnabar dissolution is derived from the experiments that showed a threshold rate was reached at a NOM concentration to cinnabar surface area ratio of about 4 mg C m^{-2} . This implies that above some specific surface coverage, the dissolution-enhancing component of NOM cannot promote dissolution because available surface sites are filled. Dissolution can proceed only when Hg is solubilized, freeing a new surface site for interaction with another NOM molecule (Waples et al., 2005).

It has been seen that as the concentration of cinnabar increases, the particles will aggregate together so that the surface available to reaction will be less as well as the dissolution rate. All these observations demonstrated that, the presence and formation of nanoparticles may be important in Hg-NOM interactions (see Appendix D). However, little research has been carried out to examine the release of Hg from the mineral surface (Stallings, 2013). It is nonetheless possible that multiple modes of interaction between NOM molecules and the cinnabar surface may have synergistic effects that have not yet been identified (Waples et al., 2005).

Since cinnabar dissolution is driven by surface interaction, it is possible that NOM-cinnabar interactions are triggered by NOM's complex structure. If reducing moieties within NOM could be isolated or concentrated, potential interactions with the surface may be increased, so redox-sensitive moieties with aromatic structures in NOM may act as electron shuttles. However, it remains to be determined if Hg(II)-sulfide bond breaks via the reduction of Hg(II) or the oxidation of S(II).

1.4.1.4. Mineral Fertilizers

Regarding to the inorganic chemistry of Hg, a lot of studies have been carried out in solution with sulfhydryl, chloride salts, and hydroxides. But a very few studies have

investigated the role of inorganic fertilization on Hg environmental fate (McLeod et al., 1996; Bolan and Duraisamy, 2003).

Hg(II) is prone to form complexes with high stability constants with many different inorganic ions: Cl^- , OH^- , S^{2-} , SO_4^{2-} , NO_3^- ; it also has a significant affinity to phosphate and NH_3 (Schuster, 1999). Further, polymer-supported pendant urea groups have been demonstrated to be very efficient in selective removal of mercuric ions from aqueous solutions (Bicak et al., 2003). Despite these evidences, not much research has investigated whether mineral fertilizers could interact with Hg and change its speciation in soils.

1.4.1.5. Organic amendments

Similarly to what reported in the previous paragraph, not much research has been carried out to investigate the role of organic amendments in changing both soil properties and Hg geochemistry (Park et al., 2011).

Organic amendments are used as a source of nutrients as well as soil conditioners to improve soil physical properties, such as particle size distribution, cracking pattern and porosity, and fertility of soils. Addition of biological waste materials has often been shown to increase the amount of organic matter in soils either by acting as a source of organic matter or by enhancing the solubilization of the soil organic matter.

The more recent concern about soil contamination has resulted in organic wastes, which have been used as materials for remediation of contaminated sites. In addition, the increase in wastewater generation and intensification of livestock has resulted in large quantities of solid organic wastes from very widely different sources with a variable composition.

Organic amendments are able to interact with metals through various processes that include complexation, reduction, volatilization and rhizosphere modification. Organic amendments play a role in metal speciation also by providing a source of electron donor and carbon substrate for microorganisms (Park et al., 2011).

1.4.1.6. Effect of root exudates on mercury mobility

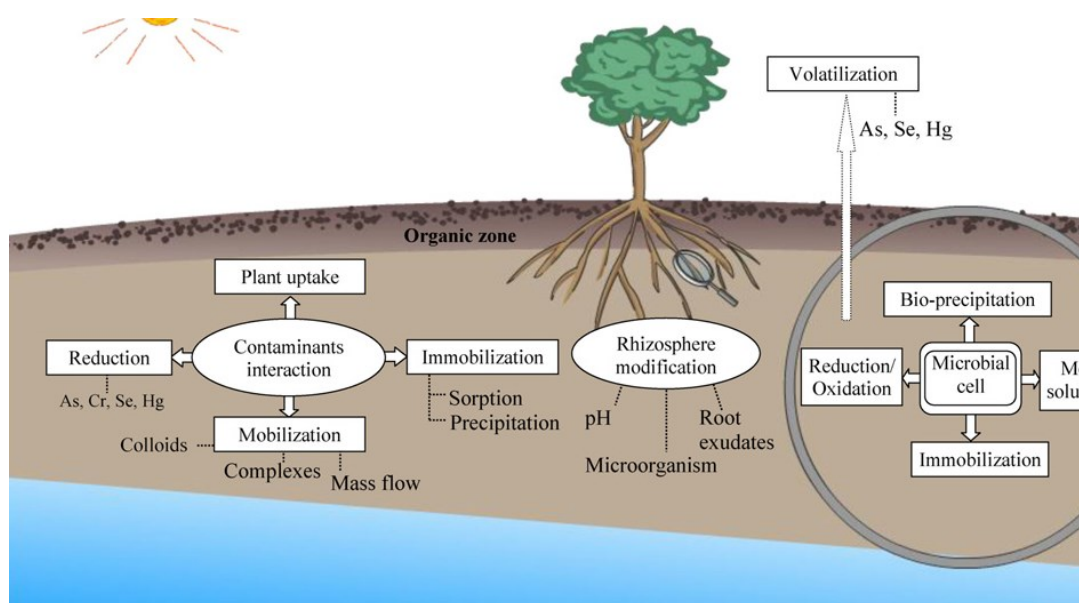


Figure 1.12. The role of organic amendments in regulating various processes that include immobilization, reduction, volatilization and rhizosphere modification (Park et al., 2011).

Factors that influence the metal bioavailability in soil include root-induced pH changes, metal binding by root exudates, detoxification of metals by siderophores, root-induced microbial activities, and root depletion as a consequence of plant uptake. Plant root exudates include a variety of soluble substances such as organic acids, which form complexes with metals and dissolve the solid phases to which metals are bound in the soil (Park et al., 2011).

Metallothioneins which are small cysteine-rich polypeptides that can bind metals, phytochelatins, cysteine-containing-glutamyl peptides, metal-thiolate clusters and microbial exopolymers composed of polysaccharide may be involved in heavy metal binding and detoxification (Park et al., 2011).

Metals can also bind to polysaccharides, proteins, lipoproteins including c-type cytochromes, phosphoryl groups associated with the membranes of microorganisms, proteins rich in acidic amino acids (including aspartic and glutamic acid), phosphate-containing nucleotides, uronic acids, carboxylic acids (malate, citrate, oxalate), simple and flavonoid type phenolics, etc. (Dohnalkova et al., 2005; Pal and Paul, 2007; Park et al., 2011).

In spite of the very low concentration of these biological products (plants and microorganisms exudates), their presence is exploited by the peculiar characteristics of rhizosphere. In a very spatially limited environment like the rhizosphere, chemical

molecules, physical parameters, plants and microorganisms interact all together so that changes in Hg behavior could result in a higher mobility, bioavailability and toxicity. Indeed, also Hg complexed by small organic molecules like amino acids may be taken up by plants.

Some research has involved quinones because of their predominance in natural organic matter and their ready participation in redox reactions. Quinones, hydroquinones, resorcinols are actively generated by microbes during processes such as respiration and are prominent in plant allelopathy. Many other aromatic compounds are known to be released from roots and microorganisms, under oxidative stress, during periods of drought or flood and in the presence of heavy metals.

The treatments, which will be used in this work, have been selected on the basis of either their capacity to improve NOM content in soil or their similarity to natural components of NOM (e.g. reducing moieties), that it is thought to be responsible for the release of Hg from cinnabar, and their natural presence in the environment.

1.4.2. Mercury reduction and volatilization

Accordingly to what stated before, as a global pollutant process, the reduction of Hg is especially important.

The reduction of Hg^{2+} to Hg^0 and further volatilization of Hg^0 are two very important surface processes because they can regulate much of the Hg load to surface water.

Hg reduction generally occurs in reducing environments such as lower soil horizons or saturated soils, and it is heavily influenced by adsorption. Generally, an inorganic Hg form that is free in solution has a higher potential of being reduced than one adsorbed to a soil component (Schuster, 1991; 2000).

Hg reduction in soil may be driven by (Schluter, 2000):

1. abiotical reactions;
2. biotical reactions.

In soils, the main reductants (electron donors) are Fe^{2+} and humic and fulvic compounds (Wilson and Weber, 1979; Allard and Arsenie, 1991; Schluter, 2000). The reason for the large reducing power of humic matter is its free radical component (Schluter, 2000). Moreover, abiotic reduction can be enhanced in the presence of sunlight (Allard and Arsenie, 1991; Zhang and Lindberg, 1999; Schluter, 2000; Gustin et al., 2002). These reactions normally progress in the visible light range but are most efficient at smaller wavelengths (UVB: 280–320 nm) (Amyot et al., 1994).

The fate of inorganic Hg in the environment have been studied for decades, with early studies focused on the reduction of Hg(II) by organic acids (Alberts et al., 1974; Skogerboe and Wilson, 1981; Allard and Arsenie, 1991). Thus, abiotic reduction of inorganic Hg by natural organic matter and native soils is well-known.

Ravichandran (2004) comprehensively reviewed the interaction between Hg and dissolved organic matter, which suggested that humic substances have a dual role in determining Hg transfer in the geochemistry cycle: complexation and reduction. However, previous studies have mainly concentrated on complexation or adsorption/desorption (Schuster, 1991; Yin et al., 1997; Xia et al., 2004; Zhang et al., 2009), while in comparison only a few references exist about the reduction process as affected by humic acids (Alberts et al., 1974; Allard and Arsenie, 1991; Matthiessen, 1998). However, humic acids are known to be redox active substances as an electron donor (Alberts et al., 1974; Kappler and Haderlein, 2003), mediator (Scott et al., 1998; Kappler et al., 2004), or acceptor (Bradley and Chapelle, 1998). Compared with studies on complexation, the abiotic reduction of Hg²⁺ by HAs was not negligible in either terrestrial or aqueous systems, though it is believed to be less obvious in terrestrial systems. Rocha et al. (2003) also found that Hg²⁺ is preferentially reduced by HAs molecules having a relatively high ratio of phenolic/carboxylic groups and a small amount of sulfur, and there exists a complicated competition between reduction and complexation of Hg²⁺ by HAs in water.

It may be speculated that the production of Hg⁰ increases when light intensity and exposure duration increase. However, additional experiments are recommended to better understand the relationships and sensitivity between the characteristics of the HA type used and the elemental Hg production under lighted conditions.

It has been widely accepted that aromatic structures are mainly functional groups for redox reactions involving electron transfer, including phenolic groups (Serudo et al., 2007) and, in particular, quinone or semi-quinone moieties (Dunnivant et al., 1992; Curtis and Reinhard, 1994; Scott et al., 1998; Struyk and Sposito, 2001; Royer et al., 2002; Kappler et al., 2004; Fimmen et al., 2007; Rakshit et al., 2009). Additionally, carboxylic and amide groups (Serudo et al., 2007) have also been found to be involved in HA redox processes. On the other hand, complexed iron in HAs can also contribute to the electron transfer process (Senesi et al., 1977; Struyk and Sposito, 2001).

Introduction

Within the last ten years, solid-bound and structural ferrous Fe(II) has been implicated in abiotic reduction of Hg(II): as a surface species sorbed to nonferruginous clay (Charlet et al., 2002) as the ferrous sulfide mineral mackinawite (Jeong et al., 2007) and as the mixed valence Fe (hydr)oxides green rust (O'Loughlin et al., 2003) and magnetite. More recent studies concerns magnetite (Wiatrowski et al., 2009; Pasakarnis et al., 2013).

Magnetite has also been implicated in the transfer of electrons between diverse microbial species in sediments, a process that relies on mineral conductivity which also varies with Fe(II) content (Kato et al., 2012). In the soil and water, there is the potential for many redox reactions to occur during water table fluctuations. Changes in magnetite Fe(II) content due to fluctuating redox conditions may have significant implications for the interaction and cooperation between subsurface microbial species. (Pasakarnis et al., 2013).

The reduction of Hg with the Hg reductase enzyme while obtaining energy for growth can occur also by various strands of bacteria, for example *Escherichia coli* and *Saccharomyces* (Hansen et al., 1984; Nakamura et al., 1988; 1990; Schluter, 2000).

Some bacteria decompose organomercurials such as Methyl-Hg and phenylHg to elemental Hg through the action of two enzymes. An organomercurial lyase cleaves the carbon-Hg bond, and a Hg reductase converts Hg ions (Hg_2C) to elemental Hg (Hg^0) (Begley et al., 1986; Schiering et al., 1991; Nakamura and Silver, 1994). Some other bacteria possess only Hg reductase, which can reduce inorganic mercurials, but not organic mercurials (Sahlman et al., 1984; Nakamura et al., 1999).

Glucose and yeast in the growth media of microorganisms are also known to reduce Hg^{2+} to Hg^0 . However, high amounts of organic matter in soil are known to inhibit biotic reduction even more so than in abiotic reduction (Schluter, 2000). A possible reason for this is due to Hg^{2+} adsorption to organic matter, therefore decreasing its availability.

Once formed, the migration of Hg^0 is largely dependent upon soil structure, sorption to soil, and ambient air temperature. Heat created from sunlight has been seen to greatly effect the volatilization of Hg^0 . While UV radiation and temperature are the primary factors controlling Hg^0 volatilization, secondary parameters are: soil moisture content (Lindberg et al., 1999; Wallschläger et al., 1999; Zhang and Lindberg 1999; Gillis and Miller, 2000), wind speed (Poissant and Casimir, 1998; Wallschläger et al., 1999; Cobos et al., 2002), relative humidity (Poissant and Casimir, 1998; Wallschläger et al., 1999; Gillis and Miller, 2000), ozone (Poissant and Casimir, 1998; Gillis and Miller, 2000) and

soil Hg content (Engle et al., 2001; Southworth et al., 2004). In general, these parameters are correlated with Hg^0 flux except for relative humidity, which is commonly inversely correlated to Hg^0 flux.

2. OBJECTIVES AND HYPOTHESES

The purpose of this research was to characterize and understand the distribution and potential mobility of Hg in agricultural soils affected by sediments transported and deposited by the Soča-Isonzo river.

Hg bioavailability, mobility and toxicity strongly depend upon Hg speciation/fractionation. Although several methods of Hg speciation/fractionation have been proposed and assessed, there is still a lack of consensus toward a valid and generally applicable Hg speciation/fractionation procedure. The major problems of Hg fractionation protocols are the lack of selectivity of reagents, readsorption and redistribution among the remaining fractions, losses by volatilization.

The soils studied in this research are low-land bank soils; they are permanently under the sea level, so are subject to frequent changes in the oxic/anoxic boundary and capillary rise flow of the water table. They are, also, intensively cultivated to arable and horticultural crops.

2.1.OVERALL AIMS AND GOALS

1. Characterize Hg distribution in the identified area, along soil profile and its partition between size-textural fractions using wet sequential extraction procedures;
2. Validate a method of temperature fractionation by coupling a multistep sequential extraction procedure with a thermodesorption technique;
3. Investigate the factors that may increase Hg mobilization (either volatilization and solubilization) in particular in soils under intensive agriculture.

2.2.HYPOTHESES

- Hg is highly concentrated in the soil of the area and its distribution along soil profile is mainly due to the process of river sediments deposition.
- The form of Hg mostly represented in the soils under investigation is HgS (cinnabar and metacinabar).
- Thermodesorption may represent a valid and quick method to identify the main Hg compounds.

Objectives and Hypotheses

- Coupling two methodologies of speciation may overcome the inherent limitation of each of them and improve their interpretation.
- Application of fertilizers, either mineral or organic, may influence Hg mobility.
- Plant root exudates may influence Hg mobility.
- Redox changes of soil may modify the behavior of Hg.

3. MATERIALS AND METHODS

The methodology of this study consisted of three main parts:

1. A survey of Hg contamination in bank soils subjects to river deposition of mine residues from Idrja mine, with pedological analyses and size fractionation of textural-size and chemical Hg speciation.
2. The second part of the study focused on a comparison between thermodesorption and a seven steps Sequential Extraction Procedure.
3. The third part investigated the potential effects of mineral, organic fertilizers and root exudates addition on Hg solubilisation and volatilization.

3.1. DESCRIPTION OF THE STUDY AREA

The area under investigation is located in the so-called Friuli plane (North-East of Italy), near the Soča-Isonzo estuary (Figure 3.1), in Fossalon di Grado (Gorizia). The area borders Isonzo river to the east and Grado-Marano Lagoon to the south-west. More specifically, the area of interest is located in the eastern sector of the Grado-Marano Lagoon at the mouth of the Soča-Isonzo river, between the Isonzato canal and the Isonzo river (Figure 3.1). Its drainage basin covers about 3400 km², extending into both Italy and Slovenia. The average annual flow rate at the river mouth is estimated to be 196.8 m³ s⁻¹, ranging monthly from 43.1 to 665.9 m³ s⁻¹ (Interreg II, 2001). The rate of flow can exceed 2500 m³ s⁻¹ during the autumn floods (RAFVG, 1986). The mean annual solid discharge is 150 g m⁻³, with peaks of 1000 g m⁻³ during extreme events (Mosetti, 1983).

The whole area of Friuli plane has alluvial soil. There are also many groundwater from -30 and -215 m depth (CBBF, 2013).



Figure 3.1. Idrija-Soča-Isonzo rivers system, Aussa river and location of sampling sites for soils (Fossilon) and sediment (Banduzzi channel), red spots.

From the geological point of view, Mesozoic limestone and Eocene flysch are the two prevalent lithologies cropping out in the Isonzo catchment area. The former prevails in the northernmost alpine chains, the latter outcrops in the hilly and pre-alpine areas bordering the alluvial plain (Stefanini, 1976; Covelli et al., 2006). Carbonate sediments dominate mineralogy.

The pedological substrate is characterized by the following sedimentary layers (ersa.fvg):

1. from 0 to 15 m depth, clays and sands;
2. from 15 to 25 m depth, gravel and sands;
3. from 25 to 50 m depth, clays with peats horizon;
4. from 50 to 60 m depth, sands;
5. from 60 to 70 m depth, sandy gravels;
6. up to 230 m depth, alternations of sand and clay;
7. 250 m bedrock.

The climate is predominantly temperate (mean annual temperature of 16 °C, mean minimum annual temperature of 7 °C and mean maximum annual temperature of 27.5 °C), with annual precipitations of 1000-1100 mm (osmer.fvg).

In the whole area, Hg concentration exceeds legislation limits. Indeed, bank soils in the Soča-Isonzo catchment are widely known to be characterized by high background values of Hg (RAFVG, 1992; Brambati, 1997). This contamination is mainly due to the mining activities in Idrija (Slovenia). The Hg mine began the extraction of cinnabar (HgS) and native Hg since 15th century. The extracting activities has continued over the years, gradually decreasing in recent decades until the final closure of the plant in 1996.

For this reason, the Isonzo river is the main source of Hg to the whole Gulf of Trieste. The Idrijca, a river with a typical torrential character, flows through the town of Idrija where the area of the former Hg mine is located, then merges with the Soča river, 40 km downstream from the mine. The Soča river is renamed as Isonzo in Italian territory (Figure 3.2) (Hines et al., 2006).

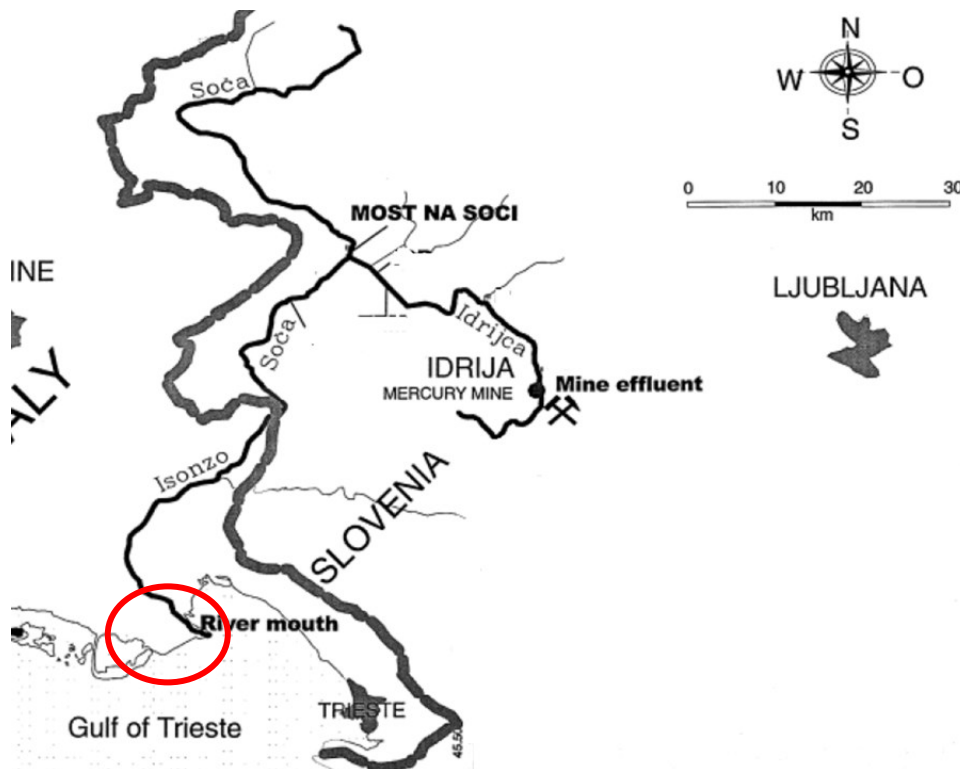


Figure 3.2. Idrija- Soča-Isonzo river system and location of sampling site (red circle) of contaminated soil (Gosar and Tersic, 2012).

Materials and Methods

The translocation of the Hg contamination from the Soča-Isonzo river to soil is possibly due to:

- the use of the same sediments for land reclamation activities,
- Hg volatilization and subsequent re-deposition,
- Hg diffusion by means of irrigation systems.

Indeed, Hg concentrations show a net gradient between the river and surrounding soils: concentrations decrease with the distance from the Isonzo estuary (CBBF, 2013).

The whole area lies within the "Bonifica della Vittoria", an agricultural soil below the sea level. The reclamation occurs after the First World War: the area has been stabilized, in order to reduce the removal of material by the sea currents. These initial works began in 1933 and ended in 1941. Agricultural activities began during the '40s. Nowadays this area is intensively cultivated with arable crops, horticulture, and fruit trees (Figure 3.3).

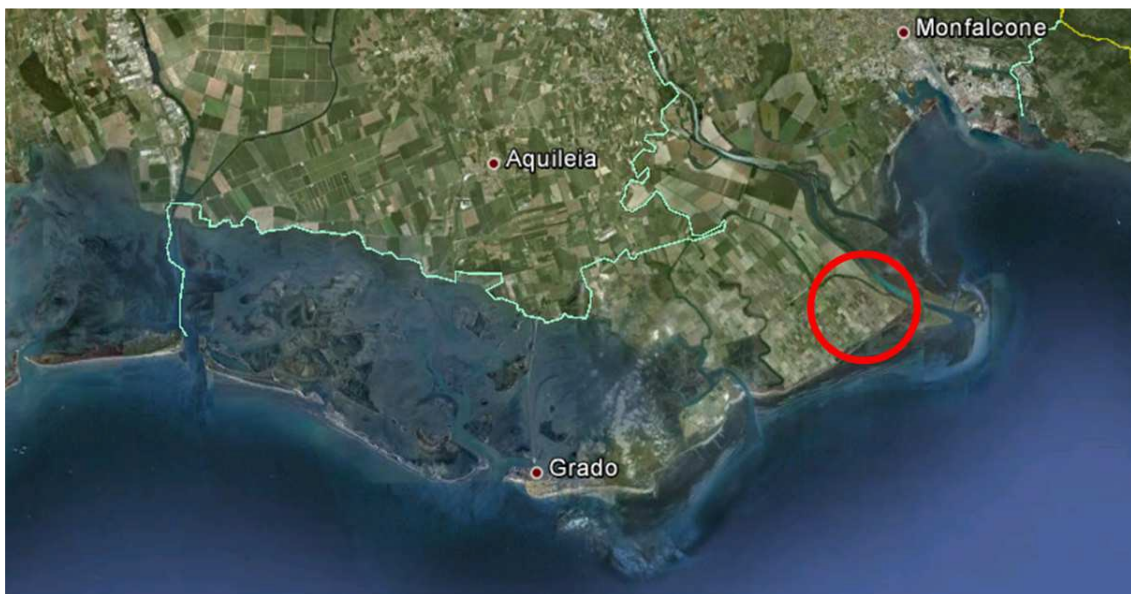


Figure 3.3. Aerial view of Isonzo river mouth and location of sampling site (red circle) of contaminated soil (Google maps).

In the Grado-Marano Lagoon, in the period between 1949 and 1984, a further contribution to Hg contamination has derived from the uncontrolled discharge of wastewater containing Hg, used as an electrode, by a chlor-alkali plant in the industrial area of Torviscosa (Figure 3.4) (Daris et al., 1993). The chlor-alkali plant began operation in 1949 and it has been estimated that a total of 186,000 kg of Hg was discharged in an artificial channel (Banduzzi channel) connecting the industrial area to the upper river

course of the Aussa-Corno. Samples of sediment were taken in this channel, close to the chlor-alkali plants (Figure 3.4). The chlor-alkali plant employed metallic Hg to electrochemically separate sodium and chlorine from brine. In addition, at the same industrial site, cellulose was produced from cane (*Arundo donax* sp), which enriched the sediments with organic carbon.

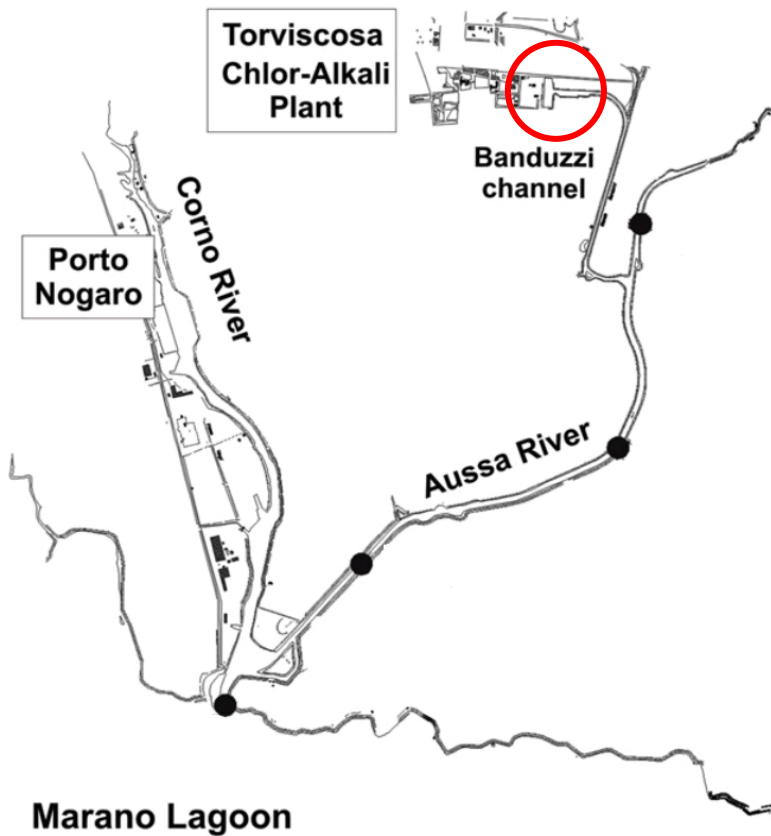


Figure 3.4. Aussa-Corno river system, Torviscosa chlor-alkali plant outflow from Banduzzi channel and location of sampling site of chlor-alkali contaminated sediment (redrawn from Covelli et al., 2009).

3.2.SOIL SAMPLING AND PROCESSING

In Figure 3.5 are shown the sampling points used for the preliminary soil survey, whereas Table 3.1 reports the georeferenced data of the sampling points.

Soil samples (0-120 cm) were collected with a Dutch Auger. Repeated drillings, have been applied to sample deep horizons. Four samples were taken for each sampling point at 0-40 cm, 40-60 cm, 60-80 cm and 80-120 cm depth. Particular care has been paid to accurately clean the sampling devices after every sampling in order to avoid cross contamination. Soil samples have been collected in clean plastic bags, and transported to the laboratory in refrigerated boxes.

Materials and Methods

For the study of the soil profile down to 2 m depth (at sampling point C23), an excavator has been used to open a trench about 1 m x 1 m wide and 2.20 m deep. During excavation, care was taken to stop just above the aquifer level.

Soil layering was investigated in a trench wall excavated from the soil surface down to the groundwater, at a depth of approximately 230 cm. The sequence and morphology of soil horizons – i.e. thickness, Munsell color, texture, structure, redoximorphic features, etc. – was recorded according to the suggestions of USDA-NRCS field book for describing and sampling soils (Schoeneberger et al., 2012). From each horizon, starting from the lowest horizon and ending with the Ap, a sample of soil was collected for chemical and physical analyses.

The soil was classified according to the World Reference Base for Soil Resources (IUSS Working Group WRB, 2014).

Among the sampling points, soils from two sampling points were chosen for the investigations on Hg speciation, thermodesorption and mobilization. These points were characterized by high Hg concentrations as well as an easy access for re-sampling operations.

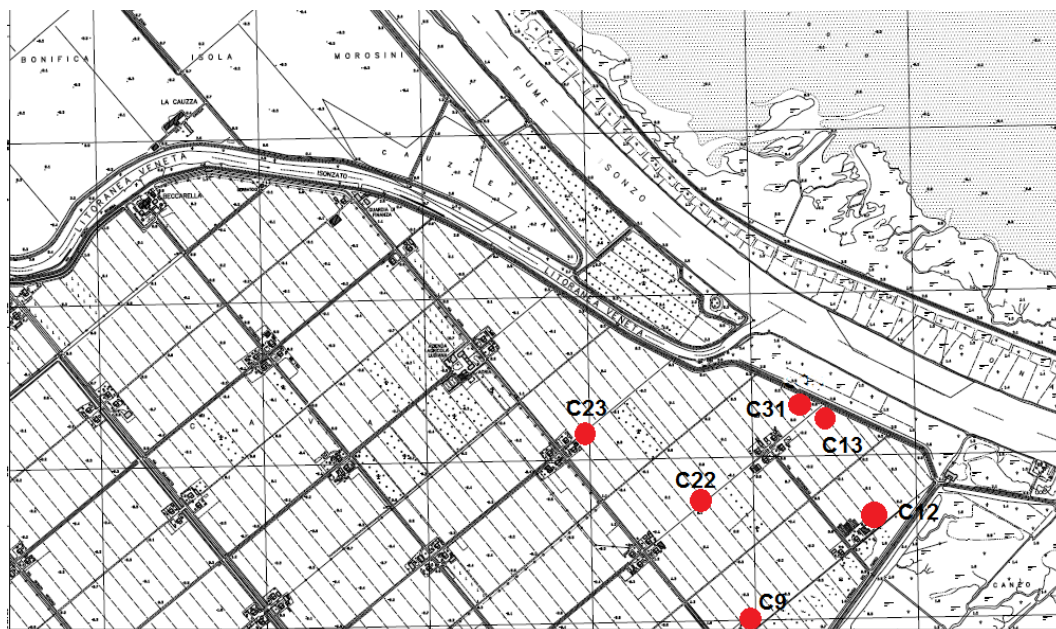


Figure 3.5. Cartography of studied area in Fossalon di Grado. Red spots indicate locations of sampling points for soil survey.

Table 3.1. Geographical coordinates of sampling points.

Sampling point	Latitude	Longitude
C9	5073398.09 N	1852415.65 E
C12	5073748.48 N	1852796.52 E
C13	5074058.70 N	1852534.28 E
C22	5073777.07 N	1852219.86 E
C23	5073967.87 N	1851850.00 E
C31	5074127.50 N	1852509.16 E

Once in the laboratory, soil samples were air dried at room temperature (temperature below 20 °C). Stones were removed and soil aggregates were gently crushed and homogenized. The dried samples were sieved to <2 mm. The <2 mm fraction was used for a general soil characterization and all further analysis.

Sieved samples were sealed in polyethylene bags and stored in a refrigerator at 4 °C until further processing.

A separate aliquot of sample was oven dried at 105 °C to constant weight for the determination of residual moisture content. Results are always expressed on a dry weight basis.

3.3.SEDIMENT SAMPLING AND PROCESSING

Surface sediment from Banduzzi channel (Figure 3.6 and Figure 3.7) was sampled near the chlor-alkaly plant using a stainless steel Van Veen grab (Figure 3.8). Four samples were collected and pooled together to obtain a homogeneous sample. Sediments were stored under water at 4 °C until analyses.

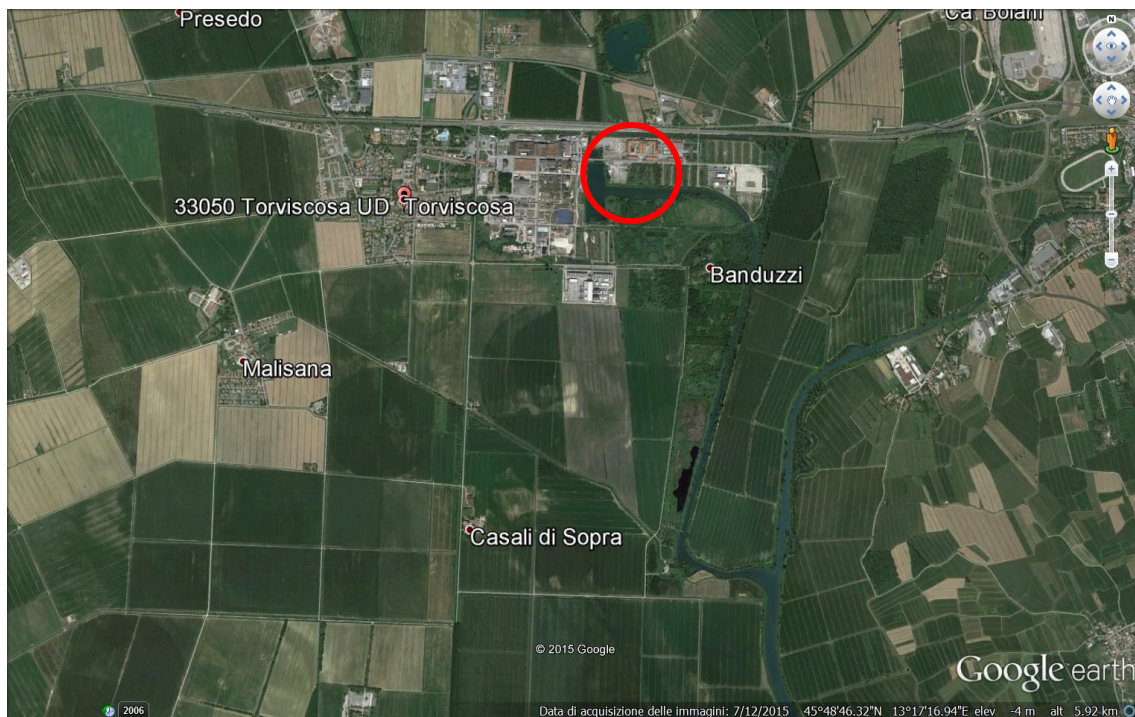


Figure 3.6. Aerial view of the industrial area in Torviscosa (Google maps).



Figure 3.7. Banduzzi channel close to the chlor-alkali plant.



Figure 3.8. Stainless steel Van Veen grab used for sediment sampling.

3.4.CLEANING PROCEDURE

Sampling devices were cleaned with an accurate removal of soil residues before washing firstly with tap water then rinsing with deionized water.

All glassware was cleaned each time, just before use, washed with tap water, then with a 2% KMnO_4 solution (15 min), and 12% $\text{NH}_2\text{OH}\cdot\text{HCl}$ solution (5 min), followed by rinse with Milli-Q[®] water. Teflon vials were pre-cleaned with acid following the procedure described by Horvat et al. (1993). After soaking the Teflon vials in 50% HNO_3 (w/w) at 70 °C overnight, the ware was rinsed with Milli-Q[®] water and then soaked in 10% HCl for 3 days, followed by thorough rinsing with Milli-Q[®] water, then filled with 1% HCl and stored in hermetically closed polyethylene bags in a Hg-free environment.

3.5.CHEMICAL ANALYSES FOR SOIL CHARACTERIZATION

3.5.1. Soil pH

The soil pH (CaCl_2) was determined using a WTW pH meter-538, according to the ISO 10390:2005 method. Briefly, it was used a glass electrode in a 1:5 (soil:solution v/v) suspension of soil in 0.01 M CaCl_2 . Soil suspension was shaken for 60 minutes. Measurement was performed after 1 hour after suspension preparation. Calibration of the

pHmeter was carried out using two buffer solutions at pH 6.88 and pH 9.22. Measurements were performed at 20 °C.

3.5.2. Soil salinity analyses

Electrical Conductivity (EC) was measured in a filtrate from 1:2 soil to water ratio (w/w) using a portable conductance meter (Crison CM 35). Instrument was calibrated with standard solutions from 147 $\mu\text{S cm}^{-1}$ to 12.88 mS cm^{-1} . Briefly, 20 ml deionized water were added to 10 g soil, shaken, and left overnight, filtered and EC measured on filtrate.

3.5.3. Cation Exchange Capacity analyses

Cation exchange capacity (CEC) was measured with BaCl_2 buffered at pH 8.2 with triethanolamine (TEA) (Mehlich, 1953). Briefly, 2 g of soil were added with 25 ml 1M BaCl_2/TEA solution and shaken for 1 h. Then the suspension was centrifuged to remove the unreacted Ba, washed, and 25 ml of MgSO_4 were added. After separation of the sediment by centrifugation, the excess of Mg was determined by complexometric titration with EDTA.

3.5.4. Redox potential

Redox potential (Eh) was determined with a platinum electrode connected with a reference electrode of Ag/AgCl , KCl 3M. Before analysis, calibration was performed using a saturated solution of $\text{K}_2\text{Cr}_2\text{O}_7$ (pH 2), at known Eh.

The following equation was used to correct measures with standard values (Zausig, 1995):

$$E_{\text{eff}} = (E_{\text{h}} + 293) - (E_0 - 636) \quad [\text{mV}]$$

Where:

E_{eff} = effective redox potential of the analytical sample;

E_{h} = measured value;

E_0 = measure of the standard ($\text{K}_2\text{Cr}_2\text{O}_7$);

293 = standard potential of the reference electrode;

636 = standard value ($\text{K}_2\text{Cr}_2\text{O}_7$).

3.5.5. Lime content analyses

Determination of total lime is based on the volumetric analysis of CO₂ liberated during the application of HCl in the Scheibler calcimeter. Briefly, 1-2 g of dry soil were weighted in a vessel and 5ml of HCl were added inside a small test-tube. The gas developed after the reaction of HCl with soil were measured volumetrically (Boero, 1992).

The concentration of CaCO₃ (g kg⁻¹) was then obtained with the following equation:

$$C = \frac{V_0 \cdot 0.0044655 \cdot 1000}{P}$$

Where:

C= lime content expressed as CaCO₃ (g kg⁻¹);

V₀= is the gas volume of CO₂ produced, normalized to 0 °C and 101,325 kPa pressure;

P= is the weight of soil in g.

3.5.6. Organic carbon and total nitrogen analyses

The organic C, as well as total N, were determined on 40 °C dried and homogenised samples, after pretreatment by acidification with HCl (1 M), using a CHN Elemental Analyser (Elementar, Vario EL Cube, Germany) at a combustion temperature of 920 °C. 200 mg of sample were weighted in Ag capsules for solids, and placed in an autosampler. Atropine sulfur was used as a standard for instrument calibration (1-2 mg).

3.5.7. Determination of total metal content

Pseudo-total metal content was determined according to USEPA 3051 method (1995a). Aliquots (< 0.2 g) of soil sample were introduced in Teflon® microwave vessels and 10 ml of concentrated HNO₃ was added. Samples were processed in a microwave digester (CEM Mars Xpress Matthews, NC, USA) at a temperature of 175 °C for 10 min. After cooling, digested solutions were filtered through a PTFE filter of 0.2 µm pore size, transferred into 20 ml volumetric flasks and stored at 5 °C for further analyses.

The concentration of metals in soil extracts was determined by ICP-AES. A Varian Vista Pro axial instrument equipped with a cross-flow nebulizer and auto-sampler was used.

The calibration was performed using an ICP-standard 23 elements solution in 5% HNO₃ (Merck solution IV). Yttrium (Y) was added as internal standard. The method detection

limit (MDL) was calculated as $3 s/m$ (where s is the standard deviation of 10 replicate blanks and m is the slope of the calibration curve) for each element. MDL were $0.02 \mu\text{g g}^{-1}$ for Cd, $0.01 \mu\text{g g}^{-1}$ for Ni, $0.2 \mu\text{g g}^{-1}$ for Zn and $0.01 \mu\text{g g}^{-1}$ for Cu.

3.5.8. Multielement analyses by neutron activation

Multielemental analyses were performed by k_0 standardization neutron activation analysis (k_0 -INAA), at JSI (Lubiana, SLO), a nondestructive method. Homogenized samples were analyzed with Thermal neutron flux irradiation in 250kW TRIGA Mark II reactor with HPGe calibrated detector (Jaćimović, 2014). The k_0 -INAA procedure is accredited according to ISO/IEC 17025:2005 by the Slovenian Accreditation Agency (Accreditation Certificate LP-090).

3.6. TOTAL MERCURY ANALYSIS

Total Hg content in native samples were determined by thermal decomposition Atomic Absorption Spectroscopy (AAS) with gold amalgamation (LECO[®] model AMA-254), a rapid total Hg determination method (US EPA Method 7473, 2007).

A mass of 20-40 mg of dry sample were weighed in a sample boat and placed in the auto-sampler. The sample was initially dried and then thermally decomposed at $850 \text{ }^\circ\text{C}$ in a quartz tube located inside a controlled heating coil. An oxygen stream passing through the tube carried the released Hg through the catalytic column, in which Hg was reduced to Hg^0 . Hg vapour was collected on a gold amalgamation trap and subsequently desorbed into the absorption cell. Hg content was determined using atomic absorption spectrometry at 253.7 nm. Three to five replicates for each sample were weighted and analyzed to obtain a reliable average value. Two certified materials were used to calibrate the instrument, Marine Sediment Reference Materials for Trace Metals and other Constituents: MESS-3 with a certified value of Hg $0.091 \pm 0.009 \text{ mg kg}^{-1}$ and PACS-2 with a certified value of Hg $3.04 \pm 0.20 \text{ mg kg}^{-1}$. The quality of results was also assessed by measuring BCR146R (sewage sludge) reference material.

3.7. PARTICLE SIZE FRACTIONATION

Particle size fractionation was performed on a soil sample collected from point C31 in the 0-40 cm horizon depth (on 26/10/2014). One portion of this sieved soil was subjected to a six steps SEP according to Lechler et al. (1997), while a second portion was subjected

to a preliminary particle size fractionation to separated the fine earth (2 mm) into four particle-size fractions according to the International Society of Soil Science (ISSS) particle size classification system (Table 3.2).

Table 3.2. Size limits of texture fractions (ISSS).

Fraction	Size limits
Coarse sand	< 2 mm and > 250 µm
Fine sand	< 250 µm and > 20 µm
Silt	< 20 µm and > 2 µm
Clay	< 2 µm

Separation was carried out without any organic matter removal pretreatment, to limit change in Hg speciation.

Coarse sand was separated by dry sieving (250 µm) using a stainless steel sieve, whereas the separation of finer fractions was carried out by sedimentation with the “Appiani” cylinder (Figure 3.9).

An aliquot of 100 g of soil was weighted in a soil dispersing cup and distilled water was added. Then 5 ml of 1M sodium hexametaphosphate were added in order to suspend soil particles. The suspension was then mixed for 15 minutes, then transferred to a sedimentation cylinder.

The suspension was transferred to a sedimentation cylinder. The cylinder was filled up to the marked level with distilled water.

Settling velocity and times were calculated according to the Stokes’s Law:

$$t = \frac{18 \cdot \eta \cdot h}{g(\rho_s - \rho_l) \cdot X^2}$$

Where:

η = viscosity [10^{-3} kg m⁻¹ s⁻¹];

h = distance from the top of the solution to the siphoning system [cm];

g = gravity acceleration [m s⁻²];

ρ_s = particle density [Mg m⁻³];

Materials and Methods

ρ_l = liquid density [Mg m^{-3}];

X = particle diameter [μm].

The fine sand fraction was separated and collected after repeated removal of unseparated suspension ($t = 8 \text{ min and } 42 \text{ s}$), collecting the sediment and air-drying; silt was separated by sedimenting the previous suspension ($t = 14 \text{ h, } 31 \text{ min, } 29 \text{ s}$), collecting the sediment and air-drying; and finally the clay fraction ($< 2 \mu\text{m}$) was collected by air drying the unseparated particles.

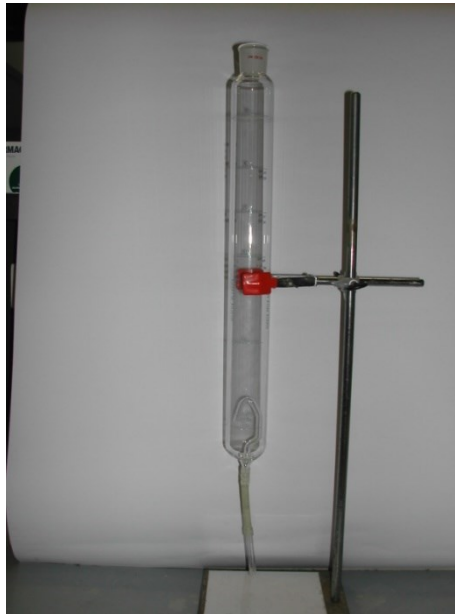


Figure 3.9. Sedimentation cylinder (Appiani).

3.8. MERCURY FRACTIONATION WITH SEQUENTIAL EXTRACTION PROCEDURES (SEP)

Since SEP procedures are operationally defined according to matrix characteristics, type of contamination and groups of Hg compounds that are intended to obtain, in this work, three different procedures were selected and retained to be suitable for the samples under investigation.

3.8.1. Sequential extraction procedure by Lechler et al.

The procedure used for Hg fractionation on size-texture fractions was proposed by Lechler et al. (1997).

It is based partially on the work of Eganhouse et al. (1978), Di Giulio and Ryan (1987), Quevauviller et al. (1992) and Biester (1994). This method allows to separate Hg in six operationally defined fractions: F1: Elemental, F2: Exchangeable, F3: Strongly bound, F4: Organic, F5: sulfides and F6: residual.

Two portions of 5 g of sample were simultaneously weighted into ceramic cups and heated at 180 °C in a ventilated oven for 48 h. Petri dishes containing activated charcoal were also inserted in the oven to captures Hg vapours and minimize Hg transfer from one sample to the other during heating.

One portion was measured by thermal decomposition AAS (LECO® model AMA-254), and the difference between total Hg in non-heated sample and heated sample represents the F1: volatile Hg.

The second heated sample was used for the determination of the other Hg species in the sample.

On the heated sample from step 1, 25 ml 0.5 M MgCl₂ were added and shaken at room temperature for 2 h, let stand for 60 min, decanted, centrifuged and the surnatant stored to determine exchangeable Hg. After each extraction, the residue was washed with 25 ml of deionised water, decanted for 60 min and centrifuged. The surnatant was then discharged and the residue collected for the following step.

On the residue from step 2, 25 ml of 0.5 N HCl were added, mixed at room temperature for 2 h, let stand for 60 min, decanted and centrifuged to separate fraction F3 in the surnatant: strongly bound Hg.

Using the sample residue from step 3, 12.5 ml 0.2 N NaOH were added, mixed at room temperature for 2 h, then 12.5 ml 4% (v/v) CH₃COOH (glacial acetic acid) were introduced, mixed at room temperature for 2 h, let stand for 60 min, decanted, centrifuged, and stored to determine F4 in the surnatant: organic Hg.

Using the residue from step 4, 12.5 ml of saturated sodium sulfide (Na₂S) solution were added, then mixed at room temperature for 24 h, centrifuged, and stored to determine F5 in the surnatant: sulphide Hg.

Residual Hg (F6) was calculated by difference between the sum of Hg extracted from the previous fractions and total Hg measured with AMA.

The samples deriving from particle fractionation and SEP leachates were analyzed for total Hg following US EPA method 1631, revision E (US EPA, 2002).

3.8.2. Tree steps Sequential extraction procedure

Air dried and sieved soil samples were divided in two aliquots and subjected to two different treatments, one including thermal heating and another without initial heating treatment.

First step (elemental Hg): soil was heated at 80 °C for 24 h in a ventilated oven with Petri dishes containing activated charcoal. A portion of the heated soil was measured for the remaining total Hg with LECO[®] model AMA-254 (see section 3.6) (Sladek and Sexauer, 2003).

Both heated and non heated soils underwent a 3-step sequential extraction:

First step (Soluble and exchangeable fraction): 4 g of soil were weighted in a PVC tube and added with 40 ml of 1.0 M Mg(NO₃)₂, then stirred for 2 h, centrifuged and filtered; the volume was made up to 50 ml (Finzgar et al., 2005).

Second step (Organically bound fraction): the residue of the previous extraction was added with 10 ml of 0.1 M NaOH and 0.1 M Na₂P₄O₇, stirred for 2 h, centrifuged and filtered; the volume was filled to 50 ml (Huang et al., 2012).

Before the ICP-MS analyses of this fraction, the organic matter was decomposed by microwave digestion according to the EPA METHOD 3015 (Microwave assisted acid digestion of aqueous samples and extracts).

Third step (residual Hg): the residue remaining after the previous extractions was air dried and analyzed with the LECO[®] model AMA-254 (see section 3.6).

3.8.3. Sequential extraction procedure by Han et al.

Mercury in soils was assumed to be present in seven operationally defined solid-phase fractions, which can be extracted by selective sequential leaching. The protocol employed in this study was performed according to Han et al. (2006). This SEP allows to distinguish between Hg as cinnabar (HgS), by using saturated Na₂S, and humic/humin bound Hg in the RES fraction.

This extraction procedure was performed in three replicates, using 1 g of dry sample each. Each leaching solution was added to the solid in Teflon vials and shaken at 300 rpm. Then, the vials were centrifuged at 10,000 rpm for 10 min at 20 °C, and the supernatant

filtered through a membrane filter of 0.2 μm pore size. These operations were repeated for each extraction step. The soil residue was kept for the next analysis/dissolution steps. The first step extract NH_4OAc -extractable Hg; this fraction includes soluble plus exchangeable Hg (EXC). Twenty-five milliliters of a 1 M ammonium acetate solution (pH adjusted to 7.0 with NH_4OH) were added to 1 g of air-dried soil in a 50-ml Teflon centrifuge tube. The mixture was shaken for 30 min at 25 $^\circ\text{C}$, and then centrifuged.

Second step: the $\text{NH}_2\text{OH}\cdot\text{HCl}$ -extractable fraction mainly comprises Hg bound to easily reducible oxides such as Mn oxides (ERO) (Shuman, 1982). Twenty-five milliliters of a 0.1 M $\text{NH}_2\text{OH}\cdot\text{HCl}$ +0.01 M HCl solution (pH 2) were added to the soil residue from the previous step and shaken for 30 min. The extracting solution might dissolve some organic matter, resulting in an underestimation of the organically bound metal. However, after extraction of the exchangeable fraction, this risk is less serious.

Third step: the H_2O_2 -oxidizable fraction mainly comprises Hg bound to organic matter (OM) (Tessier et al., 1979; Han et al., 2003a) as well as Hg^0 and some HgS (Biester and Scholz, 1997). Three milliliters of a 0.01 M HNO_3 and 5 ml of 30% H_2O_2 were added to the soil residue coming from the previous extraction step. The mixture was digested in a water-bath at 80 $^\circ\text{C}$ for 2 h. Additional 2 ml of H_2O_2 were added and the mixture was heated for 1 h. Fifteen milliliters of a 1 M ammonium acetate solution were then added and the sample shaken for 10 min.

In the fourth step, oxalate extracted Hg bound to amorphous iron oxides (AmoFe). Twenty-five milliliters of a 0.2 M oxalate buffer solution (0.2 M $(\text{NH}_4)_2\text{C}_2\text{O}_4$ –0.2 M $\text{H}_2\text{C}_2\text{O}_4$ at pH 3.25) were added to the soil residue and the sample shaken in the dark for 4 h (Shuman, 1982).

Fifth step: hot $\text{NH}_2\text{OH}\cdot\text{HCl}$ and HOAc were used to extract Hg bound to crystalline iron oxides (CryFe). Twenty-five milliliters of 0.04 M $\text{NH}_2\text{OH}\cdot\text{HCl}$ in a 25% acetic acid solution were added to the soil residue and the sample digested in a water bath at 97–100 $^\circ\text{C}$ for 3 h.

Sixth step: 4 M HNO_3 extracted the residual non-cinnabar Hg (RES), remaining from the previous extractions (mostly from the organically bound Hg, such as humin bound Hg) as well as Hg^0 (Biester and Scholz, 1997). Twenty-five milliliters of 4 M HNO_3 were added to the residue from the previous extraction and the sample was transferred to a glass digestion tube.

Digestion was conducted in a water bath at 80 °C for 16 h (Sposito et al., 1981; Han et al., 2003a).

Four milliliters of saturated Na₂S were added to the residual soil and the sample was mixed and reacted overnight. The extraction was repeated twice (Revis et al., 1989).

After all the extracting steps, the solid residue was analyzed with Atomic Absorption Spectroscopy (AAS) with gold amalgamation (LECO[®] model AMA-254).

After the extraction, the supernatants containing Hg were treated with nitric acid, perchloric acid and sulphuric acid in a ratio of 1:1 (2% v/v) and H₂SO₄ (5% v/v) in Milli-Q water at 240 °C for 20 minutes, on a hot plate, in open 50 ml volumetric flasks.

3.9. MERCURY QUANTIFICATION IN SOIL EXTRACTS

Hg was measured in the soil extracts by different methods using the instruments available in the laboratories where extractions or experiments were carried out and according to the detection limit required. Below the different methods used are described.

3.9.1. CV-AAS

Hg in both soil and sediment digestion/extracts was determined using a CV-AAS method (Automatic Mercury Analyser Model Hg-201, Sanso Seisakusho Co., LTD Instrument Model 910, Japan). The LOD was 0.1 ng l⁻¹ calculated on the basis of three standard deviations of the reagent blank (Akagi and Nishimura, 1991). Three replicates were digested for each sample to check the homogeneity and three replicates of each subsample were measured to check the repeatability of the measured Hg concentration. Each extracting solution was digested with the same procedure used for the extracts and measured as a blank. 1 ml of a solution of HgCl₂ (1 ng ml⁻¹) was measured as standard.

3.9.2. CV-AFS

Quantification of Hg in SEP fractions obtained by the Lechler et al. (1997) procedure (section 3.8.1) on size-texture fractions (section 3.7) was obtained by Cold Vapour Atomic Fluorescence Spectrometry (CV-AFS) at the ARPA laboratories in Trieste (Italy). SEP leachates were analyzed for total Hg using automated oxidation, purge and trap, desorption, and cold-vapor atomic fluorescence spectrometry (CV-AFS) (Brooks Rand Instruments) following US EPA method 1631, revision E (US EPA, 2002). Briefly, samples were first pre-oxidized using 0.2 M BrCl solution for one hour (0.5 ml), then,

pre-reduced using hydroxylamine hydrochloride to remove oxidant excess (250 μl of $\text{NH}_2\text{OH}\cdot\text{HCl}$, 12%), just before quantification by SnCl_2 reduction, dual gold amalgamation, Hg^0 release and measurement with CV-AFS.

The method detection limit (MDL) is approximately 0.2 ng l^{-1} and the reproducibility is about 5-10%.

Quality assurance (QA) procedures for total Hg analysis were guaranteed through blank analysis and duplicated measurements.

3.9.3. ICP-MS

The liquid phases from the incubation experiments (solubilization/volatilization) were analyzed with Inductively Coupled Plasma-Mass Spectrometry ICP-MS (NexIon 350X – Perkin Elmer), based on EPA Method 6020A.

The instrument was optimized daily for sensitivity, doubly charged ions (<2%) and oxides (<3%) with $1 \mu\text{g l}^{-1}$ Be, Ce, Fe, In, Li, Mg, Pb, U in HNO_3 1% solution. Data elaboration was carried out by using ICP-MS Syngistix software package (V 1.1.).

Nebulizer argon was introduced as carrier gas through the T-inlet. Tygon pump tubings were used for sample (0.76 mm i.d., black/black) and for internal standard (0.38 mm i.d., orange/green) transport.

Hg isotope 201 and 202 were measured both with and without He flow in collision cell/KED to reduce polyatomic interference. Rhodium (Rh) was used as an Internal Standard (50 ppb). After each measurement a rinse solution of Au (50 ppb in HNO_3 5%) was flown with a 90 s rinse time.

Calibration was performed before each batch of samples, with a Hg concentration range according to the expected results (generally $0.5\text{-}5 \text{ ng ml}^{-1}$).

Before analysis, samples were digested and filtered ($0.20 \mu\text{m}$). To take into account matrix interferences, standards and blanks were prepared using the same solutions used for extractions. To avoid, or reduce, Hg memory effect and contamination of the instrument, Au (10 ppb) in HNO_3 (1%) was also added in samples and standards.

3.10. Hg FRACTIONATION BY THERMO-DESORPTION

Thermodesorption was carried out at the Josef Stefan Institute (Ljubljana, SLO) with an home-made device, described below (Sedlar, 2014) (Figure 3.10 and Figure 3.11).

Apparatus: An RA-915+ Mercury Analyser with a PYRO-915+ pyrolysis unit was used for the detection of Hg. The instrument was developed for direct determination of total Hg by combustion of samples and cold vapour atomic absorption detection (CV-AAS) with a Zeeman background correction (Sholupov et al., 2004). It consisted of a gas tank (1) for supply of the carrier gas, a flow meter (2) for flow adjustment and quartz tubes. The first quartz tube, with outer diameter of 20 mm and inner diameter of 16 mm, was placed in an electric tube furnace (3). The quartz boat used for samples (4) was carefully positioned in the first quartz tube in the middle of an electric tube furnace Nabertherm RT 50/250/11, in which the thermocouple was located. The quartz boat had a semi-circular shape with inner diameter of 5 mm and was 35 mm long. The tube furnace consisted of a ceramic tube with inner diameter of 50 mm and two plugs of ceramic fiber on each side. Each plug had a hole drilled in the middle for a tight fit to a quartz tube to reduce the heat loss. The second quartz tube, with the same dimensions as the first, was packed with quartz wool (5) and heated to 800 °C by a small electric furnace with inner diameter of 27 mm (6) to ensure the transformation of all volatile Hg compounds to elemental Hg and to retain any particles that may be released from the sample. The Lumex Pyro 915+ pyrolysis unit with dimensions of 350 x 350 x 120 mm (7) ensured additional decomposition of any remaining volatile compounds of Hg that might interfere with the atomic absorption measurement (Sholupov et al., 2004). Elemental Hg was detected by a Lumex Ra-915+ atomic absorption detector with Zeeman correction, with dimensions of 470 x 210 x 110 mm (8), which was connected directly to a computer (9) for data collection. An impinger containing H₂SO₄-KMnO₄ solution (10) was connected to the exhaust from the Lumex Ra-915+ to retain Hg(0) in solution by its oxidation.

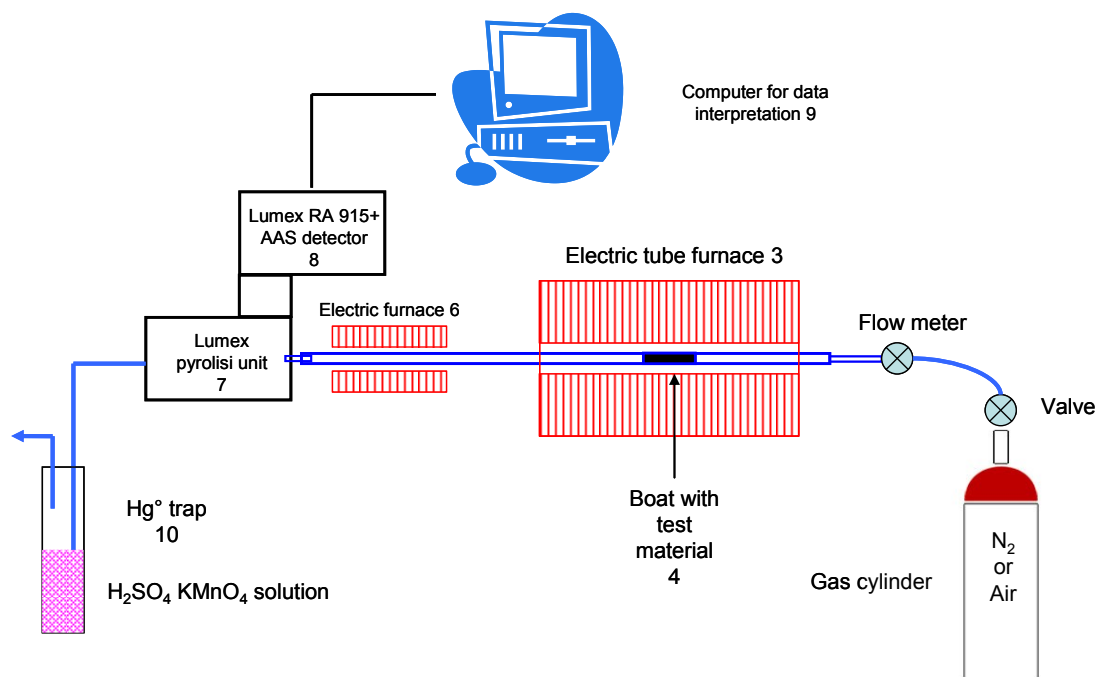


Figure 3.10. Scheme of the Thermo-desorption measuring apparatus (redrawn Sedlar, 2014).

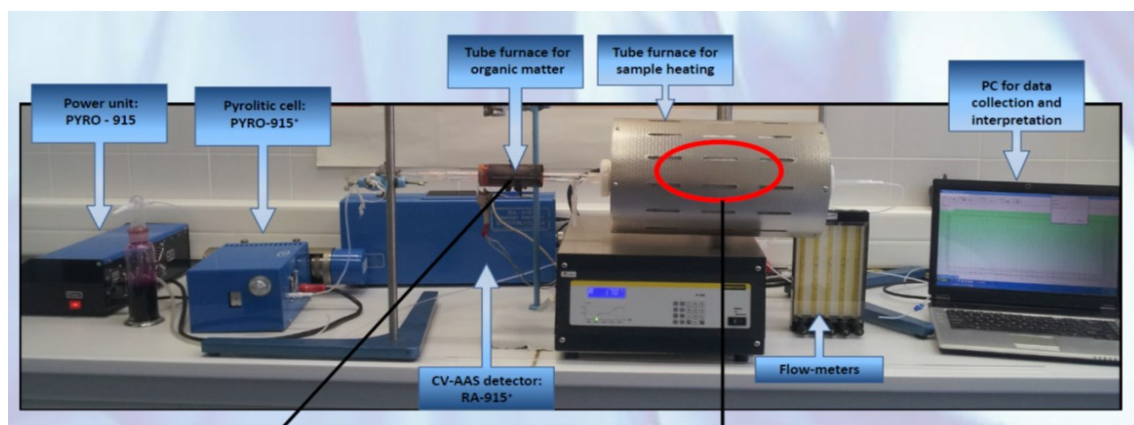


Figure 3.11. Picture of Thermo-desorption measuring apparatus.

Procedure: The sample was weighed in a quartz boat. The mass of the sample was predetermined not to exceed the upper limit of the detection range ($2 - 30000 \text{ ng Hg m}^{-3}$) (Sholupov et al., 2004). The results of mass balance for different samples also showed that the intensities of the peaks did not match perfectly to the recording units (ng m^{-3}) due to a drifting measuring baseline, as a software deficiency; however, these units served for easier comparison of the signal intensity. To resolve the drifting baseline problem, corrections on each thermogram were made by deducting the thermogram area obtained by averaging several thermograms of blank samples. In addition to the baseline correction, corrections of temperature were also considered, due to the difference in the

Materials and Methods

measured temperature of the sample and that recorded by the electric tube furnace (Figure 3.10 (3)). An independent measuring thermocouple was fused directly into the quartz tube in which the sample was located, which gave precise temperature readings and, after several experiments, the average of the obtained temperature data was calculated and deducted from the data recorded by the electric tube furnace to provide a correct temperature function.

The sample boat (Figure 3.10, (4)) was carefully positioned in the middle of the quartz tube, which was heated from room temperature to the maximum temperature at a linear heating rate of approximately $2.2\text{ }^{\circ}\text{C min}^{-1}$. The maximum temperature was $800\text{ }^{\circ}\text{C}$. Nitrogen (99.996%) was used as a carrier gas to flush Hg vapour released from the sample through the measurement train at a flow rate of 1 l min^{-1} . Mixture samples of at least two pure Hg compounds, mixed with substrate, were heated to $750\text{ }^{\circ}\text{C}$. Gypsum samples and spiked gypsum samples were heated to a maximum temperature of $700\text{ }^{\circ}\text{C}$.

Data interpretation: Data were interpreted by Lumex software as a signal for continuous measurement of the concentration in ng m^{-3} shown on the ordinate axis as a function of time in seconds displayed on the abscissa axis. Due to the known heating rate and precise temperature readings, the concentration signal per time was adapted to the concentration signal per temperature in $^{\circ}\text{C}$ to observe Hg release on increment of temperature.

Total Hg in solid samples: For quantitative determination of Hg in gypsum samples, around 0.5 g of the sample was digested in an acidic solution of $\text{HNO}_3\text{-HClO}_4$ in a ratio of 1:1 (2% v/v) and H_2SO_4 (5% v/v) in Milli-Q water at $240\text{ }^{\circ}\text{C}$ for 20 minutes. After the digestion process, Hg content was determined by the CV AAS method (Automatic Mercury Analyser Model Hg-201, Sanso Seisakusho Co., LTD). At least two replicas were prepared and measured for every sample but, for testing the homogeneity of samples, the same procedure was used whereby 6 replicas were prepared and tested to check the repeatability of the measured Hg concentration.

Preparation of pure Hg compounds: three different Hg compounds (Table 3.3) were chosen for examination (HgS , HgCl_2 , HgSO_4). The mass of the sample in the sample boat had to be as small as possible to not exceed the upper limit of detection of the measuring equipment. It did not usually exceed a few micrograms.

Pure Hg compounds were “diluted” by mixing them with SiO₂ (Merck KGaA; purity of substance is 99 – 100.5% calculated on calcinated substance) powder as a substrate. Each pure Hg compound (1-4 µg) was added to 5 g of substrate powder. The mixtures were carefully homogenized by mixing in a zirconium container placed in a planetary mill (Fritsch planetary mill Pulverisette 7) with two milling stations, each one filled with seven balls (10 mm diameter). The bulk homogeneity of the prepared mixtures was checked by 6 independent analyses of total Hg. A sample weighing from 80-140 mg was acid digested and Hg determined by CV AAS after reduction with SnCl₂ (Akagi and Nishimura, 1991). When pure Hg compounds mixed with both substrates were tested, 10 – 30 mg of the sample was weighed in the sample boat for testing by the temperature fractionation method and only 0.4 – 10 mg for testing by mass spectrometry.

Table 3.3. Type of Hg Compound, Suppliers and Purity.

Hg compound	Supplier	Declared purity of Hg compound
HgS- red	Mallinckrodt Chemical Works	99%
HgCl₂	Kemika d.d., Zagreb	99%
HgSO₄	Sigma-Aldrich Co. LLC.	99%

3.11. INTERPRETATION OF MERCURY FRACTIONATION BY COUPLING TD WITH SEP

To characterize and improve interpretation of thermo-desorption diagrams, the seven steps SEP (See section 3.8.3) was coupled with TD (see section 3.11). Thermodesorption has been carried out on native soil, and on residues after each extraction step of SEP.

A soil from Isonzo river banks (sample C13, 0-40 cm deep) and a sediment from Banduzzi channel were used for comparison of different matrix, source and characteristics of pollution.

The solid residue left from each extraction step was measured with TD to identify Hg fractions left in the residue. Each solid residue was dried in a drying oven at 20 °C and homogenized in a rotating ceramic ball mill for 15 min. Care was taken to avoid any cross-contamination during the whole sample preparation, including the sequence of

samples treatment: samples with higher Hg concentration were processed and analyzed after samples with lower Hg concentration.

3.12. SOIL SPIKING WITH MERCURY-HUMIC SUBSTANCES

To confirm TD peak interpretation, native soil (C13) was measured after spiking with Hg bound to humic and fulvic acids (Humic Acids-Hg and Fulvic Acids-Hg).

Humic and Fulvic Acids (HA and FA) were extracted from a woodland soil (Cambic Calcisol, Gleyc) according to the procedure described in De Nobili et al. (2008). Briefly, soil was extracted with 0.1M $\text{Na}_4\text{P}_2\text{O}_7$ plus 0.1M NaOH solution at soil to solution rate 1:10 under shaking for 1 h under N_2 . Humic acids were precipitated by acidification with H_2SO_4 to $\text{pH} < 2$, whereas FA were isolated by solid phase extraction (SPE) on crosslinked polyvinylpyrrolidone (PVP: Polyclar Aldrich). An appropriate aliquot of HgCl_2 solution (1000 mg l^{-1}) was added to HA and FA solutions ($\text{pH} 7$), and left to react overnight in a shaker. Then Hg-FA and Hg-HA were dialyzed to remove eventual uncomplexed Hg^{2+} and excess of salts. Total Hg concentration in HA-Hg and FA-Hg solutions was measured with direct Hg analyzer (LECO[®] model AMA-254).

Hg enriched humic solutions were used to spike the native soil (C13 sample) in an appropriate proportion to add 25, 50 and $100 \text{ mg Hg kg}^{-1}$ soil. Spiked soil samples were then air dried and homogenized before TD analysis.

3.13. EFFECT OF FERTILIZERS ADDITION ON MERCURY STABILITY

To assess potential changes in Hg stability, solubility and volatility caused by fertilizers addition, either mineral or organic fertilizers were added to soil sample C13. Fertilizers were added to fresh soil singularly, as solid powder as well as dissolved in distilled water (Figure 3.12).

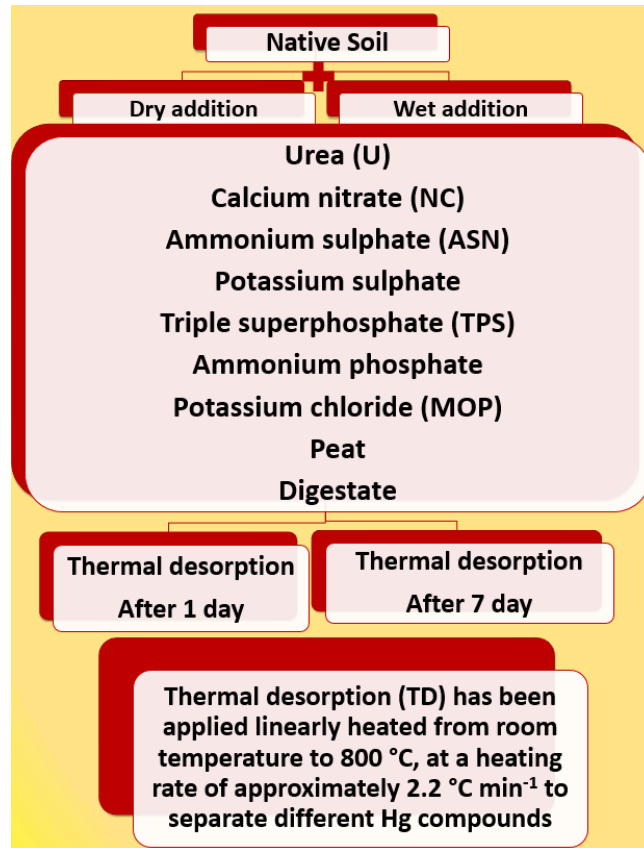


Figure 3.12. Scheme of the experimental setting with fertilizers.

The mineral fertilizers tested were: urea, calcium nitrate, ammonium sulphate, potassium sulphate, potassium chloride, triple superphosphate, diammonium phosphate (Table 3.4). Organic amendments tested were: peat and a residue from anaerobic digestion plant (digestate) (Table 3.5). The amount of each fertilizer was calculated taking into account the usual application rate to soil in crop cultivation. Each treated soil was incubated in a thermostated oven at 20 °C for 7 days.

After 1 and 7 days of incubation it was analyzed both for thermo-desorption and water solubility tests (paragraph 3.15).

Samples were homogenized in a rotating ceramic ball mill, with two milling stations, each one filled with seven balls (Fritsch planetary mill Pulverisette 7) for 15 min at room temperature. Care was taken to avoid any cross-contamination of samples: ceramic containers and balls were carefully cleaned after each sample. About 100 mg of soil were used for TD.

Materials and Methods

Table 3.4. Application doses for some fertilizers commonly used for arable crops (corn). Application rate of N (300 kg ha⁻¹), P (100 kg ha⁻¹ P₂O₅), K (100 kg ha⁻¹ K₂O) in a depth of 5 cm.

Fertilizer	Nutrient content	Application rate	
	(%)	(kg ha ⁻¹)	(mg g ⁻¹)
<i>Nitrogen</i>			
Ca(NO ₃) ₂	16	1875.00	2.88
(NH ₄) ₂ SO ₄	21	1428.57	2.20
Urea	46	652.17	1.00
<i>Phosphorus</i>			
(NH ₄) ₂ HPO ₄	46	217.39	0.33
Ca(H ₂ PO ₄) ₂ H ₂ O	46	217.39	0.33
<i>Potassium</i>			
KCl	60	166.67	0.26
K ₂ SO ₄	40	250.00	0.38

Soil density: 1300 kg/m³

Table 3.5. Application of organic amendments commonly used for arable crops (corn).

Organic amendment	Rate fresh material (t ha ⁻¹)	Moisture (%)	Dry Matter (t ha ⁻¹)	Application rate (g m ⁻²)	Concentration of amendment (mg g ⁻¹ soil)
Digestate*	100	95	5.00	500	7.69
Peat	100	95	5.00	500	7.69

Soil density: 1300 kg/m³; *Giardini, L. (2002). Agronomia generale ambientale e aziendale. Patron Editore.

Soil dept of 5 cm.

3.14. VOLATILIZATION AND SOLUBILIZATION EXPERIMENT

Inorganic and organic fertilizers as well as root exudates model molecules were tested to assess the effect on Hg reduction/volatilization and solubilization from Fossalon soil (sampling point C13, 0-40 cm deep).

The experimental apparatus consisted of two connected glass containers (Gas washing bottles, Drechsel pattern), called “reactor” and “trap” (Figure 3.13 and Figure 3.14). The reactor bottle contained 35 g of soil (aerobic incubations) or soil covered with 100 ml of solution (either water or a solution of tested amendment, for anoxic incubations). The trap bottle contained an oxidizing solution (100 ml of 0.1 M KMnO_4 in 10% w/v HNO_3). Each container was capped and fitted with silicone and Teflon™, and covered with an aluminum foil to exclude light. These two containers were tightly connected with Teflon tubes and the reactor was connected with a gas supply, nitrogen for anaerobic incubations or synthetic air for aerobic incubations. This apparatus was set out according to Stallings (2013). Experiments were conducted for 30 days at room temperature. The trap solution was replaced after 15 days with fresh oxidizing solution. Every 5 days, gas was flushed through the reacting solution, to remove Hg^0 from the solution and from the headspace of the reactor and oxidize to Hg^{2+} in the trap container. At the end of the incubation period, redox potential was measured in all reacting solutions. Hg in solutions (reactor solution, trap solution and aerobic soil stirred overnight with 100 ml of water) was analyzed by ICP-MS (Section 3.9.3).

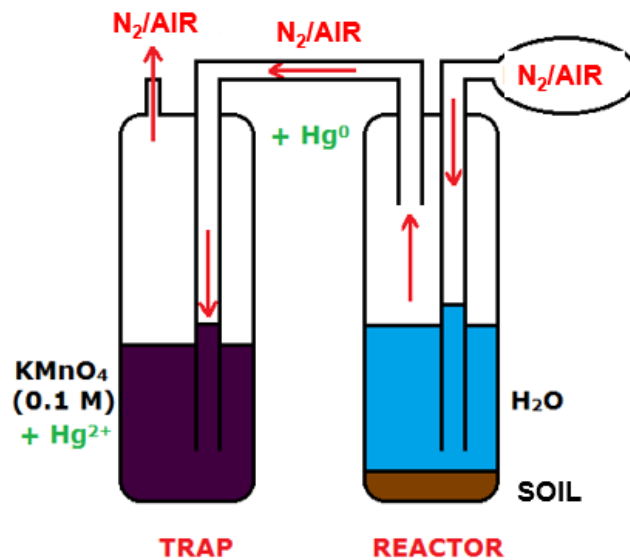


Figure 3.13. Scheme of the incubation experiments.

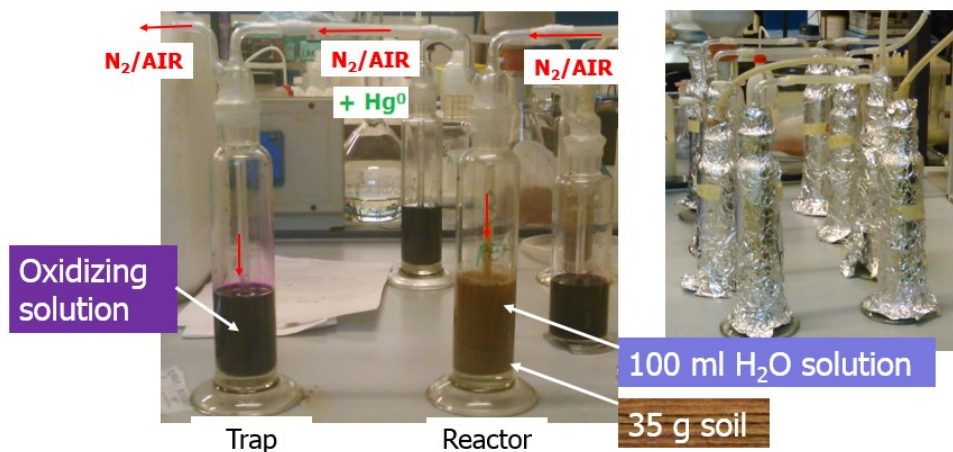


Figure 3.14. Picture of the incubation experiments.

3.14.1. Experimental set up

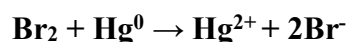
Experiments were conducted at room temperature for 60 days. The trap solution was replaced after 20 days with fresh oxidizing solution.

Then, according to these preliminary results, the next experiments were conducted over a period of 30 days, in oxic and anoxic conditions, mainly with addition of reductants and complexants. The trap solution was replaced after 15 days with fresh oxidizing solution. In Table 3.6 all the theses investigated are shown.

Table 3.6. Conditions of incubation experiments.

Treatment	Redox state	Concentration
Control	Aerobic	--
	Anaerobic	--
Poultry manure	Aerobic	0.14 g g ⁻¹
	Anaerobic	0.14 g g ⁻¹
Compost	Aerobic	0.14 g g ⁻¹
	Anaerobic	0.14 g g ⁻¹
Humic Acids	Aerobic	4.28 mg C g ⁻¹
	Anaerobic	4.28 mg C g ⁻¹
KCl	Aerobic	0.26 mg g ⁻¹
	Anaerobic	0.26 mg g ⁻¹
Urea	Aerobic	1 mg g ⁻¹
	Anaerobic	1 mg g ⁻¹
Gallic Acid	Aerobic	10 ⁻³ M
	Anaerobic	10 ⁻³ M
L-Aspartic Acid	Aerobic	10 ⁻³ M
	Anaerobic	10 ⁻³ M
L-Glutathione	Aerobic	10 ⁻³ M
	Anaerobic	10 ⁻³ M
Malic Acid	Aerobic	10 ⁻³ M
	Anaerobic	10 ⁻³ M

Upon completion of an experiment, 10 ml of sample was filtered through a 0.45 µm filter and immediately transferred to a glass test tube containing 250 µl concentrated HCl (Optima Grade) and 100 µl 0.1 M bromide/ bromate solution (Br⁻ /BrO₃⁻; Teledyne Leeman Labs) to form bromine (Br₂). Hg⁰ is oxidized by Br₂ according to the following reaction, which maintains the Hg stable in solution until analysis:



The sample was allowed to oxidize (confirmed by a persistent yellow color) for at least 30 min (maximum digestion time of 4 h), after which 400 µl of 10% (w/v) hydroxylamine (NH₂OH) was added to expel any un-reacted bromine. Some solutions, particularly those with KMnO₄, required excess NH₂OH (400 – 1600 µl). The concentration for these solutions was adjusted for the dilution. The test tube containing a 10 ml sample and digestion reagents was analyzed by ICP-MS (Section 3.9.3).

3.15. WATER LEACHING TEST

Water leaching test was carried out using 5 g of homogenized sample (native soil and soil treated with fertilizers). The sample weight to water volume ratio was of 5 to 10 ml of Milli-Q water added to the solid and subjected to end-over-end shaking at 250 rpm overnight. The vials were then centrifuged at 3,500 rpm for 15 min, the supernatant liquid decanted and analyzed in three replicates with CV AAS method (Automatic Mercury Analyser Model Hg-201, Sanso Seisakusho Co., LTD Instrument Model 910, Japan).

3.16. QUALITY CONTROL AND QUALITY ASSURANCE

All solutions were prepared from reagent-grade chemicals and before use they were tested and found to contain very low amounts of Hg (less than 10 ng l^{-1}). Analytical procedures were conducted using ultra-clean glassware, to avoid contaminating sample extracts. Care was taken to avoid cross- contamination of the samples. Each set of samples extracted included one blank, to check if both material and reagents were mercury free, and a certified reference material was also checked. Three replicates of each sample were taken for all analytical procedures, as well as blanks. The accuracy of Leco AMA-254 was assessed daily by the analysis of certified reference material (MESS-3, and PASC-2). Recoveries were within the range 80–120%. Moreover, recovery of the SEP procedure (ranging from 91-99%) were found to be acceptable.

4. RESULTS AND DISCUSSION

The results are arranged in four main parts:

1. Results of soil survey and characterization of the investigated area;
2. Results of Hg fractionation through Sequential Extraction Procedures;
3. Interpretation of thermodesorption curves by comparison with a seven steps sequential extraction procedure;
4. Investigation of the potential Hg mobilization (solubilisation and volatilization) caused by addition of either mineral and organic fertilizers and addition of organic molecules representing root exudates.

4.1. SOIL SURVEY AND CHARACTERIZATION

Six points were selected in the area of interest according to the preliminary characterization carried out by the Consorzio di Bonifica Pianura Friulana (2013).

Concentration of potentially toxic elements (PTE) in the top horizon (0-40 cm deep) shows that in the study area the only element present as a pollutant in concentrations higher than threshold limits (D.Lgs 152/2006) is Hg (Table 4.1).

Indeed, concentration of As, Cd, Cr, Cu, Ni, Pb and Zn are well below the legislation limits (D.Lgs 152/2006 "Testo Unico Ambientale", Parte quarta, Allegato 5), whereas Hg ranges between 7.32 to 50.58 mg kg⁻¹ in the top soil. These values are 1.5-10 times higher than the threshold limit for industrial and commercial use of soil, respectively 1 and 5 mg kg⁻¹. A general gradient in the direction of the Isonzo river is evident. Hg distribution in the area is confirmed also by the results of the "Piano di caratterizzazione di un'area agricola in località Fossalon di Grado" (Consorzio di Bonifica Pianura Friulana, 2013).

This Hg contamination is not attributable to a point source of pollution, but is coherent with a long-term gradual deposition of contaminated particulate material from the Isonzo river, transported from the Idrja mine (SLO).

Further monitoring has concerned the distribution of Hg in the study area along the soil profile.

Table 4.1 Concentration (mg kg^{-1}) and standard deviation ($n=3$) of potentially toxic elements in the top 0-40 horizon of six sampling points. Threshold concentration of contamination in the soil and subsoil referred to the specific intended use of the sites to be reclaimed (D.Lgs 152/2006).

Sampling point	As	Cd	Cr	Cu	Mn	Ni	Pb	Zn	Hg
C 9	1.6 ± 0.2	0.6 ± 0.3	38.9 ± 5.2	29.2 ± 3.9	725 ± 102	60.9 ± 7.9	14.6 ± 1.5	59.4 ± 9.1	7.3 ± 0.9
C 12	3.8 ± 0.6	0.5 ± 0.03	19.5 ± 0.7	14.7 ± 0.5	356 ± 38	29.8 ± 0.9	10.4 ± 0.5	42.2 ± 0.6	48.2 ± 3.8
C 13	3.1 ± 1.2	0.2 ± 0.1	49.8 ± 5.6	24.9 ± 1.3	536 ± 35	52.2 ± 6.2	15.4 ± 1.2	64.5 ± 3.6	50.6 ± 2.6
C 22	3.5 ± 0.1	0.4 ± 0.1	38.1 ± 1.3	14.8 ± 1.2	487 ± 42	34.5 ± 5.7	28.7 ± 1.9	53.9 ± 5.7	16.4 ± 1.4
C 23	1.7 ± 0.9	0.3 ± 0.3	30.8 ± 3.3	52.6 ± 5.2	483 ± 67	44.2 ± 6.6	8.9 ± 1.5	102.7 ± 11	15.2 ± 2.4
C 31	13.1 ± 4.8	0.2 ± 0.1	54.4 ± 4.9	58.5 ± 2.9	687 ± 52	80.3 ± 4.2	14.6 ± 0.5	128.4 ± 8.2	30.9 ± 2.0
Threshold limits									
Residential use	20	2	150	120	-	120	100	1	1
Industrial use	50	15	800	600	-	500	1000	350	5

Hg concentrations in soil from four different depths up to 120 cm are given in Table 4.2. This table shows that there is not a unique trend of contamination along the soil profile in the 0-120 cm depth. Hg concentration is generally higher in the top horizons. However, in some samples the layer 60-80 cm shows a lower Hg concentration than the deeper horizon (80-120 cm). There are no evidences that Hg mobilized along the soil profile, e.g. through leaching, and therefore we may hypothesize that Hg in the top profile is tightly retained to the solid soil particles.

Table 4.2. Total mercury concentration along soil profiles in the six sampling points.

Sampling point	Depth (cm)	Total Hg (mg kg⁻¹)
C 9	0-40	7.3 ± 0.9
	40-60	5.8 ± 1.1
	60-80	3.6 ± 0.8
	80-120	6.7 ± 2.1
C 12	0-40	48.2 ± 3.8
	40-60	21.5 ± 1.3
	60-80	9.2 ± 2.2
	80-120	30.9 ± 1.1
C 13	0-40	50.6 ± 2.6
	40-60	51.1 ± 6.4
	60-80	29.6 ± 1.7
	80-120	21.3 ± 3.2
C 22	0-40	16.4 ± 1.4
	40-60	14.5 ± 3.6
	60-80	10.6 ± 1.6
	80-120	8.7 ± 1.1
C 23	0-40	15.2 ± 2.4
	40-60	11.4 ± 1.5
	60-80	6.4 ± 1.1
	80-120	3.3 ± 0.6
C 31	0-40	30.9 ± 2.0
	40-60	47.0 ± 5.4
	60-80	26.9 ± 2.2
	80-120	36.0 ± 1.7

4.1.1. Pedological characterization of soil profile

The pedological study was carried out by analyzing the entire soil profile in correspondence to the sampling point identified as C23.

Variable soil textures were observed in this profile: Silty clay loam; Silty loam; Sandy loam; Loamy sand; Sand; Loam (Table 4.4).

As it was demonstrated by the soil survey (Table 4.3), the layers of the soil under study, come from sediments originated by the Soča-Isonzo river. The Soča-Isonzo river basin is in fact characterized by a significant presence of alluvial rocks with carbonates, which are typically present in sediments and water. Along the profile, below horizon 3C, a former soil has been buried by sediments deposited during river floodings.

Soil pH is sub-alkaline, due to abundance of carbonates, the typical pedogenetic substrate. Soil cation exchange capacity is low in 5C, 6A, 7C, due to the high sand content.

The pattern of EC along the soil profile highlights two points of salts accumulation driven by the following processes:

1. capillary rise from groundwater;
2. leaching of salts from the surface, by precipitations.

The relatively high molar C:N ratio throughout the profile may be attributed to the terrestrial origin of organic matter (Cifuentes, 1991).

From the literature, it is well known the paramount relevance of Hg speciation and mobilization in soils and soil mineralogical and chemical composition, along with particle-size distribution (e.g. Fernandez-Martinez et al., 2006; Reis et al., 2010; 2016). Thus, it is of primary importance to discuss Hg speciation in light of the physicochemical characterization of the soil under study.

Hg mobility in soil systems is determined by a number of factors (Kim et al., 2000):

- the mineralogical form of Hg in the soil,
- the concentration and type of organic and inorganic complexing ligands,
- the pH,
- the redox potential,
- the concentration of other elements.

For example, it is known that in the presence of organic matter Hg is effectively bound and retained to soil humic substances (Sladek and Gustin, 2000; Biester et al., 2002; WHO/IPCS, 2002). Moreover, under oxidizing conditions, hydrous oxides of Fe and Mn are excellent scavengers of Hg (Coker, 1995); pH affects all adsorption mechanisms and

the complexing of metals in the soil solution (U.S. EPA, 2002; Loredo et al., 2003), thus alkaline pH decreases the mobility of all metals.

Generally, this soil shows high pH together with high contents of carbonates, which may contribute to Hg complexation, precipitation and inhibit its mobilization. Another possible factor controlling the mobilization of Hg is the content of Ca, since the presence of Ca^{2+} may even make Hg less prone to mobilization (Melamed and Villas, 2000).

Table 4.3. Soil profile description. GENERAL FEATURES: Holocene Floods with water table at 200 cm. Headland at the side of a drainage ditch. COORDINATES: X: 2404985.54; Y: 5065087.10. LOCATION: Fossalón di Grado.

Horizon	Dept (cm)	Lower Boundary	Colour	Colour of Mottles	Texture	Structure	Special Features
A (1)(2)(3)	40	Smooth, Abrupt	5Y 4/4		Silty Clay loam (SCL)	Angular blocky, Medium and coarse, Strong, Very hard	
2C	50	Smooth, Abrupt	5Y 4/4/ 5Y 5/6		Sand/Silty loam (S/SiL)	Massive and hard/ Single grain	Succession of sandy and finer- textured layers
3C	59	Smooth, Abrupt	2.5Y 5/6		Loamy sand (LS)	Single grain	
4A	70	Smooth, Abrupt	5Y 5/2	10YR 4/6, 10%, faint	Sandy loam (SaL)	Subangular blocky, Fine and medium, Weak, Soft	Mottles related to roots of Common Reed
4Bw	100	Smooth, Clear	5Y 5/3	10YR 4/6, 10%, prominent	Sandy loam (SaL)	Subangular blocky, Fine and medium, Weak, Soft	Mottles related to roots of Common Reed, shells
5C	125	Smooth, Abrupt	5Y 6/4	10YR 4/6, 5%	Sand (S)	Single grain	Mottles related to roots of Common Reed
6A	142-150	Smooth, Abrupt	5Y 2.5/1		Loam (L)	Massive	Organic material with low grade of decomposition, slating layer with lower end towards west
7C	165	Smooth, Abrupt	5Y 6/4	10YR 4/6, 5%	Sand (S)	Single grain	Same as 5C, but with fine loam masses (from 6Cg erosion?)
8Cg	170	Smooth, Abrupt	5Y 5/1		Sand (S)	Single grain	Gley
9Cg	173	Smooth, Abrupt	3N		Sandy loam (SaL)	Massive	Gley
10Cg	185	Smooth, Abrupt	5N		Sand (S)	Single grain	Gley
11Cg	200+	Smooth, Abrupt	2.5N		Sandy loam (SaL)	Single grain	Gley, water table at the bottom, sulphide smell

Table 4.4. General characterization of soil profile C23: texture, particle size, pH, soil salinity, redox potential, total lime content, cation exchange capacity, nitrogen and organic carbon.

Horizon name	Depth	Texture	Sand	Silt	Clay	pH	EC	Eh	Total lime	CEC	Organic C	N tot	C/N ratio
	cm	(USDA)		% w/w		-	mS m ⁻¹	mV	g kg ⁻¹	cmol·kg ⁻¹		%	-
Ap1	10	SCL	15.0	50.0	35.0	8.0	0.2	450	158.9	19.8	12.3	1.1	11.7
Ap2	25	SCL	16.0	52.0	32.0	8.1	0.2	446	158.9	19.8	9.0	0.6	14.3
Ap3	40	SCL	13.0	53.0	34.0	8.0	0.2	468	158.9	19.8	10.1	0.6	16.3
2C	50	SiL	37.6	50.1	12.3	7.8	0.4	432	102.9	14.5	4.2	0.2	19.0
3C	59	LS	78.1	15.1	6.8	7.9	0.6	348	102.9	14.5	3.4	0.2	16.7
4A	70	SaL	64.5	22.5	13.0	8.1	1.0	406	102.9	14.5	6.9	0.4	19.5
2Bw	100	SaL	61.5	25.0	13.5	8.2	1.3	151	102.9	14.5	4.0	0.3	16.3
5C	125	S	89.2	6.3	4.5	8.3	2.5	86	146.7	7.3	3.2	0.2	18.8
6A	150	L	45.3	39.1	15.6	8.7	3.1	-27	146.7	7.3	29.8	1.2	24.9
7C	165	S	86.5	9.7	3.8	8.8	2.8	150	146.7	7.3	1.0	0.1	14.4
8Cg	170	S	88.3	6.4	5.3	8.4	2.1	-255	146.7	7.3	1.0	0.1	21.1
9Cg	173	SaL	66.2	22.5	11.3	8.0	3.8	-184	67.9	19.2	7.6	0.8	9.9
10Cg	185	S	91.5	5.1	3.4	8.2	4.7	-196	67.9	19.2	2.3	0.2	10.3
11Cg	200	SaL	78.8	9.1	12.1	8.3	4.8	-280	67.9	19.2	15.7	1.1	13.9

(*) SCL: Silty clay loam; SiL: Silty loam; SaL: Sandy loam; LS: Loamy sand; S: Sand; L: Loam.

Results and Discussion

The correlation coefficients (r values) between total Hg and the physico-chemical characteristics of soil are listed in Table 4.5. High r values (0.817-0.665) were observed for the correlations of Hg with:

- Organic carbon,
- Silt,
- Sand,
- Clay,
- Eh,
- EC,
- pH

suggesting that the total Hg concentration may be influenced by multiple factors, among which sand, silt and organic carbon content have a significant effect.

It is not surprising that organic carbon correlates positively with Hg content, indeed, it has a strong binding affinity for Hg, and Hg is known to form stable complexes with organic matter. It can be hypothesized that organic matter bounds Hg and thus retains it in soil, hindering Hg from being mobilized along the profile (Liu et al., 2009). Sand content negatively correlates with Hg, whereas the relationship between silt, clay and Hg concentration is positive. Indeed Hg association with fine particles is well known (e.g. Fernandez-Martinez et al., 2006). Moreover, clay and Fe and Mn oxihydroxides are known to have a strong affinity for Hg.

The influence of salinity may be interpreted in relation to seawater intrusions that can bring NaCl into the soil. Chloride is able to complex and solubilize Hg, which may both reduce Hg adsorption onto soil particles and mobilize Hg in the soil solution (e.g. Schuster, 1991; Grassi and Netti, 2000). This process may explain why salinity correlates negatively with Hg content in the horizons.

The relationship between pH and Hg is negative, but with a low level of significance because pH value is almost constant. On the contrary, and surprisingly, redox potential and Hg correlates positively, which means that in anoxic condition Hg concentration is lower than in more oxidative conditions.

Table 4.5. Pearson correlation coefficients between Total Hg concentration and soil parameters.

	Sand	Silt	Clay	pH	EC	Eh	N tot	C Org
Pearson Coefficient	-0.811	0.817	0.738	-0.665	-0.806	0.814	0.345	0.811
Significance	***	***	**	*	***	***	n.s.	***

n.s.: not significant; *: P<0.05; **: P<0.01; ***: P<0.001

Table 4.6 reports Hg concentration along the soil profile, while Figure 4.1 and Figure 4.2 highlight the pattern of Hg distribution with depth.

Accumulation of Hg is observed in the most recent surface layers, as well as in the former surface layers buried by flood deposits in ancient times (4A, 4Bw). Then, Hg concentration decreases until about 200 cm where a sudden increase is observed just upon the groundwater line.

The reason of this increase can be found in the capillary rise of salty seawater that could transport and solubilize Hg. Indeed, Covelli et al. (2004) demonstrated the effect of capillary rise on soluble Hg compounds, e.g. HgCl₂, from the seawater and a subsequent reaction of Hg²⁺ with sulphides and formation of HgS in deep anoxic horizons.

It is well known that Hg accumulates in surface organic horizons. Indeed, several studies show that the majority of the total soil Hg is concentrated in the organic matter-rich A horizon (Driscoll et al., 1994; Lindberg, 1996). Lindberg (1996) showed that in the forest ecosystem of the Walker Branch watershed (Tennessee), the largest Hg pool resided in the soil, and that about 75% of the total Hg soil pool was in the organic A horizon. However, association of Hg with organic materials is favoured by acid pH, whereas in alkaline soils Hg tends to be mainly associated with metal oxides (e.g. Schuster, 1999). Xia et al. (1999) used synchrotron-based X-ray absorption spectroscopy and showed the importance of reduced sulfur functional groups of humic substances – thiol (R-SH) and disulfide (R-SS-R)/disulfane (R-SSH) – in the complexation of Hg(II). They further observed the involvement of oxygen ligands such as carboxyl and phenol moieties in addition to the reduced S ligands in the complexation of Hg(II), due to the low density of reduced S ligands in humic substances.

When the capacity for bonding to the reduced sulfur is filled, Hg may be attracted by –NH₂ and –COOH moieties, forming weaker bonds. (Han et al., 2006).

Results and Discussion

Moreover, the Hg bound to the organically bound fraction may increase its stability with time. The stability constants for Hg–organic sulfur complexes are between 10^{25} – 10^{32} (Ravichandran, 2004).

Table 4.6. Concentration of total mercury along soil profile.

Horizon name	Depth cm	Total Hg mg kg⁻¹
Ap1	10	12.0 ± 0.9
Ap2	25	15.8 ± 1.9
Ap3	40	15.6 ± 2.5
2C	50	14.2 ± 2.2
3C	59	9.2 ± 1.2
4A	70	13.6 ± 0.6
4Bw	100	13.1 ± 2.3
5C	125	3.0 ± 1.3
6C	150	6.2 ± 0.9
7C	165	0.06 ± 0.03
8C	170	0.07 ± 0.03
9C	173	6.7 ± 2.8
10C	185	0.2 ± 0.1
11C	200	22.8 ± 1.1

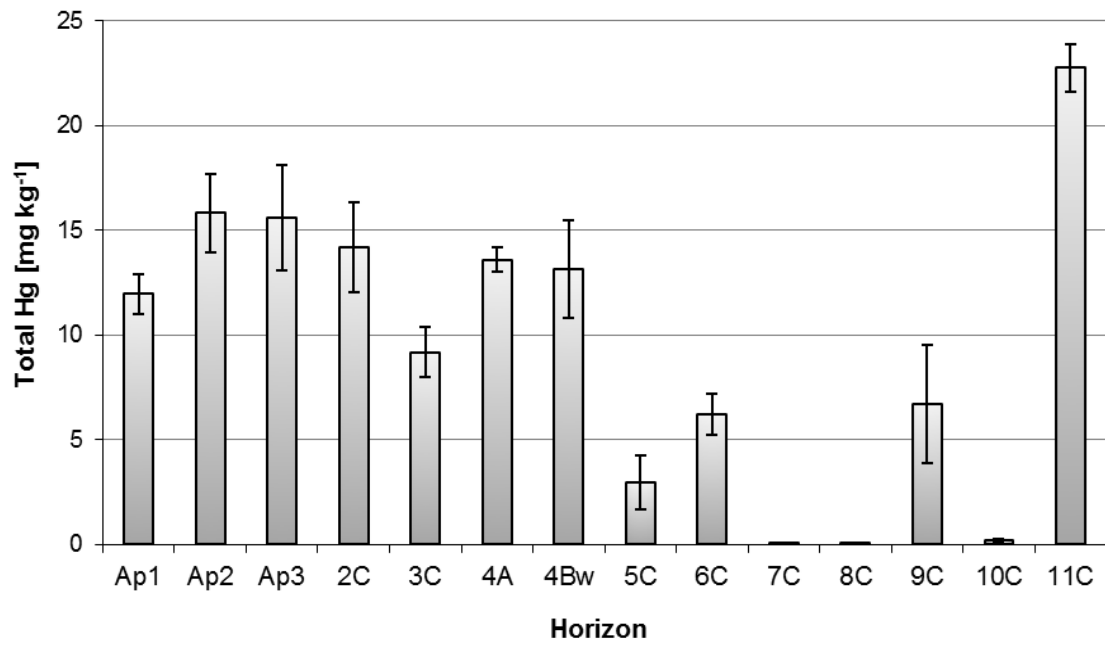


Figure 4.1. Concentration of total Hg in each horizon of C23 soil profile.

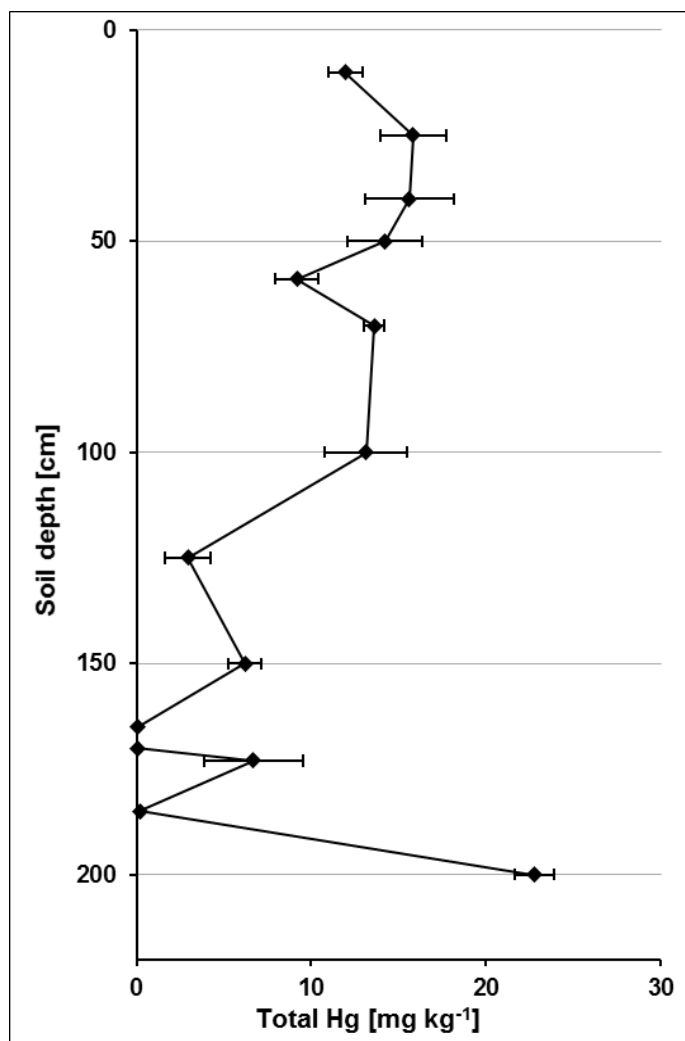


Figure 4.2. Total Hg concentration along the soil profile.

4.2.MERCURY SPECIATION/FRACTIONATION

Since different Hg species may exhibit different behavior, mobility and availability, measurements of total Hg in soils do not provide enough information on the potential toxicity of Hg in the soil (Beckvar et al., 1996; Biester et al., 2002). An assessment of the chemical forms of Hg in soil can be accomplished by the application of sequential extraction methods (Bloom and Preus, 2003; Fernández-Martínez and Rucandio, 2003; Han et al., 2003b) and is critical to evaluate its environmental risk.

Several different SEP have been proposed in the literature, which must be selected according to:

- type of matrix (e.g. physicochemical characteristics of soil and land use);
- Hg source (e.g. mining activity/chlor-alkali plant).

Since soil is a complex and variable matrix, different suitable SEP were chosen and applied to the soil under study.

Indeed, since SEP results are influenced by substrate matrix, the application and interpretation of such extractions should be carried out with caution and the substrate components with the environmental conditions associated have to be characterized (Reis et al., 2016).

4.2.1. Mercury distribution according to particle size

Table 4.7. Texture Partition of C 31 soil sample.

Texture fraction	Size	% w/w
Coarse Sand	< 2 mm and > 250 µm	11
Fine Sand	< 250 µm and > 20 µm	24
Silt	< 20 µm and > 2 µm	46
Clay	< 2 µm	19

Table 4.8. Organic C, total N and C/N ratio of particle-size fractions before and after heating at 180 °C.

	Native soil			Heated soil		
	Organic C g kg ⁻¹	Total N g kg ⁻¹	C/N ratio -	Organic C g kg ⁻¹	Total N g kg ⁻¹	C/N ratio -
Soil	14.1	1.3	10.5	10.0	1.2	8.3
Coarse Sand	20.1	1.3	15.1	13.8	1.2	11.7
Fine Sand	10.7	0.9	12.5	7.0	0.7	9.9
Silt	14.2	1.5	9.2	10.5	1.2	8.8
Clay	19.0	2.7	7.1	13.9	2.2	6.4

As it can be seen in Table 4.9, total Hg distribution among soil particles is not in accordance with previous works. Indeed, in the work of Fernandez-Martinez et al. (2006) total Hg content increases when the grain-size decreases, and it is typically triplicated in the finest subsample. However, in the work of Fernandez-Martinez et al. (2006), a large part of Hg comes from the condensation of vapors in the chimney of a metallurgical plant (Hg⁰), so it is reasonable that it was concentrated in the finest particle-size subsamples,

associated to the clay minerals. Whereas, in this work the speciation of Hg in a well-structured mineral form, coming from river floodings, may partially explain its presence in the sand fractions.

Moreover, the concentration of organic carbon is higher in the coarse sand fraction (as well as in the clay fraction), suggesting the possibility that Hg could be even bound to organic matter in the coarse sand fraction.

Besides, several works have demonstrated that non-cinnabar fractions may accumulate in fine grained particles, while cinnabar is more present in coarse grain materials (e.g. Biester et al., 2000; Tersic et al., 2011a).

Therefore, regardless of the total Hg concentration in the granulometric fraction, the speciation and thus the mobility of this element in each size-fraction could be different. Meaning that e.g. the 18.8 mg kg^{-1} Hg in the clay fraction may result to be more prone to mobilization than the 38.6 mg kg^{-1} Hg present in fine sand.

Indeed, regarding the Hg fractionation among the different granulometric fractions, in the clay fraction, 65% of Hg is just extracted in the first step of extraction compared to 46% (coarse sand), 20% (fine sand), 26% (silt) (Table 4.9). Whereas, the residual fraction accounted only to 9%. This means that Hg extraction was more complete in the clay fraction, compared to the other particle size fractions where 32% (coarse sand), 49% (fine sand) and 46% (silt) cannot be extracted (Table 4.9). The amount of Hg in the sulfide fraction is quite similar in all the fine fractions: 27% in fine sand, 29% in silt and 26% in clay. From this data it could be argued that the dimension of particles (fine particles) influences the amount of leachable Hg rather than HgS or, in other words, that the clay fraction contains easier leachable Hg compounds than sand fraction. This is in agreement with literature. Indeed, Fernandez-Martinez et al. (2006), who performed a SEP after particle size analysis, observed a higher Hg mobility in the subsamples with the finest grain size.

Moreover, the easier leachability of Hg in the clay fraction could be related to the organic carbon concentration (13.9 g kg^{-1}) further suggesting the presence of organic bound Hg in this fraction.

Accordingly, data from SEP are in agreement with literature, indeed, it has been found that Hg mobility markedly tends to increase when the grain-size decreases. Whereas, the coarsest subsamples accumulate a higher proportion of nonmobile Hg. This suggests that cinnabar particles, which show a great stability, may be present mainly in these

subsamples. On the other hand, Hg in the finest subsamples is more prone to mobilization. This higher reactivity is caused by the adsorption of Hg^{2+} or Hg^0 on clay surfaces or iron (hydr)oxides, favored by the high contact surface of these subsamples as a consequence of their small grain-size.

Finally, in this soil, the Hg mobility due to physical dispersion seems to predominate over the chemical dispersion.

Table 4.9. Sequential extraction procedure (Lerchler, 1999) from soil C31 and its particle-size fractions.

Texture	Fraction	Soil		Coarse Sand		Fine Sand		Silt		Clay	
		mg kg ⁻¹	%								
SEP	Fraction										
	Total Hg (AMA)	33.2		6.7		38.6		43.7		18.8	
F1	Volatile (180 °C)	8.5 ± 0.9*	25.6	3.1 ± 0.7	46.4	7.9 ± 1.9	20.5	11.6 ± 1.5	26.6	12.2 ± 0.2	64.9
F2	Exchangeable	0.1 ± 0.02	0.3	0.1 ± 0.01	2.0	1.1 ± 0.2	2.8	0.04 ± 0.00	0.1	0.03 ± 0.00	0.2
F3	Strongly bound	< d.l.	0.03	< d.l.	0.0	< d.l.	0.1	< d.l.	0.01	< d.l.	0.03
F4	Organic	< d.l.	0.03	< d.l.	0.1	< d.l.	0.1	< d.l.	0.03	< d.l.	0.1
F5	Sulfide	11.0 ± 1.3	33.2	1.3 ± 0.2	19.2	10.6 ± 1.3	27.4	12.5 ± 1.4	28.8	4.8 ± 0.4	25.7
F6	Residual	13.6 ± 3.1	40.9	2.2 ± 1.8	32.2	19.0 ± 6.9	49.3	19.5 ± 4.3	44.6	1.7 ± 0.6	9.1

* standard deviation (n=3)

4.2.2. Hg speciation through three steps Sequential Extraction Procedure

Table 4.10. shows thermal desorption of Hg⁰ at 80 °C, exchangeable, organic bounded and residual Hg extracted from Fossalon soil (sampling point C31, 0-40 cm deep and 40-60 cm deep). Figure 4.3 and Figure 4.4 show Hg extracted in each leaching solution. The bulk of the contamination is extracted in the residual fraction, while the easier mobile fractions, Hg⁰, soluble/exchangeable, organically bounded, are much less represented.

Table 4.10. Hg⁰ concentration desorbed from Fossalon soil at 80 °C, soluble plus excangable Hg, OM-bound Hg, resaidual Hg, total Hg.

SEP Fraction	0-40cm horizon		40-60cm horizon	
	Hg (µg kg ⁻¹)	%	Hg (µg kg ⁻¹)	%
Elemental Hg (80 °C)	542.3	1.3	1725.3	3.7
Soluble + EXC	26.3	0.1	8.0	0.02
OM bounded	337.5	0.8	406.5	0.9
Residual (AMA)	42727.1	93.4	37595.5	80.0
TOTAL AMA	39895.5		47008.9	

Results and Discussion

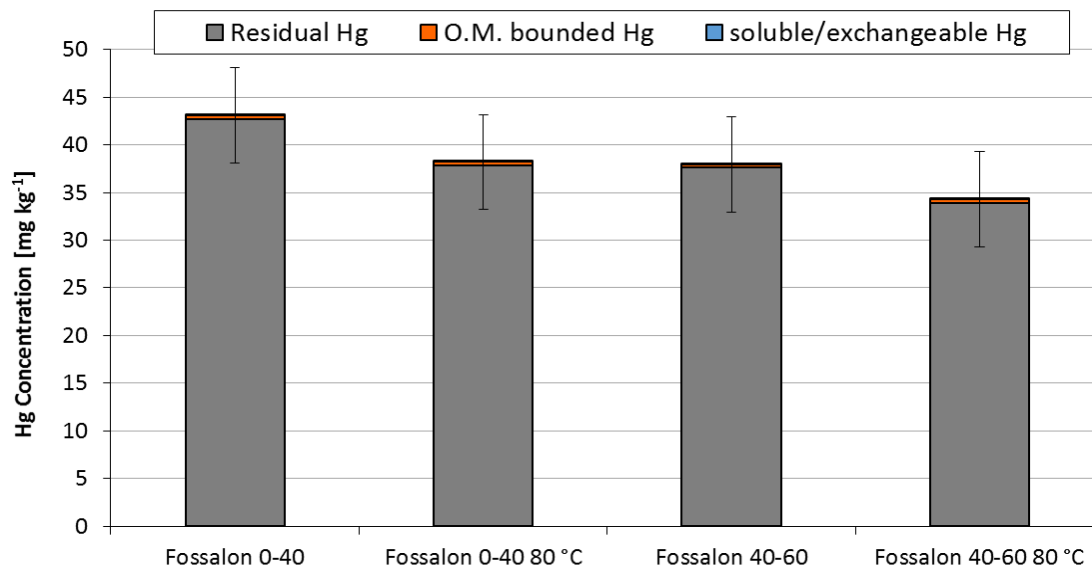


Figure 4.3. Hg concentration in the leachates of three steps SEP.

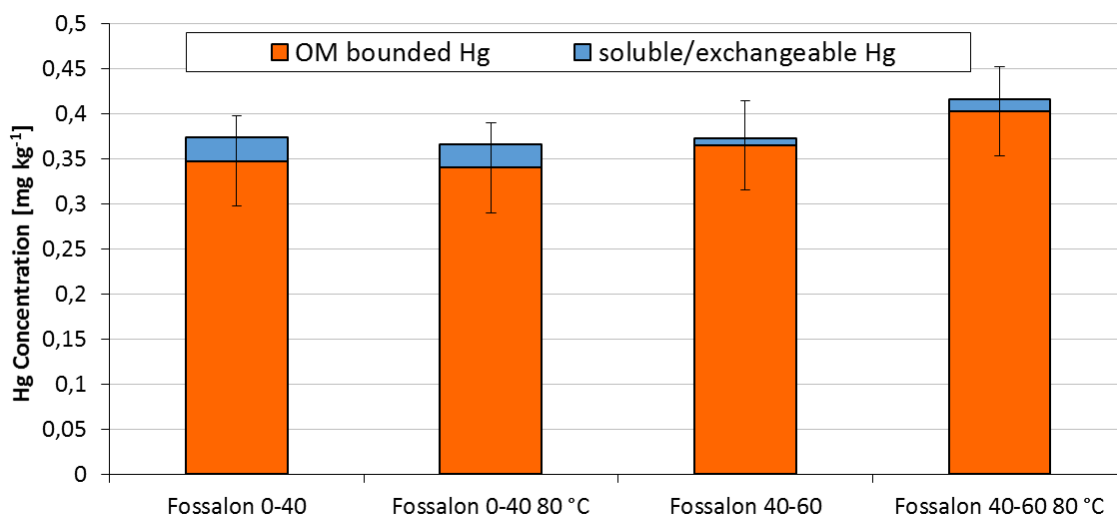


Figure 4.4. Hg concentration in the leachates of soluble plus exchangeable fraction and organic matter bound Hg.

4.2.3. Hg speciation according to Han et al.

This SEP was chosen based on the evidence that matrix substrate characteristics of Han et al. (2006) work were closer to the samples under study. Moreover, to check reliability of this procedure, another sample with different source of contamination was investigated.

This SEP was performed in parallel on Fossalon soil (sampling point C13, 0-40 cm deep) and on Banduzzi sediment.

Data in Table 4.11 are shown as total Hg concentrations in soil leachates:

1. soluble plus exchangeable (EXC-Hg);
2. easily reducible oxides or Mn oxides (ERO-Hg);
3. organic matter (OM-Hg);
4. amorphous Fe oxides (AmoFe-Hg);
5. crystalline Fe oxides (CryFe-Hg);
6. residual, non-cinnabar Hg fraction (RES-Hg)
7. cinnabar Hg (HgS).

An additional step was added in this work, consisting of a total Hg analyses (by AMA) on the soil remained after the seventh extraction step. This measurement was added because the sum of Hg extracted from the seven SEP was not able to account for the concentration of Hg measured on the soil before extractions. Indeed, it has been found that the Hg still present in the residue after SEP accounted for almost 43% in Fossalon soil and only 0.34% in Banduzzi sediment.

It is possible to rise the hypothesis that the soil to extractant ratio suggested by Han et al. (2006) was not sufficient to guarantee the complete dissolution of the high concentration of HgS in the Fossalon soil. This problem was not found in the Banduzzi sediment because the composition of Hg fractions was completely different.

This fractionation (Table 4.11, Figure 4.5) revealed that, in Fossalon soil Hg was mainly present in HgS phase, as well as in the last residue (34% and 43%). Residual non-cinnabar Hg species were the second most abundant fraction present in soil (14%). While, the mobile fraction represented a much lower contribution to the total Hg content.

Contrariwise, in Banduzzi sediment the most abundant fraction is OM-Hg (69%), followed by ERO-Hg (14%).

Hg found in the organically bound (H₂O₂- oxidizable) fraction may arise from three sources:

Results and Discussion

- the real organically bound Hg,
- partially extraction of Hg⁰,
- a possible Hg release from partial oxidization of HgS by H₂O₂ (Han et al., 2006).

Although the Hg fraction in the mobile phase generally did not exceed 0.09% of total Hg, given the high contamination of samples this fraction may still represent significant amounts of bioavailable Hg.

Additionally, although the more mobile Hg fractions are not identical to in situ pore water concentrations, it can be used as a first indicator for potential groundwater pollution or risk of metal leaching from soils.

Admissible limit for drinkable waters in Italy is 1 µg l⁻¹; EEC Regulation no. 80/788, converted to Italian law DPR 236, thus this soil does not represent a risk for leaching of pollutants in groundwaters.

However, considering that the soils in Fossalon are predominantly used for agricultural purposes, the presence of mobile and toxic Hg species, even in low concentrations, may be of concern. Indeed, because of the agricultural practices, these soils are subjected to human influence, including oxidation, by appropriate drainage and the application of fertilizers (Reis et al., 2010).

The recovery defined as the sum of extracted Hg fractions divided by the independently determined total Hg concentration is 91%, of which 34% is extracted in the HgS fraction alone.

Whereas, the recovery of extracted Hg from the sediment is 99%, of which 69% is extracted in the Organic Matter fraction (OM) alone.

These different recoveries can be explained by two aspects:

- soil complex structure make sample homogeneity and representativity more difficult to achieve;
- soil complex structure provides many different complexing site for Hg (well-structured mineral and organic aggregates) from which it could be difficult to scavenge.

Indeed recoveries far from 100% can be explained by the heterogeneity associated with soils. Because Hg is not homogeneously present in soil, it is likely that the aliquot taken for total Hg analysis does not have exactly the same Hg content as the one taken for Hg fractionation, despite the fact that each sample was thoroughly homogenised prior to analysis.

Another reason could be the loss of volatile Hg during the extracting process. The same problem was observed by Kocman et al. (2004). This recovery is, thus considered satisfactory.

Therefore, these results show that the H₂O₂-oxidizable Hg fraction (organically bound Hg) was the major solid-phase fraction in the Banduzzi sediment, while cinnabar fraction was the major solid phase fraction in Fossalon soil.

Different speciation between the soil and sediment is easily explained considering the different type of sample matrix and consequently strength of Hg bounds, as well as different source of pollution.

Indeed the Idrijca and the Soča-Isonzo rivers supply suspended material, mainly cinnabar particles in coarse grained material and organically bound Hg in fine grained material. This material has contaminated bank soils mainly during floodings (Biester et al., 2000). Whereas the sediment from Banduzzi channel, has been contaminated due to metallic Hg, used as electrode to separate sodium and chlorine from brine. In addition, at the same industrial site, cellulose was produced from cane (*Arundo donax* sp), which enriches sediments with organic carbon. Thus, these results are in agreement with previous studies on sediments of Grado marano lagoon. Piani et al. (2005) shown that, the most abundant Hg fraction in Idrijca-Isonzo river system is cinnabar, whereas the main Hg fraction transported by Aussa-Corno River system is organically bound Hg, which is potentially bioavailable.

Results and Discussion

Table 4.11. Hg concentration in SEP extracts.

SEP Fraction	Fossalon soil		Banduzzi sediment	
	Hg ($\mu\text{g kg}^{-1}$)	%	Hg ($\mu\text{g kg}^{-1}$)	%
EXC	< d.l.	0	222 \pm 19	0.09
ERO	3.8 \pm 0.11*	0.01**	32300 \pm 870	13.44
OM	10.3 \pm 0.25	0.02	165000 \pm 21000	68.65
AmoFe	16.8 \pm 4.1	0.03	19200 \pm 300	7.99
CryFe	38 \pm 5.9	0.08	10330 \pm 156	4.30
RES	7043 \pm 346	13.93	9850 \pm 140	4.10
HgS	17162 \pm 1605	33.93	167 \pm 5.8	0.07
Residue (AMA)	21679 \pm 1450	42.86	823	0.34
Total extracted	45954 \pm 2322	90.86	237892	98.98
TOTAL AMA	50579 \pm 10967		240342 \pm 21021	

* \pm standard deviation (n=3);

** percentage of recovery in each extracting step, and in the whole SEP, related to total Hg analyzed with AMA.

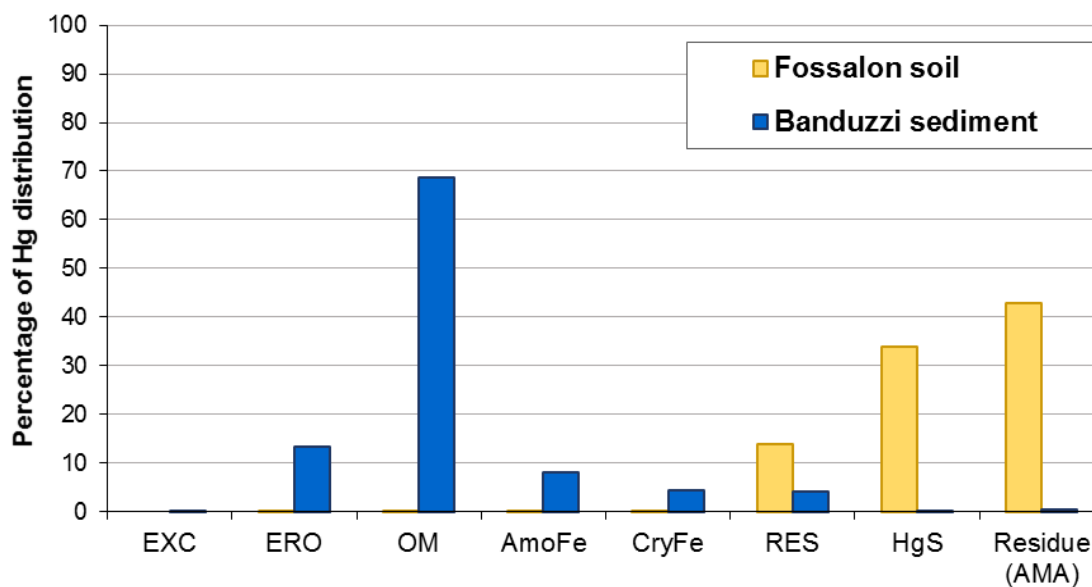


Figure 4.5. Percentage of Hg extracted in each SEP fraction.

4.3.COMBINATION OF SOIL MERCURY THERMAL DESORPTION CURVES AND SEQUENTIAL EXTRACTIONS

Hg solid thermal fractionation has been widely applied, both in soil as in sediments (Biester et al., 2000; Piani et al., 2005; Gosar et al., 2006; Teršič et al., 2011a; 2011b). However, a major problem of fractionation protocols is the lack of selectivity, meaning that it is only possible to distinguish operationally defined groups of compounds e.g “matrix-bound” Hg, not a single specie.

In fact, according to present knowledge, matrix components are known to exist as organo-mineral complexes. (Biester et al., 2000). Previous studies have shown that Hg pyrolysis combined with atomic absorption detector allowed to distinguish cinnabar from “matrix-bound” Hg also defined as non cinnabar compounds (Biester and Scholz, 1997). But, peaks overlapping among Hg bound to chloride, organic compounds and metal oxides remains an unresolved question.

In order to separately identify Hg species within the group of “matrix-bound” Hg, thermo-desorption measurements was performed after each SEP step.

In Figure 4.9 till Figure 4.30 the results are shown as graphs (thermo-desorption curves) of temperature versus the relative intensity of Hg peaks. Before elaboration, intensity outputs were divided with sample weight, to enable comparison of the results.

Pure Hg compounds (HgS, HgCl₂, HgSO₄) alone as well as mixture with silica and Gypsum, are measured as standards, to check released temperatures (Figure 4.6, Figure 4.7, Figure 4.8, Figure 4.9, Figure 4.10, Figure 4.11, Figure 4.12, Figure 4.13, Figure 4.14).

The different temperature release of Hg compound in presence of different substrates highlights the importance of matrix effect in TD curves interpretation (Sedlar, 2014).

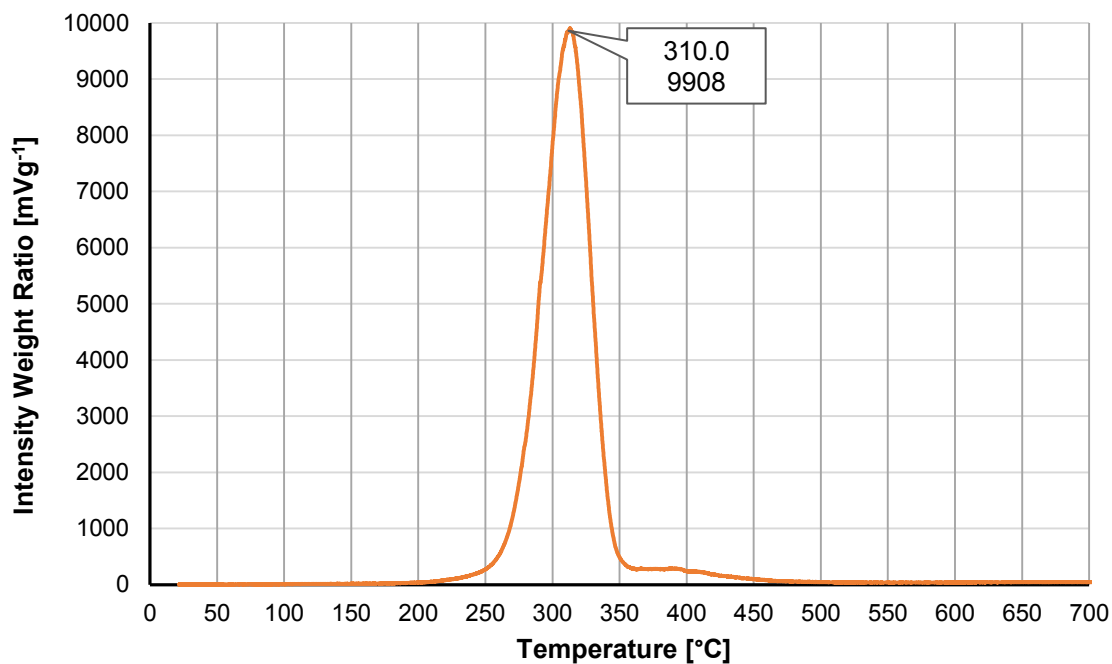


Figure 4.6. Thermo-desorption curve of Standard of HgS pure. Released temperature is plotted versus intensity/weight ratio.

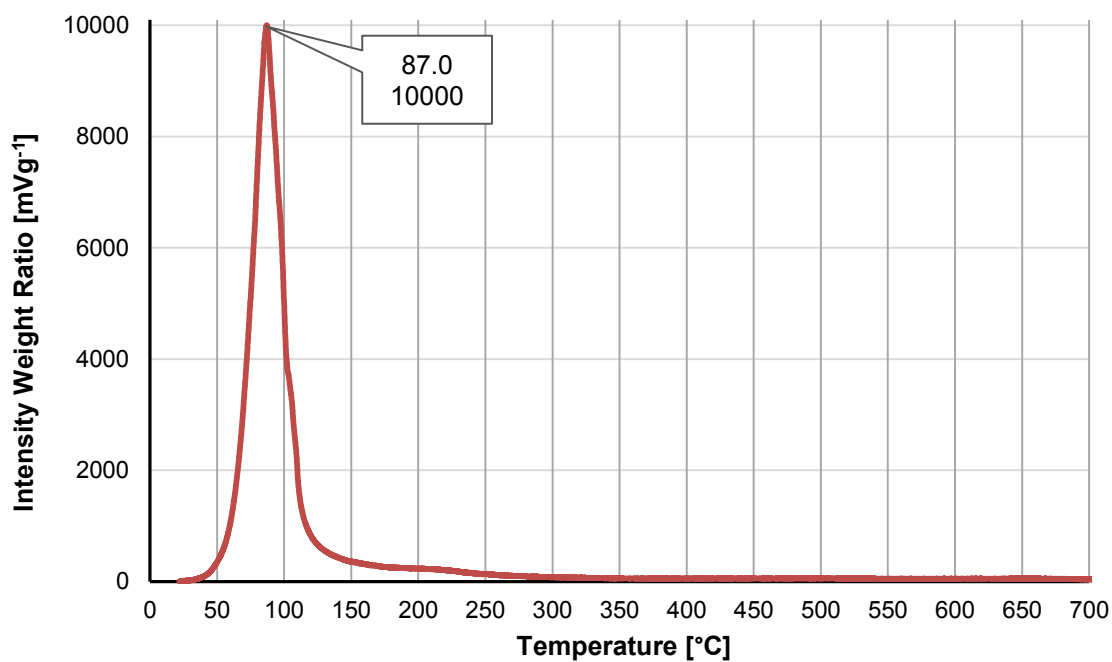


Figure 4.7. Thermo-desorption curve of Standard of HgCl₂ pure. Released temperature is plotted versus intensity/weight ratio.

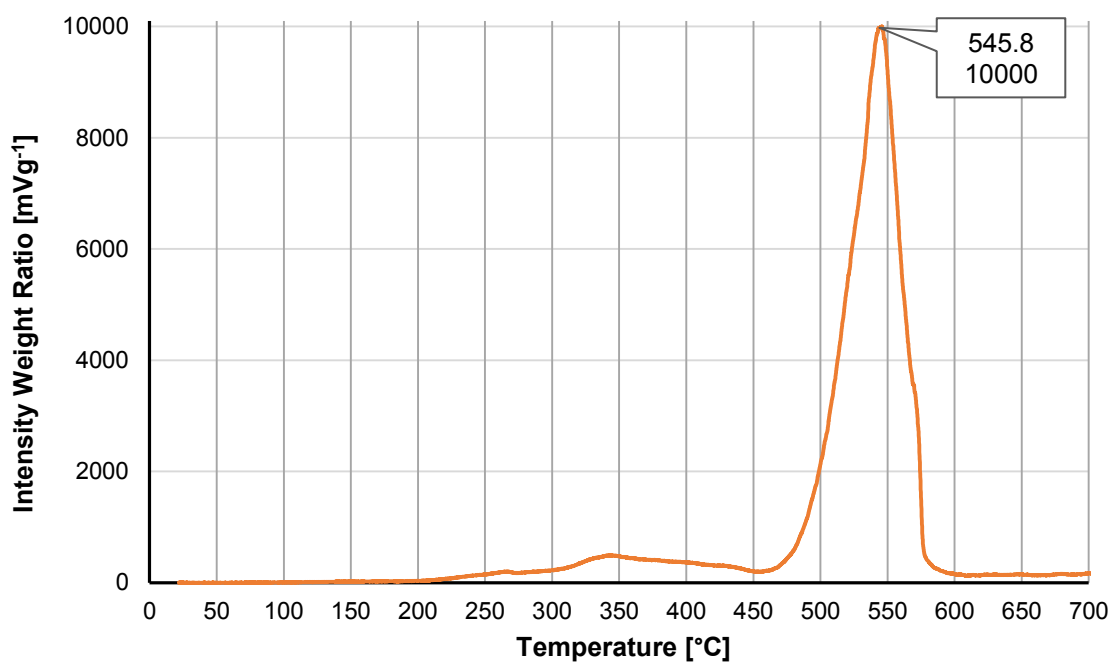


Figure 4.8. Thermo-desorption curve of Standard of HgSO_4 pure. Released temperature is plotted versus intensity/weight ratio.

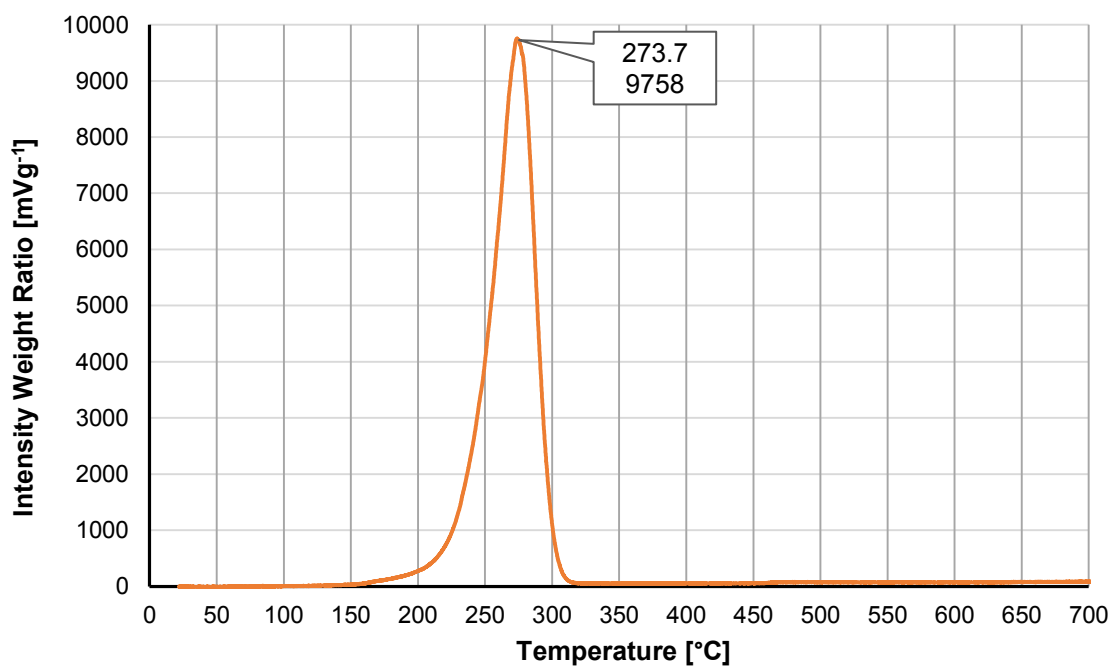


Figure 4.9. Thermo-desorption curve of Standard of HgS plus SiO_2 . Released temperature is plotted versus intensity/weight ratio.

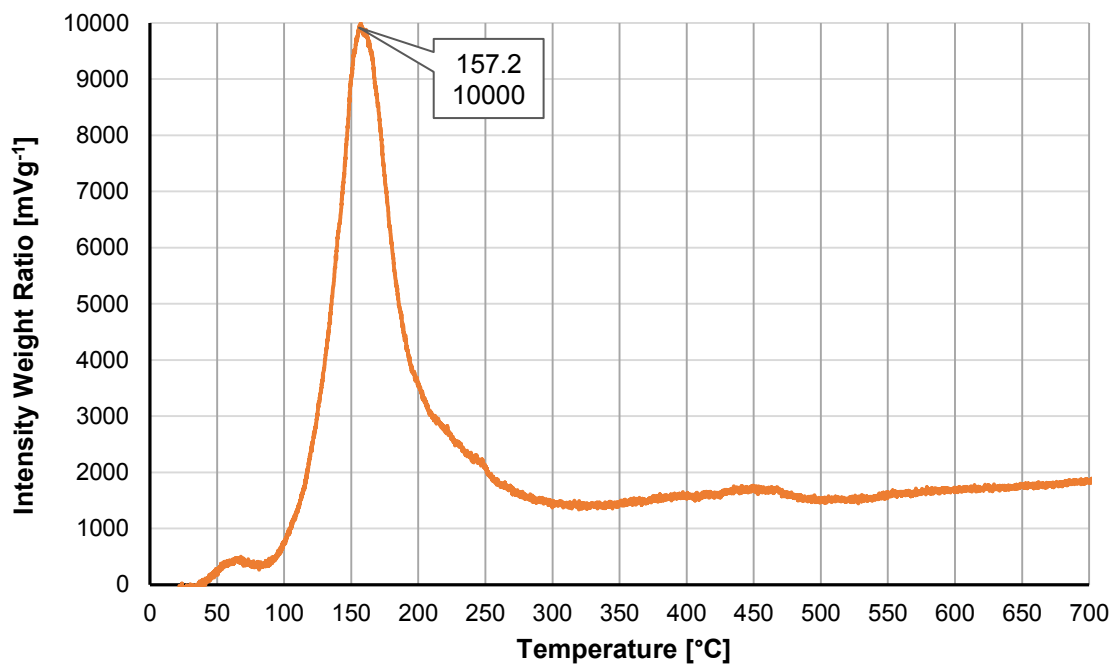


Figure 4.10. Thermo-desorption curve of Standard of HgCl_2 plus SiO_2 . Released temperature is plotted versus intensity/weight ratio.

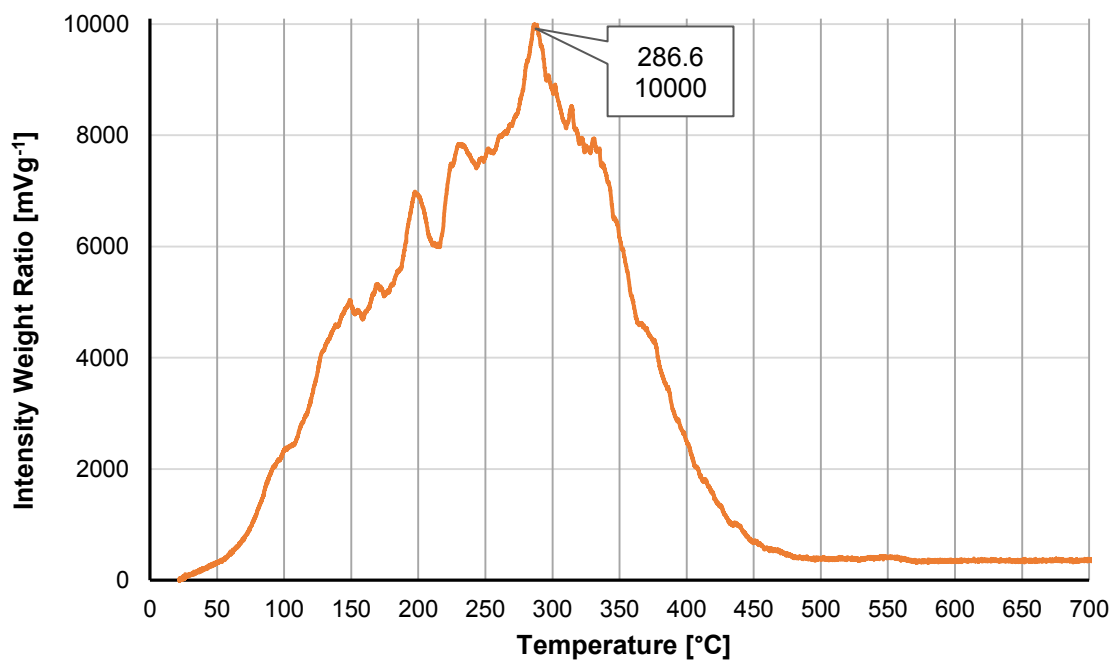


Figure 4.11. Thermo-desorption curve of Standard of HgSO_4 plus SiO_2 . Released temperature is plotted versus intensity/weight ratio.

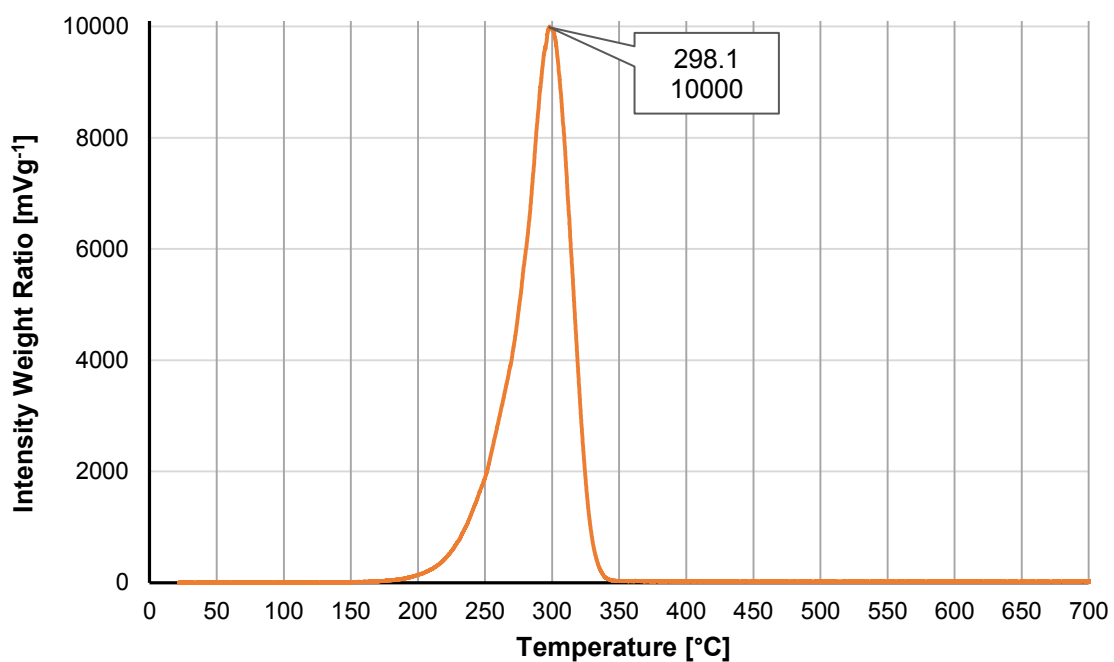


Figure 4.12. Thermo-desorption curve of Standard of HgS plus Gypsum. Released temperature is plotted versus intensity/weight ratio.

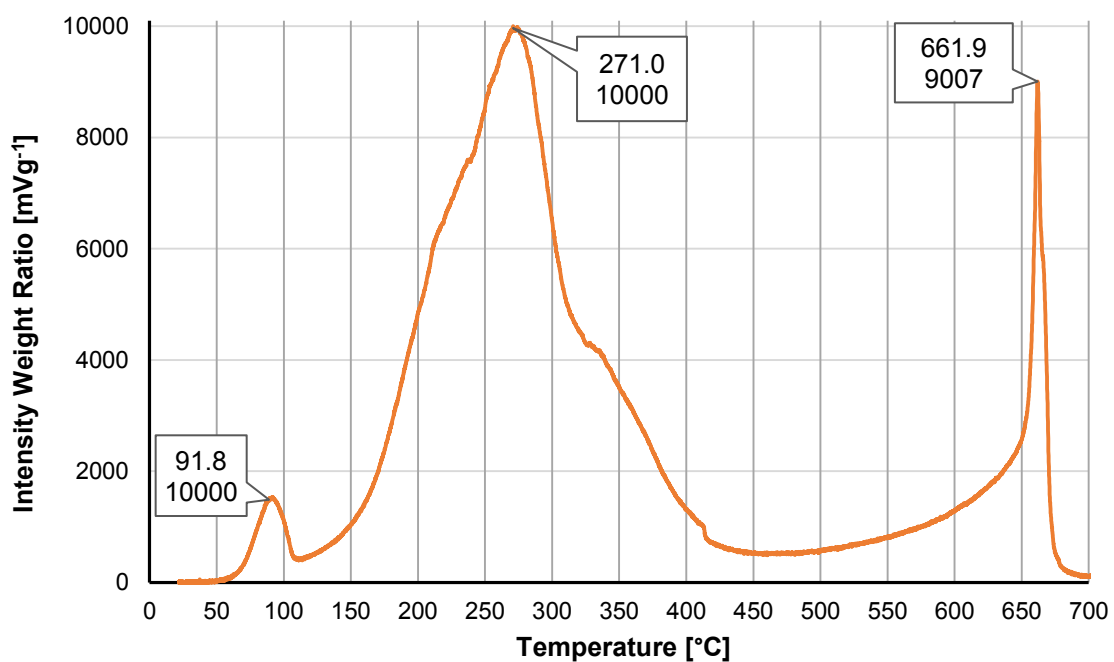


Figure 4.13. Thermo-desorption curve of Standard of HgCl₂ plus Gypsum. Released temperature is plotted versus intensity/weight ratio.

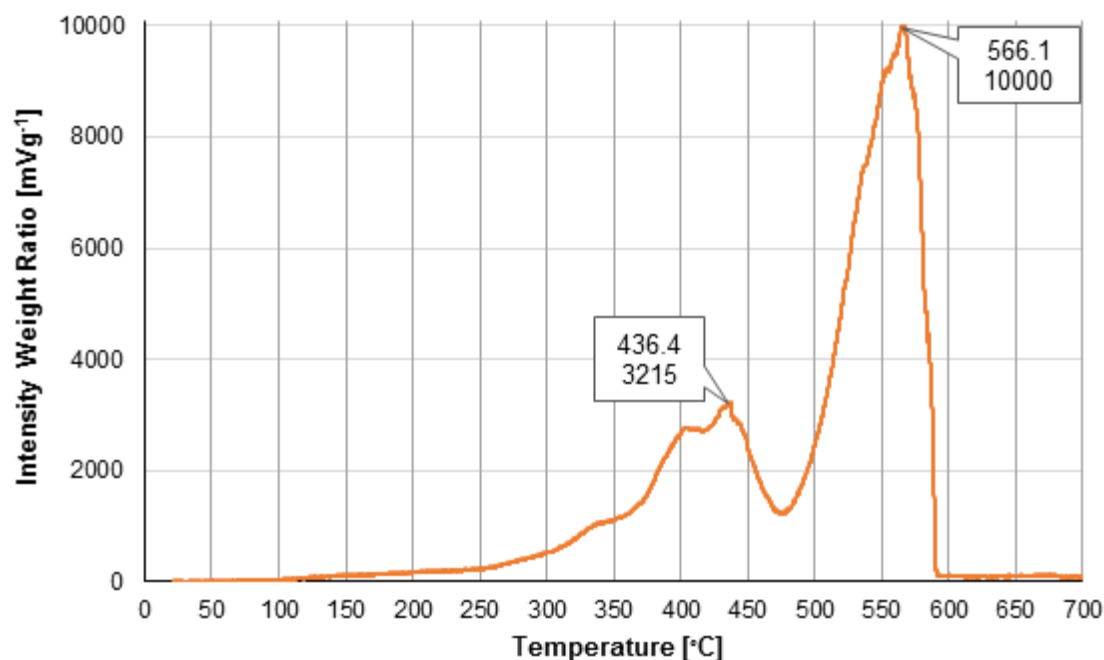


Figure 4.14. Thermo-desorption curve of Standard of HgSO_4 plus Gypsum. Released temperature is plotted versus intensity/weight ratio.

Thermo-desorption curves of native samples and of residues left from each extracting step are shown in Figure 4.15, Figure 4.16, Figure 4.17, Figure 4.18, Figure 4.19, Figure 4.20, Figure 4.21, Figure 4.22, Figure 4.23, Figure 4.25, Figure 4.26, Figure 4.27, Figure 4.28, Figure 4.29, Figure 4.30. The residues shown are: soluble plus exchangeable (EXC-Hg); easily reducible oxides or Mn oxides (ERO-Hg); organic matter (OM-Hg); amorphous Fe oxides (AmoFe-Hg); crystalline Fe oxides (CryFe-Hg); residual, non-cinnabar Hg fraction (RES-Hg) and cinnabar Hg (HgS).

Hg released pattern of native soil is shown in Figure 4.15. It can be discern two peaks corresponding to two main fraction. The peak 1 has the maximum at 214.3 °C. The peak 2 has the maximum at 320.4 °C. The higher peak, the second one, is reasonably imputable to HgS , the first one can be initially, more generally defined as “matrix bound Hg” (e.g. Biester et al., 1999; Gosar et al., 2006).

Temperature release of HgS standards are between 273-310 °C, however the matrix is different from samples, thus they are difficult to compare.

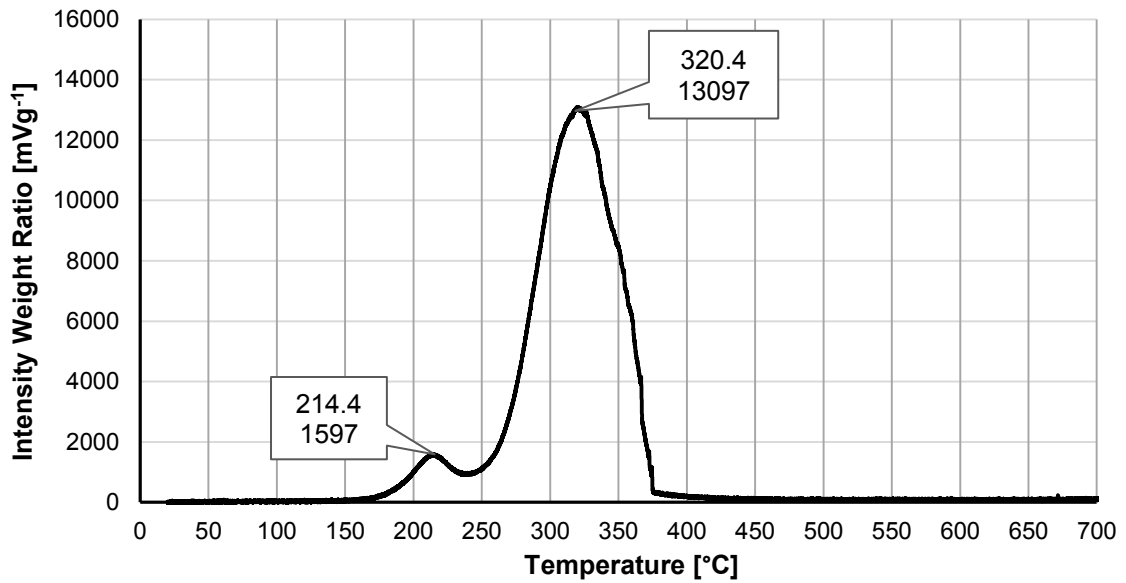


Figure 4.15. Thermo-desorption curve of Fossalon Soil. Desorption temperature is plotted versus intensity/weight ratio.

Sediment sample show out a different release pattern, in which the highest peak is the first one (252.3 °C), whereas the second one (330.1 °C) is smaller and less discernable (Figure 4.16). Likewise the soil, the two peak of sediment can be define as “matrix bound Hg” and HgS respectively. However, unlike the soil, the sediment have a higher proportion of total Hg in the matrix bound fraction than in the HgS fraction.

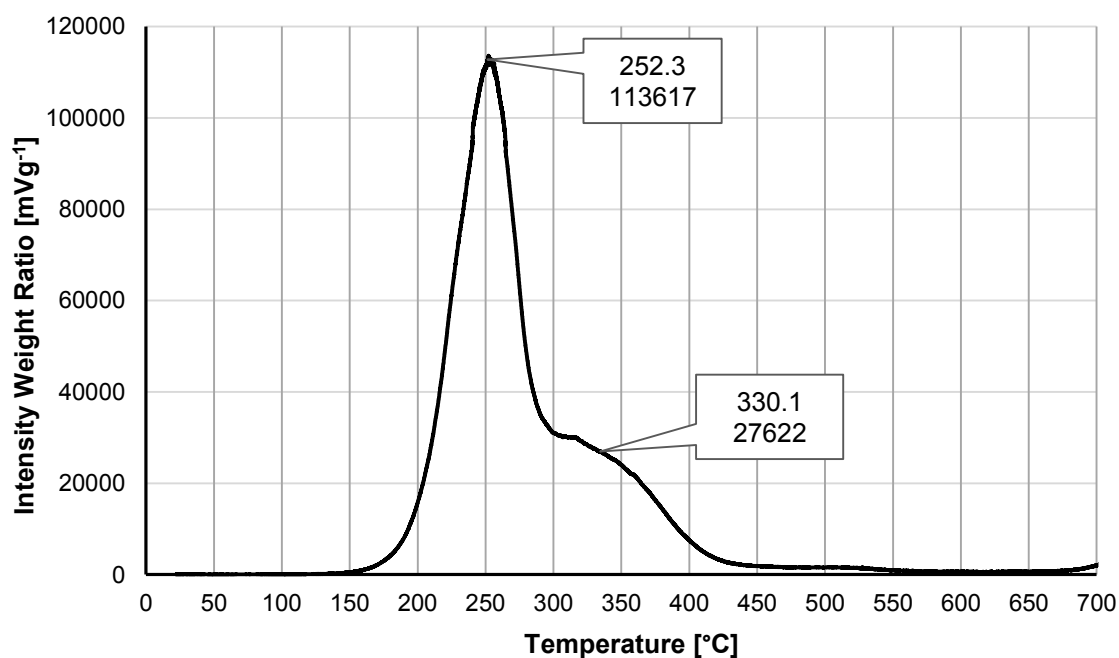


Figure 4.16. Thermo-desorption curve of Banduzzi Sediment. Desorption temperature is plotted versus intensity/weight ratio.

The released pattern of the residue left from EXC-Hg and ERO-Hg extraction of Fossalon soil shows out no relevant differences from native soil (Figure 4.17 and Figure 4.18). Indeed, the two peaks have quite the same temperature and height (see also Table 4.12). After the extraction of organically bounded Hg, OM-Hg residue, the peak 1 (214.6 °C) has similar temperature of the other fractions and native soil, but peak height is considerable smaller than peak 1 of the previous extracting step (Figure 4.19).

No differences can be seen among TD curves of OM-Hg residue, AmoFe-Hg residue and CryFe-Hg residue (Figure 4.19, Figure 4.20, Figure 4.21).

TD curve of Res-Hg residue as the peak 2 with invariable temperature and height, but before 300 °C three different fractions appear at different temperature. The peaks are not easily discernable, but they raise at temperature between 100-200 °C (Figure 4.22).

Is not easy to attribute these peaks to specific Hg compounds, it could be argued that the decomposition process affect complexed minerals structure of soil (e.g. metal oxide, or HgS) in a way that smaller, degraded, disordered structures have lower released temperatures. This behavior could even be due to a multistep breakdown of the cinnabar lattice, which explains the succession of “small peaks”. In fact, HNO₃ must be used very

carefully because some oxidizing gases produced by the traces of chloride in concentrated HNO_3 may result in the dissolution of HgS (Mikac et al., 2003)

Moreover, a little part of these degraded mineral could be further reduced to Hg^0 (which could hypothetically decompose at 100 °C).

TD curve of the last residue (Figure 4.23), after the application of the whole SEP, shows out still two peaks: peak 1 at 206.3 °C and peak 2 at 327.6 °C. The released temperatures is comparable to those of native soil. However, the height of the first peak is comparable with those of OM-Hg, Amo-Fe, Cry-Fe, whereas the height of peak 2 is 10 times smaller than the previous extraction.

In summary, the peak 1 shows a significative decrease after OM-Hg extracting step, the peak 2 after HgS extracting step, without complete. In addition RES-Hg extracting step give rise to other new peaks. In Fossalon soil sample the majour difference between the two peaks is in OM-Hg. Meaning that in this step, in relative terms, it has been extracted the majour portion of “matrix bound” Hg fraction.

Comparing these results with the wet chemistry extraction (Table 4.11), it could be seen that only the 0.02% of the total concentration is extracted in OM step, thus even that the first TD fraction is actually organic bounded Hg, it is a much less represented fraction. Moreover, after the extraction of HgS (34% of the total concentration), the 43% of Hg remains un-extracted and gives raise to the peak in the last TD residue measurement.

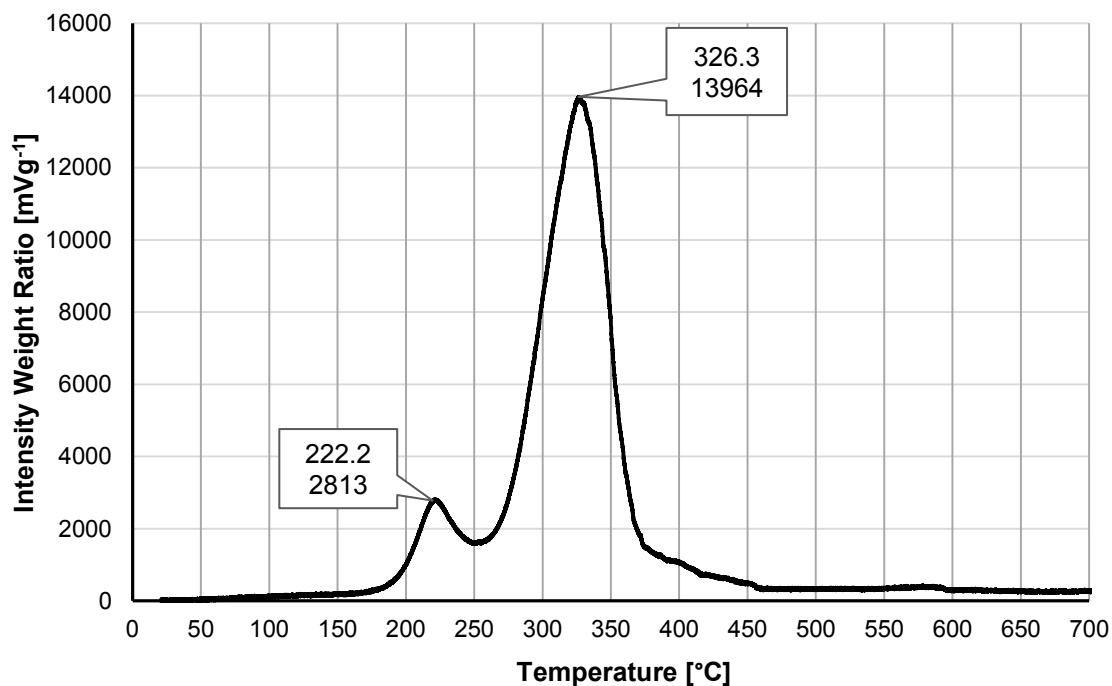


Figure 4.17. Thermo-desorption curve of Fossalon Soil after EXC-Hg extracting step. Desorption temperature is plotted versus intensity/weight ratio.

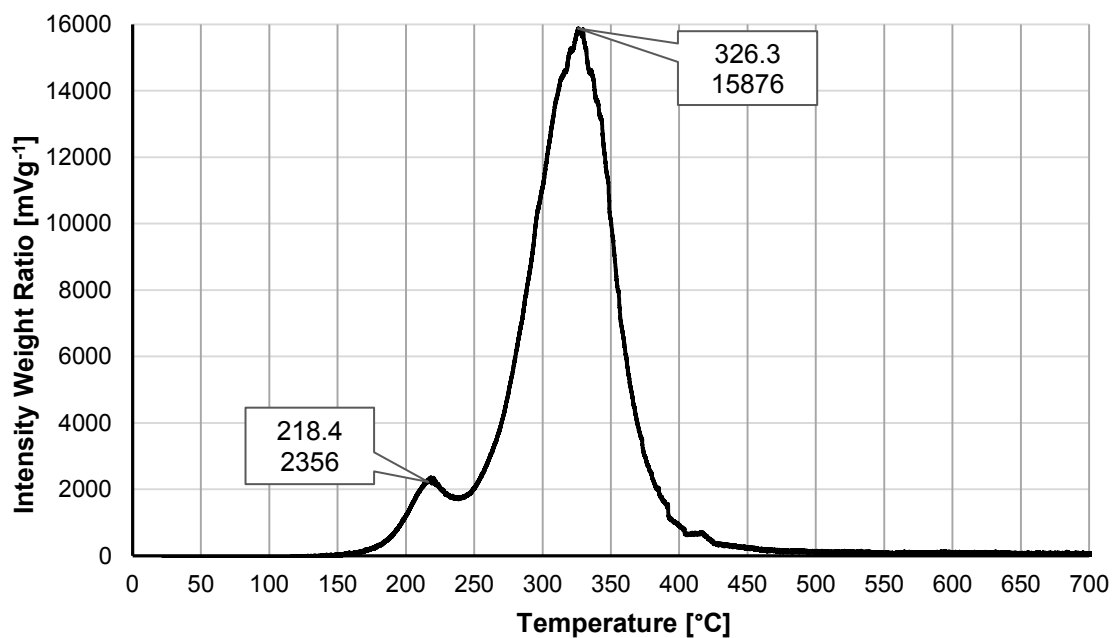


Figure 4.18. Thermo-desorption curve of Fossalon Soil after ERO-Hg extracting step. Desorption temperature is plotted versus intensity/weight ratio.

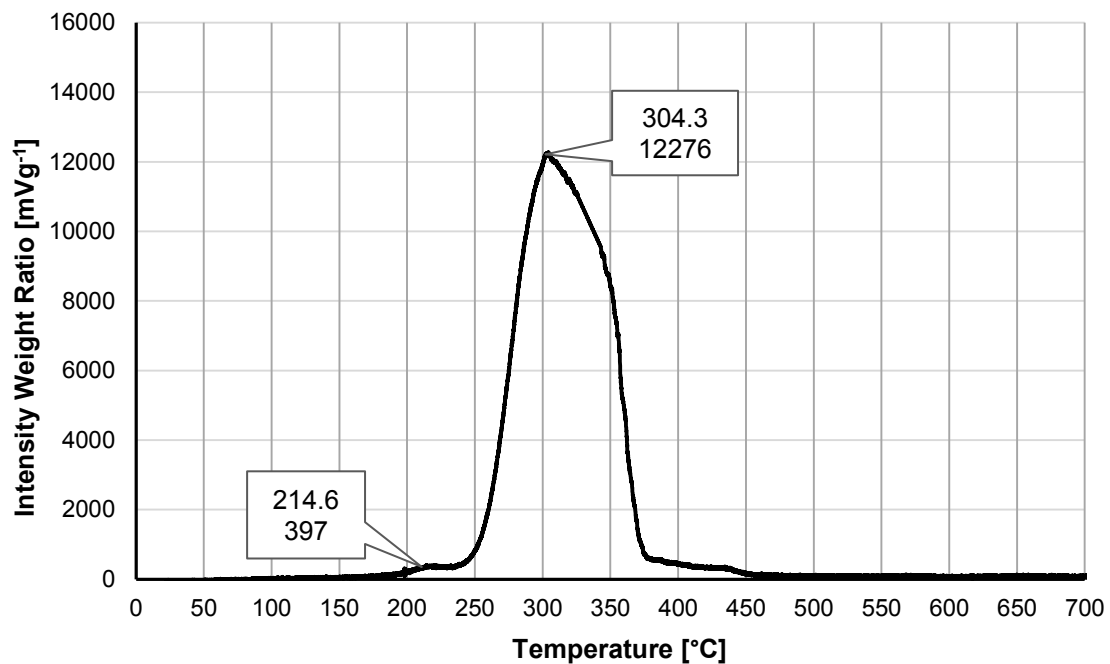


Figure 4.19. Thermo-desorption curve of Fossalon Soil after OM-Hg extracting step. Desorption temperature is plotted versus intensity/weight ratio.

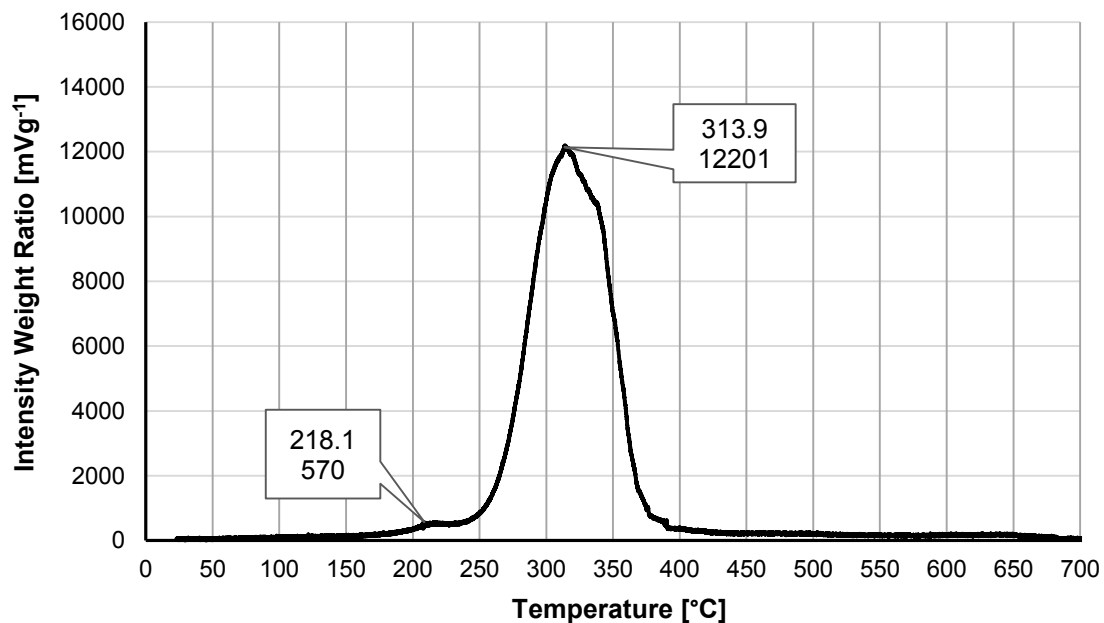


Figure 4.20. Thermo-desorption curve of Fossalon Soil after AmoFe-Hg extracting step. Desorption temperature is plotted versus intensity/weight ratio.

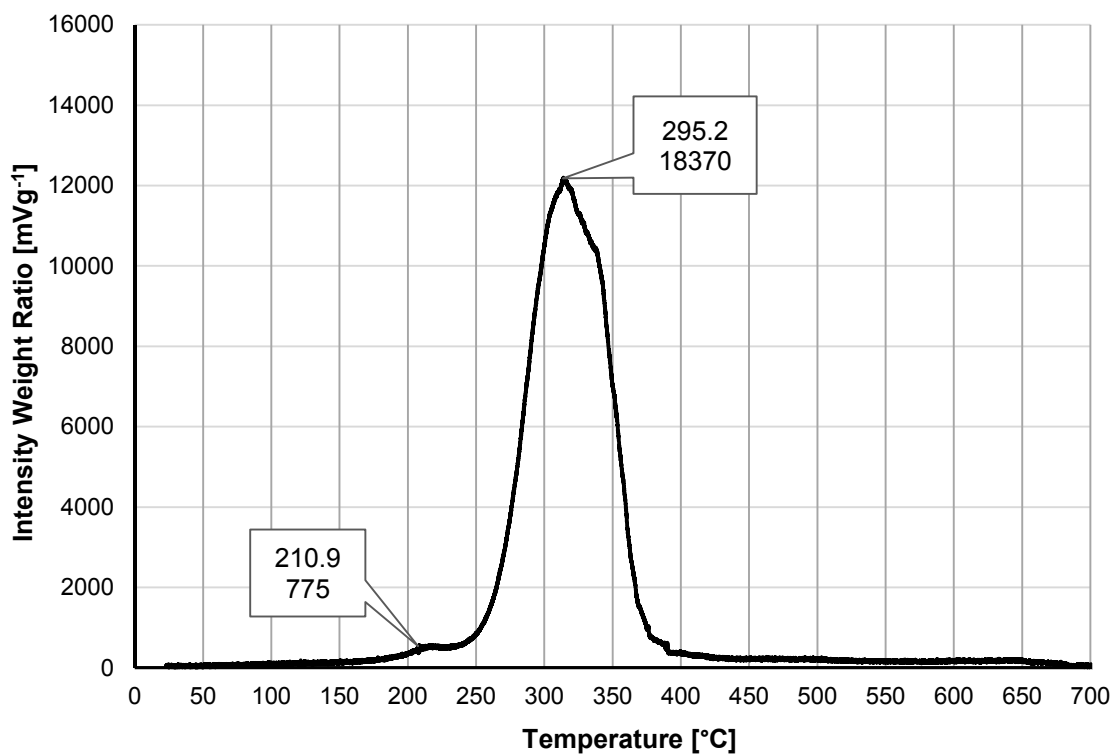


Figure 4.21. Thermo-desorption curve of Fossalon Soil after CryFe-Hg extracting step. Desorption temperature is plotted versus intensity/weight ratio.

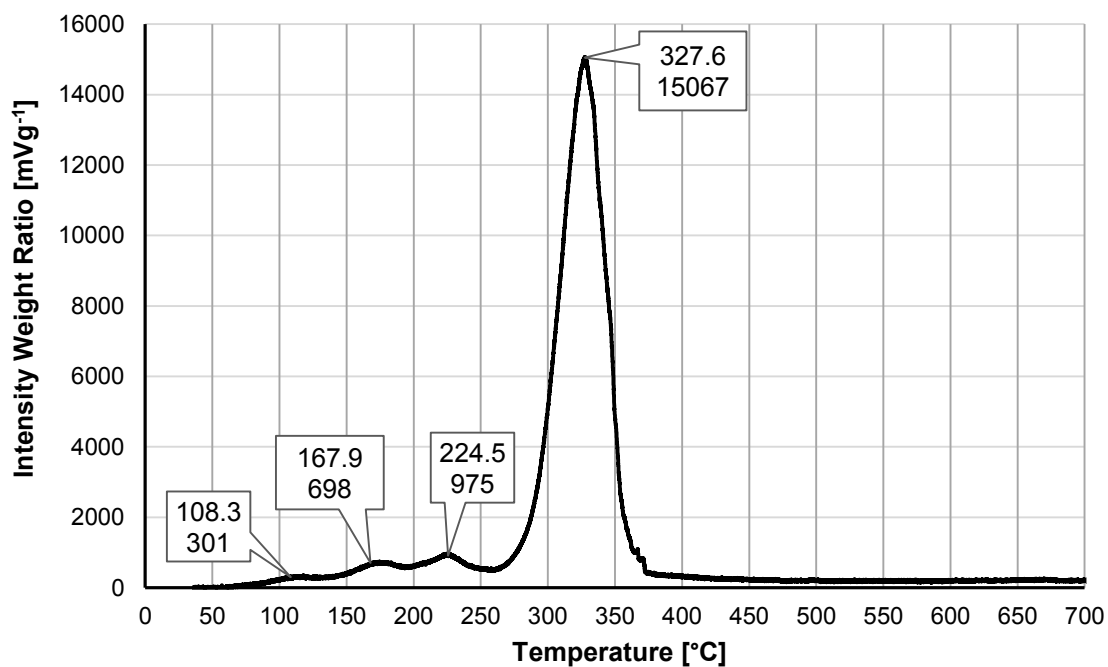


Figure 4.22. Thermo-desorption curve of Fossalon Soil after RES-Hg extracting step. Desorption temperature is plotted versus intensity/weight ratio.

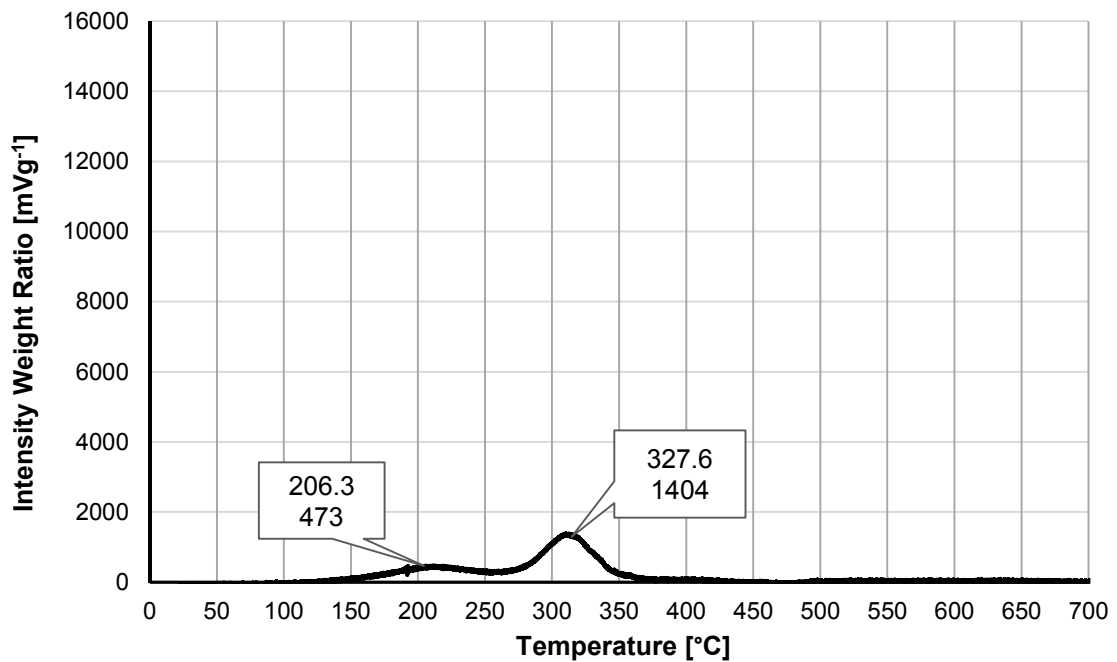


Figure 4.23. Thermo-desorption curve of Fossalon Soil after HgS extracting step. Desorption temperature is plotted versus intensity/weight ratio.

TD analysis of Banduzzi sediment raises 2 peaks: one discerned peak at 252.3 °C and a second peak at around 330.1 °C, a very broad peak (Figure 4.16). The same as TD curve pattern of EXC-Hg residue (Figure 4.24).

In the ERO-Hg residue it can be already observed a decrease in intensity of both peaks (Figure 4.25).

This decrease is in agreement with results obtained from the analysis of leachates: in the EXC-Hg leachate of Banduzzi sediment only 0.1% of total Hg is extracted, whereas in ERO-Hg it is extracted 13% of total concentration (Table 4.11).

The most evident difference of all extracting phases, it can be seen between ERO-Hg and OM-Hg (Figure 4.25 and Figure 4.26).

Indeed, TD curve of OM-Hg residue has one peak at 198.2 °C, with an intensity of 7181, and the second peak raises at 225.1 °C and it is 8452 height, therefore it shows a decrease in the released temperature of both peaks, as well as a decrease in intensity of the peak 1. Also this TD pattern is in agreement with leaching test: OM-Hg step of SEP has extracted in solution the 69% of the total content.

Results and Discussion

In TD measurement of AmoFe-Hg residue as well as CryFe-Hg residue (Figure 4.27, Figure 4.28) the released temperature remains the same as the previous phase and less than native sediment, and also intensity has no changes.

Another important difference it can be seen in TD curve of RES-Hg (Figure 4.29). One new peak at 51.2°C appears. The peak at around 250 °C disappears, and the peak at 170.9 °C is much smaller than the corresponding peak of previous steps.

After the performance of the whole SEP, the HgS residue shows out no peaks (Figure 4.30).

Even this observation is in agreement with wet chemistry, indeed in HgS step was extracted the 0.07% of total Hg, whereas in the last residue only 0.34% of the total concentration remains un-extracted. This explains the smooth line of last TD measurement (Table 4.11).

In summary, in Banduzzi sediment the difference between the two peaks is biggest in OM-Hg extracting step, meaning that in this step it has been extracted the majour portion of the first peak, “matrix bound Hg”.

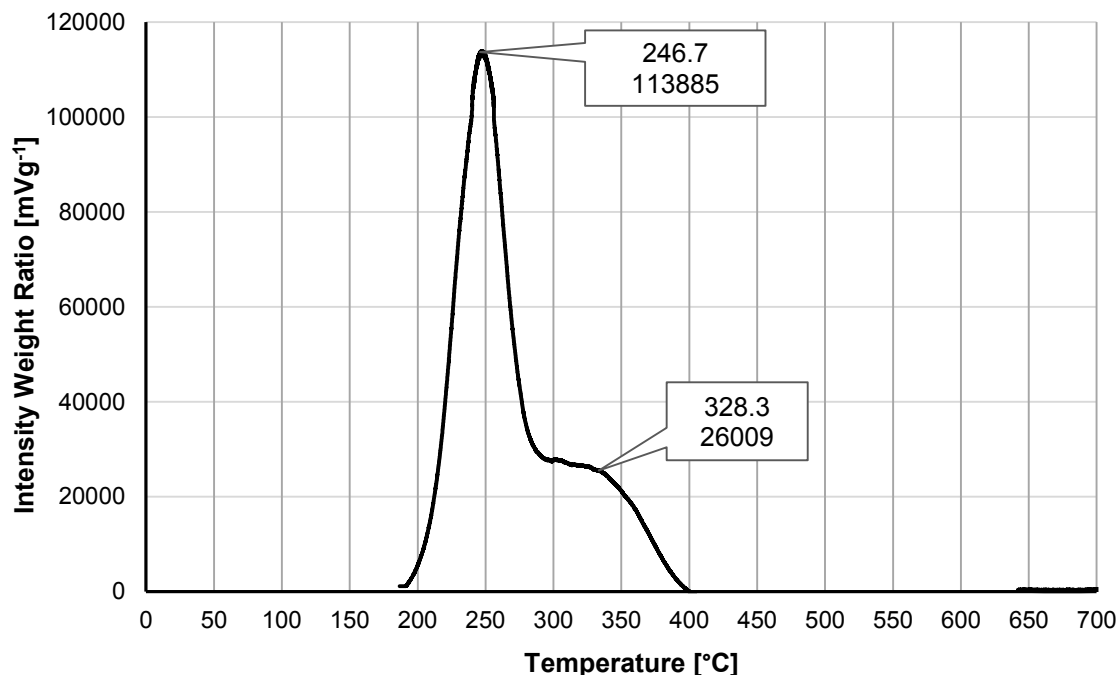


Figure 4.24. Thermo-desorption curve of Banduzzi Sediment after EXC-Hg extracting step. Desorption temperature is plotted versus intensity/weight ratio.

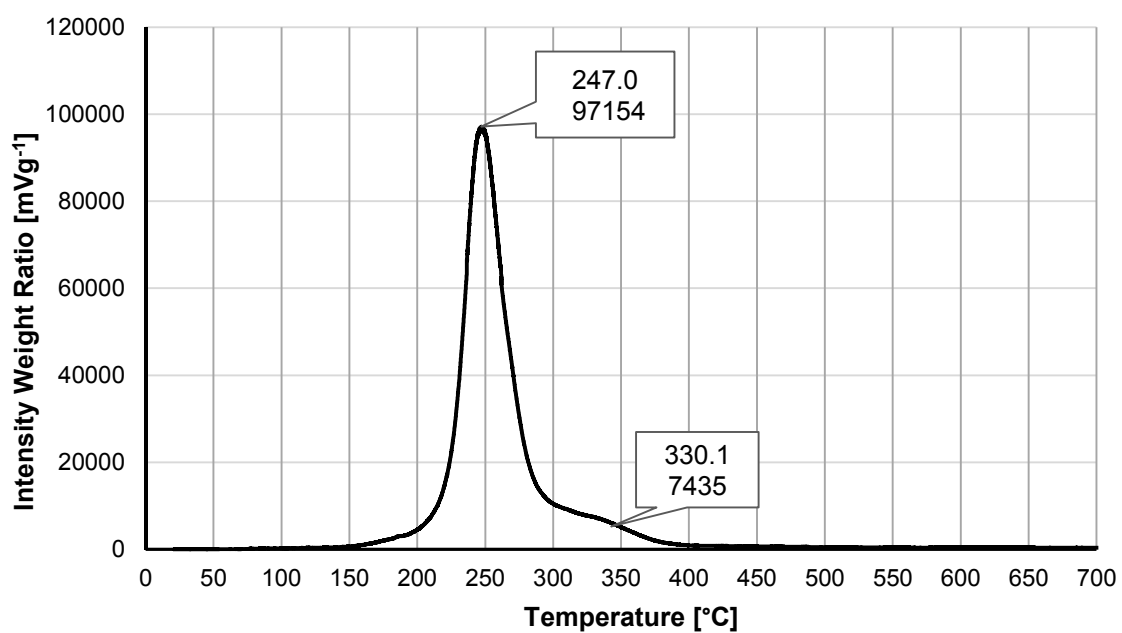


Figure 4.25. Thermo-desorption curve of Banduzzi Sediment after ERO-Hg extracting step. Desorption temperature is plotted versus intensity/weight ratio.

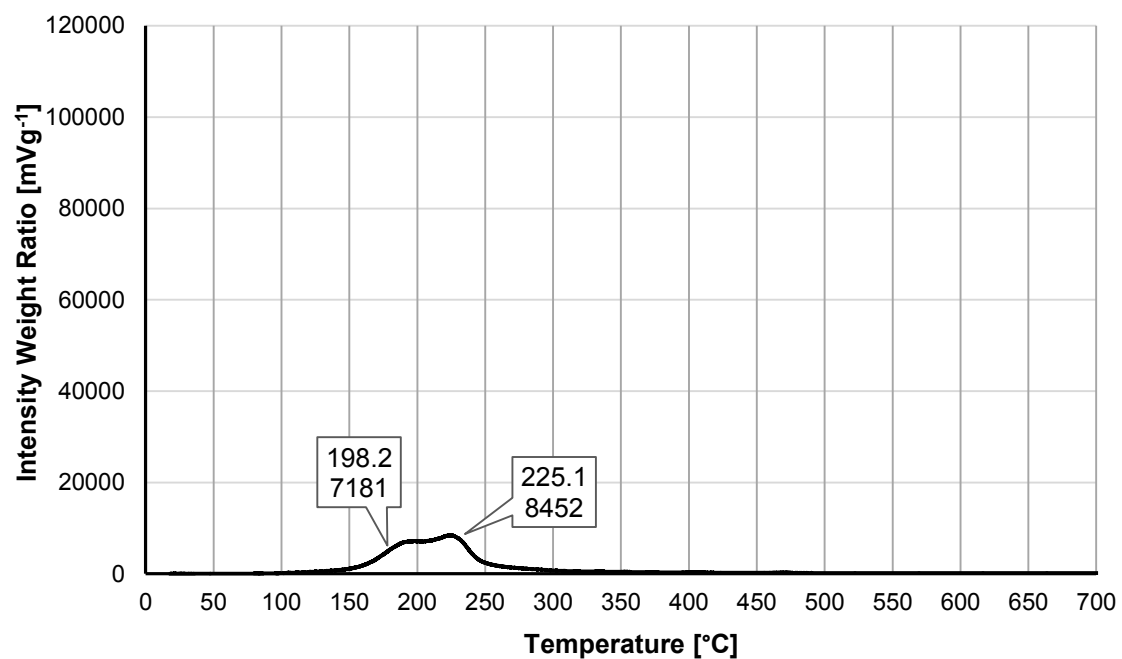


Figure 4.26. Thermo-desorption curve of Banduzzi Sediment after OM-Hg extracting step. Desorption temperature is plotted versus intensity/weight ratio.

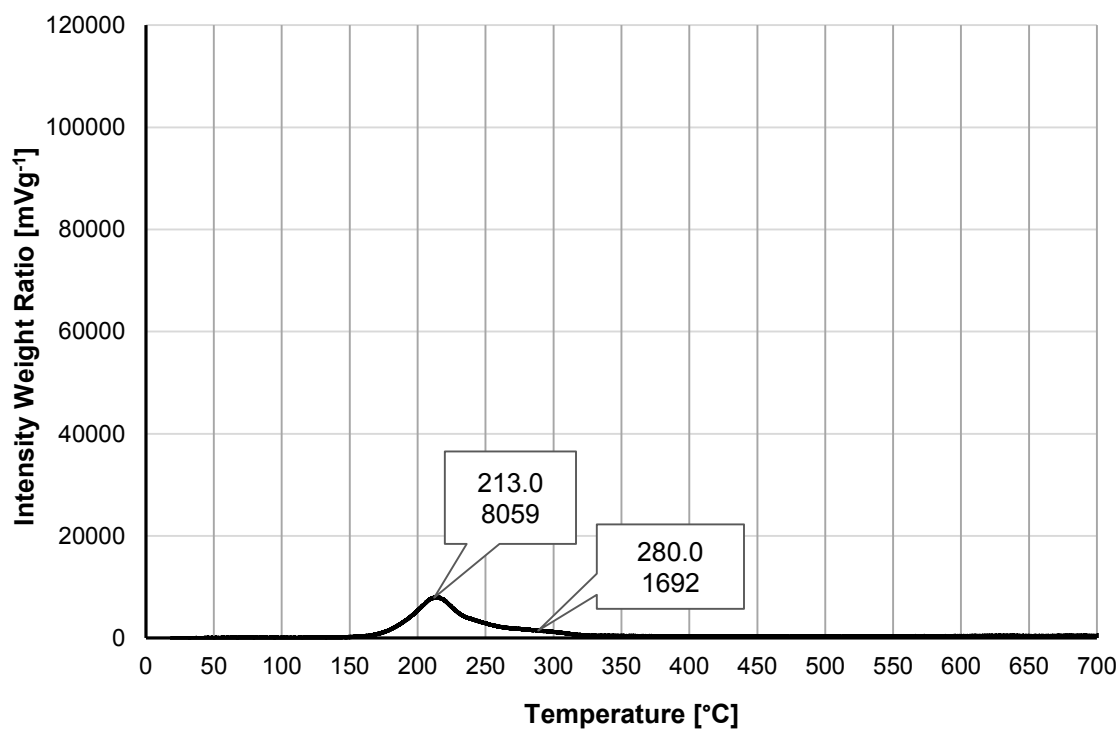


Figure 4.27. Thermo-desorption curve of Banduzzi Sediment after AmoFe-Hg extracting step. Desorption temperature is plotted versus intensity/weight ratio.

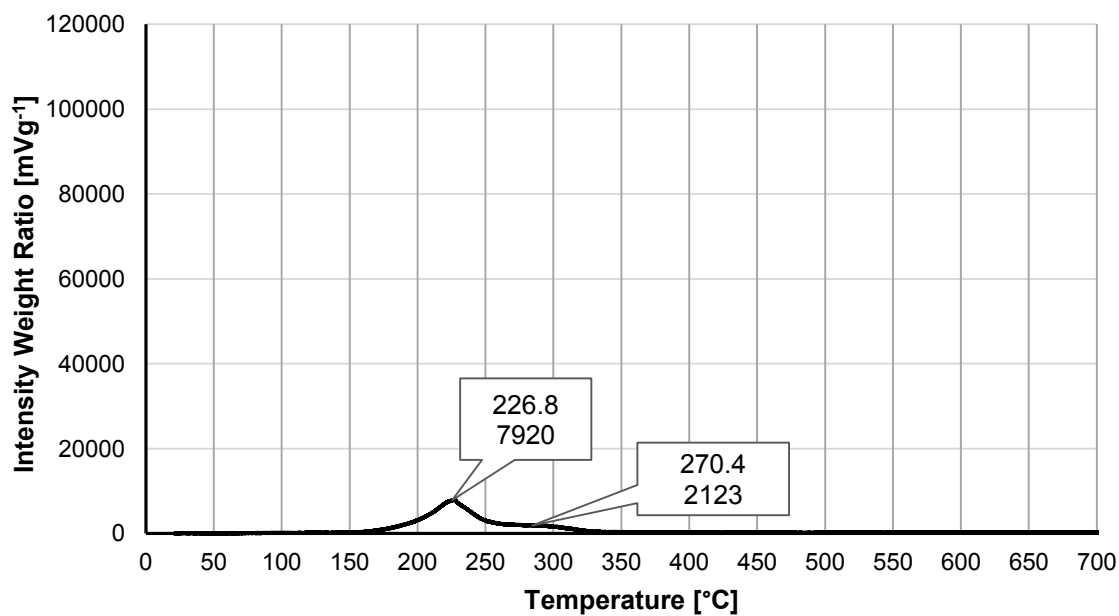


Figure 4.28. Thermo-desorption curve of Banduzzi Sediment after CryFe-Hg extracting step. Desorption temperature is plotted versus intensity/weight ratio.

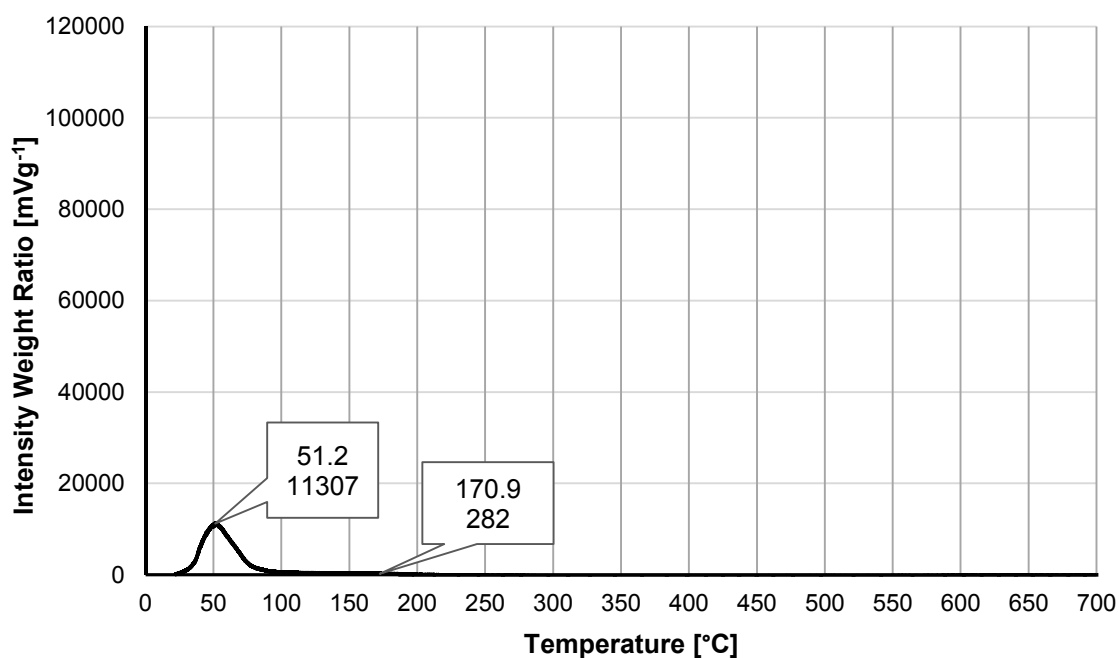


Figure 4.29. Thermo-desorption curve of Banduzzi Sediment after RES-Hg extracting step. Desorption temperature is plotted versus intensity/weight ratio.

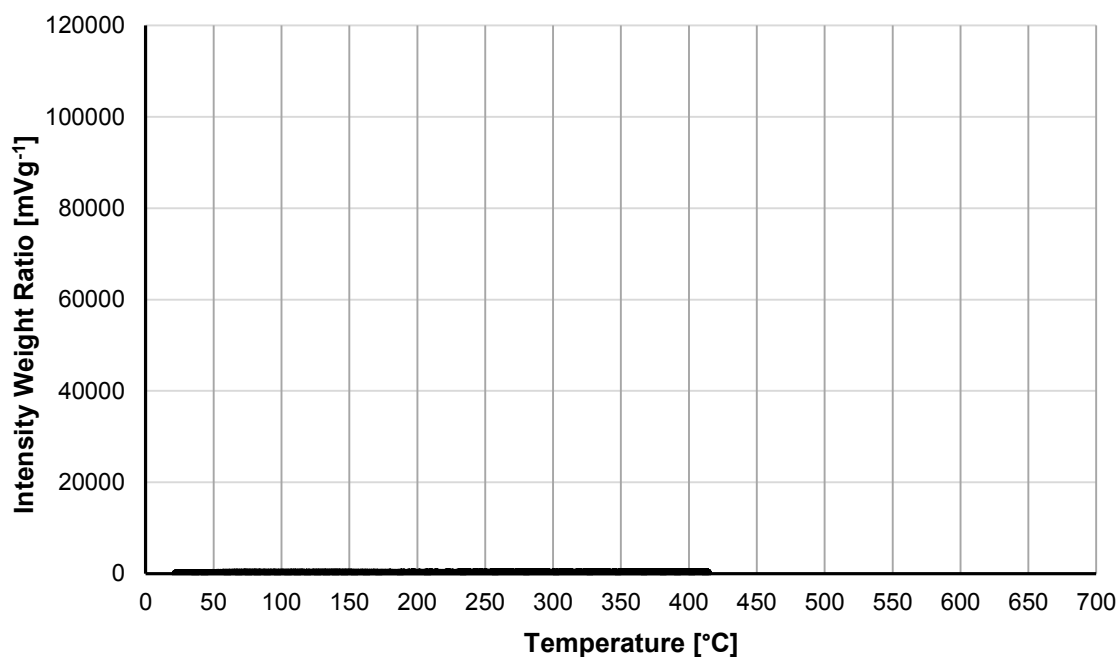


Figure 4.30. Thermo-desorption curve of Banduzzi Sediment after HgS extracting step. Desorption temperature is plotted versus intensity/weight ratio.

Thermo-desorption curves of residues left from all extracting steps are shown in Figure 4.31 (Fossalon soil) and Figure 4.32 (Banduzzi sediment). The results are shown as

Results and Discussion

graphs (thermo-desorption curves) of temperature versus the relative intensity of Hg peaks.

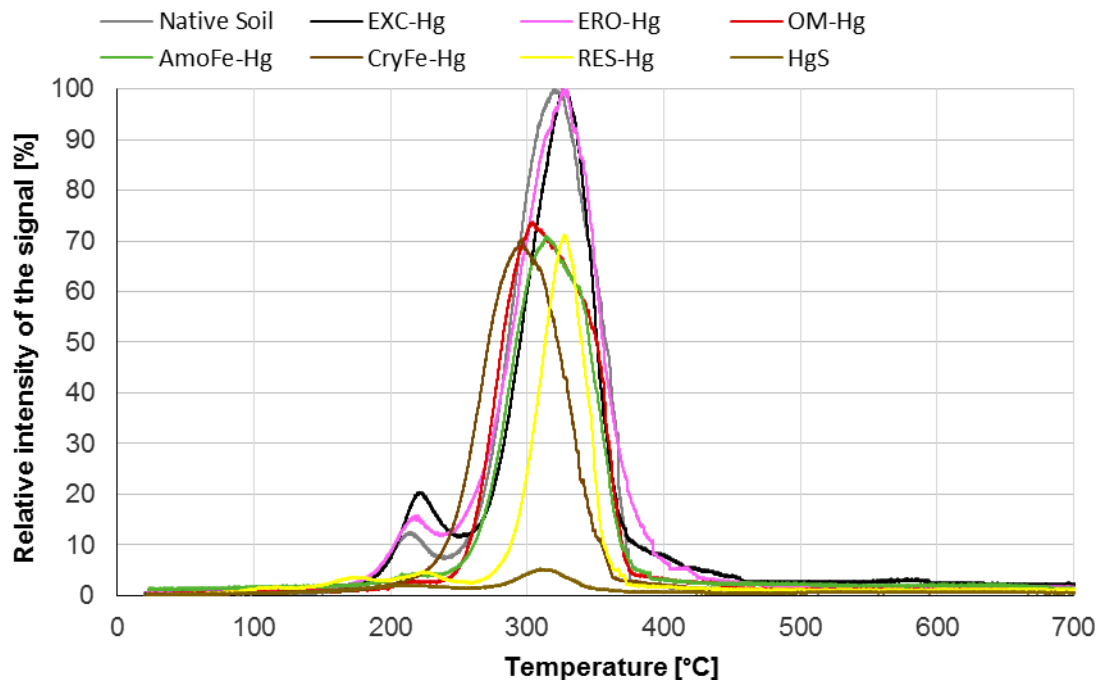


Figure 4.31. Thermo-desorption curves of Fossalon soil residues left from each extracting step: soluble plus exchangeable (EXC-Hg, black line); easily reducible oxides or Mn oxides (ERO-Hg, pink line); organic matter (OM-Hg, red line); amorphous Fe oxides (AmoFe-Hg, green line); crystalline Fe oxides (CryFe-Hg, blue line); residual, non-cinnabar Hg fraction (RES-Hg, yellow line) and cinnabar Hg (HgS, brown line).

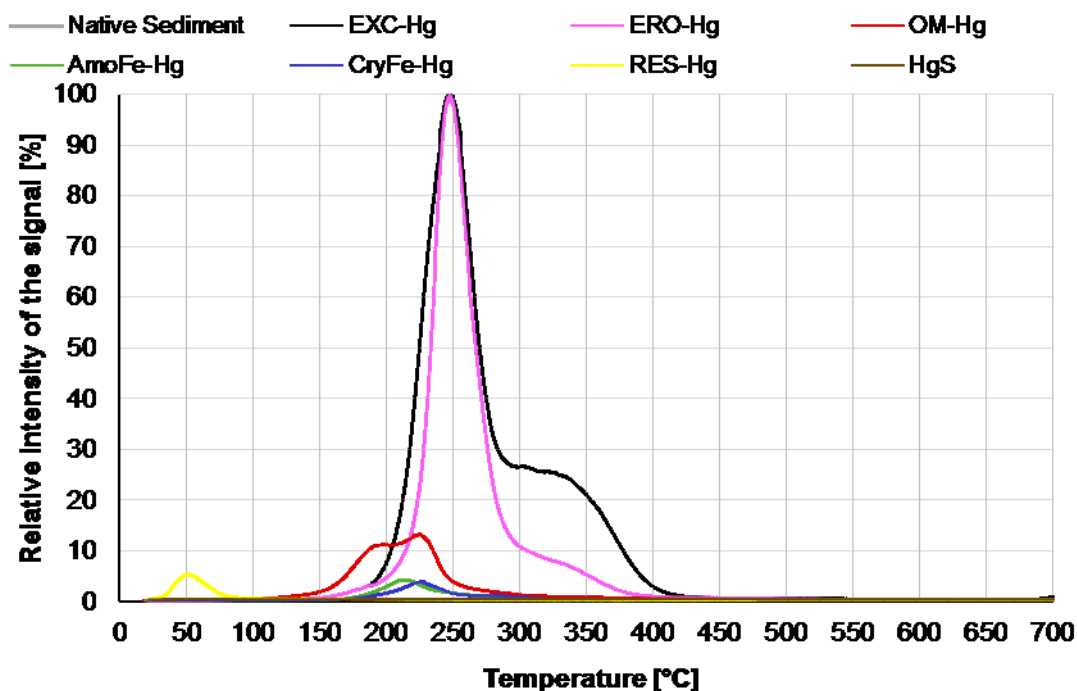


Figure 4.32. Thermo-desorption curves of Banduzzi sediment residues left from each extracting step: soluble plus exchangeable (EXC-Hg, black line); easily reducible oxides or Mn oxides (ERO-Hg, pink line); organic matter (OM-Hg, red line); amorphous Fe oxides (AmoFe-Hg, green line); crystalline Fe oxides (CryFe-Hg, blue line); residual, non-cinnabar Hg fraction (RES-Hg, yellow line) and cinnabar Hg (HgS, brown line).

Figure 4.33 and Figure 4.34 shows the ratio between the two main peaks discernable in graphs. Peak 2 is divided with peak 1. Where peak one correspond to peaks at about 200-250 °C, and peak 2 at around 280-330 °C. This ratio emphasize the difference between the two main peaks. Thus, as it can be seen, the major variation for Fossalon soil sample is in OM-Hg, Cry-Fe-Hg and AmoFe-Hg in descending order. While the majour variation for Banduzzi sediment is markly in OM-Hg fraction.

Results and Discussion

Table 4.12. Peak parameters of Fossalon Soil (peak height, released temperature, height of peak 2 vs height of peak 1 ratio).

Sample/SEP	Peak 1		Peak 2		Ratio
	temperature	height	temperature	height	
	°C	mV g ⁻¹	°C	mV g ⁻¹	
Native soil	214.35	1596.74	320.44	13097.50	8.20
EXC-Hg	222.21	2813.42	326.28	13963.82	4.96
ERO-Hg	218.36	2355.62	326.28	15876.36	6.74
OM-Hg	214.64	397.23	304.32	12276.19	30.90
AmoFe-Hg	218.08	570.11	313.87	12201.58	21.40
CryFe-Hg	210.89	775.87	295.21	18369.73	23.68
RES-Hg	224.54	975.83	327.58	15067.38	15.44
HgS	206.34	472.77	327.58	1404.52	2.97

Table 4.13. Peak parameters of Banduzzi Sediment (peak height, released temperature, height of peak 2 vs height of peak 1 ratio).

Sample/SEP	Peak 1		Peak 2		Ratio
	temperature	height	temperature	height	
	°C	mV g ⁻¹	°C	mV g ⁻¹	
Native sediment	252.26	113616.94	330.10	27621.80	0.24
EXC-Hg	246.68	113884.58	328.33	26009.34	0.23
ERO-Hg	247.01	97154.35	330.12	7435.06	0.08
OM-Hg	198.16	7181.25	225.09	8451.80	1.18
AmoFe-Hg	212.98	8059.30	280.02	1691.84	0.21
CryFe-Hg	226.76	7920.97	270.42	2123.99	0.27
RES-Hg	51.22	11306.57	170.93	281.72	0.02
HgS	-	-	-	-	-

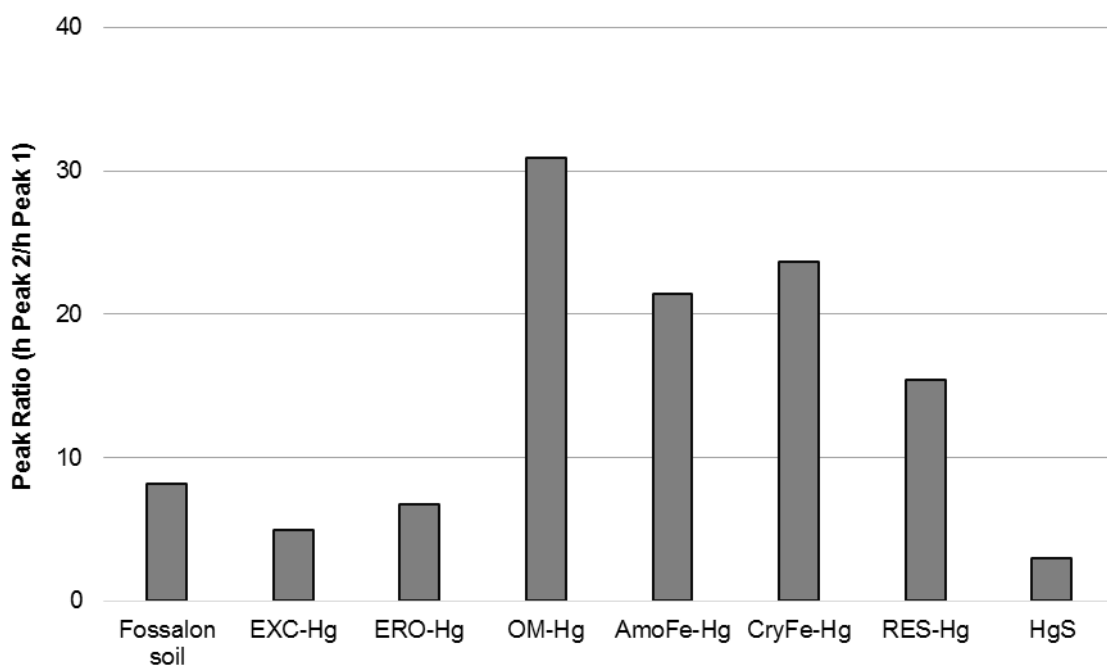


Figure 4.33. Peak ratio of Fossalon Soil (hight of peak 2 vs hight of peak 1 calculate based on the curves of .desorption temperature plotted versus intensity/weight ratio).

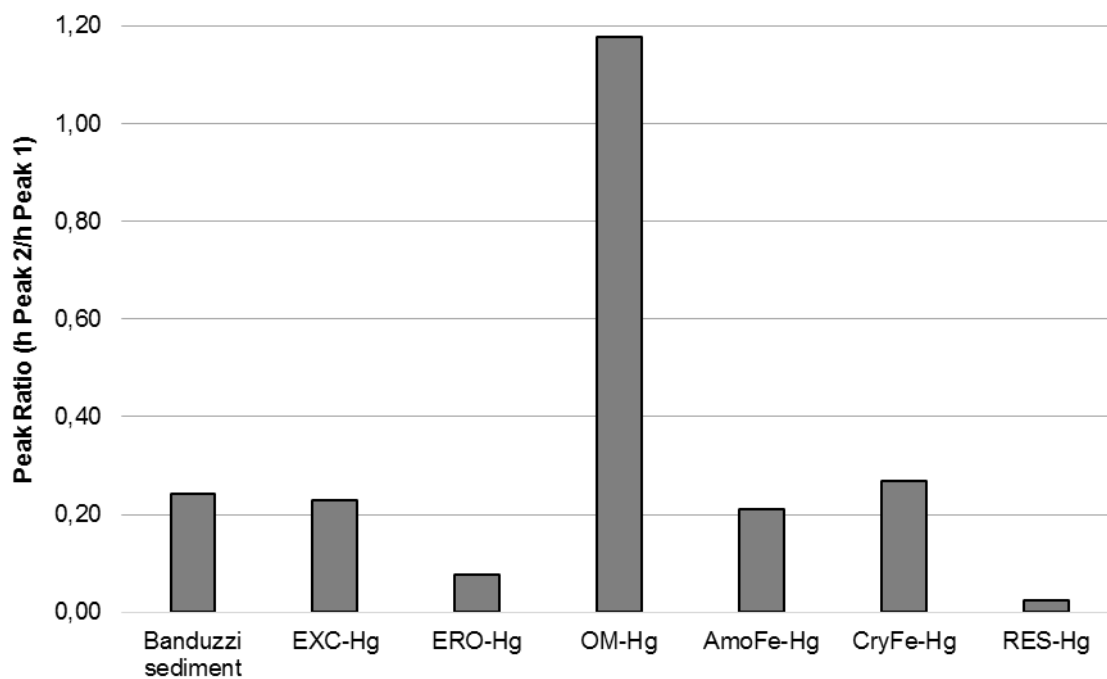


Figure 4.34. Peak ratio of Banduzzi Sediment (hight of peak 2 vs hight of peak 1 calculate based on the curves of desorption temperature plotted versus intensity/weight ratio).

4.3.1. Soil spiking

Fossalon soil (C13 sampling point, 0-40 horizon) was spiked with a solution of Humic Acids-Hg (HA-Hg) and of Fulvic acids-Hg (FA-Hg) in order to validate the hypothesized “organic“ nature of Hg desorbing at temperatures around 215 °C, corresponding to the peak 1 of curves observed either in Fossalon soil or in Banduzzi sediment (Figure 4.35). In Figure 5.35 are shown thermo-desorption curves of Fossalon soil spiked with HA-Hg and with FA-Hg.

The spike did not change the temperature of peak 2, but in the HA-Hg spiked soil the relative height of peak 2 decreased significantly. This decrease is not attributed to a reduction in the HgS fraction, but instead to a significant increase in the height of peak 1 that made a change in the relative height of two peaks.

The peak 1 (220 °C) increased significantly in both HA-Hg and FA-Hg, with a corresponding slight increase in temperature of peak in the HA-Hg (from 220 to 230 °C). Peak 1 broadened also evidently: Hg release it is due to chemical interactions between Hg and functional groups of Humic Acids. Hg is strongly bound to reduced sulfur functional groups (thiol (R-SH) and disulfide (R-SS-R)/disulfane (R-SSH)) in humic substances. Furthermore, Hg can bound with oxygen ligands such as carboxyl and phenol in addition to the reduced S ligands due to the low density of reduced S ligands (Ravichandran, 2004). The different bound forms have different stability constants, which lead to different release temperatures.

A new peak between 50 to 60 °C compared in both HA-Hg and FA-Hg spiked soil. This peak is certainly attributed to elemental Hg form (Hg^0). This peak was much higher in HA-Hg than in FA-Hg confirming the high reactivity of Hg towards matrix and the well-known reductive potential of humic acids. This behaviour of humic substances on Hg, confirms what reported by other authors (Yao et al., 2006; Navarro et al., 2008; Tao et al., 2014).

Indeed, due to complex Hg chemistry and the lack of stability of Hg compounds, the spiking of samples has to be performed and especially interpreted, very carefully, in the event that they are used for recovery evaluation.

While the Hg released at around 80 °C in the soil spiked with Fulvic acids-Hg could be reduced Hg^0 . Indeed these two compounds have the same temperature range release.

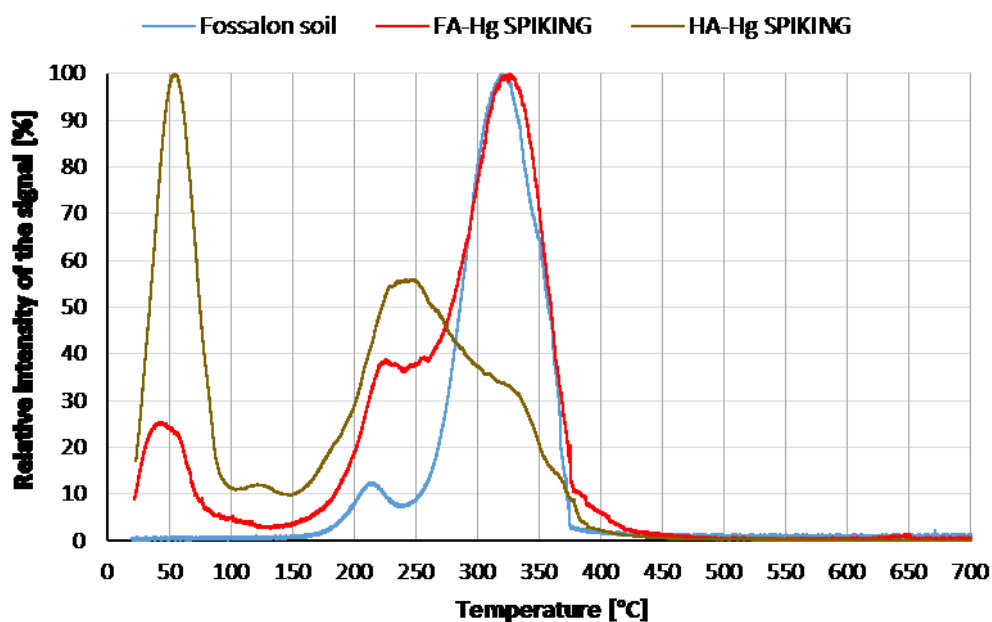


Figure 4.35. Thermo-desorption curves of Fossalon soil: soil spiked with Fulvic Acids-Hg and soil spiked with Humic Acids-Hg.

The combination of multiple methodologies has been demonstrated to be an effective way to enhance Hg fractionation, especially its interpretation.

Both methodologies suffer of numerous and important drawbacks.

Thermodesorption is strongly affected by matrix effects, as already being demonstrated by Sedlar (2014) but Hg compounds are also transformed during the course of desorption, producing new compounds, not present in the original sample, which desorb at unpredictable temperatures.

Finally, it could be infer that in both soil and sediment “matrix-bound” Hg is principally bound to organic matter and with a lesser extend to mineral components. Anyway, these results give only an estimation of the predominant Hg binding form in the investigated soil and sediment, and further differentiation between Hg sorbed to mineral or organic components is difficult not only because of methodology limitations, but mainly because matrix components in soils normally exist as organo-mineral complexes that are hard to separate. Also, metal organic complexes in soil may be specifically adsorbed onto mineral surfaces, thus Hg is bound, to a different extend, with both types of components (Schuster, 1991).

This study allowed some conclusions to be drawn about Hg speciation in soils and sediments. Thermo-desorption cannot be considered a stand-alone tool in Hg fractionation analysis, because peak overlapping remains an unresolved problem. It can

be a valid method to investigate thermal behavior of different Hg compounds at high temperatures, e.g. to assess Hg volatilization during industrial processes (Sedlar et al., 2015), or it can be used to distinguish between cinnabar and “non-cinabar” Hg. Conversely, SEP procedure allows a better identification of different Hg species. Since the different procedures are intentionally developed based on which operationally defined Hg fractions have to be separated, the procedure has to be carefully chosen according to sample characteristics and purpose of fractionation, but it allows more specific Hg binding forms to be distinguished which are not discernable with TD analysis alone.

4.4.EFFECT OF MINERAL FERTILIZERS ON MERCURY MOBILITY

Mobility of Hg has been evaluated by thermal-desorption, water extraction and incubation under oxic and anoxic conditions for 30 days.

The effect of fertilizers has been studied in Fossalon soil (sampling point C13, 0-40 cm deep.) contaminated due to mining activity.

4.4.1. Effect of mineral fertilizers on Hg thermal stability

Thermal-desorption curves of native soil and the same soil added with urea is reported Figure 4.36 as an example. Tested fertilizers gave a similar thermal fractionation pattern as the soil without any treatment and they are all shown in Appendix C.

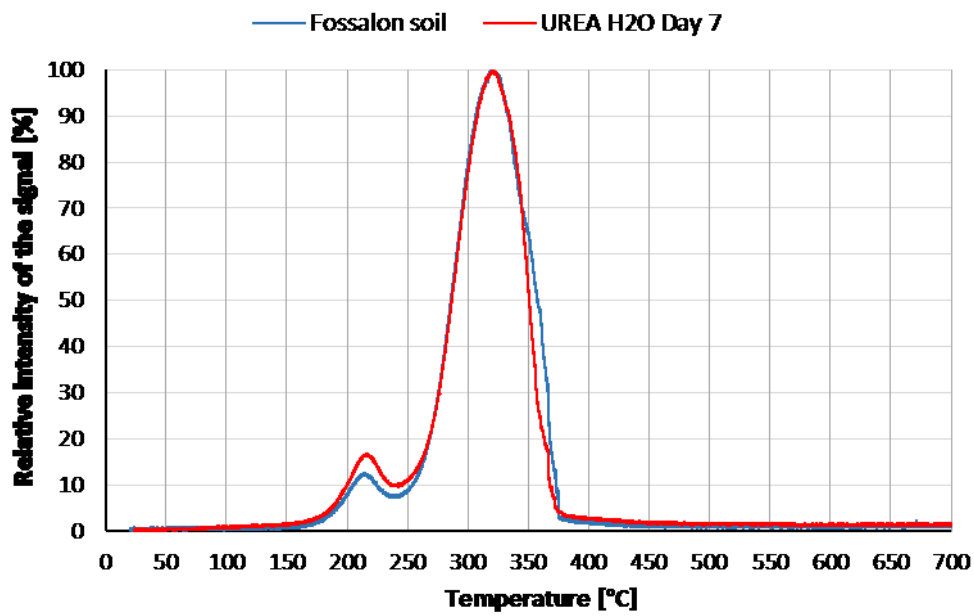


Figure 4.36. Thermo-desorption curves of native soil (sampling point C13, 0-40 cm dept) and soil amended with urea added in solution and incubated in aerobic conditions for seven days.

No significant changes can be attributed; only a slight increase in the relative height of peak 1 was evident but it is difficult to say to be significant.

4.4.2. Effect of mineral fertilizers on water extractable Hg

Water leaching test of native soil showed a very low Hg concentration after one and seven days ($0.60 \mu\text{g kg}^{-1}$). Water leaching test of soil added with fertilizers yield Hg concentrations frequently lower than unfertilizer soil; only urea increased Hg solubility up to $1.32 \mu\text{g kg}^{-1}$ (Table 4.14). Thus, the bulk of the contamination is not water soluble and not easily leachable from soil.

Table 4.14. Concentration of Hg ($\mu\text{g kg}^{-1}$) extracted with water.

Fertilizers addition	In solution		Solid	
	1 day	7 day	1 day	7 day
Native soil	0.60 ± 0.04	0.49 ± 0.09		
Fertilizers				
Urea	1.17 ± 0.06	0.54 ± 0.09	1.32 ± 0.11	0.39 ± 0.01
Ca(NO ₃) ₂	0.28 ± 0.02	0.24 ± 0.03	0.24 ± 0.03	0.24 ± 0.03
(NH ₄) ₂ HPO ₄	0.29 ± 0.02	0.45 ± 0.05	0.24 ± 0.03	0.35 ± 0.04
K ₂ SO ₄	0.29 ± 0.03	0.39 ± 0.09	0.29 ± 0.03	0.40 ± 0.02
Ca(H ₂ PO ₄) ₂	0.44 ± 0.09	0.42 ± 0.03	0.35 ± 0.03	0.40 ± 0.03
KCl	0.38 ± 0.04	0.40 ± 0.02	0.36 ± 0.02	0.36 ± 0.04
(NH ₄) ₂ SO ₄	0.25 ± 0.04	0.31 ± 0.03	0.30 ± 0.04	0.27 ± 0.03

4.4.3. Effect of mineral fertilizers on Hg solubility under aerobic and anaerobic conditions

Soils under study are characterized by shallow groundwater and frequent capillary rise. Therefore, it is worth to study Hg volatilization and solubilization under different redox changes.

Hg partitioning in solution ($\mu\text{g kg}^{-1}$) upon soil incubation in oxic vs anoxic condition, and as a result of mineral fertilizer addition, is shown in Figure 4.37

Anoxic conditions without any treatment enhanced Hg partition in solution, more than oxic incubation.

Addition of both KCl and urea in oxic conditions make no significant changes, while in anoxic environment they decreased Hg solubility in comparison to control soil (Figure 4.37).

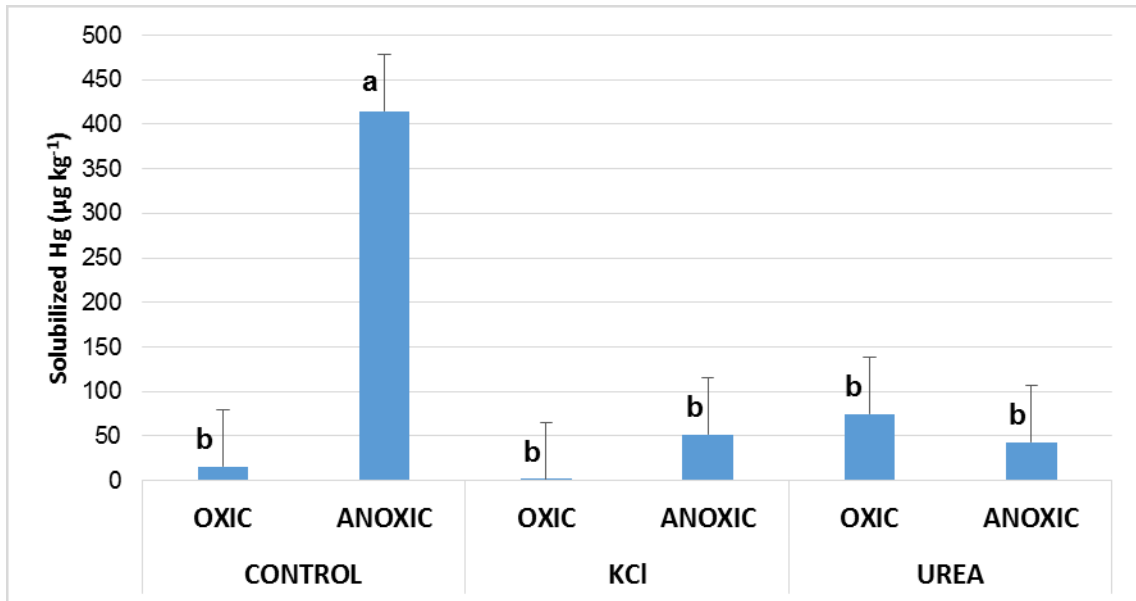


Figure 4.37. Mercury concentrations in added liquid solution of the “Reactor” container water in control soil, soil added with KCl and Urea. Different letters corresponds to significant differences ($P < 0.05$).

Urea has an amino group which is prone to bound with Hg, this complex however may be soluble in water, it could be argued that urea interacts even with soil compounds.

Salts of chloride are known to solubilize Hg (Schuster, 1999; Grassi and Netti, 2000). McLeod et al. (1996), in batch and column experiments, demonstrated that some fertilizers and NaCl solutions can remove most part of the Hg sorbed to the sediments. But in this experiment KCl did not increase Hg solubility. In anoxic condition, it played an important role in inhibiting Hg dissolution.

It can be argued that the different Hg speciation as well as soil characteristics make it tightly bound to soil.

4.4.4. Effect of mineral fertilizer on mercury volatility under aerobic and anaerobic conditions

The reduction of Hg^{2+} to Hg^0 and its further volatilization are very important surface processes in terrestrial environments because they can regulate much of the Hg load to the atmosphere.

Figure 4.38 shows the quantity of Hg collected in the “trap” over the whole period of incubation (first period of 15 days in red color, additional 15 days in orange color).

In all treatments the most part of Hg volatilized during the first 15 days of incubation. Hg reduction and volatilization from control soil was higher in anoxic incubation than in the oxic one, as expected, similarly happened for soil treated with mineral fertilizers.

Considering the Hg volatilized during the first 15 days of incubation, the addition of urea significantly reduced Hg volatilization.

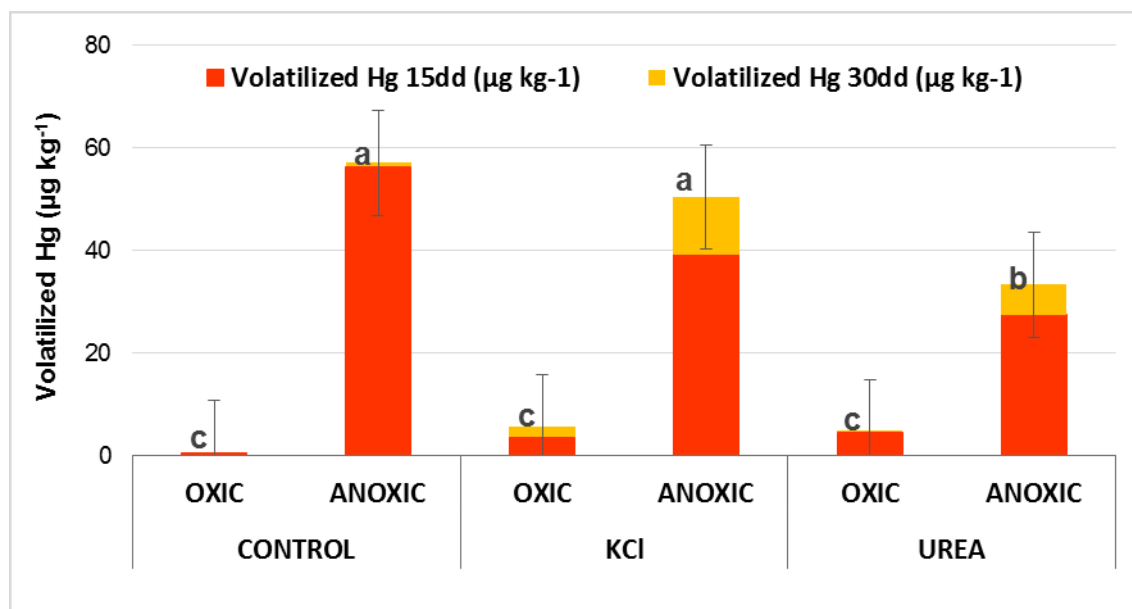


Figure 4.38. Mercury concentrations in oxidizing solution of the “Trap” container in oxidizing solution in control soil, soil added with KCl and Urea. Different letters corresponds to significant differences ($P < 0.05$).

4.5.EFFECT OF ORGANIC FERTILIZERS ON MERCURY MOBILITY

4.5.1. Effect of organic fertilizers on Hg thermal stability

Figure 4.39 and Figure 4.40 compares thermos-desorption curves of native soil with the same soil added with peat and digestate respectively. No important changes in thermal fractionation pattern can be observed, but a slight increase in relative high of peak 1 was observed in soil treated with both organic amendments (peat and digestate). It is difficult to say that these changes are significant.

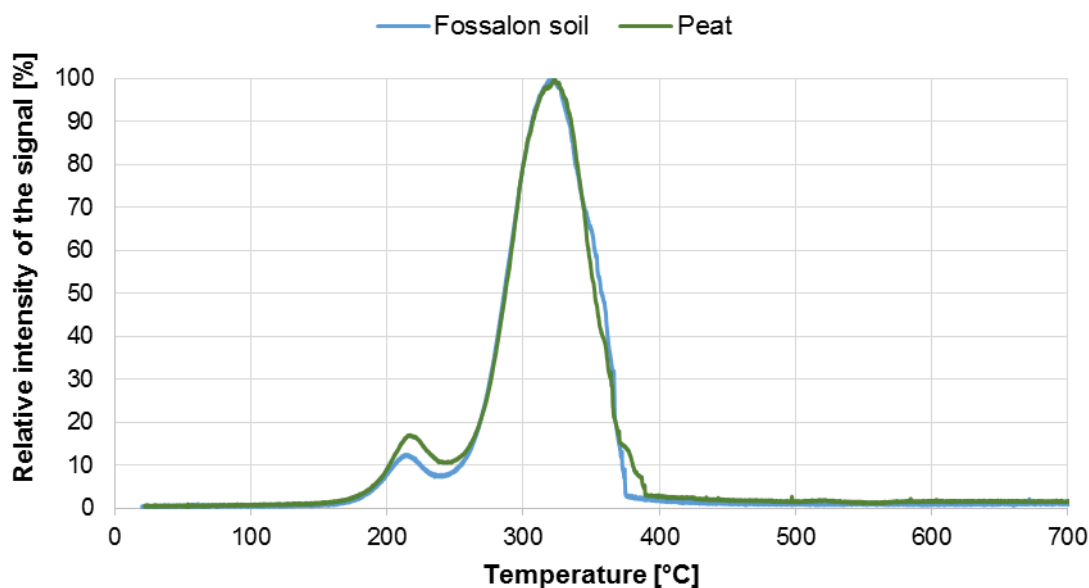


Figure 4.39. Thermo-desorption curves of Fossalon soil and soil amended with peat and incubated in aerobic conditions.

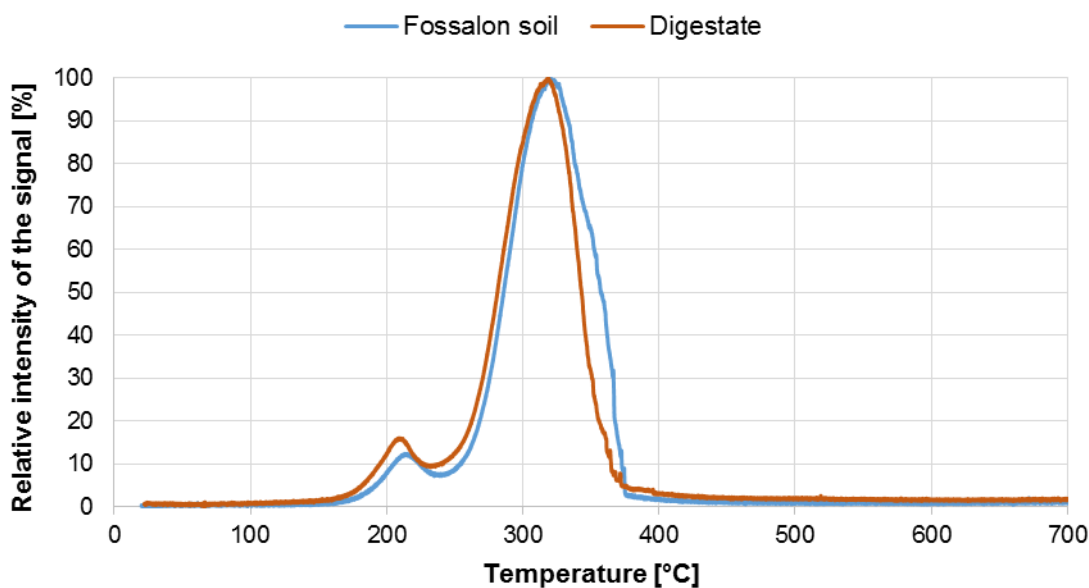


Figure 4.40. Thermo-desorption curves of Fossalon soil and soil amended with digestate and incubated in aerobic conditions.

4.5.2. Effect of organic fertilizers on water extractable Hg

Water solubility test of native soil as well as soil treated with amendments in aerobiosis yield Hg concentration below $0.5 \mu\text{g kg}^{-1}$ (Table 4.15). Thus, the bulk of the

contamination is not water soluble and not easily leachable from soil, and these two amendments did not change the solubility of Hg.

Table 4.15. Concentration of Hg ($\mu\text{g kg}^{-1}$) extracted with water.

Fertilizers addition	In solution	
	1 day	7 day
Native soil	0.60 \pm 0.04	0.49 \pm 0.09
PEAT	0.49 \pm 0.04	0.37 \pm 0.03
DIGESTATE	0.50 \pm 0.05	0.41 \pm 0.03

4.5.3. Effect of organic fertilizers on Hg solubility under aerobic and anaerobic conditions

Figure 4.41 shows Hg content in liquid phase of the “reactor” container, as well as Hg partition in solution in oxic soil incubation.

Anoxic soil (without any treatment) enhanced the Hg partitioning into liquid phase up to 414 $\mu\text{g kg}^{-1}$, respect to soil in oxic conditions.

Poultry addition enhanced Hg solubilization, both in oxic as in anoxic environment. Whereas, compost and humic acids enhanced Hg solubilization in oxic condition and decreased Hg solubilization in anoxic conditions.

It can be raised the hypothesis that poultry manure is able to complex Hg and keep it in solution, while compost and humic acids does not interact much with Hg in this soil, or they interact in a way that keep Hg bound to the solid phase.

Large and complex structures may not be able to interact with Hg inside the solid phase (Stallings, 2013).

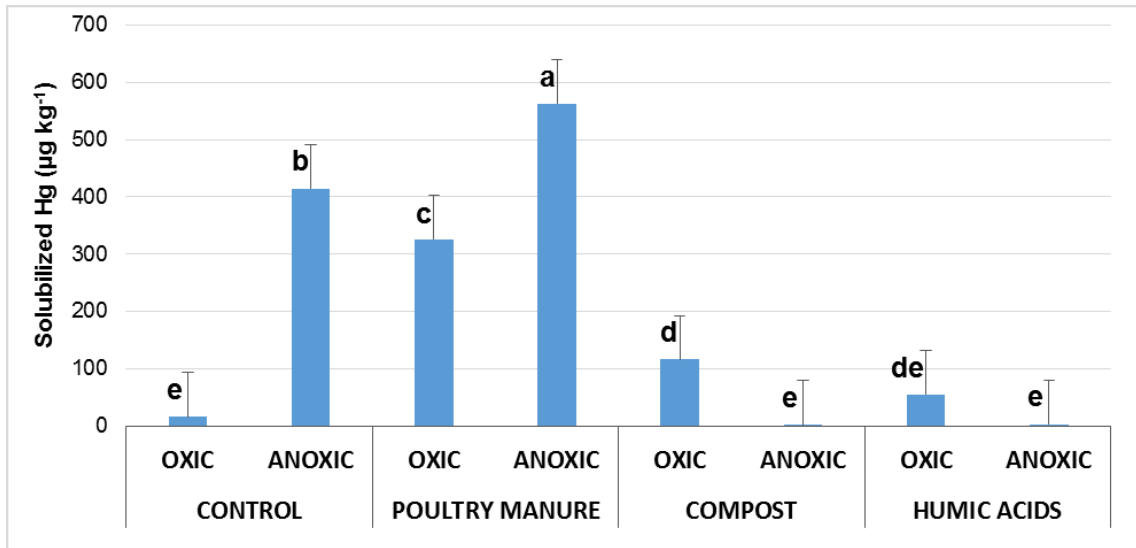


Figure 4.41. Mercury concentrations in added liquid solution of the “Reactor” container water in control soil, soil added with Poultry manure, Compost and Humic Acids. Different letters corresponds to significant differences ($P < 0.05$).

4.5.4. Effect of organic fertilizers on mercury volatility under aerobic and anaerobic conditions

Control soil shows higher volatilized Hg in anoxic conditions compared to oxic ones. While, when organic amendments are added, different results are highlight in oxic vs anoxic condition. Indeed, in oxic conditions poultry manure, compost and humic acids are able to reduce Hg and enhance its volatilization. But in anoxic conditions they are not able to reduce Hg with the same magnitude. On the other hand, volatilized Hg was lower using poultry manure, compost or humic acids under anoxic condition.

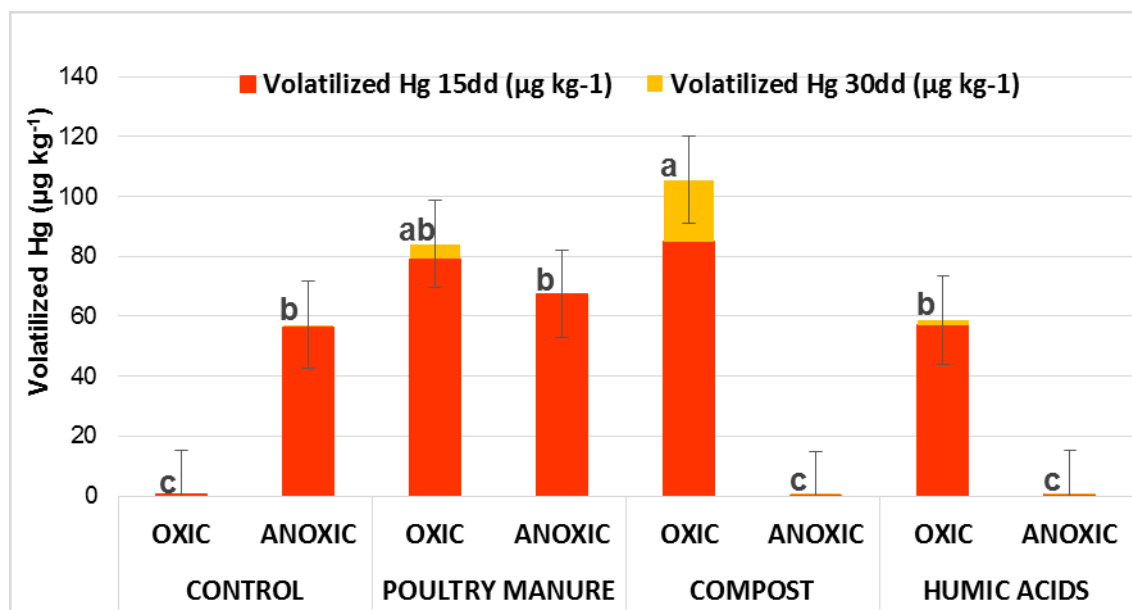


Figure 4.42. Mercury concentrations in oxidizing solution of the “Trap” container in oxidizing solution in control soil, soil added with Poultry manure, Compost and Humic Acids. Different letters corresponds to significant differences ($P < 0.05$).

It could be hypothesized that Hg, or substrate at which it is bound (i.e. organic matter, sulfur) are effectively oxidized in the presence of oxygen and made free in solution, where Hg can then be reduced by amendments. Whereas, in anoxic condition Hg remains tightly bound to solid surfaces, therefore can not be subjected to reduction.

Organic amendments are able to interact with Hg in oxic environment, while in anaerobiosis molecular structures are transformed in a way that they can not act as a reductant for Hg and may react with other species.

Organic amendments like poultry and compost can be also a growing substrate for microorganisms, which can reduce directly Hg, or indirectly by decomposing organic material and generating reductants. These microorganisms may be active in aerobic environments.

Poultry manure is mainly composed by uric acid, which may directly act as a reducing agent for Hg.

Humic substances are known to participate in redox reactions with elements in soil such as Fe, Mn, Hg. Nevertheless, few direct measurements of their redox properties, such as the formal electrode potential E_{h0} , have been reported. Standard IHSS humic acids from three sources were observed to participate in electron-transfer reactions at pH 5 with the formal electrode potential of 0.78 V (Figure 4.44). However, the origin of the HA samples

and, accordingly, their elemental and functional group composition, as well as environmental condition such as pH, determine oxidation capacity, which varied substantially.

Moreover, Scott et al. (1998) have reported that humic acids with more aromatic character also have greater electron-accepting capacity.

4.6.EFFECT OF ROOT EXUDATES ON MERCURY MOBILITY

4.6.1. Effect of root exudates on mercury solubility under aerobic and anaerobic conditions

With the addition of root exudates in anoxic condition a significant decrease of Hg in solution is highlighted for all root exudates tested, whereas in oxic soil glutathione and malate increased Hg dissolution (Figure 4.43).

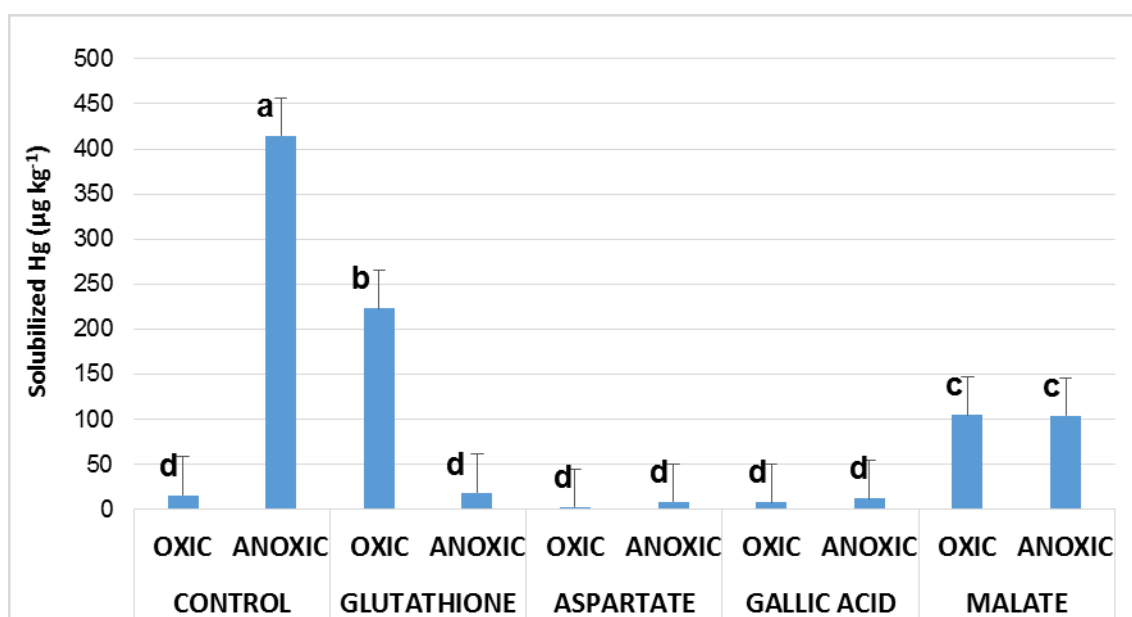


Figure 4.43. Mercury concentrations in added liquid solution of the “Reactor” container water in control soil, soil added with L-Glutathione, L-Aspartic acid, Gallic acid, Malic acid. Different letters corresponds to significant differences ($P < 0.05$).

As it can be seen from Figure 4.44, glutathione is the only compound tested heaving an SH- functional group. Therefore, it can be argued that it has the strongest affinity with Hg.

Hg²⁺, a soft, or B-type, metal cation, reacts readily with soft bases, of which inorganic sulfide (S²⁻) and organic thiolate (RS⁻) are most favorable (Haitzer et al., 2002). Weaker associations between Hg²⁺ and harder bases such as N- and O-bearing organic functional

groups (RCN⁻, RCOO⁻) can also be formed (Skylberg, 2008; Slowey, 2010). Therefore, among these molecules, glutathione may have the highest binding capacity because of its SH- functional group, which is not present in the other molecules.

Indeed, the importance of the thiol ligand in glutathione for copper complexation was shown by Leal et al. (1999) and Tang et al. (2001). A relation between glutathione and dissolved Hg has not yet been reported, though strong affinity between thiols and Hg suggests that glutathione can be an important Hg-binding organic ligand. This hypothesis is supported by the high concentration ratio of glutathione to Hg (~1000) in seawater (Han, 2004).

According to Dyrssen and Wedborg (1991), Hg-thiol complex should be a dominant species of dissolved Hg as long as sulfide concentration does not highly exceed thiol concentration based on the higher stability constants of Hg-thiol species than those of Hg-sulfide species ($\text{Hg}^{2+} + 2\text{SH}^- = \text{Hg}(\text{SH})_2$: $\text{Log } K = 37.7$; $\text{Hg}^{2+} + 2\text{RS}^- = \text{Hg}(\text{RS})_2$: $\text{Log } K = 41.6$).

However, depending on the reaction conditions, such as concentration of DOM, concentration of sulfide, and pH, the competition between the organic-Hg and sulfide-Hg complexes can occur. Evidences supporting a possible competition between sulfide and DOM species for Hg are provided by the inhibition of DOM from the nucleation of metacinnabar and by the enhanced dissolution of cinnabar in the existence of DOM (Ravichandran et al., 1998; 1999; Ravichandran, 2004).

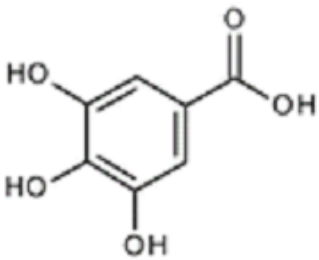
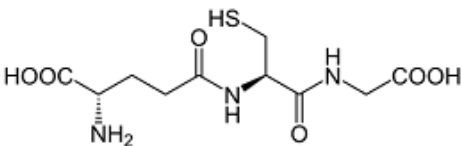
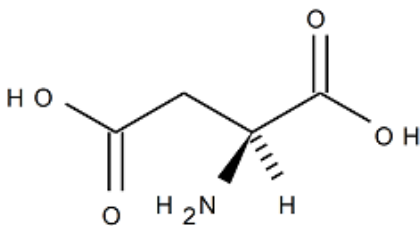
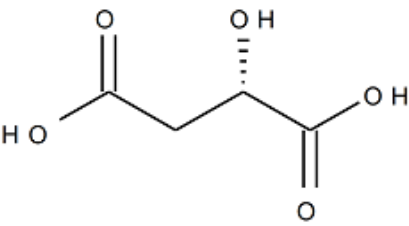
 <p>Gallic acid HA</p>	<p>Eh, pH=7, 25°C</p> <p>+ 1.04 (Abbasi et al., 2011)</p> <p>+ 0.78 (Struyk and Sposito, 2001)</p>
Hg²⁺	+ 0.69
 <p>Glutathione</p>	+ 0.35 (Rost and Rapoport, 1964)
 <p>Acido aspartico</p>	
 <p>Acido malico</p>	+ 0.17

Figure 4.44. Redox Ladder, values of Eh for the oxidation of substances used in this work.

Malate solubilized Hg possibly by altering pH condition and promoting colloidal mobilization of soil particles. Indeed, a lot of research has been carried out about LMW organic acids (malonic acid, oxalic acid, citric acid) enhanced colloid-facilitated Hg transport in tailings and contaminated soils (Slowey et al., 2005a; 2005b; Shaw et al., 2001).

Therefore, four hypothesis may be drawn to explain mechanisms involved in the Hg partitioning into liquid phase:

1. Hg complexation by functional groups (e.g. –SH) of small organic molecules.
2. Partial decomposition of organic matter, that may lead to the formation of small more soluble organic molecules (Ravichandran, 2004).
3. Microbial activity in anoxic soil, which may produce Methyl-Hg (CH_3Hg^+), (Frohne et al., 2012). It is therefore of primary importance to check the possible presence of CH_3Hg^+ in the solution.
4. Sulfide oxidation, which lead to the formation of HgSO_4 that is more soluble (Holley et al., 2007).

4.6.2. Effect of roots exudates addition on mercury volatility under aerobic and anaerobic conditions

In oxic conditions, no changes are highlighted with the addition of all root exudates in comparison with control soil (Figure 4.45).

In anoxic condition, the addition of root exudates enhanced Hg volatilization, moreover, in contrast with the other amendments tested, malic and aspartic acids lead to greater Hg volatilization even in the second period of incubation (15-30 days).

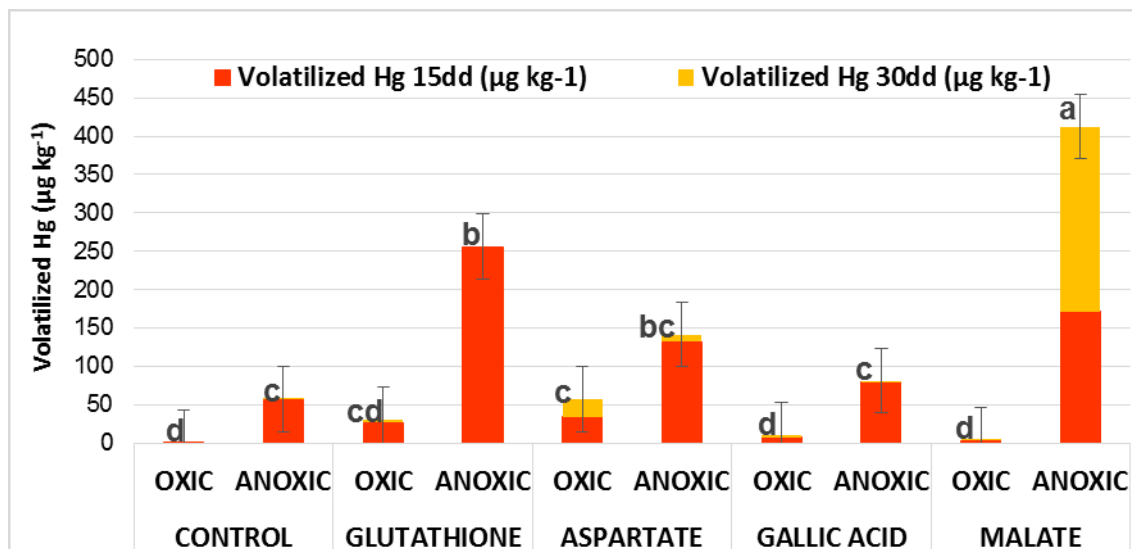


Figure 4.45. Mercury concentrations in oxidizing solution of the “Trap” container in oxidizing solution in control soil, soil added with L-Glutathione, L-Aspartic acid, Gallic acid, Malic acid. Different letters corresponds to significant differences ($P < 0.05$).

Gallic acid (3,4,5- trihydroxybenzoic acid) is a natural phenolic compound which can generate a well defined reduction peak at around -1.04 V (versus Ag/AgCl) in 0.1 M borax buffer solution (pH 7.53) (Abbasi et al., 2011).

As it can be seen in Figure 4.44 the Eh values indicate that electrons can spontaneously pass from gallic acid as well as humic acids to Hg. In other words, the reduction of Hg by gallic acids is favorable.

Moreover, it can be also observed that gallic acid has an aromatic ring which is well known to act as an electron donor (Abbassi et al., 2011; Waples et al., 2005). Despite that, this experiment shows no effect of gallic acid on Hg volatility. Maybe gallic acid is not able to interact with Hg in the conditions under study. It can be hypothesized that Hg have to be solubilized first by other complexing agents, as is the case of glutathione and malate.

Glutathione and malate can promote Hg volatilization even though that the redox potential is lower than Hg. Probably they can enhanced Hg solubilization through complexation first, afterwards Hg get free in solution is prone to be reduced by other species presented or formed in an anoxic soil e.g. Fe(II). Electron transfer at the magnetite-water interface involves direct interactions between the Hg(II) and structural ferrous iron as free electrons are not readily transferred into aqueous solution. Adsorption sites are one location where reduction of metal ions can occur. Then the adsorbed Hg(II)

interacts with magnetite surfaces by accepting electrons from Fe(II) in the magnetite structure (Wiatrowsky et al., 2009)

These results are as expected, because it has been demonstrated that the dissolution of Hg as well as cinnabar occurs under anoxic conditions and it is enhanced substantially in the presence of organic matter (Ravichandran et al., 1998; Waples et al., 2005). Moreover, amounts and rates of Hg released from cinnabar over 10 h in the presence of organic matter samples were correlated with the aromaticity of the organic matter (Waples et al., 2005). These authors hypothesized that redox sensitive aromatic moieties within the organic matter played a role in the mechanism of Hg release from HgS. However, surface contact is needed.

Under anoxic conditions and at near neutral pH, various metal oxides have been shown to dissolve more rapidly in the presence of redox compounds such as hydroquinones, resorcinols, methoxy aromatics, mono-substituted benzoic acids and non-aromatics (Stone and Morgan, 1984). For example, the dissolution of manganese (III & IV) oxides was enhanced in the presence of hydroquinone and ascorbate (Stone and Morgan, 1984). Dissolution of Hg may depend not only upon the redox reactivity of the organic matter, but also on the type of redox environment in which both organic matter and cinnabar reside. Indeed, aromatic moieties may simultaneously exist in multiple redox states within the same organic matter fraction and the overall contribution of reduced vs oxidized components changes according to redox potential of environment.

Clearly, Hg reactivity is complicated by the oxidation-reduction reactions that all species in soil may undergo.

However, although there is more research on abiotic factors, Hg can also be reduced biotically. Microorganisms might reduce Hg(II) either directly, to detoxify their immediate environment, or indirectly by either decomposing organic matter, or by converting their substrate into compounds capable of Hg(II) reduction; e.g. humic and fulvic acids (Fritsche et al., 2008; Obrist et al., 2010).

Compost and Poultry manure is a metabolic substrate for microorganisms. Carbon pools are highly dynamic and subject to mineralization processes, but little is known about the fate of Hg during decomposition. Obrist et al. (2010), performing experiments in oxic and anoxic laboratory conditions, suggested a possible involvement of microbial reduction of Hg²⁺ by anaerobes.

Our observations are supported by previous work that demonstrate a higher Hg volatilization in anoxic conditions. Obrist et al. (2010) induced changes in CO₂ respiration rates and observed Hg flux responses, including inducement of anaerobic conditions by changing chamber air supply from N₂/O₂ (80% and 20%, respectively) to pure N₂.

Unexpectedly, Hg emissions almost quadrupled after O₂ deprivation while oxidative mineralization (i.e. CO₂ emissions) was greatly reduced. This Hg flux response to anaerobic conditions was lacking when repeated with sterilized soils, possibly due to involvement of microbial reduction of Hg²⁺ by anaerobes or indirect abiotic effects such as alterations in soil redox conditions.

Therefore the possible hypothesis for Hg release through volatilization are:

1. Abiotic processes, involving reductants such as humic acids, Fe(II);
2. Microorganisms reduction;
3. Combined biotic and abiotic reduction.

5. CONCLUSIONS

This work confirmed that soils in the area near the Isonzo river are contaminated by past mining activity in Idrija (SLO). Indeed the soil survey evidenced the presence of past-buried sedimentary horizons originated from the Isonzo riverbed.

The contamination distribution is coherent with a long-term gradual deposition of contaminated particulate material. This material is showed to be principally coarse with cinnabar particles. Mercury is most concentrated in the Silt and Fine Sand texture fractions as demonstrated by particle size distribution analysis and SEP fractionation.

Moreover, as shown by using the SEP proposed by Han et al. (2006), only the 0.09% of total Hg is leached in the first extracting step (soluble plus exchangeable Hg): this imply that there is a little risk of groundwater contamination through leaching, or that all the leachable Hg has been already leached out.

By using the SEP proposed by Lechler et al. (1997), we demonstrated that, notwithstanding the Silt fraction presents the highest Hg concentration, this Hg is not easily mobilizable, being mainly extracted in the residual fraction, while Hg present in the Clay fraction is for a large part volatilized at 180 °C. It can be deduced that the coarse grained fractions contain a higher proportion of cinnabar, whereas the finest fractions are characterized by the presence of colloidal organic Hg compounds.

The second conclusion of this work is that thermo-desorption cannot be considered a stand-alone technique in soil Hg speciation analysis, because peak overlapping of different Hg species remains an unresolved question, although it can be useful to discern among elemental Hg, non-cinnabar Hg and cinnabar Hg fractions. Conversely, SEP allowed a better identification of the different Hg species.

Combining multiple methodologies together is an effective way to enhance Hg fractionation towards a complete Hg speciation. In fact, coupling TD measurements with seven steps SEP, the “matrix-bound Hg” was identified. Accordingly, it could be inferred that in both soil and sediment examined, the “matrix-bound” Hg was principally bound to organic matter and to a lesser extent to mineral components (i.e. Fe oxides, carbonates, etc.).

This study provided evidence that Hg solubilization and volatilization in soil is enhanced by anaerobiosis. Thus, the practical implication is that Hg volatilization can be controlled by soil aeration by an efficient drainage.

Conclusions

The application of mineral fertilizers had no significant effect on Hg solubility and volatility in aerobic conditions, while in anaerobiosis they reduced Hg solubility.

Organic fertilizers enhanced Hg mobilization in aerobic conditions, but not in anaerobiosis. Particularly, poultry manure, compost and humic acids have shown to increase both Hg solubility and volatility in aerobic conditions, whereas only poultry manure increased Hg solubilization in anaerobic conditions.

The root exudates have shown to decrease Hg solubility both in oxic and in anoxic soil incubation, except for glutathione and malic acid, which increased Hg solubilization. All the tested root exudates increased Hg volatilization in anoxic soil incubation.

In conclusion, in the investigated soil, the use of mineral fertilizers in aerobic conditions has no implications on Hg mobility and it is important to maintain soil in aerobic conditions through an efficient drainage, in order to reduce Hg volatilization.

REFERENCES

- Abbasi, S., Daneshfar, a., Hamdghadareh, S., & Farmany, a. (2011). Quantification of sub-nanomolar levels of gallic acid by adsorptive stripping voltammetry. *International Journal of Electrochemical Science*, 6(10), 4843–4852.
- Acquavita, A., Covelli, S., Emili, A., Berto, D., Faganeli, J., Giani, M., Rampazzo, F. (2012). Hg in the sediments of the Marano and Grado Lagoon (northern Adriatic Sea): Sources, distribution and speciation. *Estuarine, Coastal and Shelf Science*, 113, 20–31. doi:10.1016/j.ecss.2012.02.012
- Akagi, H., & Nishimura, H. (1991). Speciation of Hg in the environment. In T. Suzuki, N. Imura, & T. W. Clarkson (Eds.), *Advances in Hg Toxicology* (pp. 53–76). Springer US.
- Alberts, J. J., Schindler, J. E., Miller, R. W., & Nutter, D. E. (1974). Elemental Hg Evolution Mediated by Humic Acid. *Science*, 184(4139), 895–897. doi:10.1126/science.184.4139.895
- Allard, B., & Arsenie, I. (1991). Abiotic reduction of Hg by humic substances in aquatic system — an important process for the Hg cycle. *Water, Air, and Soil Pollution*, 56(1), 457–464.
- Amos, H. M., Jacob, D. J., Streets, D. G., & Sunderland, E. M. (2013). Legacy impacts of all-time anthropogenic emissions on the global Hg cycle. *Global Biogeochemical Cycles*, 27(2), 410–421. doi:10.1002/gbc.20040
- Amyot, M., Mierle, G., Lean, D. R. S., & McQueen, D. J. (1994). Sunlight-Induced Formation of Dissolved Gaseous Hg in Lake Waters. *Environmental Science & Technology*, 28(13), 2366–2371. doi:10.1021/es00062a022
- Andersson A., 1979. In: Nriagu J.O., ed. *The biogeochemistry of Hg in the environment*, Elsevier, Amsterdam.
- Bååth, E. (1989). Effects of heavy metals in soil on microbial processes and populations (a review). *Water, Air, and Soil Pollution*, 47(3), 335–379. doi:10.1007/BF00279331
- Babiarz, C. L., Hurley, J. P., Hoffmann, S. R., Andren, a W., & Shafer, M. M. (2001). Partitioning of Total Hg and MethylHg to the Colloidal Phase in Freshwater. *Colloidal Phase in Freshwaters. Environmental Science & Technology*, 35(24), 4773–4782.
- Bacon, J. R., & Davidson, C. M. (2008). Is there a future for sequential chemical extraction? *The Analyst*, 133(1), 25–46. doi:10.1039/b711896a
- Baldi, F., & Olson, G. J. (1987). Effects of cinnabar on pyrite oxidation by *Thiobacillus ferrooxidans* and cinnabar mobilization by a Hg-resistant strain. *Applied and Environmental Microbiology*, 53(4), 772–776. doi:10.1016/0734-9750(88)90824-5
- Barkay, T., Gillman, M., Turner, R. R., Barkay, T., & Gillman, M. (1997). Effects of dissolved organic carbon and salinity on bioavailability of Hg . *Effects of Dissolved Organic Carbon and Salinity on Bioavailability of Hg*, 63(11), 4267–4271.
- Barnett, M. O., Harris, L. a., Turner, R. R., Stevenson, R. J., Henson, T. J., Melton, R. C., & Hoffman, D. P. (1998). Formation of mercuric sulfide in soil. *Environmental Science and Technology*, 31(11), 3037–3043. doi:10.1021/es960389j

References

- Begley, T. P., Walts, a E., & Walsh, C. T. (1986). Bacterial organomercurial lyase: overproduction, isolation, and characterization. *Biochemistry*, 25(22), 7186–92. doi:10.1021/bi00370a063
- Beckvar, N., Field, J., Salazar, S., Hoff, R., (1996). Contaminants in Aquatic Habitats at Hazardous Waste Sites: Mercury. NOAA Technical Memorandum NOS ORCA 100. Department of Commerce.
- Benoit, J. M., Mason, R. P., Gilmour, C. C., & Aiken, G. R. (2001)a. Constants for Hg binding by organic matter isolates from the Florida Everglades. *Geochimica et Cosmochimica Acta*, 65(24), 4445–4451. doi:10.1016/S0016-7037(01)00742-6
- Benoit, J. M., Gilmour, C. C., & Mason, R. P. (2001)b. The influence of sulfide on solid-phase Hg bioavailability for methylation by pure cultures of *Desulfobulbus propionicus* (1pr3). *Environmental Science and Technology*, 35(1), 127–132. doi:10.1021/es001415n
- Benoit, J. M., Gilmour, C. C., Heyes, a., Mason, R. P., & Miller, C. L. (2003). Geochemical and Biological Controls over MethylHg Production and Degradation in Aquatic Ecosystems, (January), 262–297. doi:10.1021/bk-2003-0835.ch019
- Benoit, J. M., Gilmour, C. C., Mason, R. P., & Heyes, A. (1999)a. Sulfide controls on Hg speciation and bioavailability to methylating bacteria in sediment pore waters. *Environmental Science and Technology*, 33(6), 951–957. doi:10.1021/es9808200
- Benoit, J. M., Mason, R. P., & Gilmour, C. C. (1999)b. Estimation of Hg-sulfide speciation in sediment pore waters using octanol-water partitioning and implications for availability to methylating bacteria. *Environmental Toxicology and Chemistry*, 18(10), 2138–2141. doi:10.1002/etc.5620181004
- Bicak, N., Sherrington, D. C., Sungur, S., & Tan, N. (2003). A glycidyl methacrylate-based resin with pendant urea groups as a high capacity Hg specific sorbent. *Reactive and Functional Polymers*, 54(1-3), 141–147. doi:10.1016/S1381-5148(02)00189-X
- Biester, H., & Nehrke, G. (1997). Quantification of Hg in soils and sediments – acid digestion versus pyrolysis. *Fresenius' Journal of Analytical Chemistry*, 358(3), 446–452.
- Biester, H., & Scholz, C. (1997). Determination of Hg binding forms in contaminated soils: Hg pyrolysis versus sequential extractions. *Environmental Science and Technology*, 31(1), 233–239. doi:10.1021/es960369h
- Biester, H., Gosar, M., & Covelli, S. (2000). Hg speciation in sediments affected by dumped mining residues in the drainage area of the Idrija Hg mine, Slovenia. *Environmental Science and Technology*, 34(16), 3330–3336. doi:10.1021/es991334v
- Biester, H., Gosar, M., & Müller, G. (1999). Hg speciation in tailings of the Idrija Hg mine. *Journal of Geochemical Exploration*, 65(3), 195–204.
- Biester, H., Müller, G., & Schöler, H. F. (2002). Binding and mobility of Hg in soils contaminated by emissions from chlor-alkali plants. *Science of the Total Environment*, 284(1-3), 191–203. doi:10.1016/S0048-9697(01)00885-3
- Bloom, N. S., Preus, E., Katon, J., & Hiltner, M. (2003). Selective extractions to assess the biogeochemically relevant fractionation of inorganic Hg in sediments and soils. *Analytica Chimica Acta*, 479(2), 233–248. doi:10.1016/S0003-2670(02)01550-7

- Bloom, N., & Preus, E. (2003). Anoxic sediment incubations to assess the methylation potential of Hg contaminated solids. 2nd International Symposium on Contaminated Sediments Ecotoxicology, 2–7.
- Bloom, N.S., Coleman, J.A., and Barber, L. (1997). Artifact formation of methyl Hg during extraction of environmental samples by distillation. *Fresenius Journal of Analytical Chemistry*, 358, 371–377.
- Bollen, a., Wenke, a., & Biester, H. (2008). Hg speciation analyses in HgCl₂-contaminated soils and groundwater-Implications for risk assessment and remediation strategies. *Water Research*, 42(1-2), 91–100. doi:10.1016/j.watres.2007.07.011
- Boszke, L., Kowalski, a., Głosińska, G., Szarek, R., & Siepak, J. (2003). Environmental factors affecting speciation of Hg in the bottom sediments; an overview. *Polish Journal of Environmental Studies*, 12(1), 5–13.
- Bowles, K. C., & Apte, S. C. (2000). Determination of methylHg in sediments by steam distillation/aqueous-phase ethylation and atomic fluorescence spectrometry. *Analytica Chimica Acta*, 419(2), 145–151. doi:10.1016/S0003-2670(00)00997-1
- Bradley, P. M., & Chapelle, F. H. (1998). Humic Acids as Electron Acceptors for Anaerobic Microbial Oxidation of Vinyl Chloride and Dichloroethene, 64(8), 3102–3105.
- Brambati, A., 1997. *Metalli pesanti nelle Lagune di Marano e Grado. Piano di studi finalizzato all'accertamento della presenza di eventuali sostanze persistenti nelle Lagune di Grado e Marano e al loro risanamento. Regione Autonoma Friuli-Venezia Giulia, Direzione Regionale dell'Ambiente, Servizio dell'Idraulica, Trieste, 1996, 174 pp.*
- Brandon, N. P., Francis, P. a., Jeffrey, J., Kelsall, G. H., & Yin, Q. (2001). Thermodynamics and electrochemical behaviour of Hg-S-Cl-H₂O systems. *Journal of Electroanalytical Chemistry*, 497(1-2), 18–32. doi:10.1016/S0022-0728(00)00445-9
- Brondi, M., Dall'Aglio, M., Ghiara, E., & Gragnani, R. (1986). Distribuzione degli elementi minori ed in traccia di interesse tossicologico e nutrizionale nelle acque italiane. *Acqua-Aria*, 10, 1043–1061.
- Bru"mmer, G., & Herms, U. (1983). Influence of soil reaction and organic matter on the solubility of heavy metals in soils. In *Effects of Accumulation of Air Pollutants in Forest Ecosystems* (B. Ulrich and J. Pankrath, Eds.). D. Reidel, Dordrecht, 233–243.
- Buchter, B., Davidoff, B., Amacher, M. C., Hinz, C., Iskandar, I. K., & Selim, H. M. (1989). Correlation of Freundlich K_d and n retention parameters with soils and elements. *Soil Sci*, 148, 370–379.
- Buffle, J., & De Vitre, R. (1994). *Chemical and Biological Regulation of Aquatic Systems*. Lewis Publishers.
- Burkstaller, J. E., McCarty, P. L., & Parks, G. a. (1975). Oxidation of cinnabar by Fe(III) in acid mine waters. *Environmental Science and Technology*, 9(7), 676–678. doi:10.1021/es60105a004
- Calmano, W., Germany, W., & Germany, W. (1983). Chemical extraction of heavy metals in polluted river sediments in central Europe. *The Science of the Total Environment*, 28, 77–90.
- Canário, J., Antunes, P., Lavrado, J., & Vale, C. (2004). Simple method for monomethylHg determination in estuarine sediments. *TrAC - Trends in Analytical Chemistry*, 23(10-11), 799–806. doi:10.1016/j.trac.2004.08.009

References

- Charlet, L., Bosbach, D., & Peretyashko, T. (2002). Natural attenuation of TCE, As, Hg linked to the heterogeneous oxidation of Fe(II): An AFM study. *Chemical Geology*, 190(1-4), 303–319. doi:10.1016/S0009-2541(02)00122-5
- Chopin, E., & Alloway, B. (2007). Distribution and mobility of trace elements in soils and vegetation around the mining and smelting areas of Tharsis, Riotinto and Huelva, Iberian Pyrite Belt, SW Spain. *Water Air Soil Pollut.*, 183, 245–261.
- Cifuentes, L., 1991. Spatial and temporal variations in terrestrially-derived organic matter from sediments of the Delaware Estuary. *Estuaries* 14 (4), 414–429.
- Claff, S. R., Burton, E. D., Sullivan, L. a., & Bush, R. T. (2010). Effect of sample pretreatment on the fractionation of Fe, Cr, Ni, Cu, Mn, and Zn in acid sulfate soil materials. *Geoderma*, 159(1-2), 156–164. doi:10.1016/j.geoderma.2010.07.007
- Clarkson, T. W. (2002). The Three Modern Faces of Hg Methyl Hg in Fish History of Human Exposure. *Environmental Health Perspectives*, 110(1), 11–23.
- Cobos, D. R., Baker, J. M., & Nater, E. a. (2002). Conditional sampling for measuring Hg vapor fluxes. *Atmospheric Environment*, 36(27), 4309–4321. doi:10.1016/S1352-2310(02)00400-4
- Coker, W.B., 1995. Processes Effecting Mercury and Associated Metals in Lake Sediment Columns. Canadian Mercury Network Workshop, Geological Survey of Canada, 601 Booth Street, Ottawa, Ontario. K1A 0E8.
- Compeau, G. C., & Bartha, R. (1987). Effect of Salinity on Hg-Methylating Activity of Sulfate-Reducing Bacteria in Estuarine Sediments. *Applied and Environmental Microbiology*, 53(2), 261–265. Retrieved from <Go to ISI>://WOS:A1987F857600009
- Consorzio di Bonifica Bassa Friulana. 2003. Piano di Caratterizzazione di un'area agricola in località Fossalon di Grado ai sensi del D.Lgs. 152/06 e smi, Udine (I).
- Covelli S., Piani R., Faganelli J., Brambati A., 2004. Circulation and suspended matter distribution in a microti dal deltaic system: the Isonzo river mouthv(northern Adriatic Sea). *Journal of Coastal Research* 41, 130-140.
- Covelli S., Fontolan G., Faganelli J., Ogrinc N., 2006. Anthropogenic markers in the Holocene stratigraphic sequence of the Gulf of Trieste (northern Adriatic Sea). *Marine Geology* 230, 29–51
- Covelli, S., Acquavita, A., Piani, R., Predonzani, S., & De Vittor, C. (2009). Recent contamination of Hg in an estuarine environment (Marano lagoon, Northern Adriatic, Italy). *Estuarine, Coastal and Shelf Science*, 82(2), 273–284. doi:10.1016/j.ecss.2009.01.021
- Covelli, S., Emili, A., Acquavita, A., Koron, N., & Faganelli, J. (2011). Benthic biogeochemical cycling of Hg in two contaminated northern Adriatic coastal lagoons. *Continental Shelf Research*, 31(16), 1777–1789. doi:10.1016/j.csr.2011.08.005
- Covelli, S., Faganelli, J., De Vittor, C., Predonzani, S., Acquavita, A., & Horvat, M. (2008). Benthic fluxes of Hg species in a lagoon environment (Grado Lagoon, Northern Adriatic Sea, Italy). *Applied Geochemistry*, 23(3), 529–546. doi:10.1016/j.apgeochem.2007.12.011

- Covelli, S., Faganeli, J., Horvat, M., & Brambati, A. (2001). Hg contamination of coastal sediments as the result of long-term cinnabar mining activity (Gulf of Trieste, northern Adriatic sea). *Applied Geochemistry*, 16(5), 541–558. doi:10.1016/S0883-2927(00)00042-1
- Covelli, S., Piani, R., Acquavita, A., Predonzani, S., & Faganeli, J. (2007). Transport and dispersion of particulate Hg associated with a river plume in coastal Northern Adriatic environments. *Marine Pollution Bulletin*, 55(10-12), 436–450. doi:10.1016/j.marpolbul.2007.09.006
- Cranston, R., & Buckley, D. (1972). Hg pathways in a river and estuary. *Environmental Science & Technology*, 274–278. doi:10.1021/es60062a007
- Curtis, G. P., & Reinhard, M. (1994). Reductive dehalogenation of hexachloroethane, carbon tetrachloride, and bromoform by anthrahydroquinone disulfonate and humic acid. *Environmental Science & Technology*, 28(13), 2393–2401. doi:10.1021/es00062a026
- Daris F., Piani C., Mattassi G., Brisotto R. (1993). Distribuzione del mercurio in sedimenti e prodotti ittici delle Lagune di Grado e Marano. In: Atti del convegno “Il mercurio nelle Lagune di Grado e Marano – Aspetti igienico sanitari. Villa Manin di Passariano (UD) – 4 dicembre 1993: 24-45.
- Davis, A., Bloom, N. S., Que Hee, S. S., Hee, Q., & Shane, S. (1997). The environmental geochemistry and bioaccessibility of Hg in soils and sediments: a review. *Risk Analysis*, 17(5), 557–569. doi:10.1111/j.1539-6924.1997.tb00897.x
- De Nobili, M., Contin, M., Mahieu, N., Randall, E. W., & Brookes, P. C. (2008). Assessment of chemical and biochemical stabilization of organic C in soils from the long-term experiments at Rothamsted (UK). *Waste Management*, 28(4), 723–733. doi:10.1016/j.wasman.2007.09.025
- Deonaraine, A., & Hsu-Kim, H. (2009). Precipitation of mercuric sulfide nanoparticles in NOM-containing water: Implications for the natural environment. *Environmental Science and Technology*, 43(7), 2368–2373. doi:10.1021/es803130h
- Deonaraine, A., Lau, B. L. T., Aiken, G. R., Ryan, J. N., & Hsu-Kim, H. (2011). Effects of humic substances on precipitation and aggregation of zinc sulfide nanoparticles. *Environmental Science and Technology*, 45(8), 3217–3223.
- Dirk Wallschläger *, Madhukar V. M. Desai, M. S. and R.-D. W. (1998). Hg Speciation in Floodplain Soils and Sediments along a Contaminated River Transect. *J. Environ. Qual.*, 27(5), 1034–1044. doi:10.2134/jeq1998.00472425002700050008x
- Dizdarevič, T. (2001). The influence of Hg production in Idrija mine on the environment in the Idrija region and over a broad area. *RMZ- Materials and Geoenvironment*, 48/1, 56–64.
- Dohnalkova, a, Marshall, M. J., Kennedy, D. W., Gorby, Y. a, Shi, L., Beliaev, a, ... Fredrickson, J. K. (2005). The Role of Bacterial Exopolymers in Metal Sorption and Reduction. *Microscopy and Microanalysis*, 11(S02), 116–117. doi:10.1017/S1431927605506688
- Donkor, a. K., Bonzongo, J. C., Nartey, V. K., & Adotey, D. K. (2006). Hg in different environmental compartments of the Pra River Basin, Ghana. *Science of the Total Environment*, 368(1), 164–176. doi:10.1016/j.scitotenv.2005.09.046
- Driscoll CT, Otton JK, Iverfeldt A. (1994). Trace metals speciation and cycling. In: Moldan B, Cerry J, editors. *Biogeochemistry of small catchments*. New York: J Wiley;

References

- Driscoll, C. T., Mason, R. P., Chan, H. M., Jacob, D. J., & Pirrone, N. (2013). Hg as a global pollutant: Sources, pathways, and effects. *Environmental Science and Technology*, 47(10), 4967–4983. doi:10.1021/es305071v
- Drott, a, Bouchet, S., & Skyllberg, U. (2013). Re fi ning Thermodynamic Constants for Hg(II)-Sul fi des in Equilibrium with Metacinnabar at Sub-Micromolar Aqueous Sul fi de Concentrations, (Ii).
- Dunnivant, F. M., Schwarzenbach, R. P., & Macalady, D. L. (1992). Reduction of Substituted Nitrobenzenes in Aqueous Solutions Containing Natural Organic Matter. *Environmental Science & Technology*, 26(11), 2133–2141. doi:10.1021/es00035a010
- Dyrssen, D., & Wedborg, M. (1991). The sulphur-Hg(II) system in natural waters. *Water Air & Soil Pollution*, 56(1), 507–519. doi:10.1007/BF00342295
- Ebinghaus, R., Kock, H. H., Temme, C., Einax, J. W., Löwe, A. G., Richter, A., ... Schroeder, W. H. (2002). Antarctic springtime depletion of atmospheric Hg. *Environmental Science and Technology*, 36(6), 1238–1244. doi:10.1021/es015710z
- Eganhouse r.p., Young D.R., Johnson J.N., (1978). Geochemistry of mercury in Palos Verdes sediments. *Environmental Science and Technology* 12 (10), 1151-1157.
- Elliott, H. A., & Huang, C. P. (1979). The effect of complex formation on the adsorption characteristics of heavy metals. *Environment International*, 2(3), 145–155. doi:doi:10.1016/0160-4120(79)90072-2
- Engle, M. a., Gustin, M. S., & Zhang, H. (2001). Quantifying natural source Hg emissions from the Ivanhoe Mining District, north-central Nevada, USA. *Atmospheric Environment*, 35(23), 3987–3997. doi:10.1016/S1352-2310(01)00184-4
- Faganeli, J., Hines, M. E., Covelli, S., Emili, A., & Giani, M. (2012). Hg in lagoons: An overview of the importance of the link between geochemistry and biology. *Estuarine, Coastal and Shelf Science*, 113, 126–132. doi:10.1016/j.ecss.2012.08.021
- Fang, S. C. (1981). Studies on the sorption of elemental Hg vapor by soils. *Archives of Environmental Contamination and Toxicology*, 10(2), 193–201.
- Feick, G., Horne, R. A., & Yeaple, D. (1972). Release of Hg from contaminated freshwater sediments by the runoff of road deicing salt. *Science*, 175(1142).
- Fernández-Martínez, R., Rucandio, M.I. (2003). Study of extraction conditions for the quantitative determination of Hg bound to sulfide in soils from Almaden (Spain). *Anal. Bioanal. Chem.*, 375, 1089–1096.
- Fernández-Martínez, R., Loredo, J., Ordóñez, A., & Rucandio, M. I. (2006). Physicochemical characterization and mercury speciation of particle-size soil fractions from an abandoned mining area in Mieres, Asturias (Spain). *Environmental Pollution*, 142(2), 217–226. doi:10.1016/j.envpol.2005.10.034
- Fernández-Martínez, R., & Rucandio, I. (2013). Assessment of a sequential extraction method to evaluate Hg mobility and geochemistry in solid environmental samples. *Ecotoxicology and Environmental Safety*, 97, 196–203. doi:10.1016/j.ecoenv.2013.07.013
- Filgueiras, a V, Lavilla, I., & Bendicho, C. (2002). Chemical sequential extraction for metal partitioning in environmental solid samples. *Analytical and Bioanalytical Chemistry*, 374(1), 103–108. doi:10.1007/s00216-002-1427-3

- Fimmen, R. L., Cory, R. M., Chin, Y. P., Trouts, T. D., & McKnight, D. M. (2007). Probing the oxidation-reduction properties of terrestrially and microbially derived dissolved organic matter. *Geochimica et Cosmochimica Acta*, 71(12), 3003–3015. doi:10.1016/j.gca.2007.04.009
- Finzgar, N., Kos, B., & Lestan, D. (2005). Heap leaching of lead contaminated soil using biodegradable chelator [S,S]-ethylenediamine disuccinate. *Environmental Technology*, 26(5), 553–560. doi:10.1080/09593332608618537
- Fitzgerald, W. F., Lamborg, C. H., & Hammerschmidt, C. R. (2007). Marine biogeochemical cycling of Hg. *Chemical Reviews*, 107(2), 641–662. doi:10.1021/cr050353m
- Förstner, U. (1991). *Soil Pollution Phenomena — Mobility of Heavy Metals in Contaminated Soil. Interactions at the Soil Colloid — Soil Solution Interface*. Springer Netherlands. doi:10.1007/978-94-017-1909-4_17
- Fritsche, J., Obrist, D., & Alewell, C. (2008). Evidence of microbial control of Hg⁰ emissions from uncontaminated terrestrial soils. *Journal of Plant Nutrition and Soil Science*, 171(2), 200–209. doi:10.1002/jpln.200625211
- Frohne, T., Rinklebe, J., Langer, U., Du Laing, G., Mothes, S., & Wennrich, R. (2012). Biogeochemical factors affecting mercury methylation rate in two contaminated floodplain soils. *Biogeosciences*, 9(1), 493–507. doi:10.5194/bg-9-493-2012
- G.E.M. Hall, P. Pelchat, J. B. P. (2005). The design and application of sequential extractions for Hg, Part 1. Optimization of HNO₃ extraction for all non-sulphide forms of Hg. *Geochem. Explor. Environ. Anal*, 5, 107–113. doi:10.1144/1467-7873/03-061
- Gabriel, M., & Williamson, D. (2003). Principal biotechnical factor affecting the speciation and transport of Hg through terrestrial environment. *Publicación periódica; Environment and Geochemistry and Health.*, (Grigal 2002), 421–434.
- Gagnon, C., Pelletier, É., & Mucci, A. (1997). Behaviour of anthropogenic Hg in coastal marine sediments. *Marine Chemistry*, 59(1-2), 159–176. doi:10.1016/S0304-4203(97)00071-6
- Gerbig, C. a., Kim, C. S., Stegemeier, J. P., Ryan, J. N., & Aiken, G. R. (2011). Formation of nanocolloidal metacinnabar in Hg-DOM-sulfide systems. *Environmental Science and Technology*, 45(21), 9180–9187.
- Giammanco, S., Ottaviani, M., Valenza, M., Veschetti, E., E., P., Giammanco, G., & Pignato, S. (1998). Major and Trace Elements Geochemistry in the Ground Waters of a Volcanic Area : Mount Etna (Sicily , Italy), 32(1), 19–30.
- Gillis, A., & Miller. (2000). Some local environmental effects on Hg emission and absorption at a soil surface. *The Science of The Total Environment*, 260(1-3), 191–200. doi:10.1016/S0048-9697(00)00563-5
- Gilmour, J. T. (1971). Inorganic Complexes of Divalent Hg in Natural Water Systems. *Environmental Letters*, 2(3), 143–152.
- Gismera, M. J., Procopio, J. R., & Sevilla, M. T. (2007). Characterization of Hg – Humic Acids Interaction by Potentiometric Titration with a Modified Carbon Paste Hg Sensor. *Electroanalysis*, 19(10), 1055–1061. doi:10.1002/elan.200603821

References

- Gondikas, A. P., Jang, E. K., & Hsu-Kim, H. (2010). Influence of amino acids cysteine and serine on aggregation kinetics of zinc and Hg sulfide colloids. *Journal of Colloid and Interface Science*, 347(2), 167–71. doi:10.1016/j.jcis.2010.03.051
- Gorski, C. a., & Scherer, M. M. (2009). Influence of magnetite stoichiometry on FeII uptake and nitrobenzene reduction. *Environmental Science and Technology*, 43(10), 3675–3680. doi:10.1021/es803613a
- Gosar, M., & Teršič, T. (2012). Environmental geochemistry studies in the area of Idrija Hg mine, Slovenia. *Environmental Geochemistry and Health*, 34(SUPPL. 1), 27–41. doi:10.1007/s10653-011-9410-6
- Gosar, M., Šajn, R., & Biester, H. (2006). Binding of Hg in soils and attic dust in the Idrija Hg mine area (Slovenia). *Science of the Total Environment*, 369(1-3), 150–162. doi:10.1016/j.scitotenv.2006.05.006
- Graham, A. M., Aiken, G. R., & Gilmour, C. C. (2012). Dissolved organic matter enhances microbial Hg methylation under sulfidic conditions. *Environmental Science and Technology*, 46(5), 2715–2723.
- Grassi, S., & Netti, R. (2000). Sea water intrusion and Hg pollution of some coastal aquifers in the province of Grosseto (Southern Tuscany - Italy). *Journal of Hydrology*, 237(3-4), 198–211. doi:10.1016/S0022-1694(00)00307-3
- Gray, J. E., Crock, J. G., & Fey, D. L. (2002). Environmental geochemistry of abandoned Hg mines in West-Central Nevada, USA. *Applied Geochemistry*, 17(8), 1069–1079. doi:10.1016/S0883-2927(02)00004-5
- Gustin, M. S., Biester, H., & Kim, C. S. (2002). Investigation of the light-enhanced emission of Hg from naturally enriched substrates. *Atmospheric Environment*, 36(20), 3241–3254. doi:10.1016/S1352-2310(02)00329-1
- Gustin, M. S., Lindberg, S. E., & Weisberg, P. J. (2008). An update on the natural sources and sinks of atmospheric Hg. *Applied Geochemistry*, 23(3), 482–493. doi:10.1016/j.apgeochem.2007.12.010
- Gustin, M. S., Rasmussen, P., Edwards, G., Schroeder, W., & Kemp, J. (1999). Application of a laboratory gas exchange chamber for assessment of in situ Hg emissions. *Journal of Geophysical Research-Atmospheres*, 104(D17), 21873–21878. doi:10.1029/1999jd900344
- Hahne, H. C. H., & Kroontje, W. (1972). Significance of pH and Chloride Concentration on Behavior of Heavy Metal Pollutants: Hg(II), Cadmium(II), Zinc(II), and Lead(II). *Environmental Quality*, 2(4), 444–450.
- Haitzer, M., Aiken, G. R., & Ryan, J. N. (2002). Binding of Hg(II) to dissolved organic matter: The role of the Hg-to-DOM concentration ratio. *Environmental Science and Technology*, 36(16), 3564–3570. doi:10.1021/es025699i
- Hammerschmidt, C. R., & Fitzgerald, W. F. (2001). Formation of artifact methylHg during extraction from a sediment reference material. *Analytical Chemistry*, 73(24), 5930–5936. doi:10.1021/ac010721w
- Han, F. X., Banin, a., Kingery, W. L., Triplett, G. B., Zhou, L. X., Zheng, S. J., & Ding, W. X. (2003)a. New approach to studies of heavy metal redistribution in soil. *Advances in Environmental Research*, 8(1), 113–120. doi:10.1016/S1093-0191(02)00142-9

- Han, Y., Kingston, H. M., Boylan, H. M., Rahman, G. M. M., Shah, S., Richter, R. C., ... Bhandari, S. (2003)b. Speciation of Hg in soil and sediment by selective solvent and acid extraction. *Analytical and Bioanalytical Chemistry*, 375(3), 428–436. doi:10.1007/s00216-002-1701-4
- Han S., (2004). Mercury speciation in Galveston Bay, Texas: the importance of complexation by natural organic ligands. Doctor of Philosophy. Graduate Studies of Texas A&M University
- Han, F. X., Shiyab, S., Chen, J., Su, Y., Monts, D. L., Waggoner, C. a., & Matta, F. B. (2008). Extractability and bioavailability of Hg from a Hg sulfide contaminated soil in Oak Ridge, Tennessee, USA. *Water, Air, and Soil Pollution*, 194(1-4), 67–75. doi:10.1007/s11270-008-9699-7
- Han, F. X., Su, Y., Monts, D. L., Waggoner, C. a., & Plodinec, M. J. (2006). Binding, distribution, and plant uptake of Hg in a soil from Oak Ridge, Tennessee, USA. *Science of the Total Environment*, 368(2-3), 753–768. doi:10.1016/j.scitotenv.2006.02.026
- Hansen, C. L., Zwolinski, G., & Martin, D. (1984). Bacterial removal of Hg from sewage. *Biotechnology and Bioengineering*, 26(11), 1330–1333. doi:10.1002/bit.260261110
- Hardiman, R. T., Banin, A., & Jacoby, B. (1984). The effect of soil type and degree of metal contamination upon uptake of Cd, Pb and Cu in bush beans (*Phaseolus vulgaris* L.). *Plant and Soil*, 81(1), 3–15.
- Harris, R. C., Rudd, J. W. M., Amyot, M., Babiarz, C. L., Beaty, K. G., Blanchfield, P. J., ... Tate, M. T. (2007). Whole-ecosystem study shows rapid fish-Hg response to changes in Hg deposition. *Proceedings of the National Academy of Sciences of the United States of America*, 104(42), 16586–16591. doi:10.1073/pnas.0704186104
- Hedgecock, I. M., Pirrone, N., Trunfio, G. a., & Sprovieri, F. (2006). Integrated Hg cycling, transport, and air-water exchange (MECAWEx) model. *Journal of Geophysical Research Atmospheres*, 111(20), 1–13. doi:10.1029/2006JD007117
- Heitmann, T., & Blodau, C. (2006). Oxidation and incorporation of hydrogen sulfide by dissolved organic matter. *Chemical Geology*, 235(1-2), 12–20. doi:10.1016/j.chemgeo.2006.05.011
- Hesterberg, D., Chou, J. W., Hutchison, K. J., & Sayers, D. E. (2001). Bonding of HG(II) to reduced organic sulfur in humic acid as affected by S/Hg ratio. *Environmental Science and Technology*, 35(13), 2741–2745. doi:10.1021/es001960o
- Higueras, P., Oyarzun, R., Biester, H., Lillo, J., & Lorenzo, S. (2003). A first insight into Hg distribution and speciation in soils from the Almaden mining district, Spain. *Journal of Geochemical Exploration*, 80(1), 95–104. doi:10.1016/S0375-6742(03)00185-7
- Hines, M. E., Faganeli, J., Adatto, I., & Horvat, M. (2006). Microbial Hg transformations in marine, estuarine and freshwater sediment downstream of the Idrija Hg Mine, Slovenia. *Applied Geochemistry*, 21(11), 1924–1939. doi:10.1016/j.apgeochem.2006.08.008
- Hines, M. E., Horvat, M., Faganeli, J., Bonzongo, J. C., Barkay, T., Major, E. B., ... Lyons, W. B. (2000). Hg biogeochemistry in the Idrija river, Slovenia, from above the mine into the Gulf of Trieste. *Environmental Research*, 83(2), 129–139. doi:10.1006/enrs.2000.4052
- Hintelmann, H. (1999). Comparison of different extraction techniques used for methylHg analysis with respect to accidental formation of methylHg during sample preparation. *Chemosphere*, 39(7), 1093–1105. doi:10.1016/S0045-6535(99)00180-0

References

- Hogg, T. J., Stewart, J. W. B., & Bethany, J. R. (1977). Influence of the Chemical Form of Hg on its Adsorption and Ability to Leach Through Soils. *Journal of Environmental Quality*, 7(3), 440–445. doi:10.2134/jeq1978.00472425000700030029x
- Holm, H. W., & Cox, M. F. (1975). Transformation of elemental Hg by bacteria. *Applied Microbiology*, 29(4), 491–494. Retrieved from <http://www.ncbi.nlm.nih.gov/pmc/articles/PMC187012/>
- Horvat, M. (1999). Current status and future needs for biological and environmental reference materials certified for methylHg compounds. *Chemosphere*, 39(7), 1167–1179. doi:10.1016/S0045-6535(99)00185-X
- Horvat, M. (2005). Determination of Hg and its Compounds in Water, Sediment, Soil and Biological Samples. In Pirrone, N., Mahaffey, K.R. (Eds.). *Dynamics of Hg Pollution on Regional and Global Scales: Atmospheric Processes and Human Exposures Around the World*. New York: Springer Science+Business Media, Inc., 153–190.
- Horvat, M., Covelli, S., Faganeli, J., Logar, M., Mandic, V., Rajar, R., ... Zagar, D. (1999). Hg in contaminated coastal environments, a case study: the Gulf of Trieste. *Science of the Total Environment*, 238, 43–56.
- Horvat, M., Liang, L., & Bloom, N. S. (1993). Comparison of distillation with other current isolation methods for the determination of methyl Hg compounds in low level environmental samples: Part II. *Water. Analytica Chimica Acta*, 282(1), 153–168.
- Hsu, H., & Sedlak, D. L. (2003). Strong Hg (II) complexation in municipal wastewater effluent and surface waters. *Environmental Science & Technology*, 37(12), 2743–2749. doi:10.1021/es026438b
- Hsu-Kim, H., Kucharzyk, K. H., Zhang, T., & Deshusses, M. a. (2013). Mechanisms regulating Hg bioavailability for methylating microorganisms in the aquatic environment: a critical review. *Environmental Science & Technology*, 47(6), 2441–56. doi:10.1021/es304370g
- Huang, Z. Y., Qin, D. P., Zeng, X. C., Li, J., Cao, Y. L., & Cai, C. (2012). Species distribution and potential bioavailability of exogenous Hg (II) in vegetable-growing soil investigated with a modified Tessier scheme coupled with isotopic labeling technique. *Geoderma*, 189-190, 243–249. doi:10.1016/j.geoderma.2012.05.018
- INTERREG II, 2001. Progetto di monitoraggio dell'Alto-Adriatico– Relazione Conclusiva, Luglio 1998–Giugno 2001. Direzione Regionale dell'Ambiente, Laboratorio di Biologia Marina, Trieste, Italia, p. 112.
- ISO 10390:2005 Soil quality-Determination of pH (2005).
- Issaro, N., Abi-Ghanem, C., & Bermond, a. (2009). Fractionation studies of Hg in soils and sediments: A review of the chemical reagents used for Hg extraction. *Analytica Chimica Acta*, 631(1), 1–12. doi:10.1016/j.aca.2008.10.020
- IUSS Working Group WRB (2014) World Reference Base for Soil Resources 2014. International soil classification system for naming soils and creating legends for soil maps. World Soil resources Report n. 106. FAO, Rome
- Jackson, T. A. (1989). The influence of clay minerals, oxides, and humic matter on the methylation and demethylation of Hg by micro-organisms in freshwater sedimen. *Appl Organomet Chem*, 3, 1–30. doi:10.1002/aoc.590030103

- Jackson, T. A. (1998). Hg in aquatic ecosystems. *Metal Metabolism in Aquatic Environments*, 77–158. doi:10.1007/978-1-4757-2761-6_5
- Jay, J. a, Morel, F. M. M., & Hemond, H. F. (2000). Hg speciation in the presence of polysul des. *Environ. Sci. Technol.*, 342196e220(11), 2196–2200.
- Jeong, H. Y., Klaue, B., Blum, J. D., & Hayes, K. F. (2007). Sorption of mercuric ion by synthetic nanocrystalline mackinawite (FeS). *Environmental Science and Technology*, 41(22), 7699–7705. doi:10.1021/es0702891
- Jing, Y. D., He, Z. L., & Yang, X. E. (2007). Effects of pH, organic acids, and competitive cations on Hg desorption in soils. *Chemosphere*, 69(10), 1662–1669. doi:10.1016/j.chemosphere.2007.05.033
- Jing, Y. D., He, Z. L., Yang, X. E., & Sun, C. Y. (2008). Evaluation of Soil Tests for Plant-available Hg in a Soil-Crop Rotation System. *Communications in Soil Science and Plant Analysis*, 39(19-20), 3032–3046. doi:10.1080/00103620802432907
- Jiskra, M., Wiederhold, J. G., Bourdon, B., & Kretzschmar, R. (2012). Solution speciation controls Hg isotope fractionation of Hg(II) sorption to goethite. *Environmental Science and Technology*, 46(12), 6654–6662. doi:10.1021/es3008112
- Johansson, K., Aastrup, M., Andersson, A., Bringmark, L., & Iverfeldt, A. (1991). Hg in swedish forest soils and waters — Assessment of critical load. *Water Air & Soil Pollution*, 56(1), 267–281. doi:10.1007/BF00342276
- Kappler, A., & Haderlein, S. B. (2003). Natural organic matter as reductant for chlorinated aliphatic pollutants. *Environmental Science and Technology*, 37(12), 2714–2719. doi:10.1021/es0201808
- Kappler, A., Benz, M., Schink, B., & Brune, A. (2004). Electron shuttling via humic acids in microbial iron(III) reduction in a freshwater sediment. *FEMS Microbiology Ecology*, 47(1), 85–92. doi:10.1016/S0168-6496(03)00245-9
- Kato, S., Hashimoto, K., & Watanabea, K. (2012). Microbial interspecies electron transfer via electric currents through conductive minerals. *Proceedings of the National Academy of Sciences of the United States of America*, 109(25), 10042–10046. doi:10.1073/pnas.1
- Kim, C. S., Bloom, N. S., Rytuba, J. J., & Brown, G. E. (2003). Hg Speciation by X-ray Absorption Fine Structure Spectroscopy and Sequential Chemical Extractions: A Comparison of Speciation Methods. *Environmental Science and Technology*, 37(22), 5102–5108. doi:10.1021/es0341485
- Kim, C. S., Brown, G. E., & Rytuba, J. J. (2000). Characterization and speciation of Hg-bearing mine wastes using X-ray absorption spectroscopy. *The Science of the Total Environment*, 261(1-3), 157–168. doi:10.1016/S0048-9697(00)00640-9
- Kim, C. S., Rytuba, J. J., & Brown, G. E. (2004). EXAFS study of Hg(II) sorption to Fe- and Al-(hydr)oxides: I. Effects of pH. *Journal of Colloid and Interface Science*, 271(1), 1–15. doi:10.1016/S0021-9797(03)00330-8
- Kinniburgh, D. G., & Jackson, M. L. (1977). No Title. *Soil Science Society of America Journal*, 42(1), 45–47. doi:10.2136/sssaj1978.03615995004200010010x
- Kocman D, Horvat M, Kotnik J. (2004). Mercury fractionation in contaminated soils from the Idrija mercury mine region. *J Environ Monit* 6, 696–703

References

- Kodama, H., & Schnitzer, M. (1977). Effect of fulvic acid on the crystallization of Fe(III) oxides. *Geoderma*, 19(4), 279–291.
- Kostka, J. E., Dollhopf, S., Stucki, J. W., Dalton, D. D., & Skelton, H. (2002). Variety of Oxidized Iron Forms and Comparison of Growth Yields on a Acceptor Clay Minerals as the Sole Electron Growth of Iron(III)-Reducing Bacteria on. *Environ Microbiol*, 68(12), 6256–6262. doi:10.1128/AEM.68.12.6256-6262.2002
- Lamborg, C. H., Fitzgerald, W. F., Tseng, C. M., Balcom, P. H., & Hammerschmidt, C. R. (2003). Determination of the Hg complexation characteristics of dissolved organic matter in natural waters by reducible Hg titrations. *Abstracts of Papers of the American Chemical Society*, 223(15), U540–U540. Retrieved from <Go to ISI>://000176296703027
- Lamborg, C. H., Von Damm, K. L., Fitzgerald, W. F., Hammerschmidt, C. R., & Zierenberg, R. (2006). Hg and monomethylHg in fluids from Sea Cliff submarine hydrothermal field, Gorda Ridge. *Geophysical Research Letters*, 33(17), 18–21. doi:10.1029/2006GL026321
- Landa, E. R. (1978). The retention of metallic Hg vapor by soils. *Geochimica et Cosmochimica Acta*, 42(9), 1407–1411. doi:10.1016/0016-7037(78)90046-7
- Latta, D. E., Gorski, C. a., Boyanov, M. I., O’Loughlin, E. J., Kemner, K. M., & Scherer, M. M. (2012). Influence of magnetite stoichiometry on U(VI) reduction. *Environmental Science & Technology*, 46(2), 778–86. doi:10.1021/es2024912
- Le Roux, S.M., Turner, A., Millward, G.E., Ebdon, L., Apriou, P. (2001). Partitioning of mercury onto suspended sediments in estuaries. *J. Environ. Monit.* 3, 37–42.
- Leal M. F., Vasconcelos M. T. S. D., and van den Berg C. M. G. (1999) Copper-induced release of complexing ligands similar to thiols by *Emiliania huxleyi* in seawater cultures. *Limnol. Oceanogr.* 44(7), 1750 – 1762.
- Lechler, P. J. (1999). Modern Mercury Contamination from Historic Amalgamation Milling of Silver-Gold Ores in the Carson River, Nevada and Jordan Creek, Idaho: Importance of Speciation Analysis in Understanding the Source, Mobility, and Fate of Polluted Materials. *Environmental Science*, Chapter Me, 337–355.
- Lechler, P. J., Miller, J. R., Hsu, L., & Desilets, M. O. (1997). Hg mobility at the Carson River Superfund Site, west-central Nevada, USA: interpretation of Hg speciation data in mill tailings, soils, and sediments, 58, 259–267.
- Leermakers, M., Nguyen, H. L., Kurunczi, S., Vanneste, B., Galletti, S., & Baeyens, W. (2003). Determination of methylHg in environmental samples using static headspace gas chromatography and atomic fluorescence detection after aqueous phase ethylation. *Analytical and Bioanalytical Chemistry*, 377(2), 327–333. doi:10.1007/s00216-003-2116-6
- Leung, B. O., Jalilehvand, F., & Mah, V. (2007). Hg(II) penicillamine complex formation in alkaline aqueous solution. *Dalton Transactions*, (41), 4666–4674. doi:10.1039/b711436b
- Lin, C. J., & Pehkonen, S. O. (1999). The chemistry of atmospheric Hg: A review. *Atmospheric Environment*, 33(13), 2067–2079. doi:10.1016/S1352-2310(98)00387-2

- Lindberg, S. E., Jackson, D. R., Huckabee, J. W., Janzen, S. A., Levin, M. J., & Lund, J. R. (1978). Atmospheric Emission and Plant Uptake of Hg from Agricultural Soils near the Almadén Hg Mine. *Journal of Environmental Quality*, 8(4), 572–578.
- Lindberg SE. (1996). Forests and the global biogeochemical cycle of mercury. In: Baeyens W, Ebinghaus R, Vasiliev O, editors. *Regional and global mercury cycles: sources, fluxes and mass balance*. Dordrecht: Kluwer.
- Lindberg, S. E., Zhang, H., Gustin, M., Vette, a, Marsik, F., Owens, J., ... Xiao, Z. (1999). Increases in Hg emissions from desert soils in response to rainfall and irrigation. *Journal of Geophysical Research*, 104(D17), 21879–21888. doi:10.1029/1999JD900202
- Lindberg, S., Bullock, R., Ebinghaus, R., Engstrom, D., Lindberg, S., Bullock, R., ... Seigneur, C. (2007). A Synthesis of Progress and Uncertainties in Attributing the Sources of Hg in Deposition. *Ambio*, 36(1), 19–32.
- Lindberg, S., Bullock, R., Ebinghaus, R., Engstrom, D., Lindberg, S., Bullock, R., ... Seigneur, C. (2016). Royal Swedish Academy of Sciences A Synthesis of Progress and Uncertainties in Attributing the Sources of Hg in Deposition Published by : Springer on behalf of Royal Swedish Academy of Sciences Stable URL : <http://www.jstor.org/stable/4315781> REFEREN, 18–32.
- Lindqvist. (1991). Hg in the Swedish environment: recent research on causes, consequences and corrective methods. *Water Air Soil Pollut*, 55:1–261.
- Liu, G., Cai, Y., Mao, Y., Scheidt, D., Kalla, P., Richards, J., ... Appleby, C. (2009). Spatial variability in Hg cycling and relevant biogeochemical controls in the Florida everglades. *Environmental Science and Technology*, 43(12), 4361–4366. doi:10.1021/es803665c
- Lockwood, R. a, & Chen, K. Y. (1973). Adsorption of Hg(II) by hydrous manganese oxides . *Environmental Science & Technology*, 7(11), 1028–1032. doi:10.1021/es60083a006
- Loredo, J., Ordoñez, A., Baldo, C., Garcí n'a-Iglesias, C., 2003. Arsenic mobilization from waste piles of the El Terronal mine, Asturias, Spain. *Geochem. Explor. Environ. Anal.* 3, 229e237.
- Lovley, D. R., Coates, J. D., BluntHarris, E. L., Phillips, E. J. P., & Woodward, J. C. (1996). Humic substances as electron acceptors for microbial respiration. *Nature*. doi:10.1038/382445a0
- Lovley, D. R., Fraga, J. L., Blunt-Harris, E. L., Hayes, L. a., Phillips, E. J. P., & Coates, J. D. (1998). Humic substances as a mediator for microbially catalyzed metal reduction. *Acta Hydrochimica et Hydrobiologica*, 26(3), 152–157. doi:10.1002/(SICI)1521-401X(199805)26:3<152::AID-AHEH152>3.0.CO;2-D
- Lowry, G. V, Shaw, S., Kim, C. S., Rytuba, J. J., & Brown, G. E. (2004a). Macroscopic and microscopic observations of particle-facilitated Hg transport from New Idria and Sulphur Bank Hg mine tailings. *Environmental Science & Technology*, 38(19), 5101–11. Retrieved from <http://www.ncbi.nlm.nih.gov/pubmed/15506205>
- Mailman, M., & Bodaly, R. a. (2005). Total Hg, methyl Hg, and carbon in fresh and burned plants and soil in Northwestern Ontario. *Environmental Pollution*, 138(1), 161–166. doi:10.1016/j.envpol.2005.02.005
- Malm, O. (1998). Gold mining as a source of Hg exposure in the Brazilian Amazon. *Environmental Research*, 77(2), 73–8. doi:10.1006/enrs.1998.3828

References

- Mason, R. P. (2005). Monitoring the response to Changing mercury deposition. *Environmental Science & Technology*.
- Mason, R., Fitzgerald, W., & Morel, F. (1994). The biogeochemical cycling of elemental Hg: Anthropogenic influences. *Geochimica et Cosmochimica Acta*, 58(15), 3191–3198. doi:10.1016/0016-7037(94)90046-9
- Matthiessen, a. (1998). Reduction of divalent Hg by humic substances - Kinetic and quantitative aspects. *Science of the Total Environment*, 213(1-3), 177–183. doi:10.1016/S0048-9697(98)00090-4
- McLeod, C. L. (1996). Effect of Infiltrating Solutions on the Desorption of Hg from Aquifer Sediments. *Environmental Technology*, 17(5), 465–475. Retrieved from <http://dx.doi.org/10.1080/09593331708616408>
- Mehlich, A., (1953). Repid determination of cation and anion echangepropertiesand pH of soils. *Association of Official Analytical Chemists* 36, 445-457.
- Melamed, R., Villas Boas, R.C., 2000. Application of physico-chemical amendments for the counteraction of mercury pollution. *Sci. Total Environ.* 261, 203-209.
- Merritt, K. a., & Amirbahman, A. (2007). Hg dynamics in sulfide-rich sediments: Geochemical influence on contaminant mobilization within the Penobscot River estuary, Maine, USA. *Geochimica et Cosmochimica Acta*, 71(4), 929–941. doi:10.1016/j.gca.2006.10.012
- Mikac, N., Foucher, D., Niessen, S., Lojen, S., & Fischer, J. C. (2003). Influence of chloride and sediment matrix on the extractability of HgS (cinnabar and metacinnabar) by nitric acid. *Analytical and Bioanalytical Chemistry*, 377(7-8), 1196–1201. doi:10.1007/s00216-003-2204-7
- Millán, R., Gamarra, R., Schmid, T., Sierra, M. J., Quejido, a. J., Sánchez, D. M., ... Vera, R. (2006). Hg content in vegetation and soils of the Almad??n mining area (Spain). *Science of the Total Environment*, 368(1), 79–87. doi:10.1016/j.scitotenv.2005.09.096
- Miller, C. L., Mason, R. P., Gilmour, C. C., & Heyes, A. (2007). Influence of dissolved organic matter on the complexation of Hg under sulfidic conditions. *Environmental Toxicology and Chemistry / SETAC*, 26(4), 624–633. doi:10.1897/06-375R.1
- Milobowski, M. G., Amrhein, G. T., Kudlac, G. A., Yurchison, D. M. (2001). Wet FGD enhanced Hg control for coal-fired utility boilers. *Fuel and Energy Abstracts*, 43(4), 273. doi:10.1016/S0140-6701(02)86384-6
- Miretzky, P., Bisinoti, M. C., Jardim, W. F., & Rocha, J. C. (2005). Factors affecting Hg (II) adsorption in soils from the Rio Negro basin (Amazon). *Quimica Nova*, 28(3), 438–443. doi:10.1590/S0100-40422005000300014
- Morel, F. M. M., & Amyot, M. (1998). The Chemical Cycle and Bioaccumulation of Hg Author (s): François M . M . Morel , Anne M . L . Kraepiel and Marc Amyot Source : *Annual Review of Ecology and Systematics* , Vol . 29 (1998) , pp . 543-566 Published by : Annual Reviews Stable URL : ht, 29(1998), 543–566.
- Morse, J. W., & Luther, G. W. (1999). Chemical influence on trace metalsulphide interactions in anoxic sediments. *Geochim. Cosmochim. Acta*, 63(3373–3378), 3378.

- Mosetti, F., 1983. Sintesi sull'idrologia del Friuli-Venezia Giulia. Quaderni dell'Ente Tutela Pesca, vol. 6, pp. 1–295.
- Munthe, J., Bodaly, R. A. D., Branfireun, B. A., Driscoll, C. T., Gilmour, C. C., Harris, R., ... Harris, R. (2016). Royal Swedish Academy of Sciences Recovery of Hg-Contaminated Fisheries Linked references are available on JSTOR for this article : Recovery of Hg-Contaminated Fisheries, 36(1), 33–44.
- Nakamura, K., & Silver, S. (1994). Molecular Analysis of Hg-Resistant Bacillus Isolates from Sediment of Minamata Bay, Japan. *Applied And Environmental Microbiology*, 60(12), 4596–4599.
- Nakamura, K., Hagimine, M., Sakai, M., & Furukawa, K. (1999). Removal of Hg from Hg-contaminated sediments using a combined method of chemical leaching and volatilization of Hg by bacteria. *Biodegradation*, 10(6), 443–447. doi:10.1023/A:1008329511391
- Nakamura, K., Sakamoto, M., Uchiyama, H., & Yagi, O. (1990). Organomercurial-volatilizing bacteria in the Hg-polluted sediment of Minamata Bay, Japan. *Applied and Environmental Microbiology*, 56(1), 304–305.
- Nakamura, K., Sakata, T., & Nakahara, H. B. (1988). Volatilization of Hg compounds by methylHg-volatilizing bacteria in Minamata Bay sediment. *Bulletin of Environmental Contamination and Toxicology*, 41(4), 651–656.
- Navarro, A. (2008). Review of characteristics of Hg speciation and mobility from areas of Hg mining in semi-arid environments. *Reviews in Environmental Science and Biotechnology*, 7(4 SPEC. ISS.), 287–306. doi:10.1007/s11157-008-9139-6
- Navarro-Flores, A., Martinez-Frias, J., Font, X., & Viladevall, M. (2000). Modelling of modern Hg vapor transport in an ancient hydrothermal system: Environmental and geochemical implications. *Applied Geochemistry*, 15(3), 281–294. doi:10.1016/S0883-2927(99)00046-3
- Neculita, C.-M., Zagury, G. J., & Deschênes, L. (2005). Hg speciation in highly contaminated soils from chlor-alkali plants using chemical extractions. *Journal of Environmental Quality*, 34(1), 255–262. doi:34/1/255 [pii]
- Newton, D. W., Ellis, R., & Paulsen, G. M. (1976). Effect of pH and Complex Formation on Hg (II) Adsorption by Bentonite. *Journal of Environmental Quality*, 5(3), 251–254. doi:10.2134/jeq1976.00472425000500030007x
- Ning, P., Wang, H. Bin, Pan, B., Bart, H. J., & Yang, M. (2009). Isolation and Sorption Behavior of Humic Acid from Zhongdian Peat of Yunnan Province, China. *Pedosphere*, 19(5), 606–614. doi:10.1016/S1002-0160(09)60155-7
- Nriagu, J. O. (1979). The biogeochemistry of Hg in the environment.
- O'Loughlin, E. J., Kelly, S. D., Kemner, K. M., Csencsits, R., & Cook, R. E. (2003). Reduction of AgI, AuIII, CuII, and Hg II by FeII/FeIII hydroxysulfate green rust. *Chemosphere*, 53(5), 437–446. doi:10.1016/S0045-6535(03)00545-9
- Obrist, D., Fain, X., & Berger, C. (2010). Gaseous elemental mercury emissions and CO₂ respiration rates in terrestrial soils under controlled aerobic and anaerobic laboratory conditions. *Science of the Total Environment*, 408(7), 1691–1700. doi:10.1016/j.scitotenv.2009.12.008

References

- Pacyna, E. G., Pacyna, J. M., Steenhuisen, F., & Wilson, S. (2006). Global anthropogenic Hg emission inventory for 2000. *Atmospheric Environment*, 40(22), 4048–4063. doi:10.1016/j.atmosenv.2006.03.041
- Pacyna, J. M., Pacyna, E. G., & Aas, W. (2009). Changes of emissions and atmospheric deposition of Hg, lead, and cadmium. *Atmospheric Environment*, 43(1), 117–127. doi:10.1016/j.atmosenv.2008.09.066
- Pal, A., & Paul, a K. (2008). Microbial extracellular polymeric substances: central elements in heavy metal bioremediation. *Indian Journal of Microbiology*, 48(1), 49–64. doi:10.1007/s12088-008-0006-5
- Palmieri, H. E. L., Nalini, H. a., Leonel, L. V., Windmüller, C. C., Santos, R. C., & de Brito, W. (2006). Quantification and speciation of Hg in soils from the Tripu?? Ecological Station, Minas Gerais, Brazil. *Science of the Total Environment*, 368(1), 69–78. doi:10.1016/j.scitotenv.2005.09.085
- Paquette, K. E., & Helz, G. R. (1997). Inorganic speciation of Hg in sulfidic waters: The importance of zero-valent sulfur. *Environmental Science and Technology*, 31(7), 2148–2153. doi:10.1021/es961001n
- Park, J. H., Lamb, D., Paneerselvam, P., Choppala, G., Bolan, N., & Chung, J.-W. (2011). Role of organic amendments on enhanced bioremediation of heavy metal(loid) contaminated soils. *Journal of Hazardous Materials*, 185(2-3), 549–74. doi:10.1016/j.jhazmat.2010.09.082
- Pasakarnis, T. S., Boyanov, M. I., Kemner, K. M., Mishra, B., O'Loughlin, E. J., Parkin, G., & Scherer, M. M. (2013). Influence of chloride and Fe(II) content on the reduction of Hg(II) by magnetite. *Environmental Science and Technology*, 47(13), 6987–6994. doi:10.1021/es304761u
- Paustenbach, D. J., Bruce, G. M., & Chrostowski, P. (1997). Current views on the oral bioavailability of inorganic Hg in soil: implications for health risk assessments. *Risk Analysis : An Official Publication of the Society for Risk Analysis*, 17(5), 533–544.
- Piani, R., Covelli, S., & Biester, H. (2005). Hg contamination in Marano Lagoon (Northern Adriatic sea, Italy): Source identification by analyses of Hg phases. *Applied Geochemistry*, 20(8), 1546–1559. doi:10.1016/j.apgeochem.2005.04.003
- Pirrone, N., & Mahaffey, K. R. (2005). *Dynamics of Hg Pollution on Regional and Global Scales*. Springer Publishers: New York.
- Pirrone, N., & Mason, R. (2009). *Hg Fate and Transport in the Global Atmosphere Emissions, Measurements and Models*. Springer US. doi:10.1007/978-0-387-93958-2
- Pirrone, N., Cinnirella, S., Feng, X., Finkelman, R. B., Friedli, H. R., Leaner, J., ... Telmer, K. (2010). Global Hg emissions to the atmosphere from anthropogenic and natural sources. *Atmospheric Chemistry and Physics*, 10(13), 5951–5964. doi:10.5194/acp-10-5951-2010
- Poissant, L., & Casimir, A. (1998). Water-air and soil-air exchange rate of total gaseous Hg measured at background sites. *Atmospheric Environment*, 32(5), 883–893. doi:10.1016/S1352-2310(97)00132-5
- Poissant, L., & Pilote, M. (1999). Hg flux measurements in a naturally enriched area : Correlation with environmental ... *Journal of Geophysical Research Atmospheres*, 104, 21845–21857. doi:10.1029/1999JD900092
- Qian, J. (2001). *Hg Species in Environmental Samples Studied by Spectroscopic Methods*. Doctoral thesis, Swedish University of Agricultural Sciences.

- RAFVG, 1986. Caratteristiche chimico-fisiche e biologiche dei corpi idrici superficiali e profondi della regione (Allegato 5). Regione Friuli-Venezia Giulia, Direzione Regionale dell'Ambiente, Servizio per l'utilizzazione delle acque.
- Rakshit, S., Uchimiya, M., & Sposito, G. (2009). Iron(III) Bioreduction in Soil in the Presence of Added Humic Substances. *Soil Science Society of America Journal*, 73(1), 65. doi:10.2136/sssaj2007.0418
- Rallo, M., Lopez-Anton, M. A., Perry, R., & Maroto-Valer, M. M. (2010). Hg speciation in gypsums produced from flue gas desulfurization by temperature programmed decomposition. *Fuel*, 89(8), 2157–2159. doi:10.1016/j.fuel.2010.03.037
- Ramamoorthy, S., & Rust, B. R. (1978). Heavy metal exchange processes in sediment-water systems. *Environmental Geology*, 2(3), 165–172. doi:10.1007/BF02430670
- Randle, K., & Hartmann, E. H. (1987). Applications of the Continuous Flow Stirred Cell (CFSC) technique to adsorption of zinc, cadmium and Hg on humic acids. *Geoderma*, 40(3-4), 281–296. doi:10.1016/0016-7061(87)90039-5
- Ranjard, L., Richaume, a, Jocteur-Monrozier, L., & Nazaret, S. (1997). Response of soil bacteria to Hg (II) in relation to soil characteristics and cell location. *FEMS Microbiology Ecology*. doi:10.1016/S0168-6496(97)00073-1
- Ravichandran, M. (2004). Interactions between Hg and dissolved organic matter--a review. *Chemosphere*, 55(3), 319–331. doi:10.1016/j.chemosphere.2003.11.011
- Ravichandran, M., Aiken, G. R. R. J. N., & Reddy, M. M. (1999). Inhibition of precipitation and aggregation of metacinnabar (mercuric sulfide) by dissolved organic matter isolated from the Florida Everglades. *Environ Sci Technol*, 33, 1418–1423.
- Ravichandran, M., Aiken, G. R., Reddy, M. M., & Ryan, J. N. (1998). Enhanced dissolution of cinnabar (mercuric sulfide) by dissolved organic matter isolated from the Florida Everglades. *Environmental Science and Technology*, 32(21), 3305–3311. doi:10.1021/es9804058
- Reddy, M. M., & Aiken, G. R. (2001). Fulvic acid-sulfide ion competition for Hg ion binding in the Florida everglades. *Water, Air, and Soil Pollution*, 132(1-2), 89–104. doi:10.1023/A:1012073503678
- Reemtsma, T., These, A., Springer, A., & Linscheid, M. (2008). Differences in the molecular composition of fulvic acid size fractions detected by size-exclusion chromatography-on line Fourier transform ion cyclotron resonance (FTICR-) mass spectrometry. *Water Research*, 42(1-2), 63–72. doi:10.1016/j.watres.2007.06.063
- Reimers, R. S., & Krenkel, P. a. (1974). Kinetics of Hg Adsorption and Desorption in Sediments. *Water Pollution Control Federation*, 46(2), 352–365. Retrieved from <http://www.jstor.org/stable/25038128>
- Reis, a. T., Coelho, J. P., Rodrigues, S. M., Rocha, R., Davidson, C. M., Duarte, a. C., & Pereira, E. (2012). Development and validation of a simple thermo-desorption technique for Hg speciation in soils and sediments. *Talanta*, 99, 363–368. doi:10.1016/j.talanta.2012.05.065
- Reis, A. T., Duarte, A. C., Henriques, B., Coelho, C., Lopes, C. B., Mieiro, C. L., ... Pereira, E. (2015)a. An international proficiency test as a tool to evaluate Hg determination in environmental matrices. *TrAC Trends in Analytical Chemistry*, 64, 136–148. doi:10.1016/j.trac.2014.08.015

References

- Reis, A. T., Coelho, J. P., Rucandio, I., Davidson, C. M., Duarte, A. C., & Pereira, E. (2015)b. Thermo-desorption: A valid tool for Hg speciation in soils and sediments? *Geoderma*, 237-238, 98–104. doi:10.1016/j.geoderma.2014.08.019
- Reis, A. T., Davidson, C. M., Vale, C., & Pereira, E. (2016). Overview and challenges of Hg fractionation and speciation in soils. *Trends in Environmental Analytical Chemistry*, 82, 109–117. doi:10.1016/j.trac.2016.05.008
- Reis, A. T., Lopes, C. B., Davidson, C. M., Duarte, A. C., & Pereira, E. (2014). Extraction of Hg water-soluble fraction from soils: An optimization study. *Geoderma*, 213, 255–260. doi:10.1016/j.geoderma.2013.08.010
- Reis, A. T., Rodrigues, S. M., Davidson, C. M., Pereira, E., & Duarte, A. C. (2010). Extractability and mobility of Hg from agricultural soils surrounding industrial and mining contaminated areas. *Chemosphere*, 81(11), 1369–1377. doi:10.1016/j.chemosphere.2010.09.030
- Renneberg, a J., & Dudas, M. J. (2001). Transformations of elemental Hg to inorganic and organic forms in Hg and hydrocarbon co-contaminated soils. *Chemosphere*, 45(6-7), 1103–9. Retrieved from <http://www.ncbi.nlm.nih.gov/pubmed/11695587>
- Revis, N. W., Osborne, T. R., Sedgley, D., & King, A. (1989). Quantitative Method for Determining the Concentration of Hg (II) Sulphide in Soils and Sediments, 114(July), 823–825.
- Rocha, J. C., Junior, É. S., Zara, L. F., Rosa, A. H., Dos Santos, A., & Burba, P. (2000). Reduction of Hg(II) by tropical river humic substances (Rio Negro) - A possible process of the Hg cycle in Brazil. *Talanta*, 53(3), 551–559. doi:10.1016/S0039-9140(00)00532-4
- Rocha, J. C., Sargentini Jr. E., É. S., Zara, L. F., Rosa, A. H., Dos Santos, A., & Burba, P. (2003). Reduction of Hg(II) by tropical river humic substances (Rio Negro) - Part II. Influence of structural features (molecular size, aromaticity, phenolic groups, organically bound sulfur). *Talanta*, 61(5), 699–707. doi:10.1016/S0039-9140(03)00351-5
- Rost, J., Rapoport, S. (1964) Reduction-potential of Glutathione. *Letters to Nature* 201, 185; doi:10.1038/201185a0
- Royer, R. a., Burgos, W. D., Fisher, A. S., Unz, R. F., & Dempsey, B. a. (2002). Enhancement of biological reduction of hematite by electron shuttling and Fe(II) complexation. *Environmental Science and Technology*, 36(9), 1939–1946. doi:10.1021/es011139s
- Rumayor, M., Diaz-Somoano, M., Lopez-Anton, M. a., & Martinez-Tarazona, M. R. (2013). Hg compounds characterization by thermal desorption. *Talanta*, 114, 318–322. doi:10.1016/j.talanta.2013.05.059
- Rumayor, M., Diaz-Somoano, M., Lopez-Anton, M. a., & Martinez-Tarazona, M. R. (2015). Application of thermal desorption for the identification of Hg species in solids derived from coal utilization. *Chemosphere*, 119, 459–465. doi:10.1016/j.chemosphere.2014.07.010
- Sahlman, L., Lambeirs, A., Lindskogq, S., & Dunford, H. B. (1984). The Reaction between NADPH and Mercuric Reductase from *Pseudomonas aeruginosa* *. *The Journal of Biological Chemistry*, 259(20), 12403–12408.

- Sánchez, D. M., Quejido, a. J., Fernández, M., Hernández, C., Schmid, T., Millán, R., ... Morante, R. (2005). Hg and trace element fractionation in Almaden soils by application of different sequential extraction procedures. *Analytical and Bioanalytical Chemistry*, 381(8), 1507–1513. doi:10.1007/s00216-005-3058-y
- Santoro A. (2009). Innovative methods for metal speciation in soil: a case study of mercury. Dottorato di ricerca in chimica agrarian. Università degli Studi di Bari.
- Schecher, W. D., & McAvoy, D. C. (1992). MINEQL+: A software environment for chemical equilibrium modeling. *Computers, Environment and Urban Systems*, 16(1), 65–76. doi:10.1016/0198-9715(92)90053-T
- Schiering N, Kabsch W, Moore MJ, Distefano MD, W. C. & P. (1991). Structure of the detoxification catalyst mercuric ion reductase from *Bacillus* sp. strain RC 607. *Letters to Nature*, 352, 168–171.
- Schierow. (2006). Hg in the Environment : Sources and Health Risks. CRS Report for Congress., 30 p. Retrieved from Congressional Research Service, Library of Congress, Washington, D.C.
- Schindler, D. W., Hesslein, R. H., Wagemann, R., & Broecker, W. S. (1980). Effects of Acidification on Mobilization of Heavy Metals and Radionuclides from the Sediments of a Freshwater Lake. *Canadian Journal of Fisheries and Aquatic Sciences*, 37(3), 373–377.
- Schluter, K. (2000). Review: Evaporation of Hg from soils. An integration and synthesis of current knowledge. *Environmental Geology*, 39(3-4), 249–271. doi:10.1007/s002540050005
- Schoeneberger, P.J., Wysocki, D.A., Benham, E.C., and Soil Survey Staff. (2012). Field book for describing and sampling soils, Version 3.0. Natural Resources Conservation Service, National Soil Survey Center, Lincoln, NE. U.S.A.
- Scholtz, M. T., Heyst, B. J. Van, & Schroeder, W. H. (2003). Modelling of Hg emissions from background soils, 304(02), 185–207. doi:10.1016/S0048-9697(02)00568-5
- Schroeder, H., W., & Munthe, J. (1998). Atmospheric Hg - An overview. *Atmospheric Environment*, 32(5), 809–822. doi:10.1016/S1352-2310(97)00293-8
- Schuster, E. (1991). The behavior of Hg in the soil with special emphasis on complexation and adsorption processes - A review of the literature. *Water Air & Soil Pollution*, 56(1), 667–680. doi:10.1007/BF00342308
- Scott, D. T., Mcknight, D. M., Blunt-Harris, E. L., Kolesar, S. E., & Lovley, D. R. (1998). Quinone moieties act as electron acceptors in the reduction of humic substances by humics-reducing microorganisms. *Environmental Science and Technology*, 32(19), 2984–2989. doi:10.1021/es980272q
- Sedlar M. (2014) Temperature Fractionation of mercury in solid samples. Doctoral Dissertation Jožef Stefan International Postgraduate School Ljubljana, Slovenia.
- Sedlar M., Pavlin M., Popovič A., Horvat M. (2015). Temperature stability of mercury compounds in solid substrates. *Open Chem.* 13, 404–419.
- Selin, N. E. (2009). Global Biogeochemical Cycling of Hg: A Review. *Annual Review of Environment and Resources*, 34(1), 43–63. doi:10.1146/annurev.enviro.051308.084314
- Selin, N. E., Jacob, D. J., Yantosca, R. M., Strode, S., Jaeglé, L., & Sunderland, E. M. (2008). Global 3-D land-ocean-atmosphere model for Hg: Present-day versus preindustrial cycles and anthropogenic

References

- enrichment factors for deposition. *Global Biogeochemical Cycles*, 22(2), 1–13. doi:10.1029/2007GB003040
- Semu, E., Singh, B. R., & Selmer-Olsen, A. R. (1987). Adsorption of Hg compounds by tropical soils II. Effect of soil: Solution ratio, ionic strength, pH, and organic matter. *Water, Air, and Soil Pollution*, 32(1), 1–10. doi:10.1007/BF00227678
- Senesi, N., Griffith, S. M., & Schnitzer, M. (1977). Binding of Fe³⁺ by humic materials. *Geochimica et Cosmochimica Acta*, 41(7), 969–976.
- Serudo, R. L., de Oliveira, L. C., Rocha, J. C., Paterlini, W. C., Rosa, A. H., da Silva, H. C., & Botero, W. G. (2007). Reduction capability of soil humic substances from the Rio Negro basin, Brazil, towards Hg(II) studied by a multimethod approach and principal component analysis (PCA). *Geoderma*, 138(3-4), 229–236. doi:10.1016/j.geoderma.2006.11.020
- Shaw, S., Lowry, G. V., Kim, C. S., Rytuba, J. J., & Brown, G. E. (2001). The influence of colloidal phases on Hg-transport from Hg mine waste tailings : A laboratory case study of the New Idria and Sulphur Bank Mines , California , USA, 3, 3723.
- Sheng, G.-P., Yu, H.-Q., & Li, X.-Y. (2010). Extracellular polymeric substances (EPS) of microbial aggregates in biological wastewater treatment systems: a review. *Biotechnology Advances*, 28(6), 882–94. doi:10.1016/j.biotechadv.2010.08.001
- Shi, J. B., Liang, L. N., Jiang, G. Bin, & Jin, X. L. (2005). The speciation and bioavailability of Hg in sediments of Haihe River, China. *Environment International*, 31(3), 357–365. doi:10.1016/j.envint.2004.08.008
- Sholupov, S., Pogarev, S., Ryzhov, V., Mashyanov, N., & Stroganov, a. (2004). Zeeman atomic absorption spectrometer RA-915+ for direct determination of Hg in air and complex matrix samples. *Fuel Processing Technology*, 85(6-7), 473–485. doi:10.1016/j.fuproc.2003.11.003
- Shuman, L. M. (1982). Separating Soil Iron- and Manganese-Oxide Fractions for Microelement Analysis. *Soil Science Society of America Journal*, 46(5), 1099–1102.
- Siegel, S. M., & Siegel, B. Z. (1988). Temperature determinants of plant-soil-air Hg relationships. *Water, Air, and Soil Pollution*, 40(3), 443–448.
- Sierra, M. J., Rodríguez-Alonso, J., & Millán, R. (2012). Impact of the lavender rhizosphere on the Hg uptake in field conditions. *Chemosphere*, 89(11), 1457–1466.
- Skogerboe, R. K., & Wilson, S. a. (1981). Reduction of ionic species by fulvic acid. *Analytical Chemistry*, 53(2), 228–232. doi:10.1021/ac00225a023
- Skyllberg, U. (2008). Competition among thiols and inorganic sulfides and polysulfides for Hg and MeHg in wetland soils and sediments under suboxic conditions: Illumination of controversies and implications for MeHg net production. *Journal of Geophysical Research*, 113, 1–14. doi:10.1029/2008JG000745
- Skyllberg, U. (2010). Synchrotron-Based Techniques in Soils and Sediments. *Developments in Soil Science* (Vol. 34). doi:10.1016/S0166-2481(10)34013-X
- Skyllberg, U., Westin, M. B., Meili, M., & Björn, E. (2009). Elevated concentrations of methyl Hg in streams after forest clear-cut: A consequence of mobilization from soil or new methylation? *Environmental Science and Technology*, 43(22), 8535–8541. doi:10.1021/es900996z

- Sladek, C., & Sexauer, M. (2003). Evaluation of sequential and selective extraction methods for determination of Hg speciation and mobility in mine waste, 18, 567–576.
- Sladek, C., Gustin, M.S. (2000). Assessing the mobility of mercury in mine waste. *Assessing and Managing Mercury from Historic and Current Mining Activities*. U.S. Environmental Protection Agency, San Francisco, 75-77.
- Sladek, C., Gustin, M. S., Kim, C. S., & Biester, H. (2002). Application of three methods for determining Hg speciation in mine waste.
- Slowey, A. J. (2010). Rate of formation and dissolution of Hg sulfide nanoparticles: The dual role of natural organic matter. *Geochimica et Cosmochimica Acta*, 74(16), 4693–4708. doi:10.1016/j.gca.2010.05.012
- Slowey, A. J., Johnson, S. B., Rytuba, J. J., & Brown, G. E. (2005). Role of organic acids in promoting colloidal transport of Hg from mine tailings. *Environmental Science & Technology*, 39(20), 7869–74. Retrieved from <http://www.ncbi.nlm.nih.gov/pubmed/16295849>
- Smith, J. N., & Loring, D. H. (1981). Geochronology for Hg pollution in the sediments of the Saguenay Fjord, Quebec, Canada. *Environ Sci Technol*, 15(8), 944–951. doi:10.1021/es00090a010
- Smith, R. D., & Martell, A. E. (1993). NIST Critical Stability Constants of Metal Complexes Database, version 2.0. National Institute of Standards and Technology: Gaithersburg, MD.
- Snape, I., Scouller, R. C., Stark, S. C., Stark, J., Riddle, M. J., & Gore, D. B. (2004). Characterisation of the dilute HCl extraction method for the identification of metal contamination in Antarctic marine sediments. *Chemosphere*, 57(6), 491–504. doi:10.1016/j.chemosphere.2004.05.042
- Sonke, J. E., Heimbürger, L. E., & Dommergue, A. (2013). Hg biogeochemistry: Paradigm shifts, outstanding issues and research needs. *Comptes Rendus - Geoscience*, 345(5-6), 213–224. doi:10.1016/j.crte.2013.05.002
- Southworth, G. R., Lindberg, S. E., Zhang, H., & Anscombe, F. R. (2004). Fugitive Hg emissions from a chlor-alkali factory: Sources and fluxes to the atmosphere. *Atmospheric Environment*, 38(4), 597–611. doi:10.1016/j.atmosenv.2003.09.057
- Sposito, G., Lund, L. J., & Chang, A. C. (1981). Trace Metal Chemistry in Arid-zone Field Soils Amended with Sewage Sludge: I. Fractionation of Ni, Cu, Zn, Cd, and Pb in Solid Phases. *Soil Science Society of America Journal*, 46(2), 260–264. doi:10.2136/sssaj1982.03615995004600020009x
- Stalder, L., & Wilfried, P. (1980). Availability to plants of herbicide residues in soil. Part 1: A rapid method for estimating potentially available residues of herbicides. *Weed Res.*, 20(6), 341–347.
- Stallings, K. B. (2013). Hg Release from Cinnabar in Water and Aqueous Solutions of Hydroquinone or Ascorbic Acid. M.S., University of Illinois at Chicago, Chicago. Retrieved from [https://indigo.uic.edu/bitstream/handle/10027/9961/Stallings Kimberly.pdf?sequence=1](https://indigo.uic.edu/bitstream/handle/10027/9961/Stallings%20Kimberly.pdf?sequence=1)
- Stefanini, S., 1976. Composizione delle acque fluviali del Friuli-Venezia Giulia durante la fase di magra e di piena dei corsi d'acqua. *CNR Quaderni dell'Istituto di Ricerca sulle Acque*, 28, pp. 391–447.
- Stoffers, P., Survey, G., Street, B., Ka, O., & Wright, I. (1999). Elemental Hg at submarine hydrothermal vents in the Bay of Plenty, Taupo volcanic zone, New Zealand. *Geology*, 27(10), 931–934. doi:10.1130/0091-7613(1999)027<0931:EMASHV>2.3.CO;2

References

- Stone A.T.; Morgan, J.J. (1984). Reduction and dissolution of manganese (III) and manganese (IV) oxides by organics 1. Reaction with hydroquinone. *Environ. Sci. Technol.* 18: 450-456; DOI 0013-936X/84/0918-0450.
- Streets, D. G., Devane, M. K., Lu, Z., Bond, T. C., Sunderland, E. M., & Jacob, D. J. (2011). All-time releases of Hg to the atmosphere from human activities. *Environmental Science and Technology*, 45(24), 10485–10491. doi:10.1021/es202765m
- Streets, D. G., Devane, M. K., Lu, Z., Bond, T. C., Sunderland, E. M., & Jacob, D. J. (2012). NIH Public Access, 45(24), 10485–10491. doi:10.1021/es202765m.ALL-TIME
- Streets, D. G., Zhang, Q., & Wu, Y. (2009). Projections of global Hg emissions in 2050. *Environmental Science and Technology*, 43(8), 2983–2988. doi:10.1021/es802474j
- Strode, S., Jaeglé, L., & Selin, N. E. (2009). Impact of Hg emissions from historic gold and silver mining: Global modeling. *Atmospheric Environment*, 43(12), 2012–2017. doi:10.1016/j.atmosenv.2009.01.006
- Struyk, Z., & Sposito, G. (2001). Redox properties of humic acids. *Geoderma*, 102, 329–346. doi:10.1016/S0016-7061(01)00040-4
- Sunda, W. G., & Kieber, D. J. (1994). Oxidation of humic substances by manganese oxides yields low-molecular-weight organic substrates. *Nature*, 367(6458), 62–64. doi:10.1038/367062a0
- Sutherland, R. a., & Tack, F. M. G. (2008). Extraction of labile metals from solid media by dilute hydrochloric acid. *Environmental Monitoring and Assessment*, 138(1-3), 119–130. doi:10.1007/s10661-007-9748-5
- Tang D., Warnken K. W., and Santschi P. H. (2001) Organic complexaion of copper in surface waters of Galveston Bay. *Limnol. Oceanogr.* 46(2), 321-330.
- Tao, J., Shi-Qiang, W., Flanagan, D. C., Meng-Jie, L., Xue-Mei, L., Qiang, W., & Chang, L. (2014). Effect of Abiotic Factors on the Mercury Reduction Process by Humic Acids in Aqueous Systems * 1. *Pedosphere*, 24(1), 125–136. doi:10.1016/S1002-0160(13)60087-9
- Tarr RS. (1898). *Economic Geology of the United States*. London: Macmillan 38.
- Templeton, D. M., Ariese, F., Cornelis, R., Danielsson, L.-G., Muntau, H., van Leeuwen, H. P., & Lobinski, R. (2000). Guidelines for terms related to chemical speciation and fractionation of elements. Definitions, structural aspects, and methodological approaches (IUPAC Recommendations 2000). *Pure and Applied Chemistry*, 72(8), 1453–1470. doi:10.1351/pac200072081453
- Teršič, T., Gosar, M., & Biester, H. (2011a). Distribution and speciation of Hg in soil in the area of an ancient Hg ore roasting site, Frbejžene trate (Idrija area, Slovenia). *Journal of Geochemical Exploration*, 110(2), 136–145. doi:10.1016/j.gexplo.2011.05.002
- Teršič, T., Gosar, M., & Biester, H. (2011b). Environmental impact of ancient small-scale Hg ore processing at Pšenk on soil (Idrija area, Slovenia). *Applied Geochemistry*, 26(11), 1867–1876. doi:10.1016/j.apgeochem.2011.06.010
- Terzano, R.; Santoro, A.; Spagnuolo, M.; Vekemans, B.; Medici, L.; Janssens, K.; Gottlicher, J.; Denecke, M. A.; Mangold, S.; Ruggiero, P. (2010). Solving mercury (Hg) speciation in soil samples by synchrotron X-ray microspectroscopic techniques. *Environ. Pollut.* 158, 2702–2709.

- Tessier, A., Campbell, P. G. C., & Bisson, M. (1979). Sequential Extraction Procedure for the Speciation of Particulate Trace Metals, *51*(7), 844–851.
- Tossell, J. a. (2001). Calculation of the Structures, Stabilities, and Properties of Hg Sulfide Species in Aqueous Solution. *The Journal of Physical Chemistry A*, *105*(5), 935–941. doi:10.1021/jp003550s
- Tseng, C. M., De Diego, A., Martin, F. M., Amouroux, D., & Donard, O. F. X. (1997). Rapid Determination of Inorganic Hg and MethylHg in Biological Reference Materials by Hydride Generation, Cryofocusing, Atomic Absorption Spectrometry After Open Focused Microwave-assisted Alkaline Digestion. *Journal of Analytical Atomic Spectrometry*, *12*(7), 743–750. doi:10.1039/a700956i
- U.S. Environmental Protection Agency (USEPA). (1997). Hg Study Report to Congress.
- U.S. Environmental Protection Agency (USEPA). (2002). method 1631, revision E. Mercury in Water by Oxidation, Purge and Trap, and Cold Vapor Atomic Fluorescence Spectrometry.
- U.S. E.P.A., (2002). Workshop on the Fate, Transport And Transformation of Mercury in Aquatic and Terrestrial Environment. Environmental Protection Agency. EPA/625/R-02/005. Cincinnati
- U.S. Environmental Protection Agency (USEPA). (2007). method 3015A revision 1 Microwave assisted acid digestion of aqueous samples and extracts
- UNEP. (2013). Global Hg Assessment 2013: Sources, Emissions, Releases and Environmental Transport. Chemicals Branch, Geneva, Switzerland.
- US EPA Method 7473. (2007). Hg in solids and solutions by thermal decomposition, amalgamation, and atomic absorption spectrophotometry.
- USEPA, 1995. EPA Method 3051: microwave assisted acid digestion of sediments, sludges, soils, and oils, Test Methods for Evaluating Solid Waste, 3rd edition. Washington, D.C.
- Varekamp, J. C., & Buseck, P. R. (1986). Global Hg flux from volcanic and geothermal sources. *Applied Geochemistry*, *1*(1), 65–73.
- Vuceta, J. (1976). Adsorption of Pb(II) and Cu(II) on α -quartz from aqueous solutions: influence of pH, ionic strength, and complexing ligands. Retrieved from <https://books.google.com/books?hl=en&lr=&id=Rs31PfkeBaIC&pgis=1>
- Wahle, U., & Kördel, W. (1997). Development of analytical methods for the assessment of ecotoxicological relevant soil contamination. Part A - Development and improvement of soil extraction methods for the determination of the bioavailable parts of contaminants. *Chemosphere*, *35*(1-2), 223–237. doi:10.1016/S0045-6535(97)00152-5
- Wallschläger, D., Turner, R. R., London, J., Ebinghaus, R., Kock, H. H., Sommar, J., & Xiao, Z. (1999). Factors affecting the measurement of Hg emissions from soils with flux chambers. *Journal of Geophysical Research*, *104*(D17), 21859. doi:10.1029/1999JD900314
- Wang, F., & Tessier, A. (2009). Zero-valent sulfur and metal speciation in sediment porewaters of freshwater lakes. *Environmental Science and Technology*, *43*(19), 7252–7257. doi:10.1021/es8034973
- Wang, R., & Wang, W. X. (2010). Importance of speciation in understanding Hg bioaccumulation in tilapia controlled by salinity and dissolved organic matter. *Environmental Science and Technology*, *44*(20), 7964–7969. doi:10.1021/es1011274

References

- Waples, J. S., Nagy, K. L., Aiken, G. R., & Ryan, J. N. (2005). Dissolution of cinnabar (HgS) in the presence of natural organic matter. *Geochimica et Cosmochimica Acta*, 69(6), 1575–1588. doi:10.1016/j.gca.2004.09.029
- Welp, G., & Brümmer, G. W. (1997). Microbial toxicity of Cd and Hg in different soils related to total and water-soluble contents. *Ecotoxicology and Environmental Safety*, 38, 200–204. doi:10.1006/eesa.1997.1577
- Wheatley, B. (1979). MethylHg Poisoning in Canadian Indians - The Elusive Diagnosis. *The Canadian Journal of Neurological Sciences*, 6(4), 417–422.
- White, A. F., Peterson, M. L., & Hochella, M. F. (1994). Electrochemistry and dissolution kinetics of magnetite and ilmenite. *Geochimica et Cosmochimica Acta*, 58(8), 1859–1875. doi:10.1016/0016-7037(94)90420-0
- WHO/IPCS, 2002. Elemental mercury and inorganic mercury compounds. Concise International Chemical assessment Document No. 50. World Health Organisation, Geneva, Switzerland, 73 pp.
- Wiatrowski, H. A., Das, S., Kukkadapu, R., Ilton, E. S., Barkay, T., & Yee, N. (2009). Reduction of Hg (II) to Hg (0) by Magnetite. *Science and Technology*, 43(14), 5307–5313.
- Wilson, S. A., & Weber, J. H. (1979). An EPR study of the reduction of vanadium(V) to vanadium(IV) by fulvic acid. *Chemical Geology*, 26(3-4), 345–354.
- Winfrey, R., & Rudd, W. M. (1990). Formation Of Methylhg In Low pH Lakes, 9, 853–869.
- Wollast, R., Billen, G., & Mackenzie, F. T. (1975). Behavior of Hg in Natural Systems and Its Global Cycle. In *Ecological Toxicology Research* (pp. 145–166). Springer US. doi:10.1007/978-1-4615-8945-7_7
- Xia K, Skyllberg UL, Bleam WF, Bloom PR, Nater EA, Helmke PA. (1999). X-ray absorption spectroscopic evidence for the complexation of Hg (II) by reduced sulfur in soil humic substances. *Environ Sci Technol*, 33 (3), 257–261.
- Xin, M., & Gustin, M. S. (2007). Gaseous elemental Hg exchange with low Hg containing soils: Investigation of controlling factors. *Applied Geochemistry*, 22(7), 1451–1466. doi:10.1016/j.apgeochem.2007.02.006
- Yao A, Qing C, Mu S, Reardon EJ (2006) Effects of humus on the environmental activity of mineral-bound Hg: influence on Hg volatility. *Appl Geochem* 21:446–454. doi:10.1016/ j.apgeochem.2005.10.003
- Yin, Y., Allen, H. E., Huang, C. P., & Sanders, P. F. (1997). of Hg (II) with soil-derived humic substances. *Analytica Chimica Acta*, 341, 73–82.
- Zausig, J. (1995) Redox potential measurements in : Alef. K., P. *Methods in Applied Soil Microbiology and Biochemistry*, ACADEMIC PRESS INC, London.
- Zhang, H., & Lindberg, S. E. (1999). Processes influencing the emission of Hg from soils: A conceptual model. *Journal of Geophysical Research*, 104(D17), 21889–21896. doi:10.1029/1999JD900194
- Zhang, H., Lindberg, S. E., Marsik, F. J., & Keeler, G. J. (2001). Hg air/surface exchange kinetics of background soils of the Tahquamenon River watershed in the Michigan Upper Peninsula. *Water, Air, and Soil Pollution*, 126(1-2), 151–169. doi:10.1023/A:1005227802306

Zhang, J., Dai, J., Wang, R., Li, F., & Wang, W. (2009). Adsorption and desorption of divalent Hg (Hg²⁺) on humic acids and fulvic acids extracted from typical soils in China. *Colloids and Surfaces A: Physicochemical and Engineering Aspects*, 335(1-3), 194–201. doi:10.1016/j.colsurfa.2008.11.006

Zheng, W., Liang, L., & Gu, B. (2012). Hg reduction and oxidation by reduced natural organic matter in anoxic environments. *Environmental Science and Technology*, 46(1), 292–299. doi:10.1021/es203402p

APPENDIX A

A.1. RELEVANCE OF MERCURY POLLUTION IN THE AREA STUDIED

In the northern Adriatic Sea, Marano and Grado lagoons have experienced significant historic Hg inputs from both mining and industrial sources. Thus, it is an effective example of different Hg speciation depending on different pollution sources. The primary and long-term source of Hg originates from the Isonzo river outflow that partly affects the eastern sector (Grado) in the Marano and Grado Lagoon. This latter Hg, primarily in the form of cinnabar particles from the Idrija Hg mine (Biester et al., 2000), is further distributed by tidal fluxes (Covelli et al., 2007)

so that it is present throughout the entire lagoon system (Piani et al., 2005). Meanwhile, the western sector (Marano) of the Marano and Grado Lagoon system has been contaminated by Hg due to uncontrolled discharge of effluents from a chlor-alkali plant located in the drainage basin of the Aussa Corno River flowing in the basin (Piani et al., 2005; Covelli et al., 2009). The industrial plant has been producing cellulose, chlor-alkali and textile artificial fibres since the 1940s.

Hg in these two lagoon basins is primarily associated with fine-grained sediments, probably in the form of Hg^{2+} , Hg^+ and Hg^0 that are weakly adsorbed on the silty-clay fraction. However, in the Grado sector, as also observed at the Isonzo River mouth in the Gulf of Trieste (Biester et al., 2000), the sandy component appears significantly enriched in Hg present as sulphide (HgS). The Hg-rich coarse fraction of the sediment is apparently comprised of detritic Hg (microcrystalline cinnabar) (Acquavita et al., 2012).

Conversely, non-cinnabar compounds were found to be enriched in fine grained material and organic matter near the inner margin of the Marano sector and, particularly within the Aussa-Corno river system (Piani et al., 2005). A speciation technique applied to river bottom sediments demonstrated the presence of a high percentage (from 64 to 91%) of $\text{Hg}(0)$ as expected considering the large quantity of the metal discharged in this fluvial system by the industrial plant (Covelli et al., 2009).

Biester et al. (2000) have shown that cinnabar is the predominant form of Hg at the Isonzo River mouth, whereas organically bound Hg forms, which are mainly associated with fine particles, are subject to long range transport. Results of Hg thermo-desorption measurements performed on bottom samples demonstrate that both cinnabar and non-

cinnabar compounds are present in lagoon sediments and that the relative contribution to total Hg contents can be assessed.

Almost all samples show curves with two peaks. A first maximum was detected between 230 and 260 °C, which represents Hg released from non-cinnabar compounds such as humic acids, according to the curves of standard Hg compounds reported by Biester et al. (2000). Similarly, the second peak (300–350 °C) is related to red cinnabar. As noted by the same authors, several high narrow Hg peaks usually appear in the curves due to slight differences in the crystallinity and grain-size of cinnabar, which influences Hg release temperatures.

Non-cinnabar Hg is relatively more abundant, especially in the lower course of the tributary streams and in the lagoon just in front of the river mouths. This evidence confirms that most of the Hg discharged into the Aussa River from the industrial complex preferentially accumulates in the river itself and in the inner part of the lagoon (Piani et al., 2005).

The fine grained sediments in the Gulf of Trieste (Covelli et al., 2001) have recorded the historical evolution of Hg production at Idrija mine through an exponential increase of metal concentrations since 1800 (although mining activity began in 1496). Between 1850 and 1970 the amount of excavated ore increased as much as the Hg production although the ore grade decreased from several tens to less than 1%. This activity produced an increasing amount of mining residues along with an improved efficiency of the roasting processes, including intensive crushing of the ore, which would have significantly increased the amount of fine grained material in the mining residues (Biester et al., 2000). In the Grado and Marano Lagoons sediments both the fine particles and organic matter play an important role in transferring and accumulating the metal.

In areas where chlor-alkali plants are responsible for Hg contamination of sediments, up to 70–90% of the total metal in sediments can be associated with easily oxidizable organic matter, which is easily degraded and may then be released from the substrate (Smith and Loring, 1981; Gagnon et al., 1997; Biester et al., 2002). Indeed, Hg is preferentially adsorbed to the finest particles in the form of Hg(II), Hg(I) and Hg(0), due the higher specific surface area of each particle; although the presence of micro-crystalline cinnabar cannot be excluded (Covelli et al., 2001).

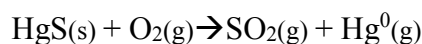
Presence and abundance of the non-cinnabar component in bottom sediments of some sampling sites may identify those areas in the lagoon where Hg is present in chemical

forms that may be more mobile and/or involved in methylation processes. While Hg in sediments impacted by industrial discharges can be primarily composed of Hg(0) with some Hg(I) (Piani et al., 2005; Covelli et al., 2009), cinnabar and Hg(0) predominates in lagoons affected by mining activities (Piani et al., 2005; Covelli et al., 2011). The more “bioavailable” water-soluble fraction present in all locations constitutes the least abundant component (<1%) while the organically bonded Hg fraction (humics) seems more important in the industrially Hg-polluted sediments. This Hg speciation in the sediment solid phase is probably reflected in the porewater composition leading to generally low porewater concentrations of dissolved Hg (high K_d) in sites with which Hg is more thoroughly bound to solid phase (Faganeli et al., 2012)

A.2. IDRIJA MERCURY MINE

Hg has been extracted, mainly, from cinnabar (HgS), although the following are also phase minerals of Hg: livingstonite (HgSb₄S₈), corderoite (Hg₃S₂Cl₂), metacinnabar (cubic HgS), schuetteite (Hg₃(SO₄)O₂), montroydite (HgO), calomel (Hg₂Cl₂), tiemannite (HgSe) and kleinite (Hg₂N [Cl SO₄] · nH₂O).

The main process for obtaining Hg from cinnabar is to roast the ore at 500–600 °C, which liberates Hg(0) in the following reaction:



The release of Hg into the environment in Hg mining areas is generally associated with the abandonment of mine waste, which is mainly composed of calcines (waste originated in the metallurgy of Hg) and mine waste impoundments; which contain waste rock and low-grade ore stockpiles (Navarro et al., 2008).

Mine waste, includes several types of material (mainly mine waste and calcines) with varying Hg content and speciation depending on the ore deposit and processing technology.

At mining sites, the weathering of waste materials and mankind’s action can redistribute Hg, if present, in additional chemical forms, facilitate dispersion in watersheds or through atmospheric emissions, and increase its bioavailability for organisms (Reis et al., 2010).

A lot of papers and reviews have been published regarding ore extraction activity and contamination in the area of Idrija, as well as the related terrestrial, atmospheric and aquatic environments (e.g. Hines et al., 2000; Gosar et al., 2006; Teršič et al., 2011a; Teršič et al., 2011b; Gosar and Teršič, 2012) (Figure A.1).



Figure A.1. Regional map presenting location of Idrija mercury mine, Idrija and Soča Rivers flow, and Gulf of Trieste (Gosar and Teršič, 2012).

The Idrija Mine, the second largest Hg mine in the world, opened in the late 15th century and ceased operation in 1995, but still delivers large quantities of Hg downstream including into the northern Adriatic Sea. Runoff from the mine into streams and rivers still delivers annually about 1.5 tons of Hg to the sea, which is about 100 km away from Idrija. Thus, Hg and MeHg is elevated in the marine environment (Horvat et al., 1999). The retorting of Hg ore at Idrija mercury mine (primarily cinnabar, HgS) produces elemental Hg (Hg(0)), a significant amount of which is lost into the environment.

Inefficient processing of ore leads to mine tailing and calcines (previously roasted ore) that are significantly laden with Hg, which can be transported great distances downstream, thereby posing a threat well away from the source (Gray et al., 2002). Hg deposited downstream can be remobilized and made available for conversion to MeHg and eventual bioaccumulation (Hines et al., 2000). Hence, it is possible to encounter dangerous concentrations of MeHg many km away from the primary inorganic source of Hg (Figure A.2) (Hines et al., 2006).

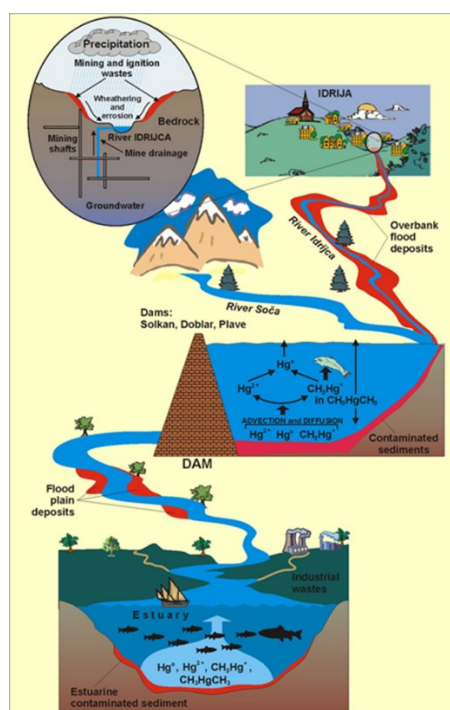


Figure A.2. Mercury contamination from the Idrija mine region to the Gulf of Trieste.

During the operating period of the mine, 107,500 t of Hg were produced. Taking into account the losses during mining and inefficient smelting, the total amount of mercury mined is estimated to be at least 153,000 t (Dizdarevič, 2001). It has been estimated that 45,500 t of mercury were emitted into the environment during the operating period of the mine, which ceased production in 1995 (Dizdarevič, 2001). The mine is currently in the final stage of its gradual shut down due to the lack of reserves, low ore grade, low Hg prices and environmental reasons (Goser et al., 2006).

APPENDIX B-PICTURES OF THE STUDY AREA AND THE SOIL PROFILE



Figure landscape of field crops and greenhouses in Fossalon di Grado.



Figure Bottom of the excavation of soil profile, water table outcropping can be seen.



Figure Detail of the soil profile between 0 and 50 cm.



Figure Detail of the soil profile between 40 and 110 cm.



Figure Detail of the soil profile between 100 and 155 cm.



Figure Detail of the soil profile between 150 and 190 cm. Grey sands at 180 cm depth can be seen.



Figure Detail of the organic horizon at 145 cm depth.

APPENDIX C-THERMO-DESORPTION CURVES OF FOSSALON SOIL TREATED WITH FERTILIZERS

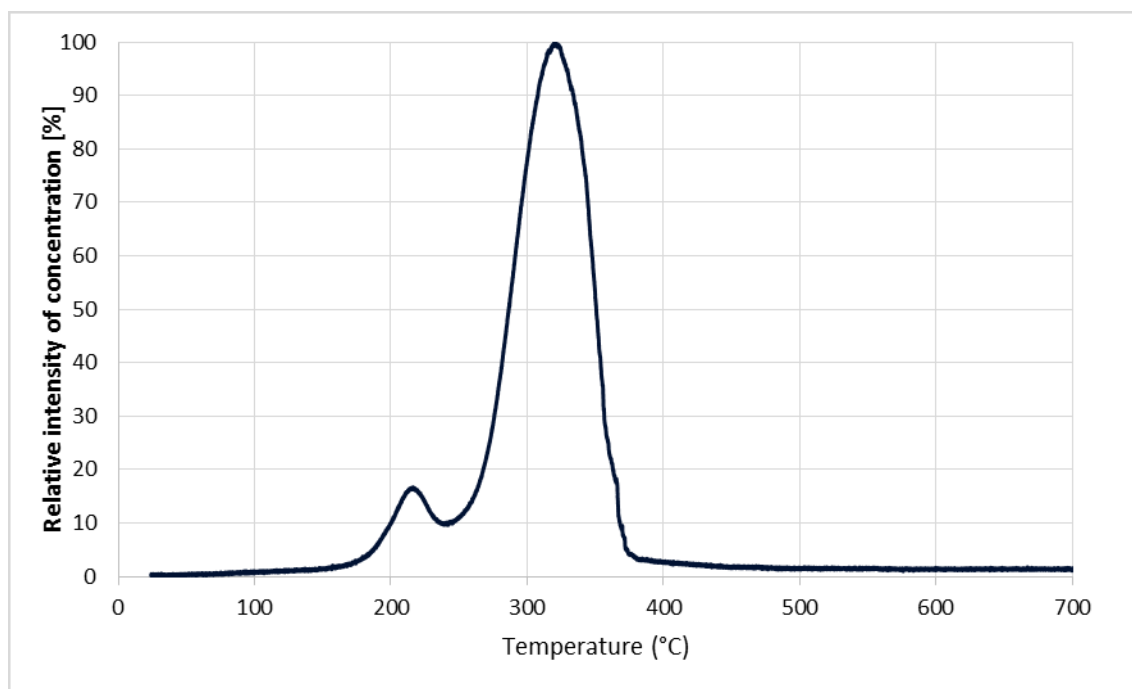


Figure. Thermo-desorption curves of Fossalon soil amended with Urea in solution and incubated in aerobic conditions for one day.

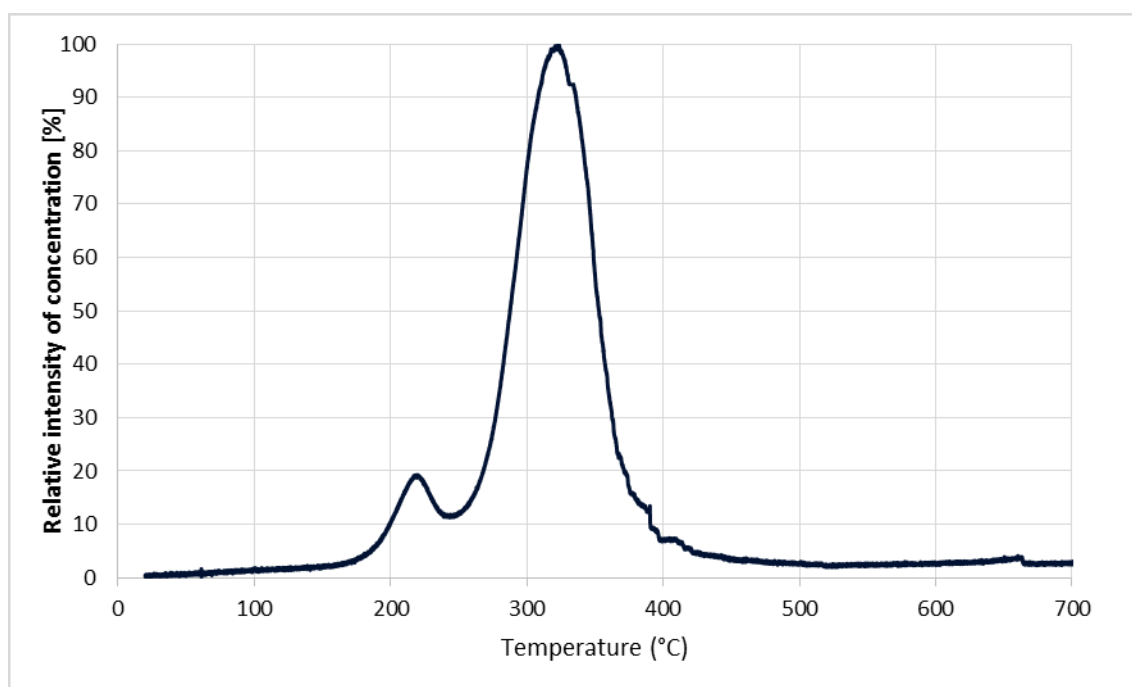


Figure. Thermo-desorption curves of Fossalon soil amended with dry Urea and incubated in aerobic conditions for one day.

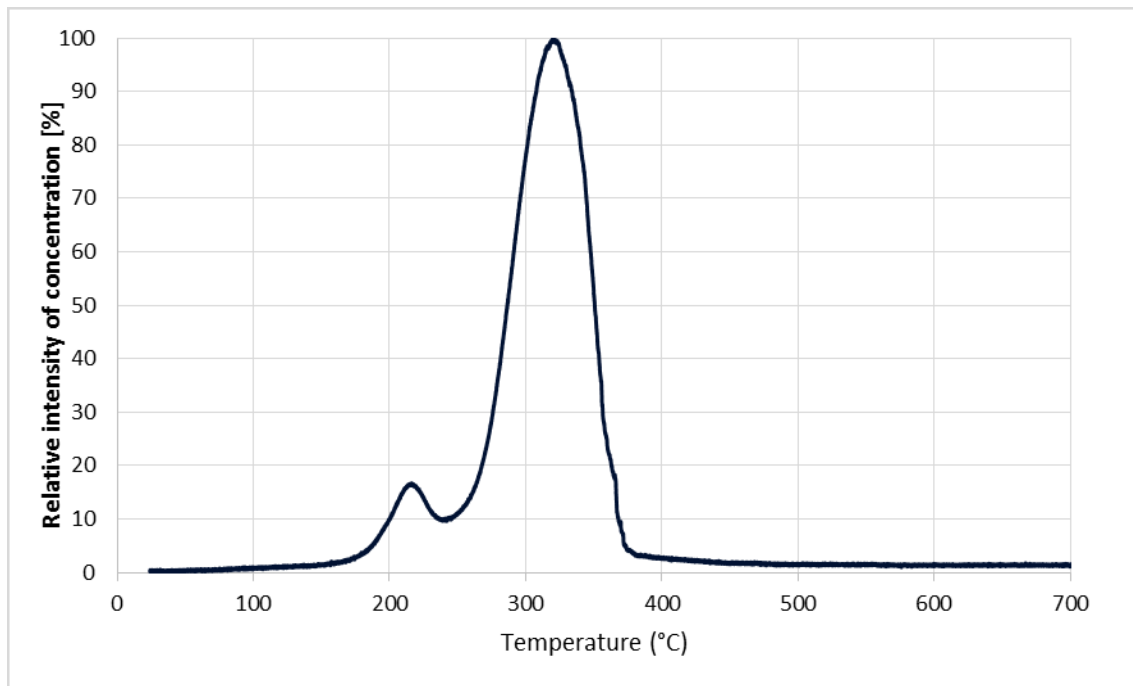


Figure. Thermo-desorption curves of Fossalon soil amended with Urea in solution and incubated in aerobic conditions for seven day.

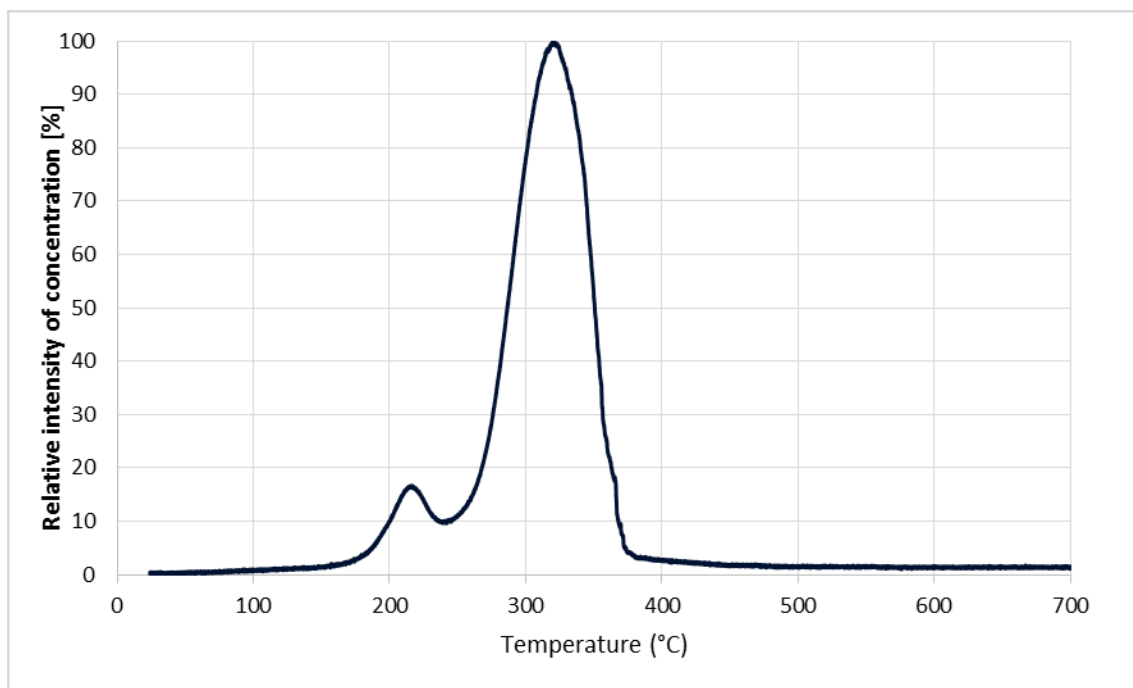


Figure. Thermo-desorption curves of Fossalon soil amended with dry Urea and incubated in aerobic conditions for seven day.

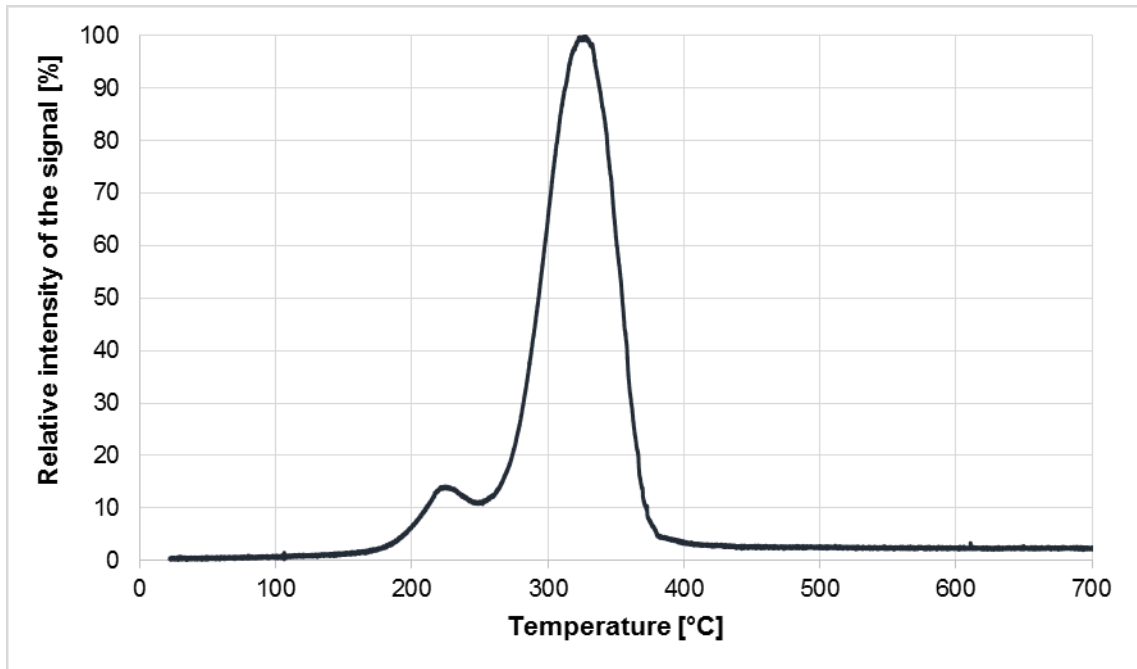


Figure. Thermo-desorption curves of Fossalon soil amended with Calcium nitrate in solution and incubated in aerobic conditions for one day.

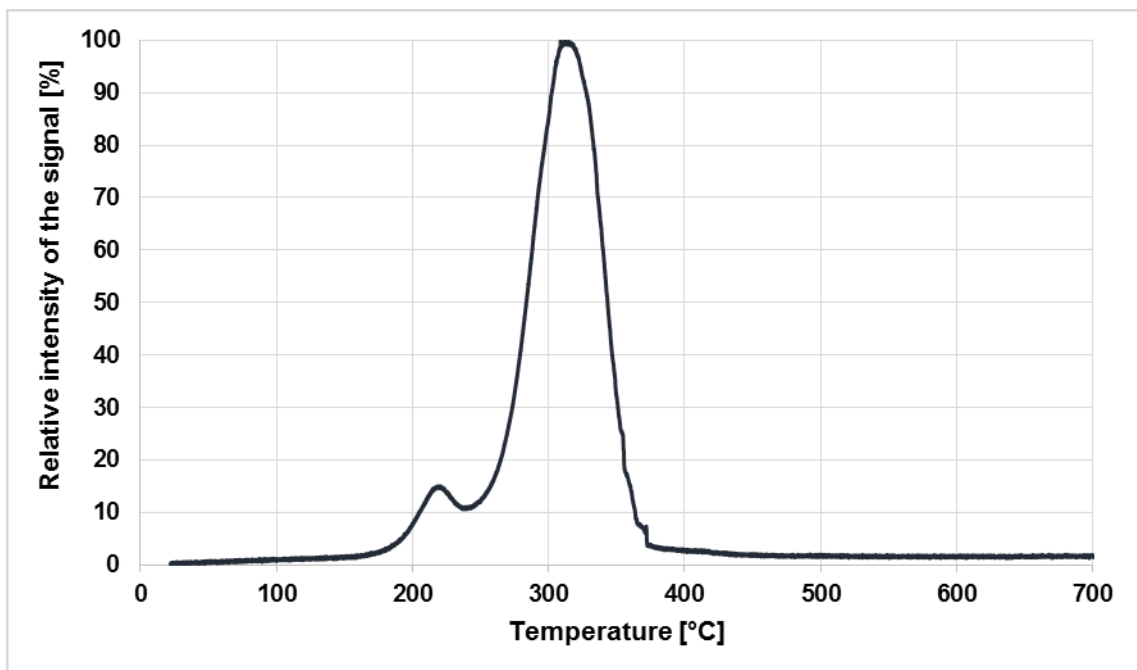


Figure. Thermo-desorption curves of Fossalon soil amended with dry Calcium nitrate and incubated in aerobic conditions for one day.

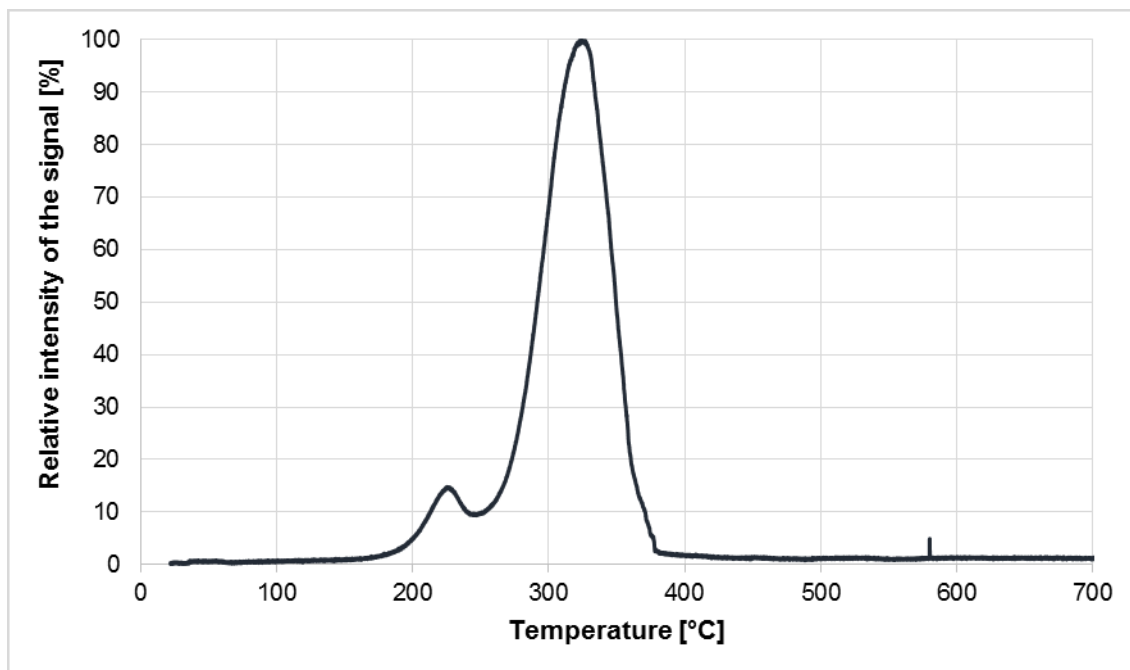


Figure. Thermo-desorption curves of Fossalon soil amended with Calcium nitrate in solution and incubated in aerobic conditions for seven day.

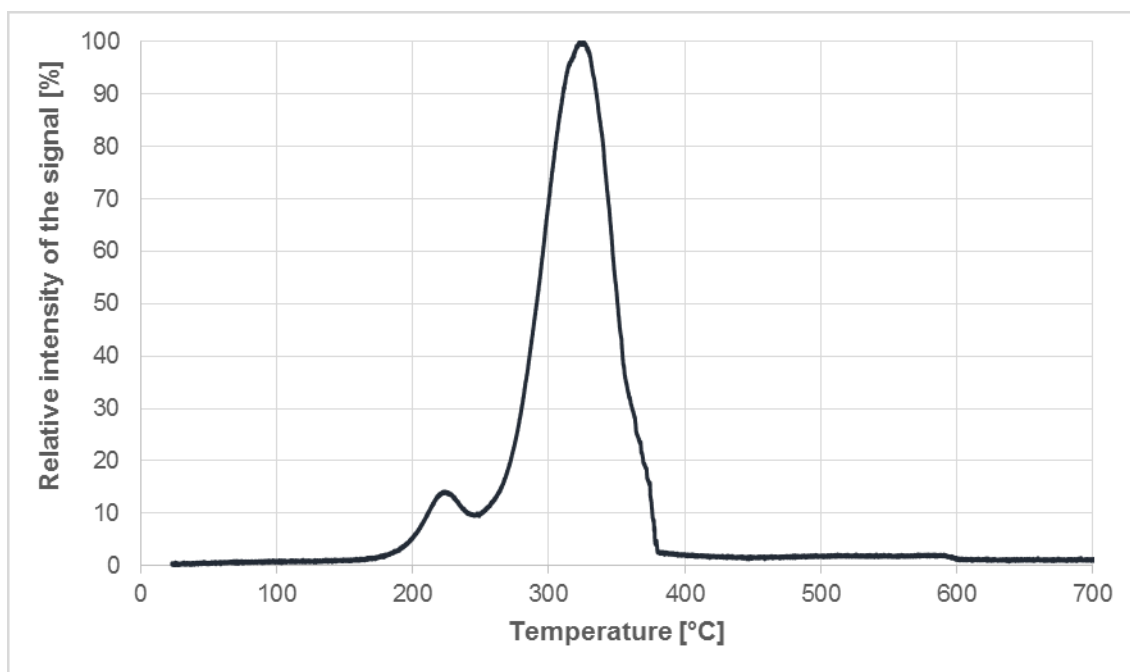


Figure. Thermo-desorption curves of Fossalon soil amended with dry Calcium nitrate and incubated in aerobic conditions for seven day.

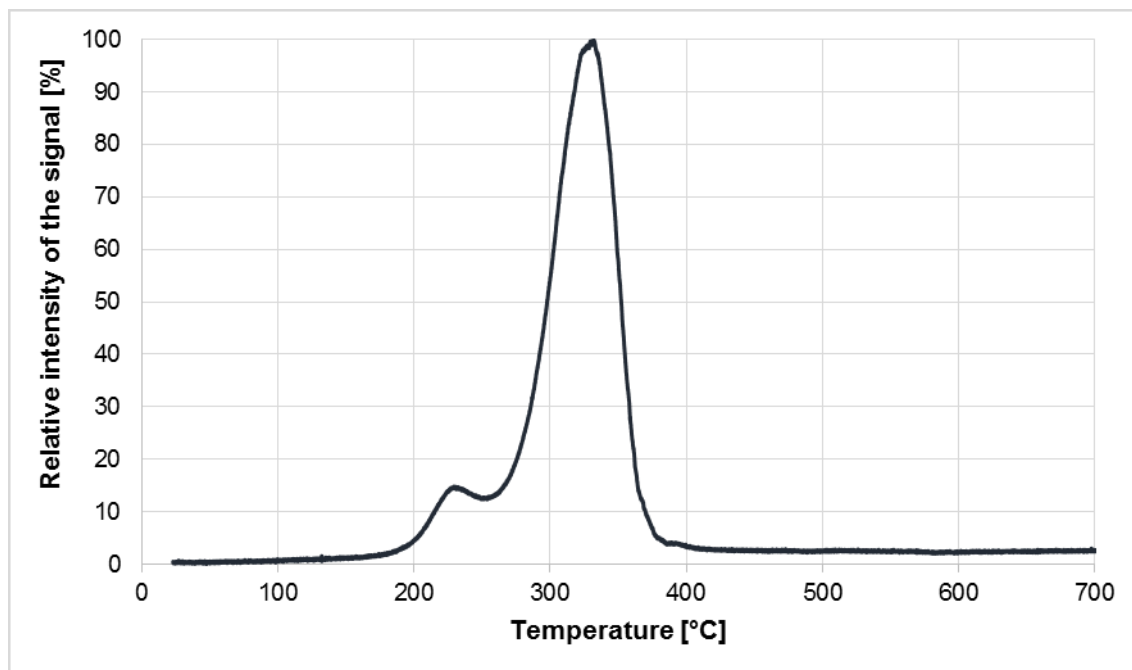


Figure. Thermo-desorption curves of Fossalon soil amended with Ammonium sulphate in solution and incubated in aerobic conditions for one day.

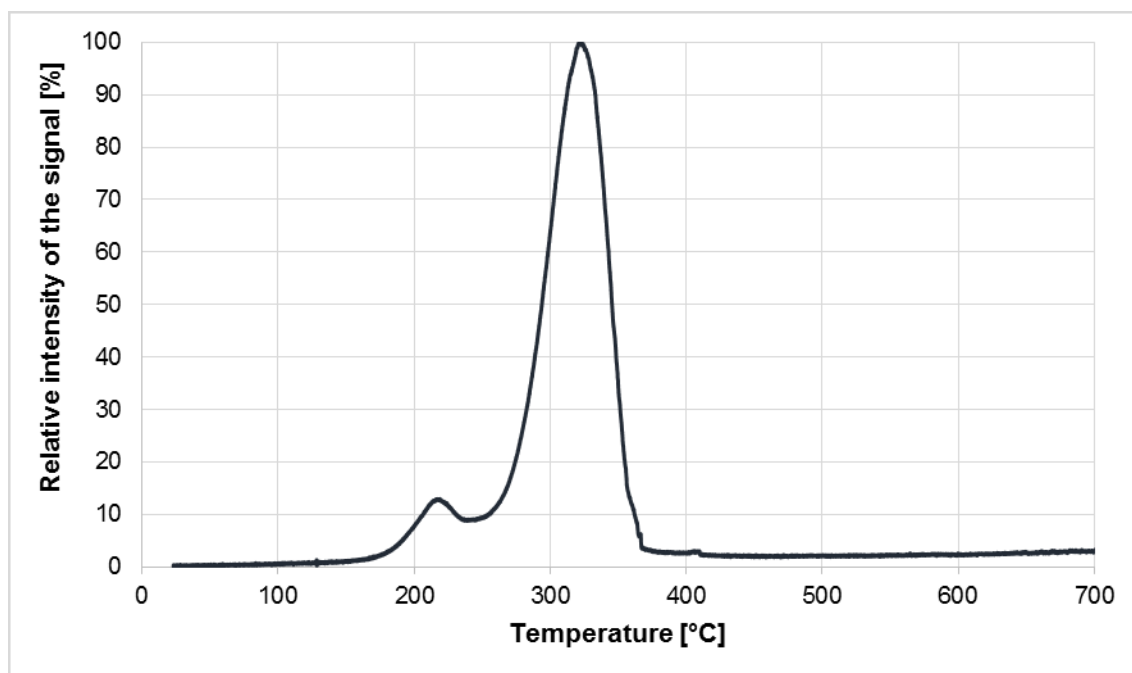


Figure. Thermo-desorption curves of Fossalon soil amended with dry Ammonium sulphate and incubated in aerobic conditions for one day.

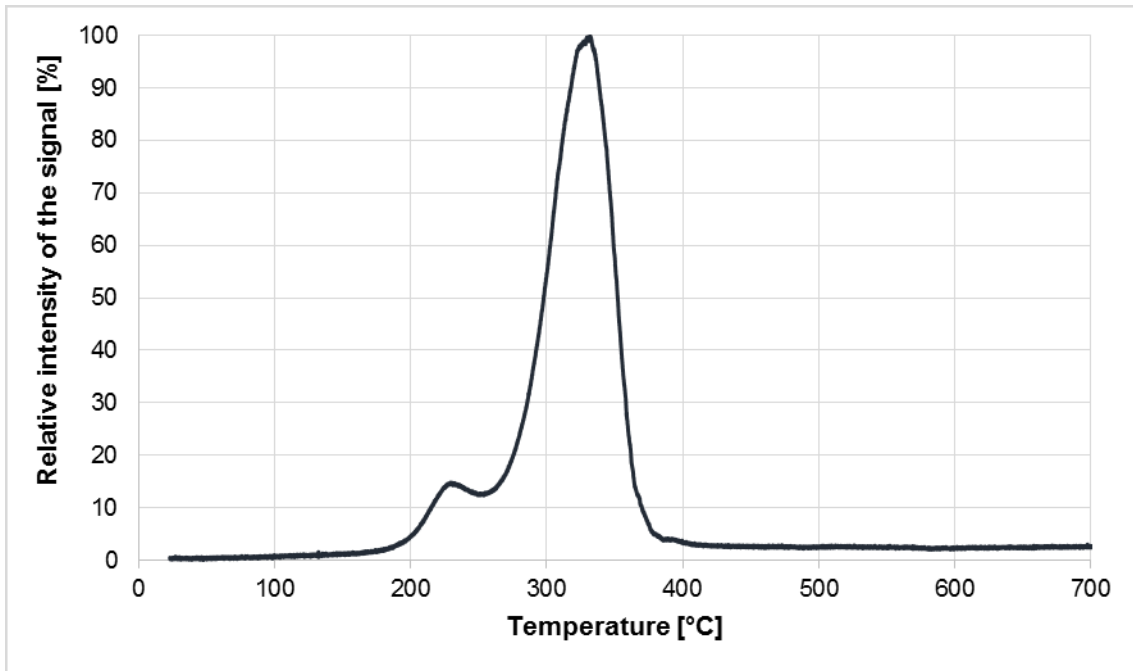


Figure. Thermo-desorption curves of Fossalon soil amended with Ammonium sulphate in solution and incubated in aerobic conditions for seven day.

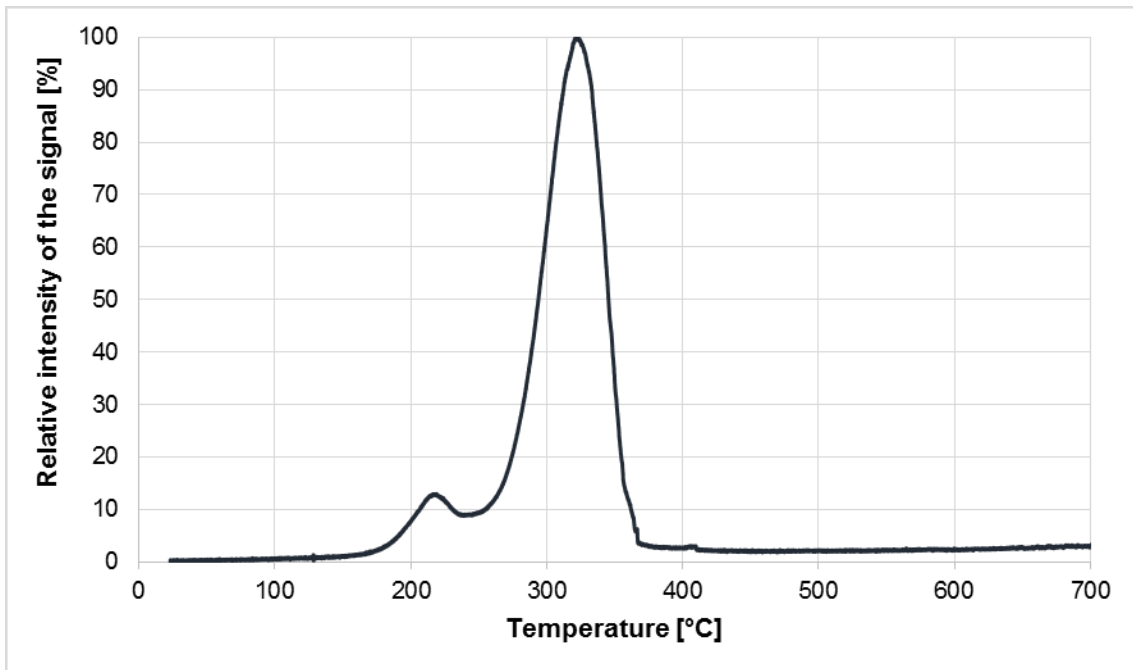


Figure. Thermo-desorption curves of Fossalon soil amended with dry Ammonium sulphate and incubated in aerobic conditions for seven day.

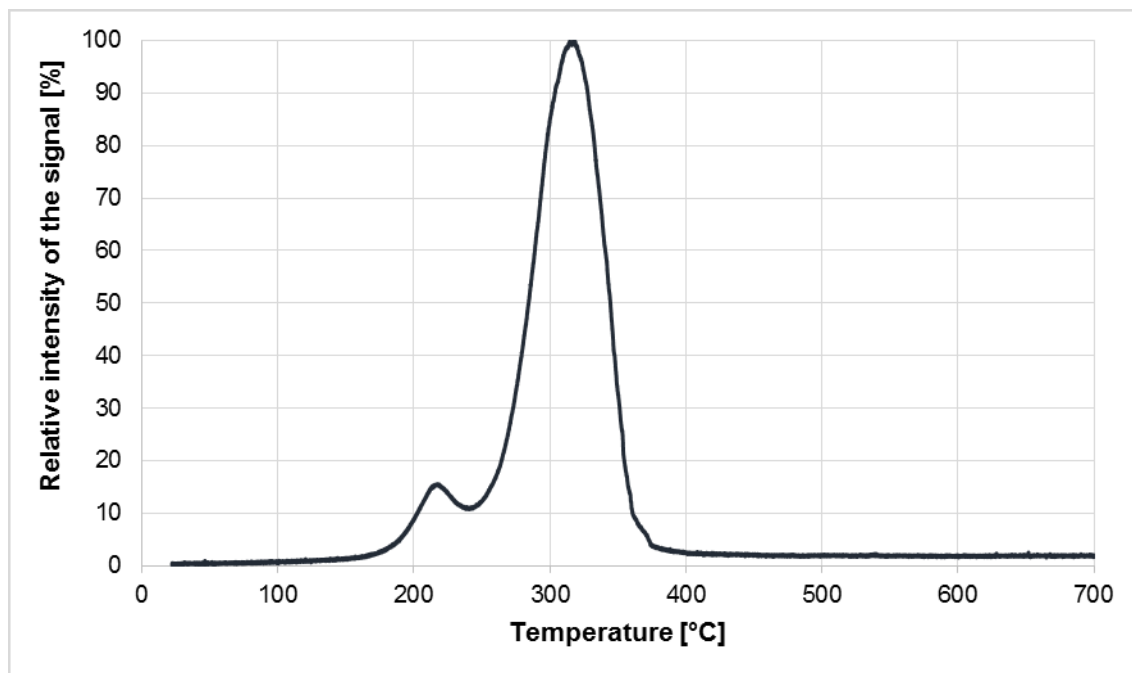


Figure. Thermo-desorption curves of Fossalon soil amended with Ammonium phosphate in solution and incubated in aerobic conditions for one day.

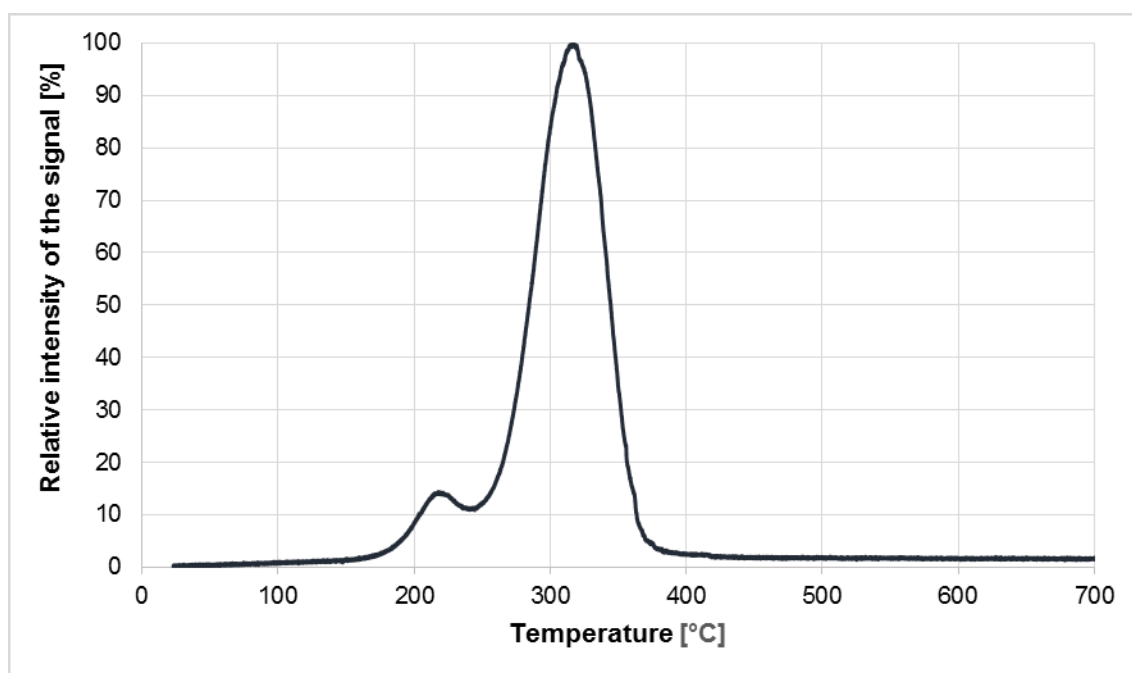


Figure. Thermo-desorption curves of Fossalon soil amended with dry Ammonium phosphate and incubated in aerobic conditions for one day.

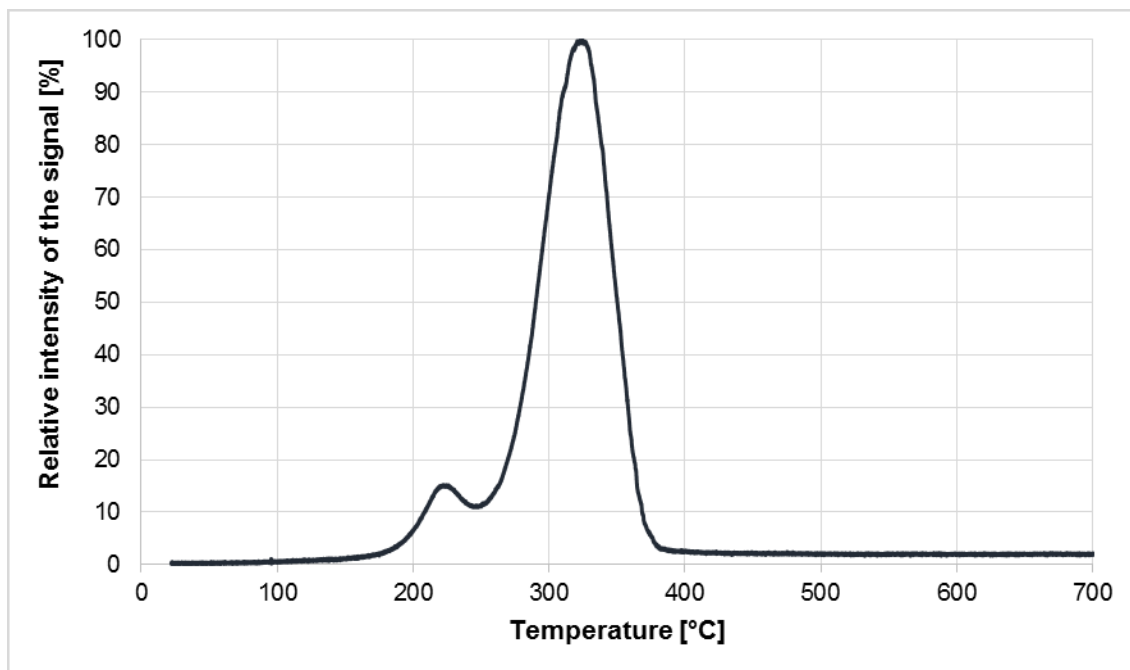


Figure. Thermo-desorption curves of Fossalon soil amended with Ammonium phosphate in solution and incubated in aerobic conditions for seven day.

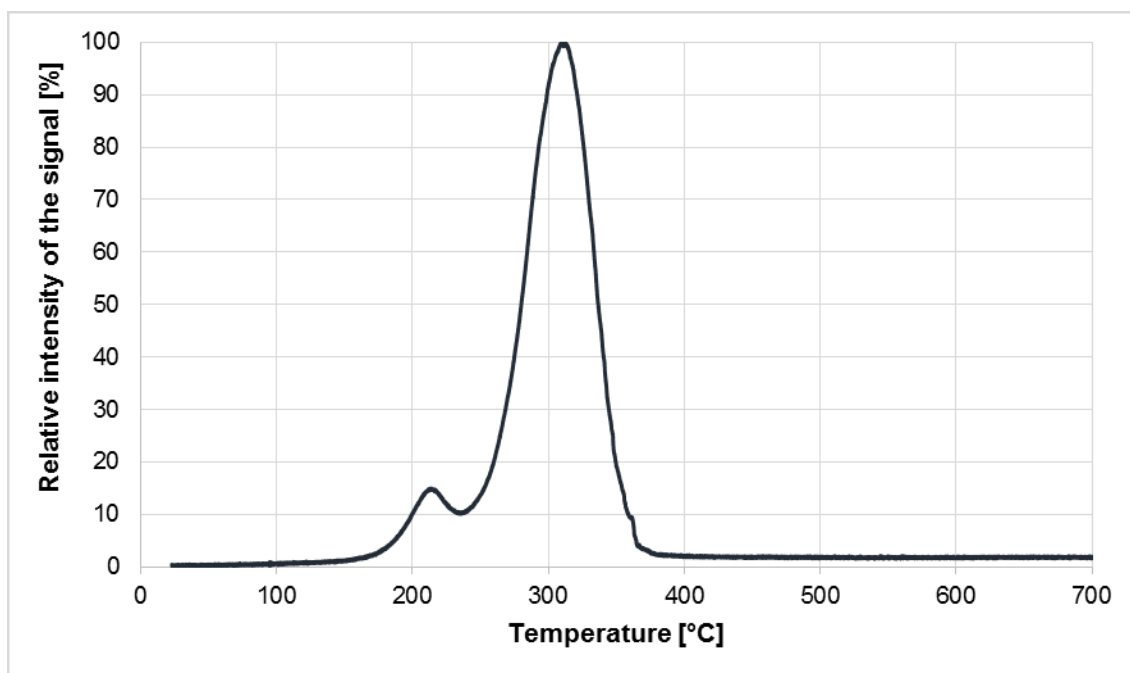


Figure. Thermo-desorption curves of Fossalon soil amended with dry Ammonium phosphate and incubated in aerobic conditions for seven day.

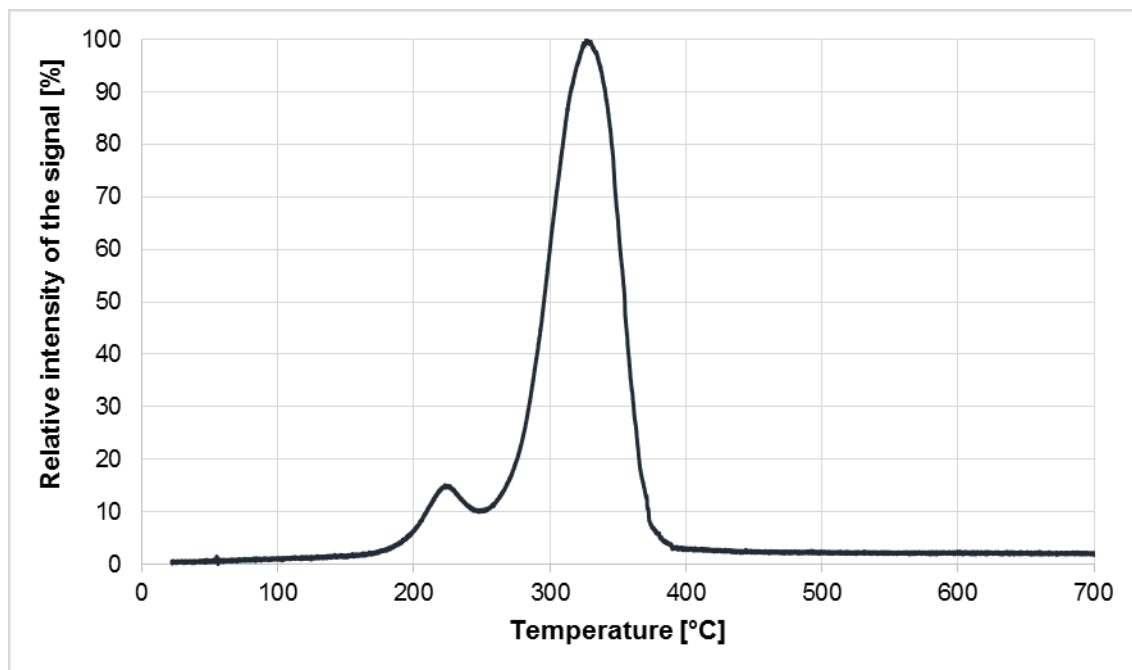


Figure. Thermo-desorption curves of Fossalon soil amended with Potassium sulphate in solution and incubated in aerobic conditions for one day.

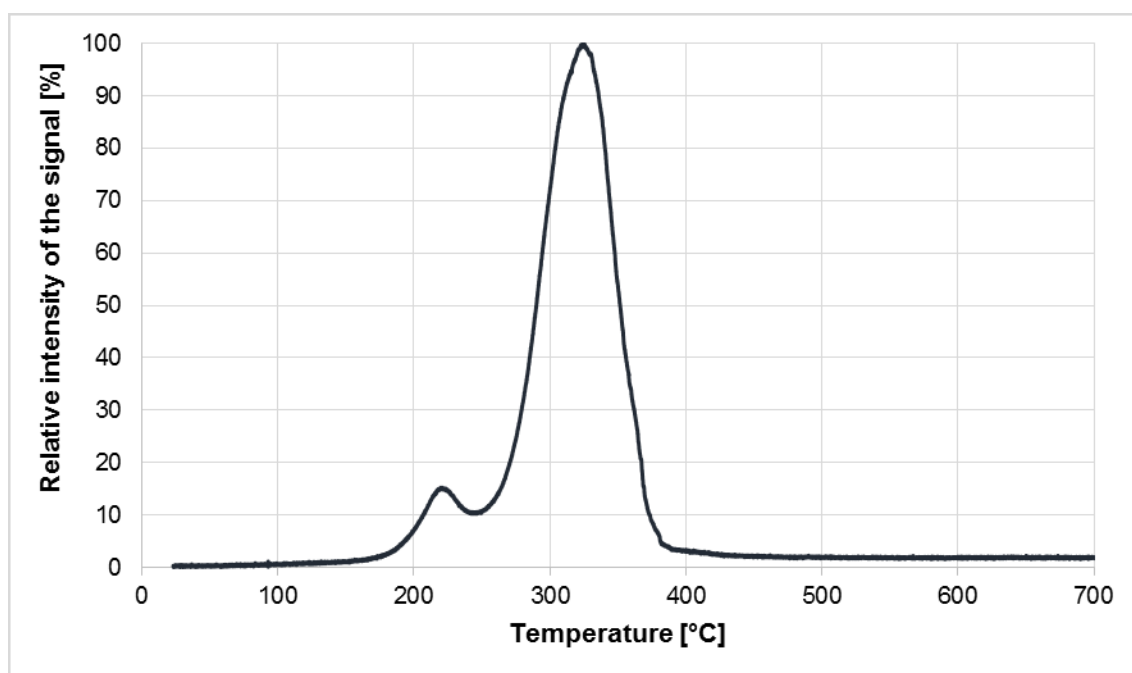


Figure. Thermo-desorption curves of Fossalon soil amended with dry Potassium sulphate and incubated in aerobic conditions for one day.

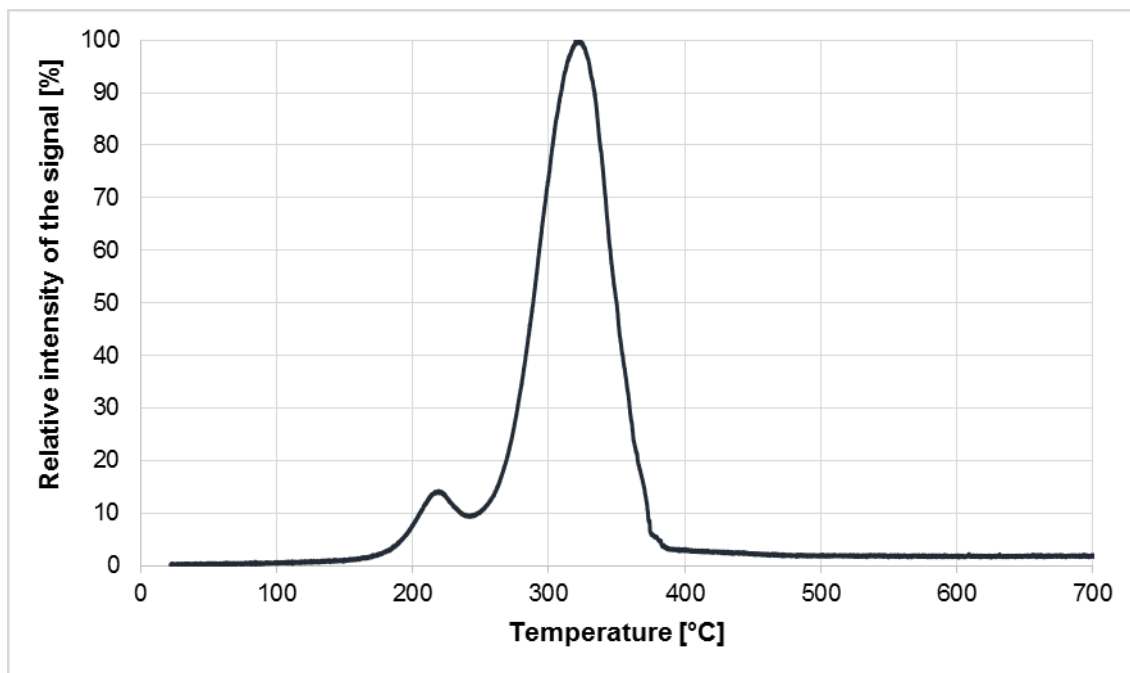


Figure. Thermo-desorption curves of Fossalon soil amended with Potassium sulphate in solution and incubated in aerobic conditions for seven day.

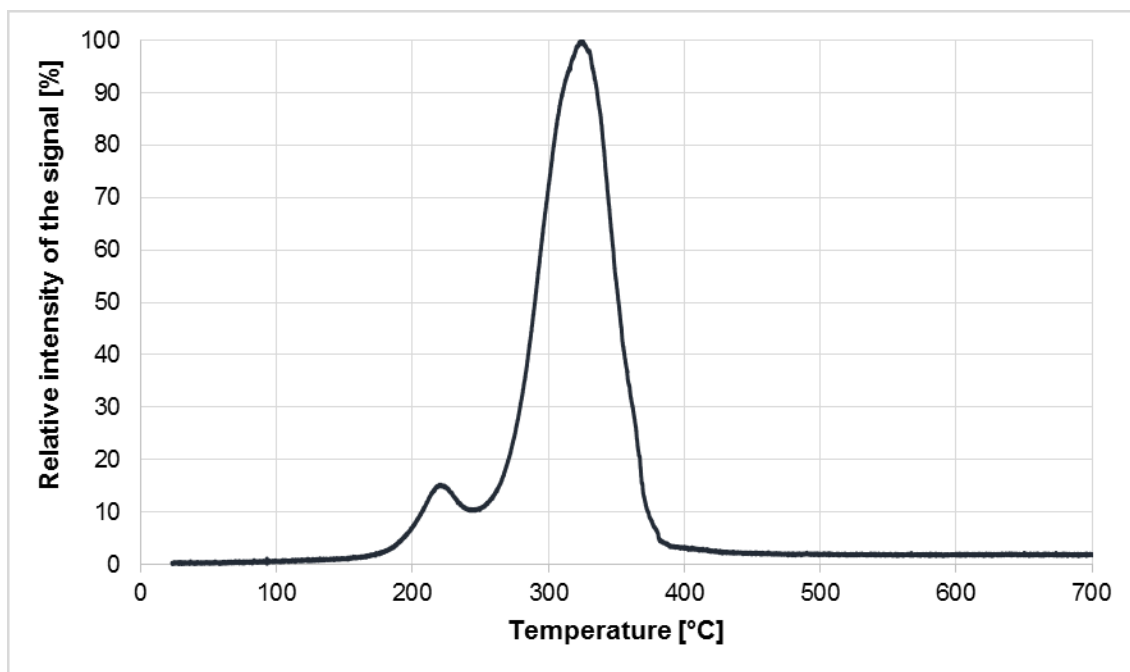


Figure. Thermo-desorption curves of Fossalon soil amended with dry Potassium sulphate and incubated in aerobic conditions for seven day.

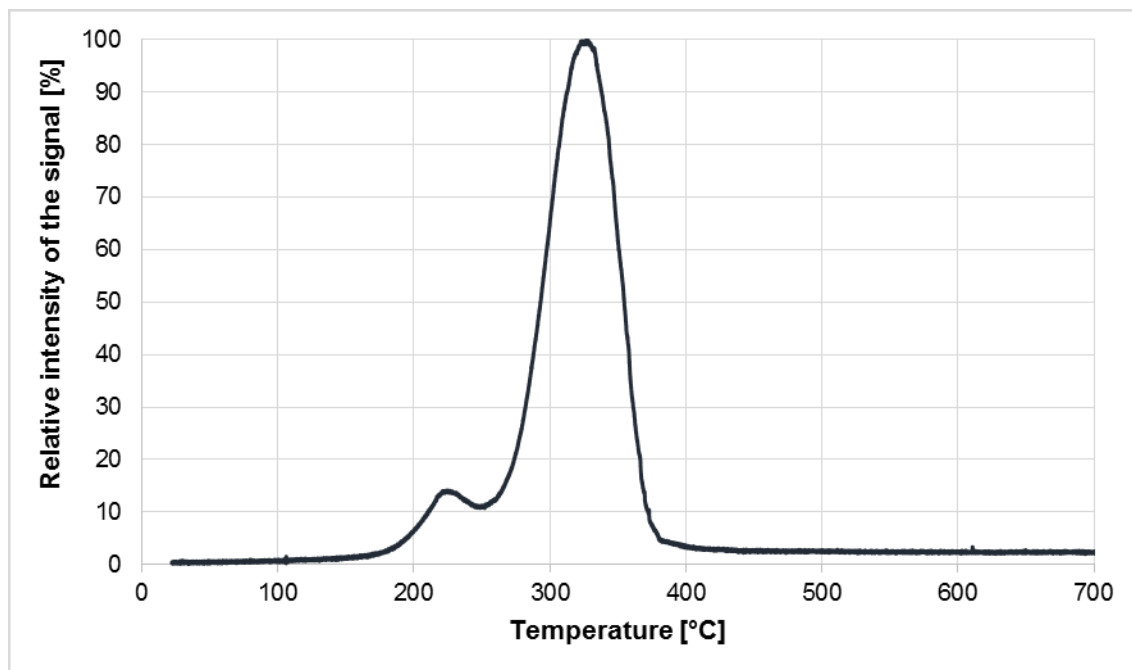


Figure. Thermo-desorption curves of Fossalon soil amended with Calcium Phosphate in solution and incubated in aerobic conditions for one day.

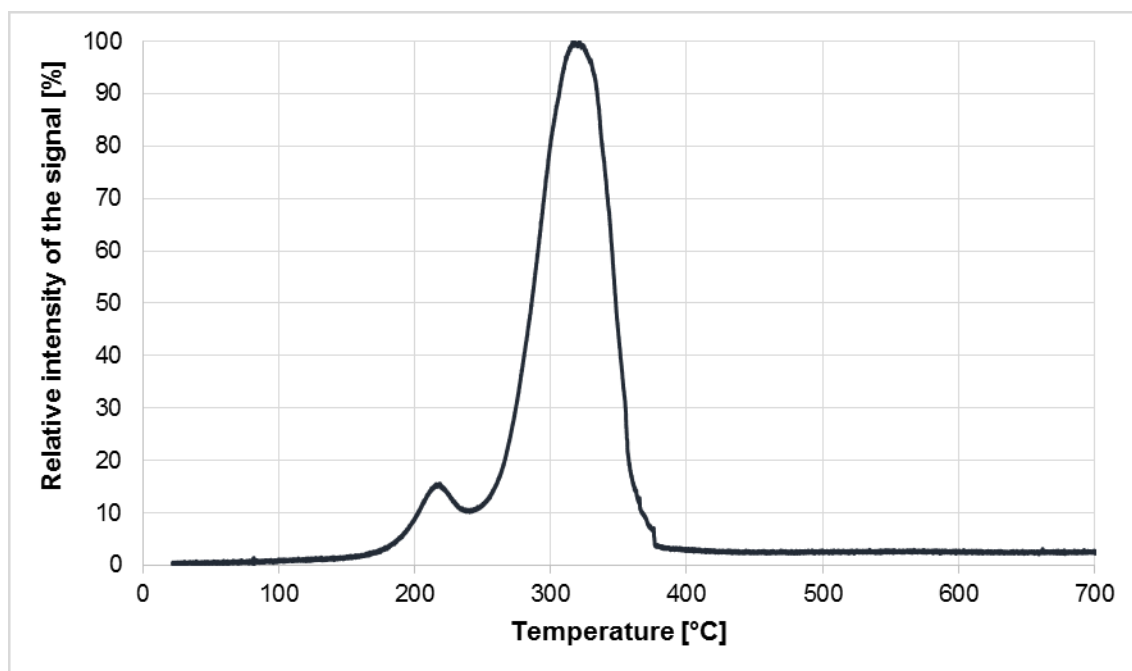


Figure. Thermo-desorption curves of Fossalon soil amended with dry Calcium Phosphate and incubated in aerobic conditions for one day.

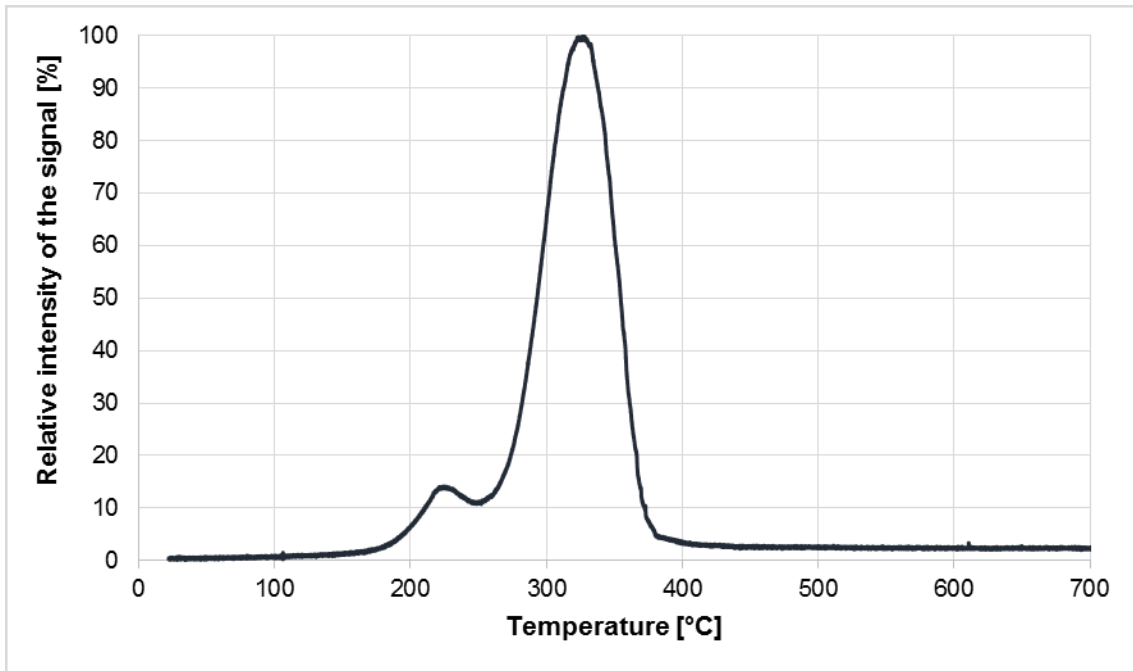


Figure. Thermo-desorption curves of Fossalon soil amended with Calcium Phosphate in solution and incubated in aerobic conditions for seven day.

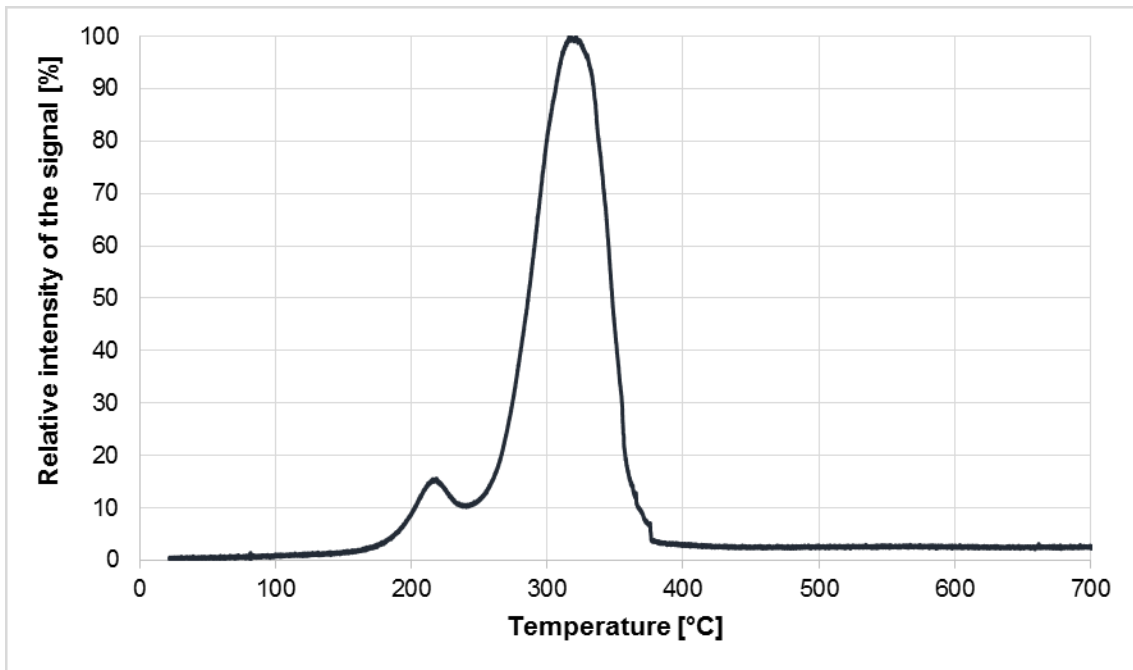


Figure. Thermo-desorption curves of Fossalon soil amended with dry Calcium Phosphate and incubated in aerobic conditions for seven day.

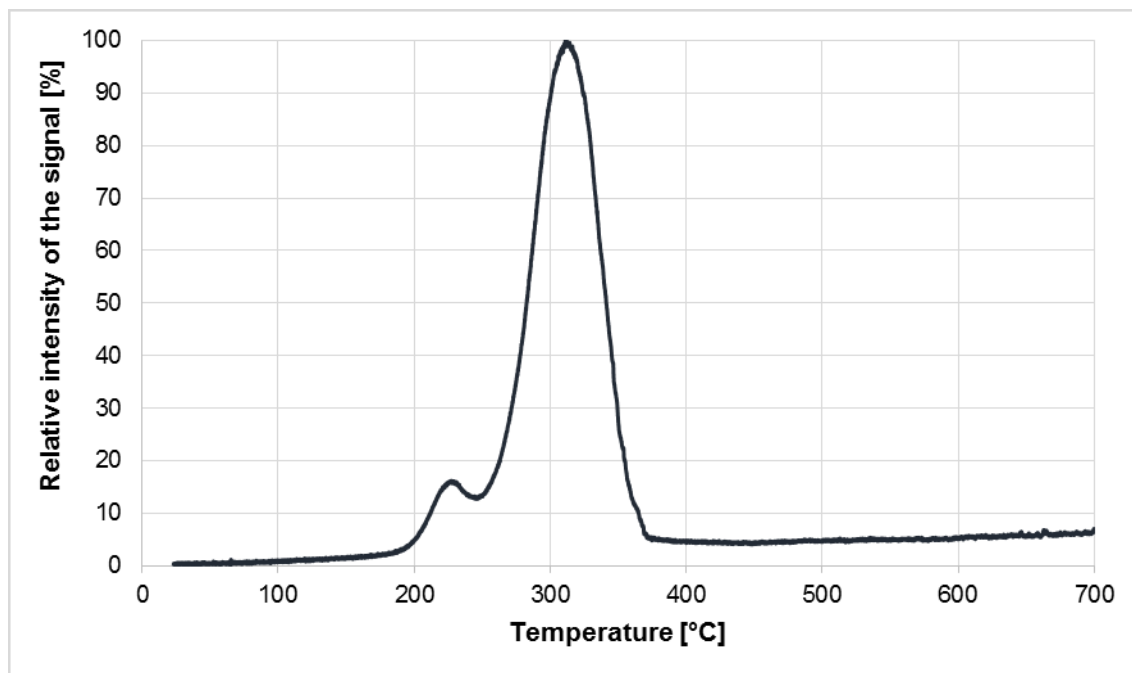


Figure. Thermo-desorption curves of Fossalon soil amended with Potassium chloride in solution and incubated in aerobic conditions for one day.

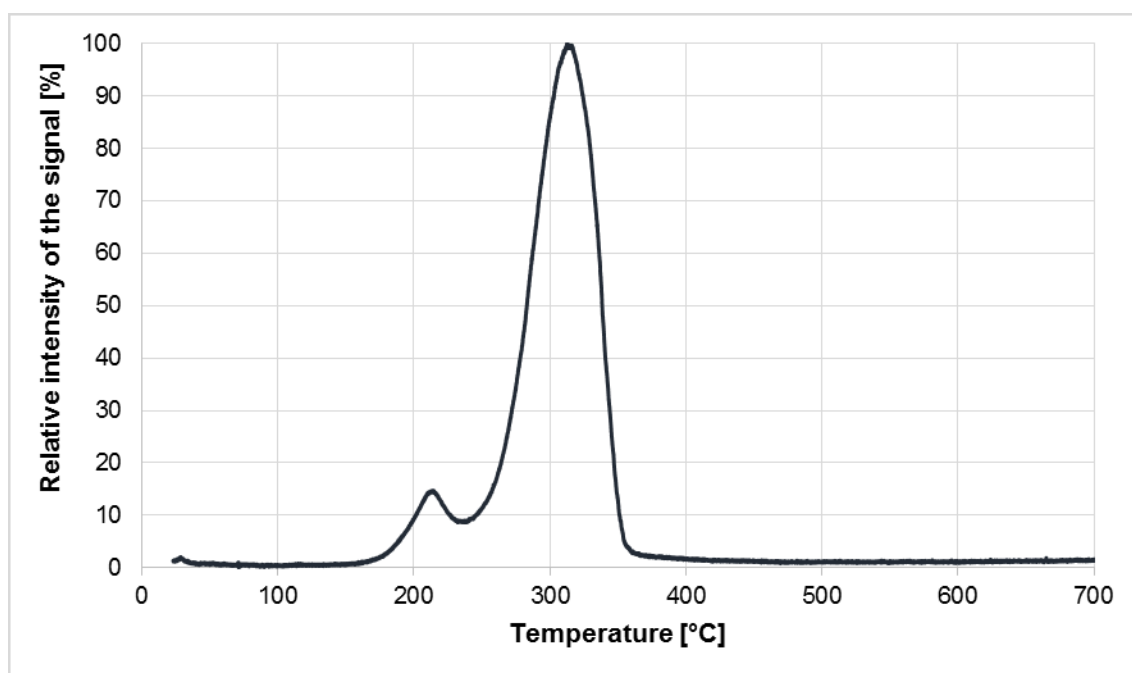


Figure. Thermo-desorption curves of Fossalon soil amended with dry Potassium chloride and incubated in aerobic conditions for one day.

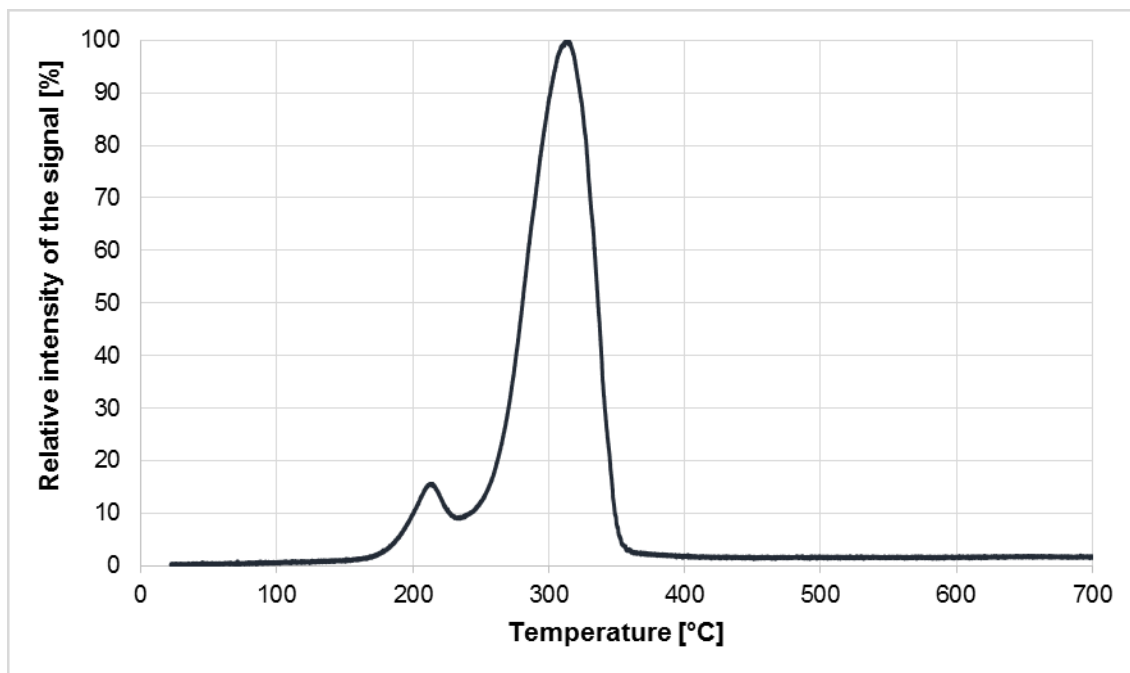


Figure. Thermo-desorption curves of Fossalon soil amended with Potassium chloride in solution and incubated in aerobic conditions for seven day.

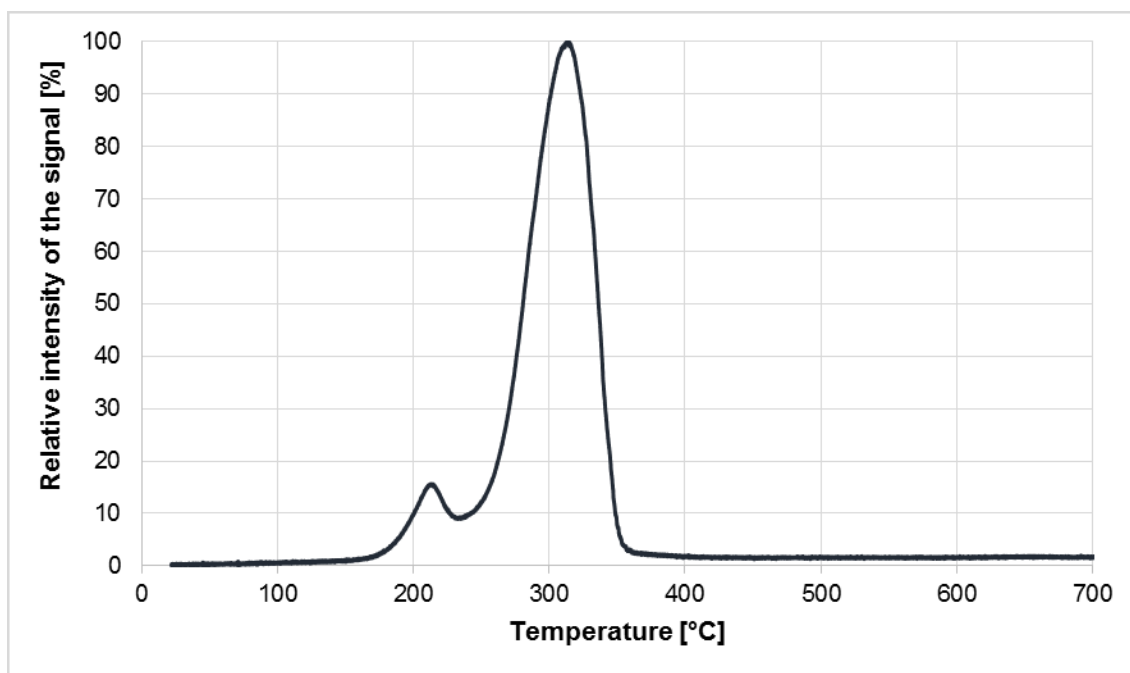


Figure. Thermo-desorption curves of Fossalon soil amended with dry Potassium chloride and incubated in aerobic conditions for seven day.

APPENDIX D-PROPOSALS FOR FURTHER RESEARCH

D.1. IMPORTANCE OF NANOPARTICLES IN CINNABAR'S MOBILIZATION

Dissolved phases are commonly considered to be the most efficient means of aqueous contaminant transport in the environment. Recently, however, a number of field studies have implicated particle-associated transport of metal contaminants in a variety of environments.

Indeed significant colloid-associated transport of a variety of metal contaminants has been demonstrated (Slowey et al., 2005).

Soil particle based mobilization is driven by:

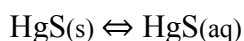
- Changes in pH;
- Changes in Ionic Strength (IS);
- Adsorption of anions, above all Low Molecular Weight (LMW) organic adsorbents, particular via specific binding with sulfhydryl functional groups.

Changes in pH and IS will occur due to seasonal variation in rainfall, so leaching can mobilized colloids.

Colloids may be stabilized through charge stabilization or steric stabilization.

Thiol-containing organics may prevent metal sulfide particle aggregation or enhance it, depending on the size, structure, and hydrophobicity of the organic compounds. Moreover, nonspecific processes such as hydrophobic interactions may be important for sorption of humic substances and other NOM macromolecules. Further studies should address both specific and nonspecific surface interactions and the implications of these interactions for colloidal stability of mineral sulfides (Gondikas et al., 2010).

Cinnabar is low soluble in water according to the reaction below (Hsu-Kim et al., 2013):



solubility product $\log K_s =$ between -10 -22.3

On this basis, mercury nanoparticles formation is important because they can modify mercury mobility in soils contaminated by cinnabar. Such Hg minerals pose a significant environmental hazard due to release of soluble Hg, and therefore potentially bioavailable Hg (Slowey et al., 2005).

In the past decade, geochemists and aquatic chemists have realized that nanoscale particles are ubiquitous in the environment. Much of this work has involved metal elements that are much more abundant than mercury (e.g. iron, aluminum, manganese,

titanium, zinc). Nanoparticles of metal sulfides such as ZnS and CuS have been observed in settings such as the biofilms of sulfate-reducing (and sulfide-generating) bacteria and in wastewater effluent. Discrete nanoparticles of HgS have been detected directly in soil, sediment, and biofilms on plant roots (Hsu-Kim et al., 2013).

Nanoscale particles are expected to behave differently than the compositionally identical, larger materials due to the high specific surface areas and unique reactivity of materials at the nanoscale. Indeed, the defining characteristics of nanoparticles are not only the small size (i.e. at least one 2 dimension smaller than 100 nm) but also size-specific reactivity exhibited by the nanomaterials and different levels of crystallization or structural disorder. Nanoscale-specific reactivity may include:

- increased sorption capacity (normalized to surface area);
- enhanced transport;
- faster rates of dissolution and renucleation;
- increased bioavailability of the metal constituents of the nanoparticle (Hsu-Kim et al., 2013).

In Figure D.1, Figure D.2, Figure D.3 and Figure D.4 an example of soil characterization using SEM-EDX is shown.

One particle in the range of 1-2 μm is detected, TEM is needed for a better characterization of the particles.

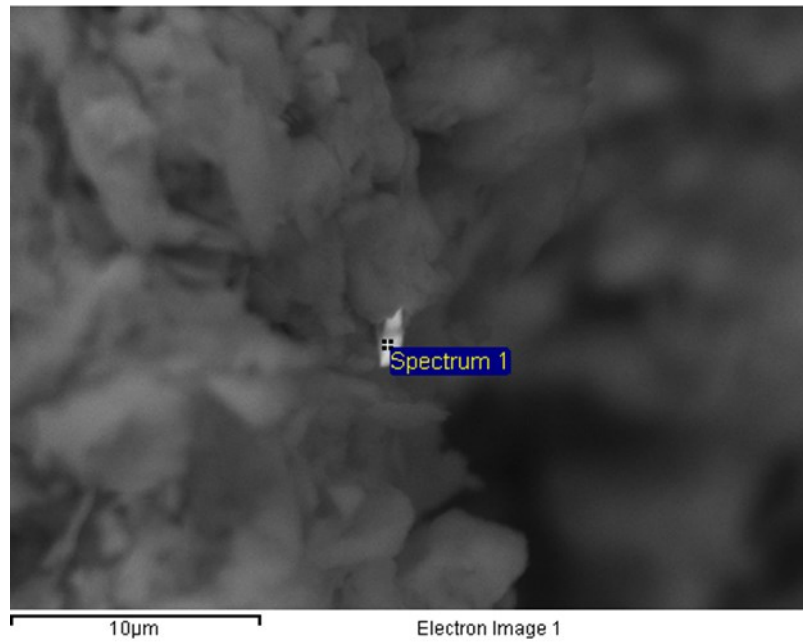


Figure D.1. SEM image of a grain containing Hg.

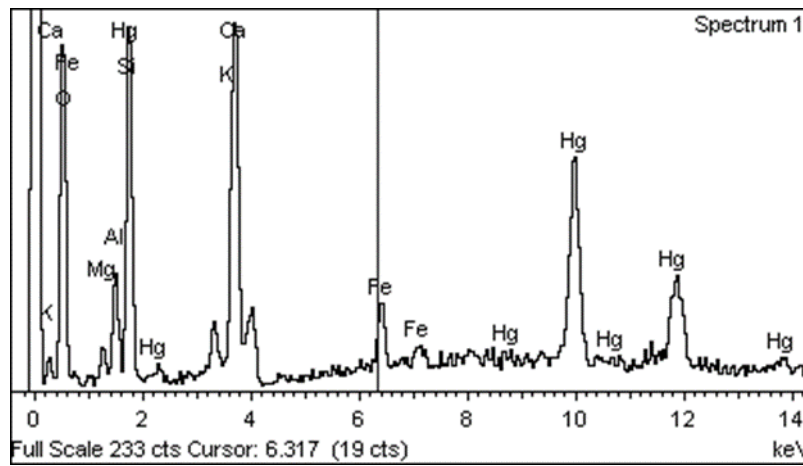


Figure D.2. EDX spectrum for an Hg-rich particle.

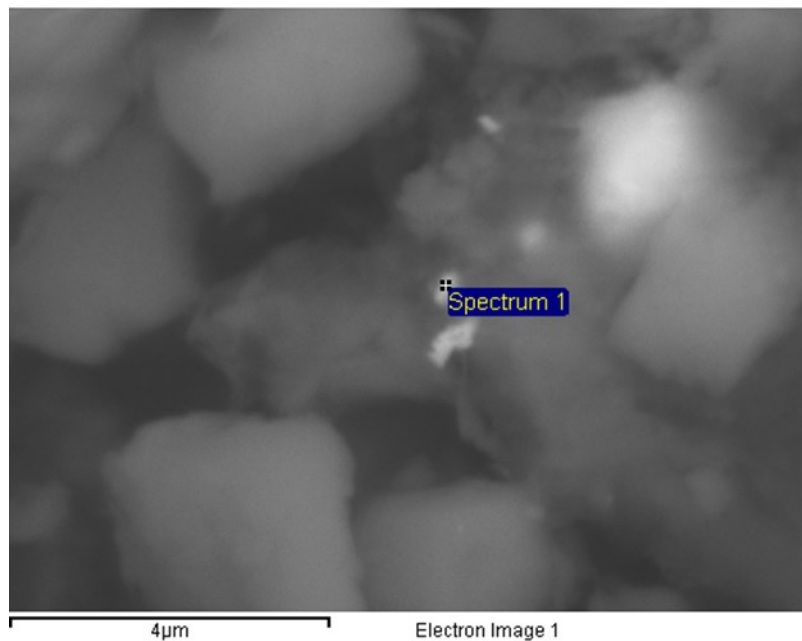


Figure D.3. SEM image of a grain containing Hg.

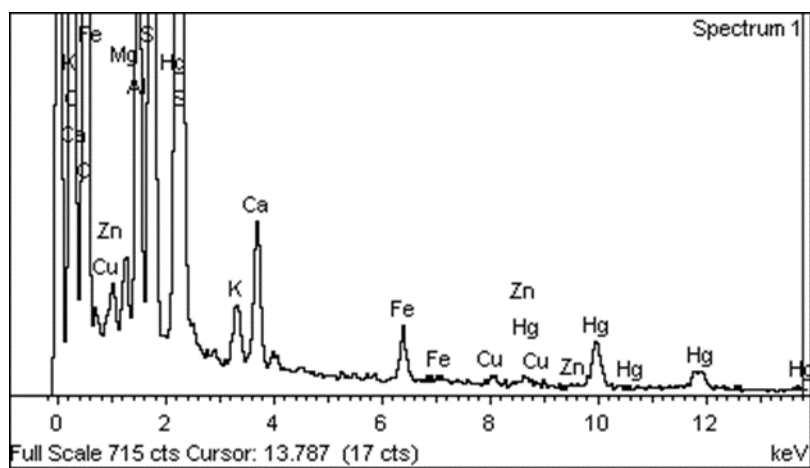


Figure D.4. EDX spectrum for an Hg-rich particle.

ACKNOWLEDGMENTS

Several experiments and analytical procedure performed during my PhD work have been carried out in different Institutes and with the kindly helpfulness of many people in them.

First and foremost, all experiments involving Thermal Desorption apparatus have been carried out at "Jožef Stefan" Institute in Ljubljana, Slovenia.

So, first of all I want to express great appreciation to Prof. Milena Horvat for the precious suggestions about the development of my research work, for her assiduous supervision and help during all my work in Ljubljana, and lastly for made me available several analytical tools and instruments in the "Reactor centre" Labs, which were indispensable for my research work.

Then, I would like to thank Dr. Vesna Fajon for her support and teachings in lab works;

Dr. Radojko Jaćimović for his kindly help during my stay in Ljubljana and for the Multielement analyses by neutron activation;

Dr. Majda Pavlin for her suggestions about results elaboration and thesis writing;

Dr. Eva Vezenkoska for her friendly help in the lab work that I greatly appreciate.

Sincere thanks to Prof. Stefano Covelli and Dr. Elisa Petranich from the University of Trieste (Dipartimento di Matematica e Geoscienze) for Hg analysis in liquid samples.

Special thanks to Prof. Daniele Goi and Dr. Andrea Fattori from the University of Udine for made me able to use LECO® model AMA-254;

Michele Magnan (Parco Scientifico e Tecnologico di Udine "Luigi Danieli") for his help in preliminary SEM-EDX analysis.

I also thank Prof. Iztok Arčon and Dr. Iuliia Mikulska from the University of Nova Gorica, for their help in performing preliminary EXAFS analysis.

Finally, I like to thank Dr. Roberto Terzano who, in the revising procedure, gives me special advises to significantly improve all the structure, informativity and readability of this thesis.